D. A. Leigh, F. Zerbetto, and E. R. Kay

DOI: 10.1002/anie.200504313

Molecular Devices

Synthetic Molecular Motors and Mechanical Machines

Euan R. Kay, David A. Leigh, and Francesco Zerbetto**

Keywords:
molecular devices · nanotechnology · noncovalent interactions · supramolecular chemistry

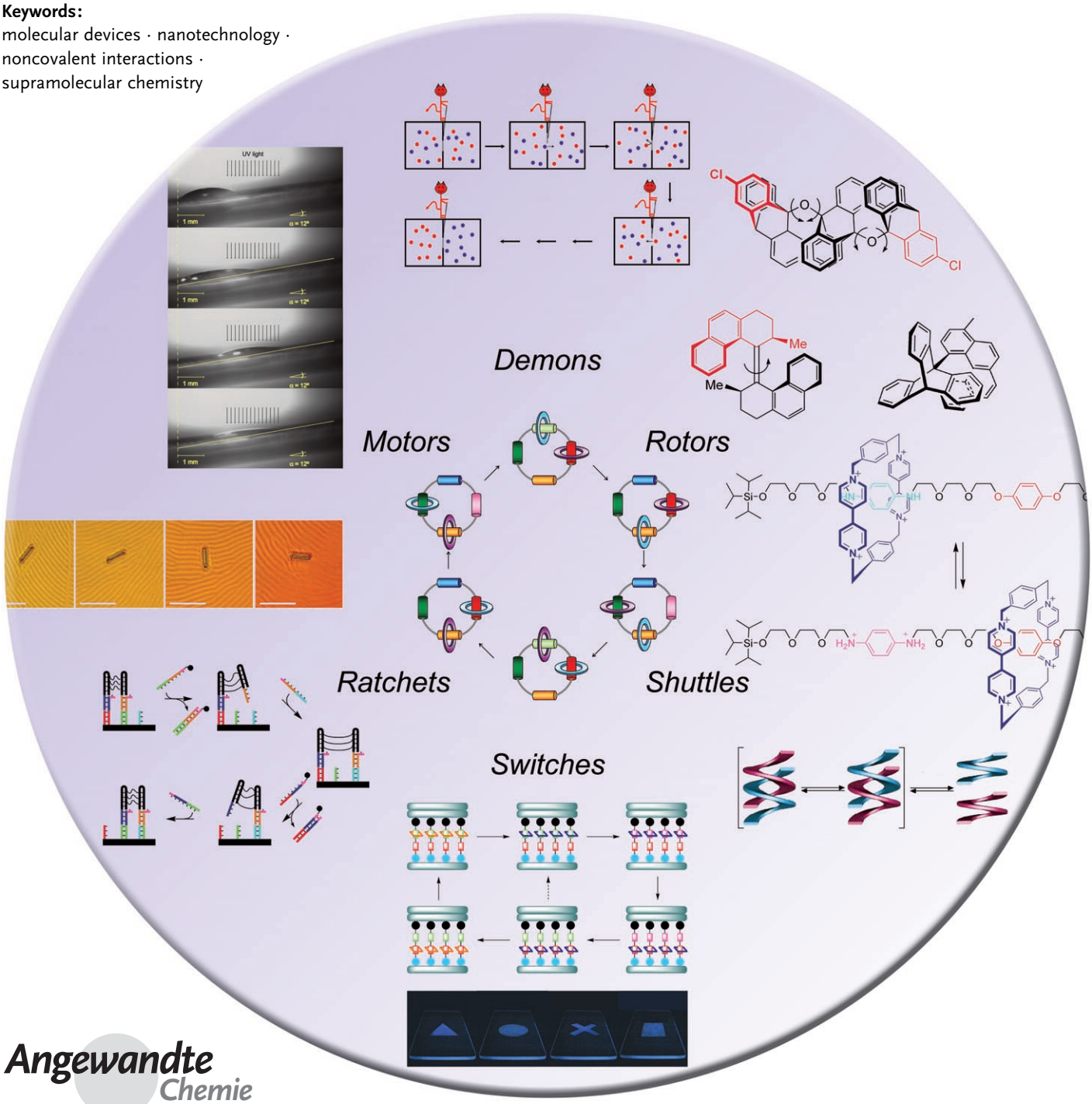

The widespread use of controlled molecular-level motion in key natural processes suggests that great rewards could come from bridging the gap between the present generation of synthetic molecular systems, which by and large rely upon electronic and chemical effects to carry out their functions, and the machines of the macroscopic world, which utilize the synchronized movements of smaller parts to perform specific tasks. This is a scientific area of great contemporary interest and extraordinary recent growth, yet the notion of molecular-level machines dates back to a time when the ideas surrounding the statistical nature of matter and the laws of thermodynamics were first being formulated. Here we outline the exciting successes in taming molecular-level movement thus far, the underlying principles that all experimental designs must follow, and the early progress made towards utilizing synthetic molecular structures to perform tasks using mechanical motion. We also highlight some of the issues and challenges that still need to be overcome.

From the Contents

1. Design Principles for Molecular-Level Motors and Machines

In recent years chemists have demonstrated imagination and considerable skill in the design and construction of synthetic molecular systems in which positional displacements of submolecular components result from moving downhill in terms of energy.[1] But what are the structural features necessary for molecules to use chemical energy to repetitively do mechanical work? How can we make a molecular machine that pumps ions to reverse a concentration gradient, for example, or moves itself uphill in terms of energy? How can we make nanoscale structures that traverse a predefined path across a surface or down a track by responding to the nature of their environment so as to change direction? How can we make a synthetic molecular motor that rotates against an applied torque? Artificial compounds that can do such things have yet to be realized. Moreover, and perhaps more surprisingly given that nature has developed such machines and refined them to a high degree of efficiency, the literature is still largely bereft of the fundamental guidelines necessary to invent them. In this Review we try to address this deficiency by using theory to outline, develop, and present the underlying mechanisms and principles required for future generation synthetic molecular-level machine systems alongside the current experimental state of the art.

Perhaps inevitably in an emerging field, there is not even a clear consensus as to what constitutes a molecular machine and what differentiates them from other molecular devices. Initially, the categorization of molecules as machines by chemists was purely iconic—the structures "looked" like pieces of machinery—or they were so-called because they carried out a function that in the macroscopic world would require a machine to perform it. Many of the chemical systems first likened to pistons and other machines were simply host–guest complexes in which the binding could be switched "on" or "off" by external stimuli such as light.[1] Whilst such studies were instrumental in popularizing the notion of molecular-level machines amongst chemists, it is fair to say (with considerable hindsight[2]) that the effects of scale tell us that supramolecular decomplexation events have little in common with the motion or function of a piston (the analogy is somewhat better applied to shuttling within a rotaxane architecture because the components are always kinetically associated, but the implication of imparting momentum is still unfortunate). Similarly, a photosensitizer is not phenomenologically related to a "light-fueled motor". Here we choose to differentiate machines from other devices on the basis that the etymology and meaning of "machine" generally implies mechanical movement—that is, a net nuclear displacement in the molecular world—which causes something useful to happen. Thus, for our purposes, "molec-

[*] E. R. Kay, Prof. D. A. Leigh
School of Chemistry
University of Edinburgh
The King's Buildings, West Mains Road, Edinburgh EH93JJ (UK)
Fax: (+44) 131-650-6453
E-mail: david.leigh@ed.ac.uk
Prof. F. Zerbetto
Dipartimento di Chimica "G. Ciamician"
Università di Bologna
v. F. Selmi 2, 40126 Bologna (Italy)
Fax: (+39) 051-209-9456
E-mail: francesco.zerbetto@unibo.it

ular machines" are a defined subset of "molecular devices" (functional molecular systems) in which some stimulus triggers the controlled, large amplitude or directional mechanical motion of one component relative to another (or of a substrate relative to the machine) which results in a net task being performed. Accordingly, we shall not discuss here supramolecular complexes in which the components are able to exchange with others in the bulk, or systems that function solely through changes in their electronic structure. Rather we will limit our scope to mechanical molecular-level devices, systems that feature—or attempt to feature—a degree of control over the motion of the components or substrates. The examples are chosen to help demonstrate the requirements for performing mechanical tasks at the molecular level.

1.1. Molecular-Level Machines and the Language Used to Describe Them

Language—especially scientific language—has to be suitably defined and correctly used to accurately convey concepts in a field. Nowhere is the need for accurate scientific language more apparent than in the discussion of the ideas and mechanisms by which nanoscale machines could—and do—operate.[3] Much of the terminology used to describe molecular-level machines has its origins in the observations of physicists and biologists, but their findings and descriptions have at times been misunderstood or under-appreciated by chemists. Similarly, the chemistry of molecular systems can sometimes be overlooked by other disciplines.[4]

As mechanism replaces imagery as the driving force behind advances in this field, it may be helpful for the terminology used to discuss molecular-level machine systems to become more phenomenologically based. When describing molecular behavior scientifically, the standard dictionary definitions meant for everyday use are not always appropriate for a regime that the definitions were never intended to cover. The difference between a "motor" and a "switch" as basic molecular machine types, for example, is significant because "motor" and "switch" become descriptors of very different types of behavior at molecular length scales, not simply iconic images (Figure 1). A "switch" influences a system as a function of state whereas a "motor" influences a system as a function of the trajectory of its components or the substrate. Returning a molecular-level switch to its original position undoes any mechanical effect it has on an external system (naturally, the molecules heat up their surroundings as the energy from the switching stimulus is dissipated); when the components of a rotary motor return to their original position through a different pathway to the one they left by (namely, a 360° directional rotation), a physical task performed by the machine is not inherently undone (for example, the rotating components could be used to wind up a polymer chain).

This difference is profound and the terms really should not be used interchangeably as sometimes happens in the chemistry (but not physics[5] or biology) literature. That is not to say that molecular switches cannot use chemical energy to do mechanical work. They can, but it is undone by resetting the switch to its original state. The key reason why this point is important is that switches cannot use chemical energy to repetitively and progressively drive a system away from equilibrium, whereas a motor can.[6] Other molecular machine types, also differentiated on the basis of their fundamental behavior, can also be identified (see Section 4.4). It is an accurate reflection of the current state of the art that the vast majority of the molecular-level machines discussed in this Review are switches, not motors. Similarly, thus far only "influence-as-a-function-of-state" rather then "influence-as-a-function-of-trajectory" molecular-level machines have been developed to the level that they can be exploited to perform tasks in the outside world.

1.2. The Effects of Scale

The path towards synthetic molecular machines can be traced back nearly two centuries to the observation of effects that pointed directly to the random motion experienced by all molecular-scale objects. In 1827, the Scottish botanist Robert Brown noted through his microscope the incessant, haphaz-

Euan Kay was born in Lanarkshire (Scotland) and educated at Hutchesons' Grammar School. He received his MChem from the University of Edinburgh in 2002. He is currently a Carnegie Trust Scholar working towards a PhD in the group of David Leigh on developing and demonstrating mechanisms for the control of molecular-level motion in mechanically interlocked molecules.

David Leigh was born in Birmingham (UK) and obtained his BSc and PhD from the University of Sheffield. After postdoctoral research at the NRC of Canada in Ottawa (1987–1989) he returned to the UK as a lecturer at UMIST. In 1998 he moved to the University of Warwick, and in 2001 he took up the Forbes Chair of Organic Chemistry at the University of Edinburgh. He holds both an EPSRC Senior Research Fellowship and a Royal Society-Wolfson Research Merit Award, and is a Fellow of the Royal Society of Edinburgh, Scotland's National Academy of Science and Letters. His research interests include molecular-level motors and machines.

Francesco Zerbetto received his PhD from the University of Bologna in 1986. From 1986 to 1990 he was a postdoctoral research associate at the National Research Council of Canada in Ottawa. He is currently Professor of Physical Chemistry at the University of Bologna. His current research interests focus on the simulation of large systems that range from mechanically interlocked molecules, to fullerenes and nanotubes, to the interface between inorganic surfaces and organic materials. He is the author of more than 200 papers.

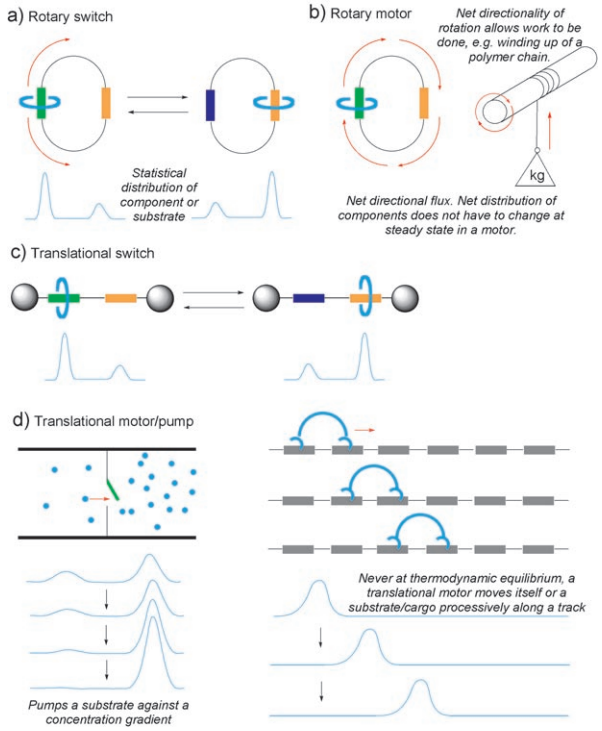

Figure 1. The fundamental difference between a "switch" and a "motor" at the molecular level. Both translational and rotary switches influence a system as a function of the switch state. They switch between two or more, often equilibrium, states. Motors, however, influence a system as a function of the trajectory of their components or a substrate. Motors function repetitively and progressively on a system; the affect of a switch is undone by resetting the machine. a) Rotary switch. b) Rotary motor. c) Translational switch. d) Translational motor or pump.

ard motion of tiny particles within translucent pollen grains suspended in water.[7] An explanation of the phenomenon—now known as Brownian motion or movement—was provided by Einstein in one[8] of his three celebrated papers of 1905 and was proven experimentally[9] by Perrin over the next decade.[10] Scientists have been fascinated by the implications of the stochastic nature of molecular-level motion ever since. The random thermal fluctuations experienced by molecules dominate mechanical behavior in the molecular world. Even the most efficient nanoscale machines are swamped by its effect. A typical motor protein consumes ATP fuel at a rate of 100–1000 molecules every second, which corresponds to a maximum possible power output in the region of 10^{-16} to 10^{-17} W per molecule.[11] When compared with the random environmental buffeting of approximately 10^{-8} W experienced by molecules in solution at room temperature, it seems remarkable that any form of controlled motion is possible.[12]

When designing molecular machines it is important to remember that the presence of Brownian motion is a consequence of scale, not of the nature of the surroundings. It cannot be avoided by putting a molecular-level structure in a near-vacuum, for example. Although there would be few random collisions to set such a Brownian particle in motion, there would be little viscosity to slow it down. These effects always cancel each other out, and as long as a temperature can be defined for an object it will undergo Brownian motion appropriate to that temperature (which determines the kinetic energy of the particle) and only the mean-free path between collisions is affected by the concentration of particles. In the absence of any other molecules, heat would still be transmitted from the hot walls of the container to the particle by electromagnetic radiation, with the random emission and absorption of the photons producing the Brownian motion. In fact, even temperature is not a particularly effective modulator of Brownian motion since the velocity of the particles depends on the square root of the temperature. So to reduce random thermal fluctuations to 10% of the amount present at room temperature, one would have to drop the temperature from 300 K to 3 K.[12,13] It seems sensible, therefore, to try to utilize Brownian motion when designing molecular machines rather than make structures that have to fight against it. Indeed, the question of how to (and whether it is even possible to) harness the inherent random motion present at small length scales to generate motion and do work at larger length scales has vexed scientists for some considerable time.

1.2.1. *The Brownian Motion "Thought Machines"*

The laws of thermodynamics govern how systems gain, process, and release energy and are central to the use of particle motion to do work at any scale. The zeroth law of thermodynamics tells us about the nature of equilibrium, the first law is concerned with the total energy of a system, while the third law sets the limits against which absolute measurements can be made. Whenever energy changes hands, however, (body to body or form to form) it is the second law of thermodynamics which comes into play. This law provides the link between the fundamentally reversible laws of physics and the clearly irreversible nature of the universe in which we exist. Furthermore, it is the second law of thermodynamics, with its often counterintuitive consequences, that governs many of the important design aspects of how to harness Brownian motion to make molecular-level machines. Indeed, the design of tiny machines capable of doing work was the subject of several celebrated historical "thought-machines" intended to test the very nature of the second law of thermodynamics.[14–18]

1.2.1.1. *Maxwell's Demon*

Scottish physicist James Clerk Maxwell played a major role (along with Ludwig Boltzmann) in developing the kinetic theory of gases, which established the relationship between heat and particle motion and gave birth to the concept of statistical mechanics. In doing so, Maxwell realized the profundity of the statistical nature of the second law of thermodynamics which had recently been formulated[19] by Rudolf Clausius and William Thomson (later Lord Kelvin). In an attempt to illustrate this feature, Maxwell devised the thought experiment which has come to be known as Maxwell's demon.[14,15,20]

Maxwell envisaged a gas enclosed within a container, to and from which no heat or matter could flow. The second law of thermodynamics requires that no gradient of heat or pressure can spontaneously arise in such a system, as that would constitute a reduction in entropy. Maxwell imagined the system separated into two sections by a partition (Figure 2). Having just proven that the molecules in a gas at a particular temperature have energies statistically distributed about a mean, Maxwell postulated a tiny "being" able to detect the velocities of individual molecules and open and close a hole in the partition so as to allow molecules moving faster than the average to move in one direction (R→L in Figure 2) and molecules moving slower than the average to move in the other (L→R in Figure 2). All the time, the number of particles in each half and the total amount of energy in the system remains the same. The result of the demon's endeavors being successful would be that one end of the system (the "fast" end, L) would become hot and the other (the "slow" end, R) cold; thus a temperature gradient is set up without doing any work, contrary to the second law of thermodynamics.

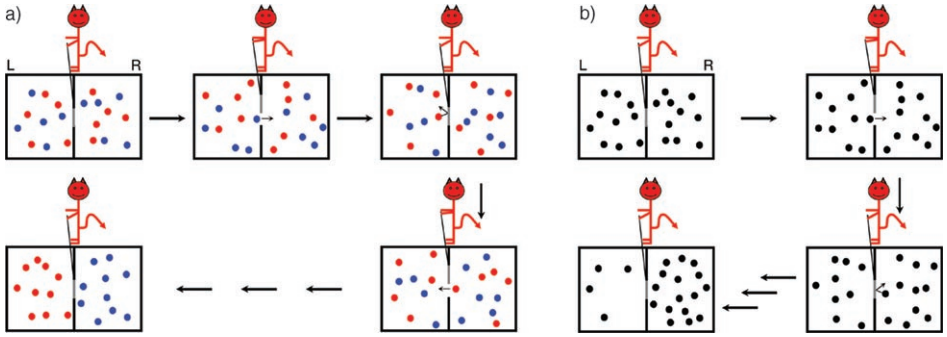

Figure 2. a) Maxwell's "temperature demon" in which a gas at uniform temperature is sorted into "hot" and "cold" molecules.[15] Particles with energy higher than the average are represented by red dots while blue dots represent particles with energies lower than the average. All mechanical operations carried out by the demon involve no work—that is, the door is frictionless and it is opened and closed infinitely slowly. The depiction of the demon outside the vessel is arbitrary and was not explicitly specified by Maxwell. b) A Maxwellian "pressure demon" in which a pressure gradient is established by the door being opened only when a particle in the left compartment approaches it.[15c]

After its publication in "*Theory of Heat*",[15b] Thomson expanded upon Maxwell's idea in a paper[21] read before the Royal Society of Edinburgh on 16 February 1874, and published a few weeks later in *Nature*,[22] introducing the term "demon" for Maxwell's being.[23] In using this word, Thomson apparently did not intend to suggest a malicious imp, but rather something more in keeping with the ancient Greek roots of the word (more usually daemon) as a supernatural being of a nature between gods and humans. Indeed, neither Maxwell nor Thomson saw the demon as a threat to the second law of thermodynamics, but rather an illustration of its limitations—an exposition of its statistical nature. This, however, has not been the view of many subsequent investigators, who have perceived the demon as an attempt to construct a perpetual motion machine driven by thermal fluctuations. The term "Maxwell's demon" has come to describe all manner of hypothetical constructs designed to overcome the second law of thermodynamics by continually extracting energy to do work from the thermal bath.[14]

Maxwell noted that the demon principle could be demonstrated in a number of different ways; a "pressure" demon, for example, (Figure 2b) could sort particles so that more end up in one end of a vessel than the other, which required different information to operate from the original temperature demon (the direction of approach of a particle, not its speed).

1.2.1.2. Szilard's Engine

Both Maxwell and Thomson appreciated that the operation of these systems for separating Brownian particles appeared to rely on the demon's "intelligence" as an animate being, but did not try to quantify it. Leo Szilard made the first attempt to mathematically relate the demon's intelligence to the thermodynamics of the process by considering the performance of a machine based on the "pressure demon", namely, Szilard's engine (Figure 3).[17] Szilard realized that the operations which the demon carries out can be reduced to a simple computational process. In particular, he recognized the process requires measurement of the approach of the particle to gain information about its direction and speed, which must be remembered and then acted upon.[24]

1.2.1.3. Smoluchowski's Trapdoor

The concept of a purely mechanical Brownian motion machine which does not require any intelligent being to operate it was first explored by Marian von Smoluchowski who imagined the Maxwell system as two gas-containing compartments with a spring-loaded trapdoor in place of the demon-operated hole (Figure 4a).[16] If the spring is weak enough, it might appear that the door could be opened by collisions with gas molecules moving in one direction (L→R in Figure 4a) but not the other, and so allow transport of molecules preferentially in one direction thereby creating a pressure gradient between the two compartments. Smoluchowski recognized (although could not prove) that if the door had no way of dissipating the energy it gains from Brownian collisions it would be subject to the same amount of random thermal motion as the rest of the system and would not then function as the desired one-way valve.

1.2.1.4. Feynman's Ratchet and Pawl

Richard Feynman revisited these ideas in his celebrated discussion of a miniature ratchet and pawl—a construct

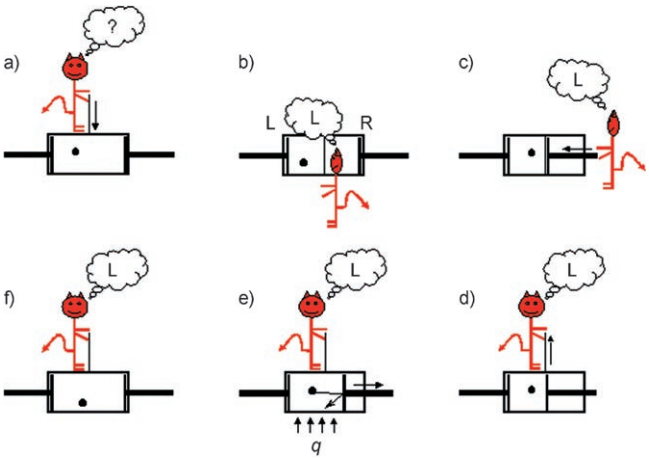

Figure 3. Szilard's engine which utilizes a "pressure demon".[17] a) Initially a single Brownian particle occupies a cylinder with a piston at either end. A frictionless partition is put in place to divide the container into two compartments (a→b). b) The demon then detects the particle and determines in which compartment it resides. c) Using this information, the demon is able to move the opposite piston into position without meeting any resistance from the particle. d) The partition is removed, allowing the "gas" to expand against the piston, doing work against any attached load (e). To replenish the energy used by the piston and maintain a constant temperature, heat must flow into the system. To complete the thermodynamic cycle and reset the machine, the demon's memory of where the particle was must be erased (f→a). To fully justify the application of a thermodynamic concept such as entropy to a single-particle model, a population of Szilard devices is required. The average for the ensemble over each of these devices can then be considered to represent the state of the system, which is comparable to the time average of a single multi-particle system at equilibrium, in a fashion similar to the statistical mechanics derivation of thermodynamic quantities.

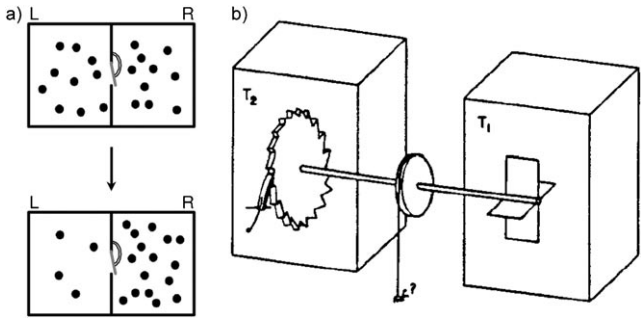

Figure 4. a) Smoluchowski's trapdoor: an "automatic" pressure demon (the directionally discriminating behavior is carried out by a wholly mechanical device, a trapdoor which is intended to open when hit from one direction but not the other).[16] Like the pressure demon shown in Figure 2b, Smoluchowski's trapdoor aims to transport particles selectively from the left compartment to the right. However, in the absence of a mechanism whereby the trapdoor can dissipate energy it will be at thermal equilibrium with its surroundings. This means it must spend much of its time open, unable to influence the transport of particles. Rarely, it will be closed when a particle approaches from the right and will open on collision with a particle coming from the left, thus doing its job as intended. Such events are balanced, however, by the door snapping shut on a particle from the right, pushing it into the left chamber. Overall, the probability of a particle moving from left to right is equal to that for moving right to left and so the trapdoor cannot accomplish its intended function adiabatically. b) Feynman's ratchet and pawl.[18] It might appear that Brownian motion of the gas molecules on the paddle wheel in the right-hand compartment can do work by exploiting the asymmetry of the teeth on the cog of the ratchet in the left-hand compartment. While the spring holds the pawl between the teeth of the cog, it does indeed turn selectively in the desired direction. However, when the pawl is disengaged, the cog wheel need only randomly rotate a tiny amount in the other direction to move back one tooth whereas it must rotate randomly a long way to move to the next tooth forward. If the paddle wheel and ratchet are at the same temperature (that is, $T_1 = T_2$) these rates cancel out. However, if $T_1 \neq T_2$ then the system will directionally rotate, driven solely by the Brownian motion of the gas molecules. Part (b) reprinted with permission from Ref. [18].

designed to illustrate how the irreversible second law of thermodynamics arises from the fundamentally reversible laws of motion.[18] Feynman's device (Figure 4b) consists of a miniature axle with vanes attached to one end, surrounded by a gas at temperature T_1. At the other end of the axle is a ratchet and pawl system, held at temperature T_2. The question posed by the system is whether the random oscillations produced by gas molecules bombarding the vanes can be rectified by the ratchet and pawl so as to get net motion in one direction. Exactly analogous to Smoluchowski's trapdoor, Feynman showed that if $T_1 = T_2$ then the ratchet and pawl cannot extract energy from the thermal bath to do work. Feynman's major contribution from the perspective of molecular machines, however, was to take the analysis one stage further: if such a system cannot use thermal energy to do work, what is required for it to do so? Feynman showed that when the ratchet and pawl are cooler than the vanes (that is, $T_1 > T_2$) the system does indeed rectify thermal motions and can do work (Feynman suggested lifting a hypothetical flea attached by a thread to the ratchet).[25] Of course, the machine now does not threaten the second law of thermodynamics as dissipation of heat into the gas reservoir of the ratchet and pawl occurs, so the temperature difference must be maintained by some external means. Although insulating a molecular-sized system from the outside environment is difficult (and temperature gradients cannot be maintained over molecular-scale distances, see Section 1.3), what this hypothetical construct provides is the first example of a plausible mechanism for a molecular motor—whereby the random thermal fluctuations characteristic of this size regime are not fought against but instead are harnessed and rectified. The key ingredient is the external addition of energy to the system, not to generate motion but rather to continually or cyclically drive the system away from equilibrium, thereby maintaining a thermally activated relaxation process that directionally biases Brownian motion towards equilibrium.[26] This profound idea is the key to the design of molecular-level systems that work through controling Brownian motion and is expanded upon in Section 1.4.

1.2.2. *Machines That Operate at Low Reynolds Number*

Whilst rectifying Brownian motion may provide the key to powering molecular-level machines, it tells us nothing about how that power can be used to perform tasks at the nanoscale and what tiny mechanical machines can and cannot be

expected to do. The constant presence of Brownian motion is not the only distinction between motion at the molecular level and in the macroscopic world. In the macroscopic world, the equations of motion are governed by inertial terms (dependent on mass). Viscous forces (dependent on particle dimensions) dampen motion by converting kinetic energy into heat, and objects do not move until they are provided with specific energy to do so. In a macroscopic machine, this is often provided through a directional force when work is done to move mechanical components in a particular way. As objects become less massive and smaller in dimensions, inertial terms decrease in importance and viscosity begins to dominate. A parameter which quantifies this effect is the Reynolds number R, which is essentially the ratio of inertial to viscous forces, and is given by Equation (1) for a particle of length a that is moving at velocity v in a medium with viscosity η and density ρ.[27]

$$R = \frac{a v \rho}{\eta} \quad (1)$$

Size affects the modes of motion long before the nanoscale is reached. Even at the mesoscopic level of bacteria (length dimensions ca. 10^{-5} m), viscous forces dominate. At the molecular level, the Reynolds number is extremely low (except at low pressures in the gas phase or, possibly, in the free volume within rigid frameworks in the solid state) and the result is that molecules, or their components, cannot be given a one-off "push" in the macroscopic sense. Thus, momentum is irrelevant. The motion of a molecular-level object is determined entirely by the forces acting on it at that particular instant—whether they are externally applied forces, viscosity, or random thermal perturbations and Brownian motion. Furthermore, the tiny masses of nanoscopic objects means that the force of gravity is insignificant for them. Since the physics which governs mechanical dynamic processes in the two size regimes is completely different, macroscopic and nanoscale motors require fundamentally different mechanisms for controlled transport or propulsion. Moreover, the high ratios of surface area to volume for molecules mean they are inherently sticky and this will have a profound effect on how molecular-sized machines are organized and interact with one another. In general terms, this analysis leads to a central tenet: while the macroscopic machines we encounter in everyday life may provide the inspiration for what we might like molecular machines to achieve, drawing too close an analogy for how they might do it may not be the best design strategy. The "rules of the game" at large and small length scales are simply too different.[1m,12,13,28]

1.3. Lessons to Learn from Biology

Help is at hand, however, because despite all these problems, we know that motors and machines at the molecular level are conceptually feasible—they are already all around us. Nature has developed a working molecular nanotechnology that it employs to astonishing effect in virtually every significant biological process.[11] Appreciating in general terms how nature has overcome the issues of scale, environment, equilibrium, Brownian motion, and viscosity is useful for indicating general traits for the design of synthetic molecular machine systems and how they might be used.

The membranes which encase cells and their organelles allow the compartmentalization of cellular processes and constituents, thereby maintaining the non-equilibrium distributions essential for life. These lipophilic barriers contain a diverse range of functionality which facilitate the movement of various ionic and polar species through channels, through relays or the use of mobile carrier species.[29] A number of different mechanisms are employed to power motion from one compartment to another. Besides passive diffusion down a concentration gradient in the transported species, an electrochemical gradient (a transmembrane electrical potential, a concentration gradient, or, most commonly, a combination of the two) originating from another species can be used. Such "gradient pumping" mechanisms move one species against its concentration gradient at the expense of another gradient. The motion of the two species can be in the same direction (symport) or in opposite directions (antiport). If the sole power source is an electrical potential, only one species crosses the membrane (a uniport mechanism). These processes are governed by sophisticated control mechanisms which open or close highly selective channels, carriers, and cotransporters in response to different stimuli, yet they all operate by relaxation down a directional transmembrane electrochemical gradient towards the thermodynamic equilibrium position.

The primary concentration gradients which are used to power subsequent secondary transport processes are maintained by a smaller number of ion pumps. These transmembrane mechanical devices convert nondirectional chemical reactions (the most abundant family, the ATPases, harness the hydrolysis of ATP) into vectorial transport of ionic species against an electrochemical gradient. The precise mechanisms by which these devices operate are still a subject of intense investigation. However, certain principles are becoming apparent. In particular, changes in the binding affinity at selective sites in the transmembrane region of the pump must be coupled to conformational changes which also modulate access to these sites from either side of the membrane so that only motion in the desired direction is achieved.[30]

A recent series of structures has outlined how just such a mechanism operates in the sarcoplasmic reticulum Ca^{2+}-ATPase pump.[31] Calcium ions bind to two high affinity sites which are open to the cytoplasm (B, Figure 5). Phosphorylation of the enzyme by ATP then results in a conformational change which shuts off access from either side (ratcheting[32]). Release of ADP is concomitant with a further conformational change which opens up access to the lumen side and disrupts the Ca^{2+}-binding residues (A, Figure 5). The calcium ions are released (escapement[32]) and swapped for protons which are subsequently occluded from the lumen by binding of a water molecule. Release of phosphate occurs with regeneration of the starting state, once again making the high-affinity Ca^{2+}-binding sites accessible to the cytoplasm. Similar mechanisms

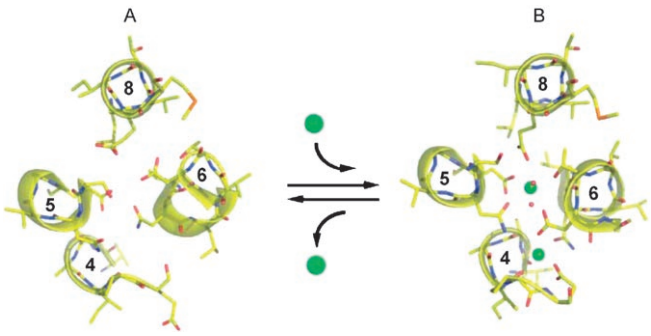

Figure 5. Crystal structures of the calcium-binding region in Ca^{2+}-ATPase in both low Ca^{2+}-affinity (A) and high Ca^{2+}-affinity (B) conformations.[31] Calcium ions are shown in green, and the numbers correspond to specific protein helices. The crystal structure pictures are reprinted with permission from Ref. [30b].

are thought to be responsible for the operation of the other members in the ATPase family.

The pumping of protons across the energy-transducing membranes of mitochondria, chloroplasts, and photosynthetic and respiratory bacteria is a particularly important process as it generates the protonmotive force necessary to operate ATP synthase (and also directly or indirectly powers the secondary transport of other species across these membranes). The ways in which nature achieves this pumping function are surprisingly diverse (by contrast, ATP synthase is highly conserved across organisms).[33] In most examples, charge-separated states and electron-transfer processes are used to generate transmembrane electric potentials. Overall, therefore, a directional electrochemical driving force is set up to drive the translocation of protons, somewhat similar to the gradient pumping secondary transport processes discussed above. Proton transport is concomitant with the resetting of the redox centers in processes often termed "redox loops" or "Mitchell loops".[34] Only in the case of bacteriorhodopsin (the photosynthetic center of certain purple bacteria) does it appear that light energy is directly converted into protonmotive force by a purely conformational pumping mechanism.[35] Again, the details of this process are not yet fully understood, but the correlation of conformational changes that control the direction in which the protons can move with changes in the affinity (that is, pK_a) of binding sites are likely to be involved.[36]

Nature also uses molecular machines to transport objects around within cells (for example, kinesin or dynein); to move whole organisms or their parts (for example, myosin or the bacterial flagellar motor); to process DNA and RNA (for example, helicases or polymerases); to convert protonmotive force into the synthesis of ATP (ATP synthase); and for may other functions besides. In these cases, too, much has been learnt about the various ways in which they perform their remarkable tasks, yet much remains to be discovered about each before the precise mechanisms can be elucidated.[11]

Accordingly, we can see that there are many general and fundamental differences between biological molecular machines and the man-made machines of the macroscopic world. Listed below are what appear to us to be the most significant aspects of biological machines to bear in mind when considering synthetic molecular machine design.

1) Biological machines are soft, not rigid.
2) Biological systems operate at near-ambient temperatures (heat is dissipated almost instantaneously at small length scales so they cannot exploit temperature gradients).
3) Biological motors utilize chemical energy, in the form of covalent-bond breaking/formation of high-energy compounds such as ATP, NADH, and NADPH or concentration gradients.
4) Biomachines operate in solution, or at surfaces, under conditions of intrinsically high viscosity.
5) Nature utilizes—rather than opposes—Brownian motion. Biomolecular machines need not use chemical energy to initiate movement—their components are constantly in motion—rather, they function by manipulating (ratcheting) that movement. Furthermore, constant thermal motion and small "reaction vessels" (cells and their organelles) ensure that the mixing of biological machines, their substrates, and their fuel is extremely rapid, in spite of the high viscosity they experience.
6) The viscous environment and constant thermal motion mean that biological machines have no use for smooth, low-friction surfaces. Genuinely smooth features are not possible on the molecular scale, of course, since the machine-component dimensions are close to the dimensions of the intrinsic unit of matter—the atom.
7) Biomotors and other mobile machines utilize architectures (for example, tracks) which serve to restrict most of the degrees of freedom of the machine components and/or the substrate(s) they act upon. The molecular machine and the substrate(s) it is acting upon remain kinetically associated during the operation of the machine. For example, kinesin only functions as it "walks" processively down a microtubule, not by simply binding to the microtubule at different places (that is, not by completely detaching, exchanging with the bulk, and rebinding). Similarly, pumps work by internally compartmentalizing ions so that they cannot exchange with others outwith the machine.
8) The operation and structure of biological machines are governed by noncovalent interactions (intramolecular and intermolecular), many of which exploit the aqueous environment in which the machines assemble and operate.
9) Biological machines are made by combinations of multiple parallel synthesis and self-assembly processes utilizing a relatively small range of building blocks: amino acids nucleic acids, lipids, and saccharides.
10) Living organisms intrinsically and necessarily function far from equilibrium—a state maintained by the compartmentalization of processes into cells, vesicles, and organelles.

We should also remember, however, that the mechanisms and function of biomolecular machines are restricted by evolutionary constraints. Over billions of years, evolution has led to machines of a complexity not yet possible through rational design, but it intrinsically proceeds through small

iterations and tends to retain the first successful solution arrived at for each problem. The human molecular-machine designer has at his or her disposal a much larger chemical toolbox, a wider range of possible operating conditions, and, as we shall see, a design approach that favors innovation.

Furthermore, whilst an appreciation of the characteristics of biological machines can give us broad clues about how to make molecular-level devices that exploit mechanical motion, we understand few of the precise details of how their designs work. How does an inherently mechanically directionless chemical reaction—the conversion of ATP into ADP—drive the directional motion of calcium ions by Ca^{2+}-ATPase? What is the detailed nature of the conformational changes which can set-up or disrupt the highly selective binding sites? Why exactly do the movements of the individual peptide subunits that cause this to happen occur in that particular sequence? What are the details of the pathways connecting the binding sites with the outside? What is the role of the kinetics and thermodynamics of each amino acid in this mechanism? In fact, biological motors and machines are so complex that studying simple synthetic chemical systems may help in the understanding of exactly how they work. Likewise, fully understanding the biological systems can only aid the design of sophisticated artificial systems. At present, however, much of the most detailed information for devising the basic mechanisms for synthetic molecular machines comes not from biology, but from non-equilibrium statistical mechanics.

1.4. Lessons To Learn from Physics, Mathematics, and Statistical Mechanics

1.4.1. Breaking Detailed Balance

The Principle of detailed balance[37] states that at equilibrium, transitions between any two states take place in either direction at the same rate so that no net flux is generated. This rules out the maintenance of equilibria by cyclic processes such as $A \rightarrow B \rightarrow C \rightarrow A$ rather than $A \rightleftharpoons B + B \rightleftharpoons C + C \rightleftharpoons A$[12] and is a formal indication that machines such as Smoluchowski's trapdoor and Feynman's ratchet and pawl cannot operate adiabatically. However, in an out-of-equilibrium system (for example, if $T_1 \neq T_2$ for the Feynman ratchet and pawl), "detailed balance" is broken, and net work can be done by the fluxional exchange process as the system moves spontaneously towards equilibrium.

To understand the mechanisms by which mechanical machines can operate on length scales at which Brownian motion occurs it is useful to appreciate precisely why work can be done by a random exchange process between two states only while detailed balance is broken. A simple analogy helps illustrate why detailed balance holds in a fluxionally exchanging system at equilibrium and the requirements necessary to break it. Consider a pair of scales with many ants running randomly between the two sides, the scales will be statistically balanced (but not necessarily horizontal, that only occurs if the pivot of the scale is positioned in the middle) and remain more or less steady at a stable angle. Even if a barrier is suddenly placed between the scales, thus stopping the two sides being in equilibrium, they remain balanced. However, if ants are added to one side or the other the scales become unbalanced and will tip accordingly. If the barrier is removed, the ants (assuming they can overcome the effect of gravity!) resume scurrying between the two sides and eventually equilibrium—and balance—will be restored. Note that even if we start without the barrier in place, if ants are suddenly added to one side balance will be broken for some time—and the scale will tip—until the roaming ants establish equilibrium and balance is restored. The breaking of balance allows a task to be performed as the exchanging system returns toward equilibrium. The net displacement that arises as the scales tip over (or as they right themselves) could be used to lift a feather to which the scale was attached. Breaking detailed balance is the key to doing work with a machine that operates at length scales on which Brownian motion occurs.

During the past decade, a number of remarkable theoretical formalisms have been developed in mathematics (particularly game theory) and non-equilibrium statistical physics that explain how the directional transport of Brownian particles over periodic potential-energy surfaces can occur from unbiased periodic or stochastic perturbations of the system.[38,39] Underlying each of these Brownian ratchet or motor mechanisms are three components:[39b] 1) a randomizing element;[40] 2) an energy input to avoid falling foul of the second law of thermodynamics; and 3) asymmetry in the energy or information potential in the dimension in which the motion occurs.[41] It is now widely accepted that ratchet mechanisms have a central role in explaining the operation of biological motor proteins.[42,43] They have also been successfully used to develop transport and separation devices for mesoscopic particles and macromolecules, microfluidic pumping, as well as quantum and electronic applications.[43,44] For molecular-level motors and other machines, the necessary randomizing element can be Brownian motion of the substrate or the machine components. The other two requirements (energy and anisotropy) can be supplied in different ways according to the type of fluctuation-driven transport mechanism.

1.4.2. Fluctuation-Driven Transport Mechanisms

Many different possible types of theoretical fluctuation-driven ("Brownian ratchet") mechanisms have been proposed, including flashing ratchets, tilting ratchets, Seebeck ratchets, drift ratchets, Hamiltonian ratchets, temperature ratchets, and entropic ratchets.[39] They can be classified and grouped together in many different (not always mutually exclusive) ways, and mechanisms that might be indistinguishable in chemical terms can be differentiated because of the nature of the physics involved. Whilst it is not clear (at least to us!) how some of the theoretical mechanisms could be applied to molecular structures, many offer clear design opportunities for the synthetic chemist. The details of the various mechanisms have been discussed extensively in the physics literature, so we will limit our discussion here to some specific variations which appear particularly well-suited for chemical systems. We choose to distinguish between two overarching classes of mechanism: energy ratchets, which fall

into two basic types—pulsating ratchets and tilting ratchets—and are the subject of a recent major review by Reimann,[39f] and information ratchets, which are much less common in the physics literature, but have been discussed by Parrondo, Astumian, and others.[39h,42b,45] Both energy ratchets and information ratchets bias the movement of a Brownian substrate.[46] However, we will also show (Sections 1.4.3 and 4.4) that they offer clues for how to go beyond a simple switch with a chemical machine to enable tasks to be performed through the non-equilibrium control of conformational and co-conformational changes within molecular structures.

1.4.2.1. *Pulsating Ratchets*[39f]

Pulsating ratchets are a general category of energy ratchet in which potential-energy minima and maxima are varied in a periodic or stochastic fashion, independent of the position of the particle on the potential-energy surface. In its simplest form this can be considered as an asymmetric sawtooth potential being repetitively turned on and off faster than Brownian particles can diffuse over more than a small fraction of the potential energy surface (an "on–off" ratchet, Figure 6). The result is net directional transport of the particles across the surface (left to right in Figure 6).

More general than the special case of an on–off ratchet, *any* asymmetric periodic potential may be regularly or stochastically varied to give a ratchet effect (such mechanisms are generally termed "fluctuating potential" ratchets). As with the simple on–off ratchet, most commonly encountered examples involve switching between two different potentials and are therefore often termed "flashing" ratchets. A classic example, which has particular relevance for explaining a number of biological processes[42b] as well as being the basis for a [2]catenane rotary motor (see Section 4.6.3), is illustrated in Figure 7. It consists in physical terms of an asymmetric potential-energy surface (comprising a periodic series of two different minima and two different maxima) along which a Brownian particle is directionally transported by sequentially raising and lowering each set of minima and maxima. The particle starts in a green or orange well (Figure 7a or c). Raising that energy minimum while lowering those in adjacent wells provides the impetus for the particle to change position by Brownian motion (Figure 7b→7c or 7d→7e). By simultaneously (or beforehand) changing the relative heights of the energy barrier to the next energy well, the kinetics of the Brownian motion in each direction are different and the particle is transported from left to right. Note that the position of the particle does not influence the sequence in which (or when, or if) the energy minima and maxima are changed. Furthermore, the switching of the

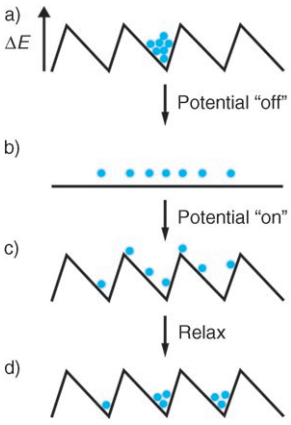

Figure 6. An example of a pulsating ratchet mechanism—an on–off ratchet.[39f] a) The Brownian particles start out in energy minima on the potential-energy surface with the energy barriers $\gg k_B T$. b) The potential is turned off so that free Brownian motion powered diffusion is allowed to occur for a short time period (much less than required to reach global equilibrium). c) On turning the potential back on again, the asymmetry of the potential means that the particles have a greater probability of being trapped in the adjacent well to the right rather than the adjacent well to the left. Note this step involves raising the energy of the particles. d) Relaxation to the local energy minima (during which heat is emitted) leads to the average position of the particles moving to the right. Repeating steps (b)–(d) progressively moves the Brownian particles further and further to the right.

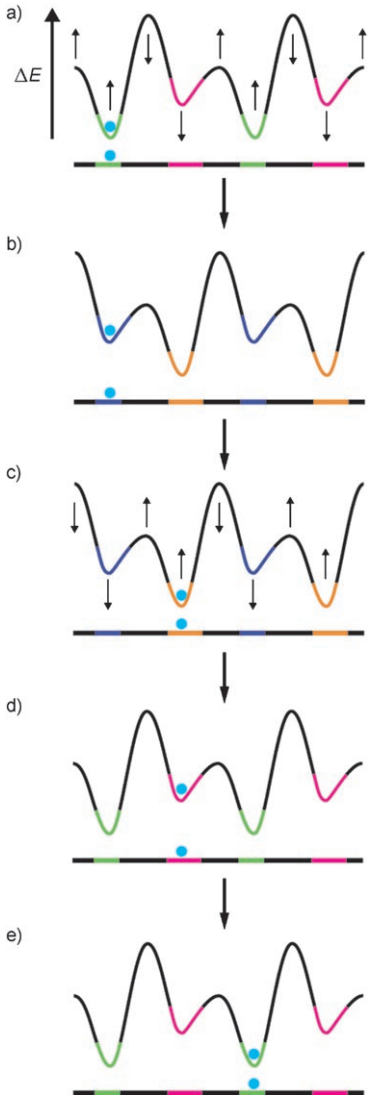

Figure 7. Another example of a pulsating ratchet mechanism—a flashing ratchet.[42b] For details of its operation, see the text.

potential does not have to be regular. As long as the two sets of energy minima and maxima are repetitively switched in the same order, the particle will tend to be transported from left to right in Figure 7, even though occasionally it may move over a barrier in the wrong direction.

The basic pulsating ratchet requirements can also be realized in another way. A potential such as that shown in Figure 7a can be given a directional drift velocity. Such systems are often termed "traveling potential" ratchets. This principle is essentially the same as macroscopic devices such as Archimedes' screw, yet in the presence of thermal fluctuations these systems exhibit Brownian ratchet characteristics and are closely related to tilting the potential in one direction (as discussed in Section 1.4.2.2). Clearly, however, an asymmetric potential is not absolutely required, nor in fact are thermal fluctuations; imagine, for example, a particle "surfing" on a traveling wave on the surface of a liquid. This category of mechanism is at the boundary between fluctuation-driven transport and transport as a result of potential gradients, with the precise location on this continuum dependent on the importance of thermal fluctuations and spatial asymmetry under the conditions chosen. In terms of chemical systems, the traveling-potential mechanism has most relevance for the field-driven processes discussed in Section 5 and the self-propulsion mechanisms of Section 6, while in Section 7 we shall discuss some situations in which the balance between random fluctuations and external directional driving force is shifted strongly towards the latter. The traveling motion does not have to be continuous, but rather may take place in discrete steps. Furthermore, arranging a continuously traveling potential to "jump" distances which are multiples of its period, at random or regular intervals, can be used to escape from the inherent directionality of the traveling-wave scheme and it has been shown that the ratchet dynamics are essentially unaffected. In the limiting situation, this can be reduced to dichotomous switching between two spatially shifted potentials which are otherwise identical, which is very similar to a rocking ratchet (see Section 1.4.2.2) and is also relevant to the unidirectional motors discussed in Section 2.2.

1.4.2.2. *Tilting Ratchets*[39f]

In this category, the underlying intrinsic potential remains unchanged and the detailed balance is broken by application of an unbiased driving force to the Brownian particle. Perhaps the most apparent unbiased driving force is heat, and ratchet mechanisms based on periodic or stochastic temperature variations are generally termed "temperature" or "diffusion" ratchets. In its simplest form (Figure 8) this mechanism is very similar to the on–off ratchet. Initially the thermal energy is low so that the particles cannot readily cross the energy barriers. A sudden increase in temperature can be applied so that $k_B T$ is much greater that the potential amplitude causing the particles to diffuse as if over a virtually flat potential-energy surface (Figure 8b). Returning to the original, lower, temperature (Figure 8c) is equivalent to turning the potential back on in Figure 6c and more particles will have moved to the next well to the right than to the left. Under this scheme,

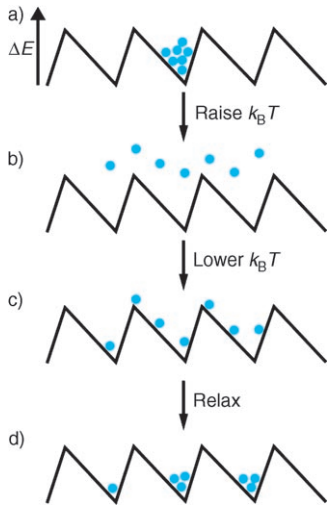

Figure 8. A temperature (or diffusion) ratchet.[39f] a) The Brownian particles start out in energy minima on the potential-energy surface with the energy barriers $\gg k_B T_1$. b) The temperature is increased so that the height of the barriers is $\ll k_B T_2$ and effectively free diffusion is allowed to occur for a short time period (much less than required to reach global equilibrium). c) The temperature is lowered to T_1 once more, and the asymmetry of the potential means that each particle is statistically more likely to be captured by the adjacent well to the right rather than the well to the left. d) Relaxation to the local energy minimum (during which heat is emitted) leads to the average position of the particles moving to the right. Repeating steps (b)–(d), progressively moves the Brownian particles further and further to the right. Note the similarities between this mechanism and that of the on–off ratchet shown in Figure 6.

therefore, it seems that applying temperature variations to any process which involves an asymmetric potential-energy surface could result in a ratchet effect.[47] In chemical terms, this means that the rotation of a chiral group around a covalent bond can, at least in principle, be made unidirectional in such a manner. This concept is explored further in relation to a molecular ratchet system in Section 2.1.2.

An unbiased driving force can also be achieved by applying a directional force in a periodic manner so that, over time, the bias averages to zero, thus generating a "rocking" ratchet. The simplest form of this is shown in Figure 9. Periodic application (to the left and then right) of a driving force that allows the particle to surmount the barriers (for example, by applying an external field if the particle is charged) results in transport. Motion over the steep barrier is again most likely as it involves the shortest distance. Such a mechanism is physically equivalent to tilting the ratchet potential in one direction then the other. Of course, if the driving force is strong enough and is constantly applied in one direction or the other, thermal fluctuations are not necessary, which would then correspond to a power stroke.

Analogues of a rocking ratchet in which the applied driving force is a form of stochastic noise are known as "fluctuating force" ratchets (in certain cases, also "correlation" ratchets). Finally, a tilting ratchet can be achieved in a symmetric potential if the perturbation itself results in spatial asymmetry (becoming very similar to the travelling-potential models in Section 1.4.2.1). This may be rather clear for the

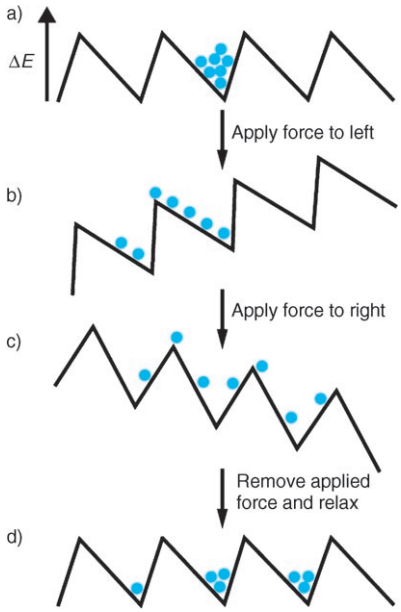

Figure 9. A rocking ratchet.[39f] a) The Brownian particles start out in energy minima on the potential-energy surface with the energy barriers $\gg k_B T$. b) A directional force is applied to the left. c) An equal and opposite directional force is applied to the right. d) Removal of the force and relaxation to the local energy minimum leads to the average position of the particles moving to the right. Repeating steps (b)–(d) progressively moves the Brownian particles further and further to the right.

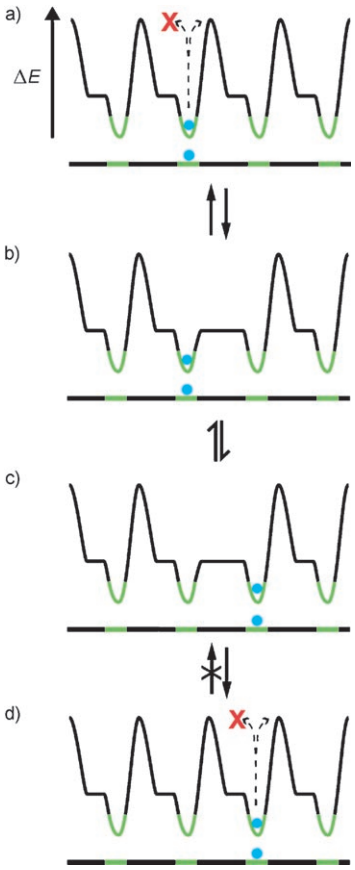

Figure 10. A type of information ratchet mechanism for transport of a Brownian particle along a potential-energy surface.[39h,42b,45] Dotted arrows indicate the transfer of information that signals the position of the particle. If the signal is distance-dependent—say, energy transfer from an excited state which causes lowering of an energy barrier—then the asymmetry in the particle's position between two barriers provides the "information" which transports the particle directionally along the potential energy surface.

periodic force cases (imagine applying the electric field discussed above for longer in one direction than the other), but is less so for stochastic driving forces. In general, these mechanisms are known as "asymmetrically tilting" ratchets.

1.4.2.3. *Information Ratchets*[39h,42b,45]

In the pulsating and tilting types of energy ratchet mechanisms, perturbations of the potential-energy surface—or of the particle's interaction with it—are applied globally and independent of the particle's position, while the periodicity of the potential is unchanged. Information ratchets (Figure 10) transport a Brownian particle by changing the effective kinetic barriers to Brownian motion depending on the position of the particle on the surface. In other words, the heights of the maxima on the potential-energy surface change according to the location of the particle (this requires information to be transferred from the particle to the surface) whereas the potential-energy minima do not necessarily need to change at all. This switching does not require raising the potential energy of the particle at any stage, rather the motion can be powered with energy taken entirely from the thermal bath by using information about the position of the particle. This is directly analogous to the mechanism required of Maxwell's pressure demon (Figure 2b, Section 1.2.1.1), but does not break the second law of thermodynamics as the required information transfer (actually, information erasure[48]) has an intrinsic energy cost that has to be met externally.

It appears to us that information-ratchet mechanisms of relevance to chemical systems can arise in at least three ways: 1) a localized change to the intrinsic potential-energy surface depending on the position of the particle (Figure 10); 2) a position-dependent change in the state of the particle which alters its interaction with the potential-energy surface at that point; or 3) switching between two different intrinsic periodic potentials according to the position of the particle.[39h,49] An example of the first of these types, in which the system responds to the "information" from the particle by lowering the energy barrier to the right-hand side (and only to the right-hand side) of the particle, is shown in Figure 10.

The particle starts in one of the identical-minima energy wells (Figure 10a). The position of the particle lowers the kinetic barrier for passage to the adjacent right-hand well and it moves there by Brownian motion (10b→10c). At this point it can sample two energy wells by Brownian motion, and a random reinstatement of the barrier has a 50% chance of returning the particle to its starting position and a 50% chance of trapping it in the newly accessed well to the right

(Figure 10d, of course a more efficient mechanism could be envisaged in which a second information transfer signals the occupation of the right-hand well and raises the barrier at this point only). The particle can no longer go back to the starting well but is now allowed access to the next well further to the right. Even though no enthalpic driving force ever exists for the particle to move from left to right, it is inevitably transported in that direction through such a mechanism. The potential-energy surface in Figure 10 is asymmetric, but this is not necessary if some other means can be devised of communicating the position of the particle (and therefore breaking spatial inversion symmetry).

Both energy ratchets and information ratchets could provide valid operating mechanisms for synthetic molecular-level machines. Furthermore, hybrid mechanisms appear to be possible. For example, by using asymmetry in the Brownian particle (for example, a cyclodextrin) rather than in the potential-energy surface to induce directionality of motion.[50] Indeed, it seems that the realization of functioning synthetic chemical machine systems could have as much to offer theoretical non-equilibrium statistical physics as the other way around.

1.4.3. *From Motors to Driving Non-equilibrium Changes in Chemical Systems*

Theoretical fluctuation-driven transport mechanisms have generally been considered in terms of either two-minima potential-energy surfaces or an infinitely repeating potential-energy surface. The former can be the basis for molecular switches, while the latter can be employed directly as designs for molecular-level motors.[51] What other general ideas can we glean from how these systems work from the viewpoint of designing other types of synthetic molecular-level machines that exploit Brownian motion?

1) Asymmetry in some part of the fluctuation-driven transport cycle is necessary to ensure that time-reversal symmetry is broken, which means that the particles undergo nonreciprocal motion during the operating cycle, thus generating a directional flux. This means that the particles are not subjected to the opposite of the initial transport process as the potential is being reset to begin another cycle.
2) In all these mechanisms (for example, Figures 6–10) we can see that the particles are always under the influence of the potential-energy surfaces responsible for transporting them. Even in the on–off ratchet (Figure 6), the sawtooth potential can only be switched off for a short time. If it were switched off for long enough for the particles to reach an equilibrium distribution over the surface, then the mechanism would not be able to directionally transport the particles progressively, it could only switch between one (average) equilibrium distribution and another. In other words, for a machine to operate by these types of mechanisms which manipulate non-equilibrium states, Brownian substrates must remain kinetically associated with the machine throughout its operation—not necessarily in physical contact but rather not able to exchange with substrates in the bulk, which are not under the influence of the machine. (This is why we rule out host–guest complexes that are under thermodynamic control acting as such machines (Section 1.1).) Exchanging with the bulk while entering the machine at one end and when leaving at the other is allowed when the two bulk regions are themselves otherwise separated (for example, a transmembrane pump).
3) The particles in all fluctuation-driven transport mechanisms can be considered to be "compartmentalized", in that at any moment the particles are free to move only over a localized area (which continually changes during the operating cycle of the machine). The compartment boundaries are not necessarily physical ones; when the sawtooth potential in the on–off ratchet in Figure 6 is switched off, it is the short time before the potential is re-applied that prevents the particles coming to global equilibrium over the surface.
4) It is the manipulation of the Brownian particles in terms of which and when compartments are "linked" (able to exchange particles) and the statistical balance of the populations of linked compartments with respect to the potential-energy surface (in the case of energy ratchets) or information (in the case of information ratchets) that enables the transport mechanism to function.
5) Energy ratchets (in which the Brownian substrate is passive) have been the most widely considered fluctuation-driven transport mechanisms in the physics literature. However, the components of chemical systems are not always passive. For molecular structures it seems likely that information ratchets (where the position of the Brownian particle or fragment affects the potential-energy surface) will also prove of great utility and importance.
6) Fluctuation-driven transport mechanisms are often considered in terms of charged particles, with electric fields being applied, typically to generate an infinitely repeating potential-energy surface. In chemical systems, noncovalent interactions and binding interactions can provide the necessary changing potential-energy surface, which can be of limited length and not uniform, with the Brownian substrate being either another ion or molecule or it could be another fragment of the same molecule.[52]
7) *Although the mechanisms for fluctuation-driven transport have been developed to direct the flow of particles in a given direction, we can consider applying the same sorts of ideas to generate other sorts of non-equilibrium distributions within molecular-level structures.* It should be possible to design molecular-level machine systems that are neither switches nor motors by utilizing small numbers of real or virtual "compartments" within a molecular (or supramolecular) structure that can be "linked" (and "unlinked") and "balanced" (and "unbalanced") in particular ways, perhaps by using Boolean logic operations, and addressed through orthogonal inputs to perform some function (see, for example, the "sorting and separating" machine suggested in Section 4.4). Fluctuation-driven transport mechanisms are illustrative of the general principles through which non-equilibrium distributions of supramolecular, molecular, and submolecular struc-

tures can be created, controlled, ordered, and manipulated by inputs of energy.

These are the principles used to develop the concepts for the compartmentalized molecular machines described in Section 4.4. However, it is interesting to consider that they are equally relevant for the design of interacting chemical reaction cascades and catalytic cycles that operate far from equilibrium.

If biology, mathematics, and physics provide the inspiration and strategies for controlling molecular-level motion, it is through chemistry that artificial molecular-level machine mechanisms must be designed, constructed, and made to work. The minimum requirements for such systems must be the restriction of the 3D motion of the machine components and/or the substrate as well as a change in their relative positions induced by an input of energy. Ways of achieving control over conformational dynamics involving single bonds and double bonds, as well as over co-conformational dynamics in kinetically stable supramolecular and mechanically bonded systems, are discussed in Sections 2–7.

2. Controlling Motion in Covalently Bonded Molecular Systems

2.1. Controlling Conformational Changes

2.1.1. Correlated Motion through Nonbonded Interactions

In compounds where two or more bulky planar substituents are geminally or vicinally connected, the congested steric environment often demands a helical ground state where all the rings are tilted in the same direction, thus generating a structure reminiscent of the macroscopic screw propellers found on aeroplanes and boats. The lowest energy rotational processes in such systems generally involve correlated motion of the planar "blades" (known as "cogwheeling"), and their investigation played an important early role in illustrating how motion can be controlled by molecular structure.[53] Inspired by the work of Ōki on the high threefold torsional barrier in bridgehead-substituted triptycenes,[54] the research groups of Mislow and Iwamura independently replaced the twofold aryl "rotators"[1k] of molecular propellers with 9-triptycyl units, thereby creating so-called "molecular gears".[53c,55–57] In these systems, the blades of each triptycyl group are tightly intermeshed, so that correlated disrotatory motion is strongly preferred. Such "dynamic gearing" mirrors the operation of a macroscopic bevel gear,[58] with correlated conrotation or uncorrelated rotation amounting to gear slippage. This threshold mechanism maintains the relationship between torsional angles of the two rotators. Changing this relationship can only occur by one of the higher energy rotational processes, so that stereoisomerism arises when at least one blade of each triptycyl is differentiable (illustrated for **1**, Scheme 1a).[59] As the isomers differ in the phase relationship between the substituted rings, the term "phase isomers" was coined for this subset of residual isomerism.[56c] Experimental and theoretical studies confirm that the correlated disrotation is generally favored over other torsional processes by 30–40 kcal mol^{-1} in these systems, largely because of the remarkable ease of the disrotary motion ($\Delta G^{\neq}$ = ca. 1–2 kcal mol^{-1}). This result actually represents stricter selectivity than occurs for the selection rules that govern correlated torsions under orbital symmetry control (see Section 2.1.5).

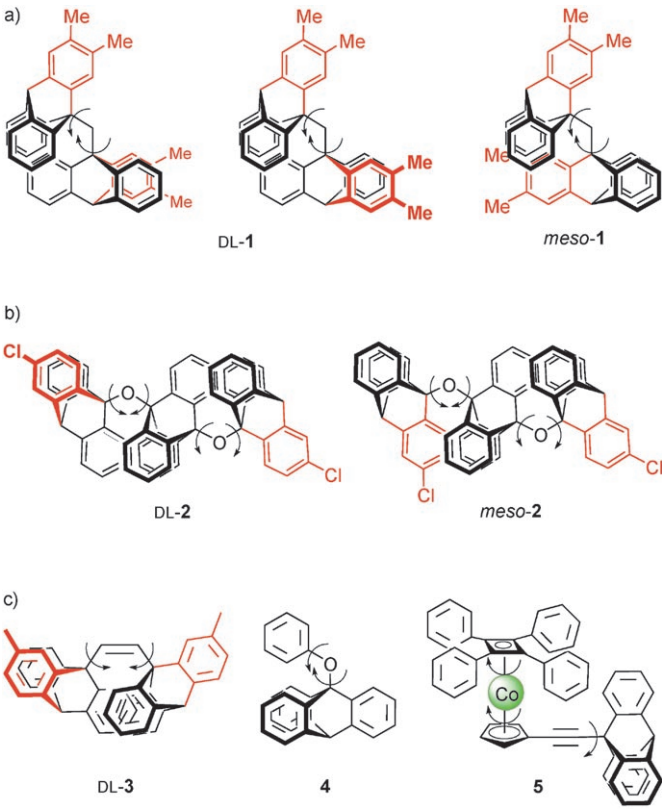

Scheme 1. a) The three residual diastereoisomers of molecular gear **1**.[57b] Correlated disrotation maintains the phase relationship between the labeled blades (shown here in red) for each isomer. Interconversion between isomers ("gear slippage") requires correlated conrotation or uncorrelated rotation. b) Molecular gear train **2**.[60] c) Vinyl molecular gear **3** (shown as the racemic residual diastereomer);[61] a molecular gear **4** with a 2:3 gearing ratio;[62i] and a molecular gear **5** based on revolution around a metallocene and with a 3:4 gearing ratio.[63] The arrows show correlated motions but are not meant to imply intrinsic directionality.

Iwamura and co-workers successfully extended the dynamic gearing concept to multiple gear systems in which each adjacent pair must disrotate, so that the behavior of the outermost rotators is dependent of the number of linkages in the chain. In **2** therefore (Scheme 1b), despite the large number of possible conformations and increased flexibility of the chain, the two outer triptycyl units conrotate and the phase relationship of the two chlorine labels is strictly maintained in both phase isomers.[60]

Dynamic gearing has also been realized in vicinally linked triptycyl rotors, such as **3** (Scheme 1c),[61] and in systems with gearing ratios other than 3:3, for example, 2:3 (**4**),[62] and 3:4 (**5**).[63] Although the low-energy dynamic processes observed in **5** could not be unequivocally shown to be correlated, this

system is one of the first molecular structures in which the facile rotation of π fragments in metallocenes was utilized, thus prompting analogy with a ball bearing.[64]

The same comparison can be applied to a more recent series of trinuclear sandwich complexes in which multiple correlated motions have been demonstrated.[65] Each silver cation in $[Ag_3(\mathbf{6})_2]$ has a linear coordination geometry, bound to one nitrogen donor from each tris-monodentate disk-shaped ligand (red)—the resulting complex is helical, with all the thiazolyl rings tilted in the same direction (Figure 11b). Random helix inversion is a low-energy process, which occurs through a nondissociative "flip" motion whereby rotation of the heteroaromatic rings so that they point in the opposite direction is accompanied by a 120° relative rotation of the two large disks (illustrated for $[Ag_3(\mathbf{6})(\mathbf{7})]$ in Figure 11c).[65a] In the heteroleptic analogue $[Ag_3(\mathbf{6})(\mathbf{7})]$, a similar coordination geometry is adopted so that only every alternate thiazolyl ring in the hexakis-monodentate disk ligand (blue) is bound at any one time. The "flip" helix reversal, during which the ligand and metal partners do not change, can clearly still occur. Ligand exchange is also rapid, however, and most likely occurs via the trigonal transition state illustrated in Figure 11c. The overall result is a correlated rotation of the heteroaromatic rings together with a 60° relative rotation of the two disks. If a ligand exchange and a flip step occur concurrently, the sense of rotation in each step is opposite, so that overall a 60° relative rotation of the disk-shaped ligands occurs.[65b,c]

While all these and other[66] related studies clearly demonstrate the role steric interactions can play, at equilibrium the submolecular motions are nondirectional even within a partial rotational event. Simply restricting the thermal rotary motion of one unit by a larger blocking group or by the similarly random motion of another unit cannot, in itself, lead to directionality. A molecular machine requires some form of external modulation over the dynamic processes to drive the system away from equilibrium and break detailed balance.

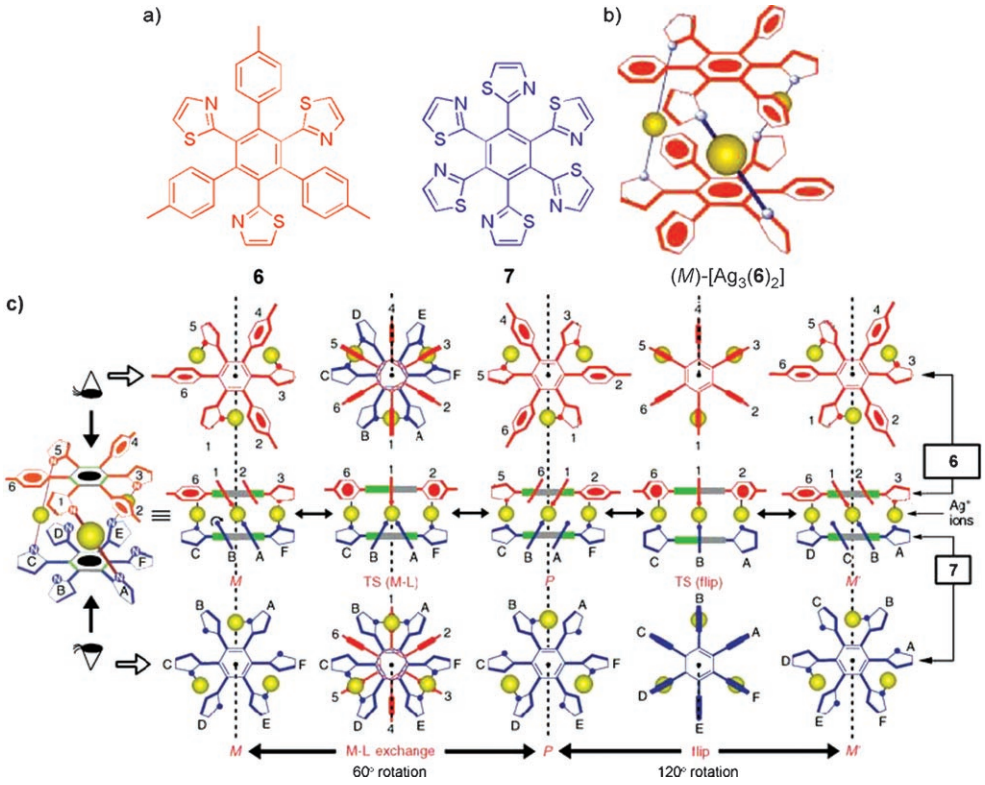

Figure 11. a) Chemical structure of tris-monodentate disk-shaped ligand **6** and hexakis-monodentate ligand **7**.[65] b) Schematic representation of complex $[Ag_3(\mathbf{6})_2]$ arbitrarily shown as its *M*-helical enantiomer. c) Description of the two correlated rotation processes occurring in $[Ag_3(\mathbf{6})(\mathbf{7})]$. The direction of rotation for an $M \rightarrow P$ transition through ligand exchange is opposite to that for the potentially subsequent $P \rightarrow M'$ transition by the nondissociative flip mechanism. Schematic representations reprinted with permission from Refs. [65a,c].

2.1.2. *Stimuli-Induced Conformational Control around a Single Covalent Bond*

As a first step towards achieving controlled and externally initiated rotation around C–C single bonds, Kelly and coworkers combined triptycene structures with a molecular-recognition event.[67] In the resulting "molecular brake" **8**

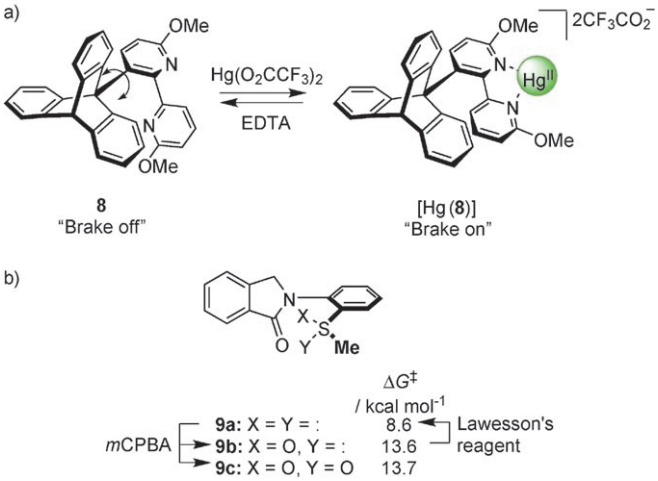

Scheme 2. "Molecular brakes" induced by a) metal-ion binding[68] and b) redox chemistry.[70] EDTA = ethylenediaminetetraacetate, *m*CPBA = *meta*-chloroperbenzoic acid.

(Scheme 2a),[68] free rotation of a triptycyl group is halted by the conformational change brought about by complexation of the appended bipyridyl unit with Hg^{2+} ions, thus effectively putting a "stick" in the "spokes".[69] A similar "braking effect" has been demonstrated by using redox chemistry and *N*-arylindolinone **9** (Scheme 2b); both oxidized forms of the sulfur side chain exhibit markedly increased barriers to rotation around the N–aryl bond (see also **45**, Scheme 21).[70,71]

Kelly et al. next extended their investigation of restricted Brownian rotary motion to a molecular realization (**10**) of the Feynman adiabatic ratchet and pawl,[72] in which a helicene plays the role of the pawl in attempting to direct the rotation of the attached triptycene "cog wheel" in one direction as a result of the chiral helical structure. Although the calculated energetics for rotation showed an asymmetric potential energy profile (Figure 12b), ^{1}H NMR experiments confirmed that rotation occurred with equal frequency in both directions. This result is, of course, in line with the conclusions of the Feynman thought experiment (Section 1.2.1.4).[73] The rate of a molecular transformation (clockwise and anticlockwise rotation in **10** included) depends on the energy of the transition state (and the temperature), not the shape of the energy barrier: state functions such as enthalpy and free energy do not depend on a system's history.[74] Thus, although rotation in **10** follows an asymmetric potential-energy surface, the principle of detailed balance at equilibrium requires that transitions in each direction occur at equal rates.[75]

The essential element missing from **10** needed to turn the triptycene directionally is some form of energy input to drive it away from equilibrium and break the detailed balance. In principle, this could be achieved rather simply for **10** by a periodic fluctuation in temperature (causing directional rotation in chemical structures does not have to be complicated), thus constituting a temperature ratchet.[75] However, proving this experimentally by quantifying the net rotation appears to be nontrivial. As a different solution, Kelly et al. proposed a modified version of the ratchet structure (**11a**, Scheme 3), in which a chemical reaction is used as the source of energy.[76] If the amino group is ignored, all three energy minima for the position of the helicene with respect to the triptycene "teeth" are identical: the energy profile for 360° rotation would appear as three equal energy minima, separated by equal barriers. As the helicene oscillates back and forth in a trough, however, sometimes it will come close enough to the amine for a chemical reaction to occur (as in **12b**). Priming the system with a chemical "fuel" (phosgene in this case to give the isocyanate **12a**) results in "ratcheting" of the motion some way up the energy barrier (**13a**). Continuation of the rotation in the same direction, over the energy barrier, can occur under thermal control and is now an exergonic process (giving **13b**) before cleavage of the urethane gives the system rotated by 120° (**11b**). Although the current version of the system can only carry out one third of a full rotation, it demonstrates the principles required for a fully operating and cyclable rotary system under chemical control and represents a major advance in the experimental realization of molecular-level machines.

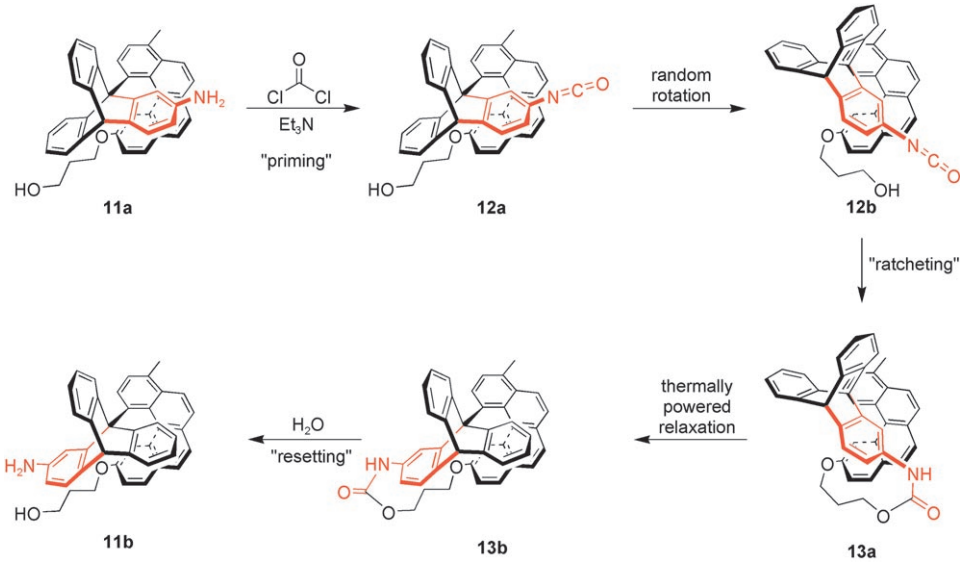

Scheme 3. A chemically powered unidirectional rotor.[76] Priming of the rotor in its initial state with phosgene (**11a**→**12a**) allows a chemical reaction to take place when the helicene rotates far enough up its potential well towards the blocking triptycene arm (**12b**). This gives a tethered state **13a**, for which rotation over the barrier to **13b** is an exergonic process that occurs under thermal activation. Finally, the urethane linker can be cleaved to give the original molecule with the components rotated by 120° with respect to each other (**11b**).

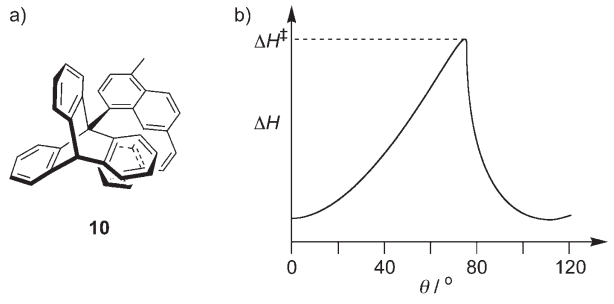

Figure 12. a) Kelly's molecular realization (**10**) of Feynman's adiabatic ratchet and pawl which does not rotate directionally at equilibrium.[72] b) Schematic representation of the calculated enthalpy changes for rotation around the single degree of internal rotational freedom in **10**.

Mock and Ochwat have proposed **14**, which undergoes the catalytic cycle illustrated in Scheme 4, as a minimalist model of a molecular motor.[77] In the process of catalyzing the hydration of its ketenimine fuel (red box) to give a carboxamide waste product (blue box), epimerization of the stereogenic center in the motor occurs—formally rotation around a C–O bond (as indicated for (*R*)-**14** in Scheme 4). The cycle operates (Scheme 4) under the specific kinetic conditions $k_2, k_4 > k_1[\mathrm{AcCH{=}C{=}N}t\mathrm{Bu}] > k_3[\mathrm{H_2O}]$. Kinetic analysis based on spectrophotometric measurements was used to identify reaction conditions under which this relation is satisfied. Over a single catalytic cycle, therefore, the molecular chirality should ensure some biasing of the rotational direction for formal 180° rotation around the C–O bond. However, the subsequent cycle on the opposite enantiomer will experience the antipodal directing effect so that the biasing effect is the exact reverse to before.[78]

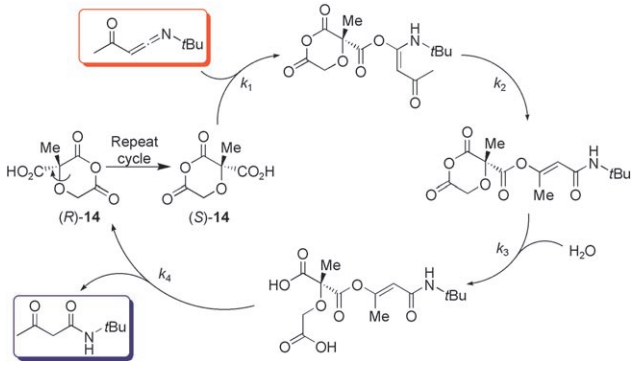

Scheme 4. Proposed system for chemically driven directional 180° rotary motion fueled by hydration of a ketenimine (red box).[77] For clarity, the catalytic cycle for a single enantiomer of motor **14** is shown. This cycle produces the opposite enantiomer, which undergoes an analogous cycle in which rotation must be biased in the opposite direction. A number of potential side reactions (not illustrated) which would divert the system from the catalytic cycle were found to be kinetically insignificant under the reaction conditions employed.

The restriction of rotational motion arising from steric interactions between *ortho* substituents in biphenyl systems forms the basis for another system designed to exhibit directional rotation through ring opening/ring closing of a chiral lactone (Scheme 5).[79] Ring opening of lactone **15** with a bulky nucleophile should proceed preferentially through attack at one of the two diastereotopic faces ($k_{\mathbf{15}\rightarrow\mathbf{16}\text{-a}S} > k_{\mathbf{15}\rightarrow\mathbf{16}\text{-a}R}$). Equilibration of the ring-opened diastereomers should then occur by random oscillations around the aryl–aryl bond, with the bulky nucleophile preferentially avoiding passing over the cyclohexanol ring. Ring closing is then proposed to be faster from the **16**-a*R* isomer because of the proximity of the reacting groups, so that a net 360° rotation will be accomplished by a number of molecules in the system. Experimentally, equilibration of the two ring-opened diastereomers in the current system occurs too fast for determination of the selectivity of the ring-opening reaction. Similarly, demonstrating directional selectivity for the ring-closing step will present a significant challenge. A further

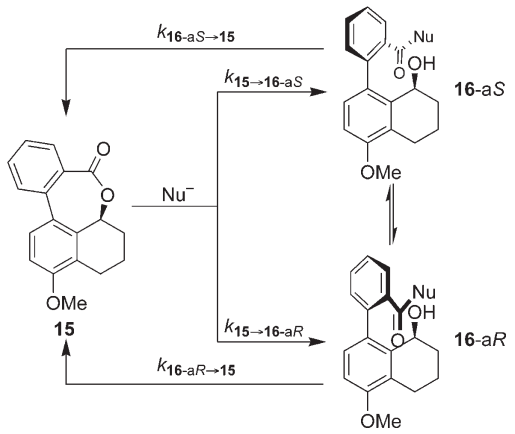

Scheme 5. Proposed system for unidirectional rotation around an aryl–aryl bond based on ring opening/ring closing of a chiral lactone.[79] Although this cannot function at equilibrium, it could if additional features were added such that $k_{\mathbf{15}\rightarrow\mathbf{16}\text{-a}S} \neq k_{\mathbf{16}\text{-a}S\rightarrow\mathbf{15}}$ and $k_{\mathbf{15}\rightarrow\mathbf{16}\text{-a}R} \neq k_{\mathbf{16}\text{-a}R\rightarrow\mathbf{15}}$.

modification is also necessary to achieve directional 360° rotation; since the ring-closing step is the exact reverse of the ring-opening step, both must proceed by the same transition state so that the rate in either direction is the same ($k_{\mathbf{15}\rightarrow\mathbf{16}\text{-a}S} = k_{\mathbf{16}\text{-a}S\rightarrow\mathbf{15}}$ and $k_{\mathbf{15}\rightarrow\mathbf{16}\text{-a}R} = k_{\mathbf{16}\text{-a}R\rightarrow\mathbf{15}}$). No energy would be consumed by the mechanism proposed in Scheme 5 and, of course, the principle of detailed balance (Section 1.4.1) demands that unidirectional rotation cannot occur in a system at equilibrium.

Stereoselective ring opening of racemic biaryl lactones using chiral reagents results in a directional rotation of about 90°, which can be extended to a full half-turn by chemoselective ring closing to give the lactone by using a hydroxy group in the other *ortho* position. This effect has been demonstrated by Branchaud and co-workers[80] and, in an independent effort, Feringa and co-workers have successfully extended this strategy to obtain a full 360° rotation around a C–C single bond.[81] The process involves four intermediates (**A**–**D**, Figure 13a), in each of which rotation around the biaryl bond is restricted: by covalent attachment in **A** and **C**, and through nonbonded interactions in **B** and **D**. Directional rotation to interchange these intermediates requires a stereoselective bond-breaking reaction in steps (1) and (3) and a regioselective bond-formation reaction in steps (2) and (4). Unlike **15** above, lactones **17** and **19** (Figure 13b) exist as racemic mixtures as a result of a low barrier for small amplitude rotations around the aryl–aryl bond. Reductive ring opening with high enantioselectivity is, however, achievable for either lactone by using a homochiral borolidine catalyst, and the released phenol can subsequently be orthogonally protected to give **18a** or **20a**. The ring-opened compounds are produced in near-enantiopure form in a process which involves directional rotation of 90° around the biaryl bond, governed by the chirality of the catalyst, and powered by consumption of borane. The *ortho* substitution of these species results in a high barrier to axial rotation. Oxidation of the benzylic alcohol (**18a**→**18b** or **20a**→**20b**) primes the motor for the next rotational step. Selective

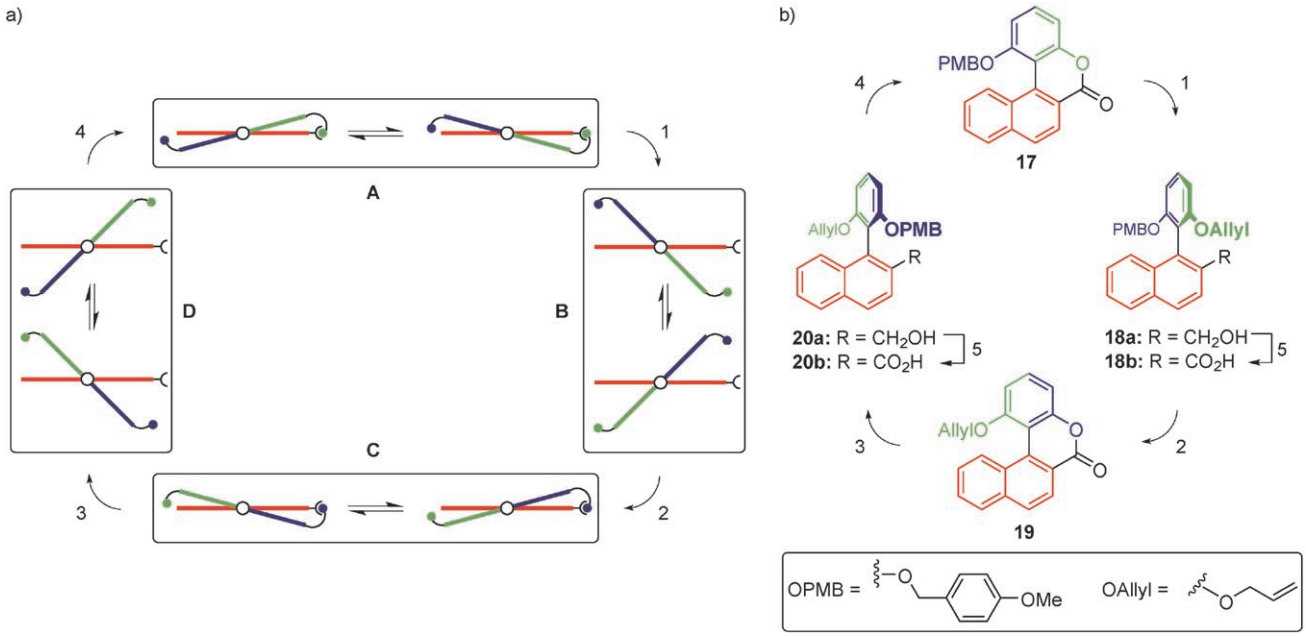

Figure 13. a) Schematic representation of unidirectional rotation around a single bond, through four states.[81] In states **A** and **C** rotation is restricted by a covalent linkage, but the allowed motion results in helix inversion. In states **B** and **D** rotation is restricted by nonbonded interactions between the two halves of the system (red and green/blue). These forms are configurationally stable. The rotation relies on stereospecific cleavage of the covalent linkages in steps (1) and (3), then regiospecific formation of covalent linkages in steps (2) and (4). b) Structure and chemical transformations of a unidirectional rotor. Reactions: 1) Stereoselective reduction with (*S*)-CBS then allyl protection. 2) Chemoselective removal of the PMB group resulting in spontaneous lactonization. 3) Stereoselective reduction with (*S*)-CBS then protection with a PMB group. 4) Chemoselective removal of the allyl group resulting in spontaneous lactonization. 5) Oxidation to carboxylic acid.

removal of one of the protecting groups on the enantiotopic phenols results in spontaneous lactonization when thermally driven axial rotation brings the two reactive groups together—again probably a net directional process because of the steric hindrance of the *ortho* substituents (although this is not demonstrated because the chirality is destroyed in this step). Figure 13b illustrates the unidirectional process achieved using the (*S*)-Corey–Bakshi–Shibata ((*S*)-CBS) catalyst; rotation in the opposite sense can be achieved by employing the opposite borolidine enantiomer and swapping the order of phenol protection and deprotection steps.

2.1.3. *Stimuli-Induced Conformational Control in Organometallic Systems*

Controlling the facile rotary motion of ligands in metal sandwich or double-decker complexes (introduced in Section 2.1.1) is conceptually similar to controlling rotation around covalent single bonds, and stimuli-induced control in such metal complexes has also been demonstrated. In metal bisporphyrinate complexes such as [Ce(**21**)] (Scheme 6) rotary motion corresponds to enantiomerization when the ligands possess D_{2h} symmetry. This situation provides a convenient handle for monitoring the kinetics of rotation.[82] In complex [Ce(**21**)], rotation around the metal center is slow enough to permit isolation of the two enantiomers by chiral HPLC. However, reduction of the metal center ([Ce^{IV}(**21**)]→[Ce^{III}(**21**)]$^-$) increases the rate of racemization by over 300-fold.[82c] This effect is thought to derive from a reduced π–π interaction between the two ligands as a consequence of the larger ionic radius of the metal center in the lower oxidation state. Similarly, complexes formed around the smaller Zr^{IV} ion show very slow rotational dynamics at pH 7,[83] yet protonation results in facile racemization.[82a] The effect is retarded by oxidation of the porphyrin ligands, probably as a result of electrostatic repulsion of incoming protons, but also because of the fact that the highest occupied molecular orbital (HOMO) of the complex is antibonding, so removal of electrons should

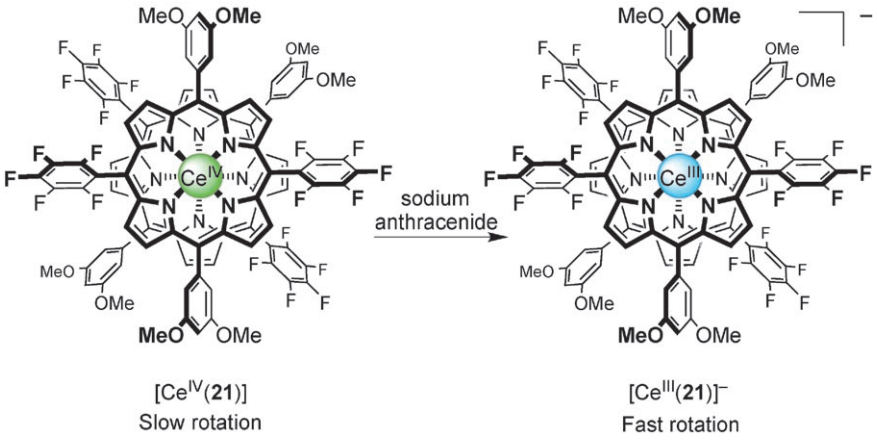

Scheme 6. Controlling the rate of relative rotations of porphyrin ligands in cerium bis[tetrakis-arylporphyrinate] double-decker complex [Ce(**21**)].[82c]

increase the π–π bonding interaction between the two porphyrin rings.[82c]

Rotary motion in sandwich complexes can be interrupted by the binding of a ditopic guest between recognition sites on each of the two rings. If more than one such pair of binding sites exists, a positive, homotropic allosteric effect is observed.[84] This principle has been exploited to create allosteric receptors (for example, **22**) for γ-dicarboxylic acids (Scheme 7),[85] β-dicarboxylate anions,[86] potassium

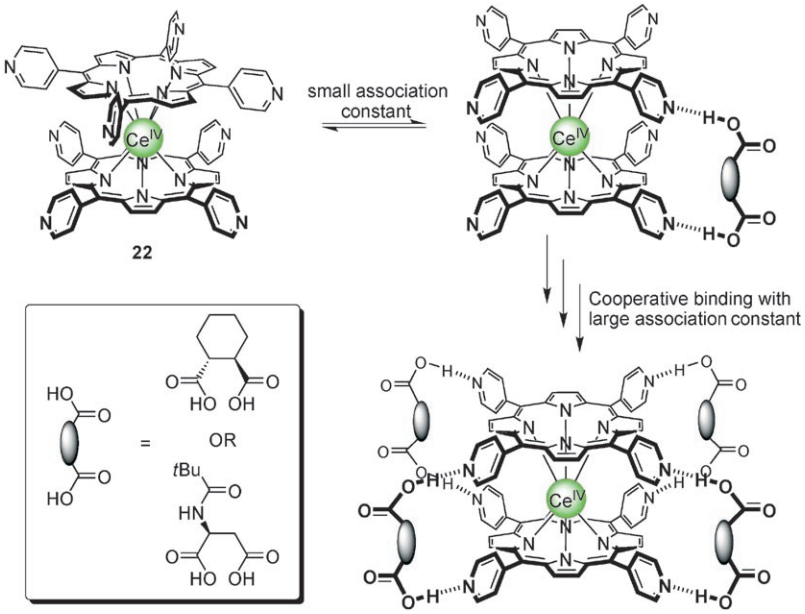

Scheme 7. Positive homotropic allosteric binding in a double-decker complex **22**.[85] A result of the cooperative binding is pronounced guest selectivity; for example, δ-dicarboxylic acids are not bound. The chirality of the guest is communicated to the host, thus determining the sense of the axial chirality induced about the metal–porphyrin axis.

ions,[87] silver ions,[88] as well as mono- and oligosaccharides (even in aqueous solution).[89] It was originally proposed that such effects were primarily a result of the restriction of the motion of the porphyrin ring when the first guest binds, thus reducing the entropic cost of subsequent identical binding events.[85–87,89] In the case of cooperative binding of silver ions, however, it is observed that binding of the guest species progressively and nonlinearly increases the rate of rotation.[88b] Here, cation binding induces a deformation of the porphyrin rings away from planarity to generate a more domed structure, simultaneously weakening the π–π interactions between the porphyrin rings and preorganizing the remaining silver binding sites. Recent results suggest that torsional strain induced by binding may play a significant role in the cooperative binding in all these systems.[90,91]

Ferrocene has long been known to exhibit a low barrier to cyclopentadienyl (Cp) ring rotation.[92] Recently, a gas-phase experimental and theoretical study of dianionic $\mathbf{23}^{2-}$ and anionic $[\mathbf{23}\cdot H]^-$ indicated that a two-state rotary switch could be operated by monoprotonation and deprotonation (Scheme 8).[93] The conformation of the dianion is governed by coulombic repulsions, while an intramolecular hydrogen bond stabilizes the observed conformation in the monoanion.

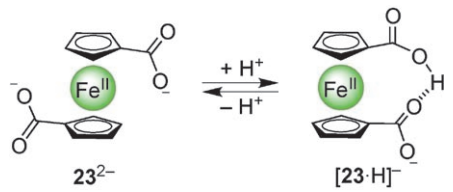

Scheme 8. Proton-switched intramolecular rotation in a ferrocene derivative.[93] The amplitude of relative rotary motion of the two cyclopentadienyl ligands is about 112°.

In contrast to these simpler metallocene or bis(porphyrinate) examples, metallacarboranes tend to have rather high barriers to rotation around the metal–ligand axis. Dicarbollide ligand $\mathbf{24}^{2-}$ features two adjacent carbon atoms on its bonding face which imparts a dipole moment perpendicular to the metal–ligand axis (Figure 14a). Transoid complexes are normally preferred to minimize electrostatic repulsion.[94] Two exceptions, however, are the Ni^{IV} or Pd^{IV} complexes which are cisoid.[95] Complex $[Ni(\mathbf{24})_2]$ can therefore operate as a reversible rotary switch on manipulation of the oxidation state or by photoexcitation (Figure 14b).[96]

2.1.4. Stimuli-Induced Conformational Control around Several Covalent Bonds

With an external stimulus, it is possible to control the conformation around not just one bond, but several all at once. Conformational control in biopolymers is of great importance in structural biology, and a vast array of methods for artificially triggering, altering, and reversing folding in polypeptides and polysaccharides now exists.[97] In nature, as in artificial systems, host–guest binding is often used to trigger complex conformational changes in one or both of the interacting species. In some cases this involves no more than minor bond deformations or the restriction of a few rotational degrees of freedom. In others, molecular recognition results in significant changes to a single degree of freedom (see Section 2.1.3), yet binding of one chemical species to another can also often result in significant changes to the conforma-

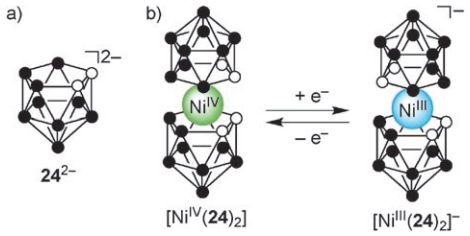

Figure 14. a) Dicarbollide ligand $\mathbf{24}^{2-}$. b) Metallacarborane $[Ni(\mathbf{24})_2]$ as an electrochemically controlled rotary switch.[96] The cisoid–transoid exchange involves a rotation of 144°. Both formal reduction and photochemical excitation of $[Ni^{IV}(\mathbf{24})_2]$ populate the lowest unoccupied molecular orbital (LUMO) and therefore elicit similar dynamic responses. Black spheres represent boron atoms, white spheres carbon atoms.

tion and internal motion around several bonds. Such "induced fit" mechanisms are the basis of many allosteric systems, whereby recognition of one species affects the binding properties or enzymatic activity at a remote site in the same molecule. Allosterism, cooperativity, and feedback are central to many functional biological systems[98] and synthetic approaches towards achieving similar effects have been extensively reviewed elsewhere.[84,99] Here we are interested primarily in the dynamic processes themselves and, therefore, in many cases where the conformational changes are rather small or poorly defined, such systems do not fall under our definition of molecular machines. However, certain examples do exhibit impressive control over the molecular shape or conformation and merit discussion here in their own right, together with other examples of stimuli-induced conformational changes around several bonds.

Some of the first and most elegant examples of synthetic allosteric receptors were introduced by Rebek et al. (Scheme 9).[99a,100] In **25**, the binding of a metal ion such as tungsten to the bipyridyl ligand forces coplanarity of this unit, thus distorting the crown ether conformation and diminishing its ability to bind potassium ions—a negative heterotropic allosteric effect. The same research group later developed this concept to create positive, homotropic allosteric receptor **26**, in which binding one molecule of $Hg(CN)_2$ preorganizes the remaining binding site for a second binding event.[101] These strategies have since either directly spawned or indirectly inspired an extraordinarily wide range of increasingly sophisticated synthetic allosteric receptors.[84,99]

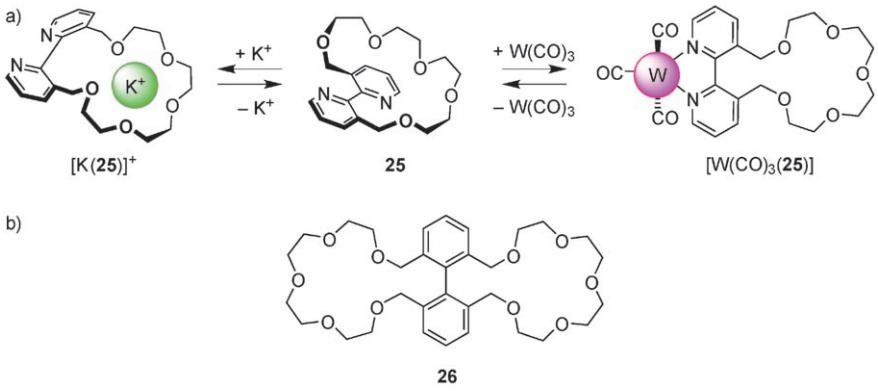

Scheme 9. a) Negative heterotropic allosteric receptor **25** binds alkali metal ions, with selectivity for K^+.[100] Chelation of tungsten to the bipyridyl moiety forces this unit to adopt a rigid conformation in which the 3 and 3′ substituents are brought close together. The resulting conformation of the crown ether does not favor binding through all the oxygen atoms and so affinity for K^+ ions is reduced. In fact [$W(CO)_3$(**25**)] shows a preference for binding the smaller Na^+ ion. b) Positive homotropic allosteric receptor **26**.[101]

Binding to molecular tweezer and clip receptors (Figure 15) can result in significant conformational changes in the host, as favorable interactions with the guest are maximized. In **27**, for example, the distance between the sidewalls decreases from 14.5 to 6.5 Å on binding to aromatic guests,[102] while diphenylglycouril-based clips such as **28** do

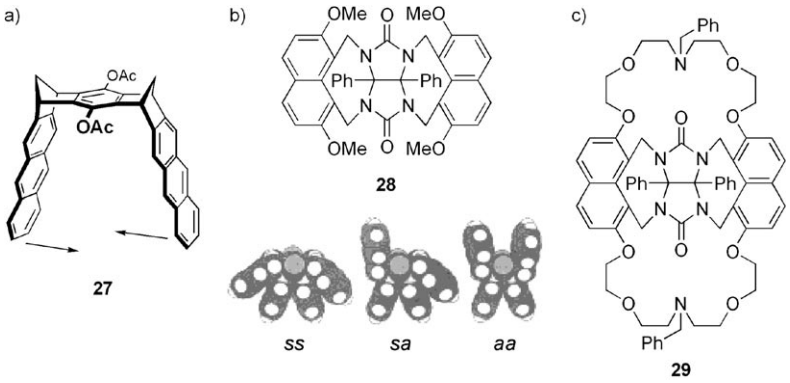

Figure 15. Binding-induced conformational changes in molecular clips. a) Dimethylene-bridged aromatic clip **27** in which binding to 1,2,4,5-tetracyanobenzene results in a large-amplitude induced-fit conformational change (motion indicated by arrows).[102] b) The three accessible conformations of the diphenylglycouril-based clips illustrated for simple derivative **28** (methoxy substituents are not shown on the space-filling models).[103] The *syn*,*anti* (*sa*) form dominates in solution, but only the *anti*,*anti* form is able to bind aromatic guests—in an induced-fit mechanism. c) Glycouril-based clip **29** in which an additional binding site (a crown ether) can control the conformation of the clip molecule, preorganizing the π-electron-rich binding site and resulting in a positive, heterotropic allosteric effect.[104] The space-filling representations are reprinted with permission from Ref. [103a].

not principally adopt the *anti*,*anti* (*aa*) binding conformation, only doing so in the presence of a suitable guest.[103] Similar structures can incorporate two conformationally coupled binding sites and exhibit allosteric effects. Glycouril-based clip **29** bears two crown ether substituents and binds potassium ions to form a complex with 1:2 stoichiometry. The binding event stabilizes the *aa* conformation, preorganizing the electron-rich naphthalene units in a pseudoparallel arrangement, thus increasing the binding affinity for simple electron-poor aromatic compounds such as 1,3-dinitrobenzene.[104] In atropoisomeric host molecules, an induced-fit binding process at elevated temperatures can be used to dynamically select the single optimal binding conformation for a particular guest, which can then be "saved" by cooling the system to ambient temperature and removal of the templating guest.[105]

The addition of an external ligand or guest can also be used to disrupt a preexisting intramolecular interaction and cause a change in conformation. This is the case for 4,4′-bipyridyl-capped zinc porphyrin **30** in which the pyridyl and porphyrin planes are switched from perpendicular to mutually parallel on addition of pyridine (Scheme 10).[106]

It is well known that the relative stabilities of the two different chair forms of six-membered alicyclic rings can be manipulated by covalent substitutions.[107,108] However, in trisaccharide **31** this conformational change can be achieved by adding and removing metal ions (Scheme 11).[109] In the absence of metal ions, the $^4C_1$ conformation is preferred for

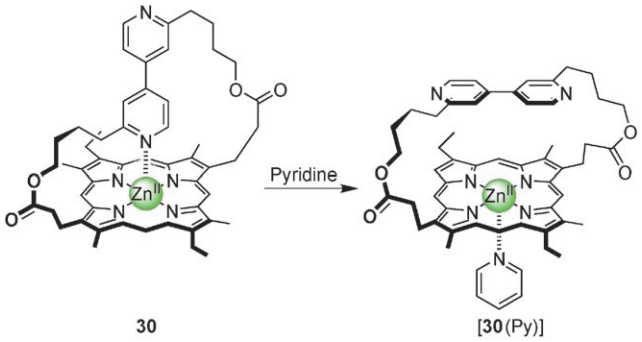

Scheme 10. Conformational switching in capped porphyrin **30**.[106]

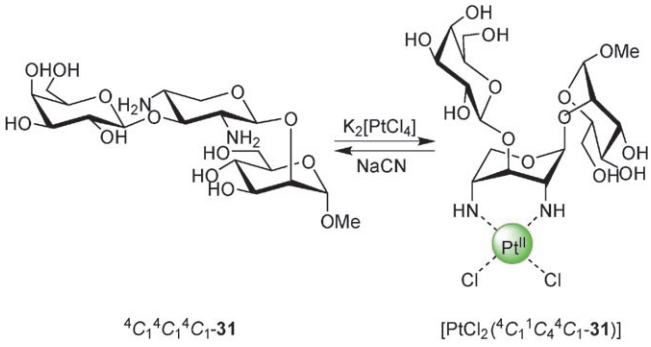

Scheme 11. Chelation-induced conformational control in a trisaccharide.[109b]

the central "hinge" pyranose unit, in which all the substituents are equatorial and both ends of the molecule are far apart. On addition of Pt^{II} ions, however, a ring flip to the $^1C_4$ form is observed so that the amine units can chelate to the metal ion and results in a major change in the shape of the oligosaccharide. Removal of the metal ions with NaCN returns the trisaccharide to its original extended conformation. Such stimuli-induced conformational switching has been achieved in a variety of cyclic systems through binding of metal ions[110] and variation of the pH value.[111] In addition to having significance for the control and modeling of biologically relevant oligosaccharides,[112] such systems have served as inspiration for the development of synthetic conformational switches (see Section 8.2.1).

Well-defined large amplitude (sometimes very large amplitude; see Section 8.2.1) conformational changes can be induced in cavitands derived from resorcin[4]arenes (for example, **32**, Scheme 12).[113] These molecules can exist in either an open "kite" conformation or a narrower "vase" form. As a result of solvation effects, the kite form is generally favored at low temperatures and the vase form at high temperatures.[114] Recently, it has been demonstrated that reversible switching between the two can also be achieved at room temperature through protonation of the quinoxaline nitrogen atoms,[115] or coordination of metal ions to these same atoms,[116] while the switching can also be highly dependent on the solvent.[115b,c] In a related series of cavitands bearing amide substituents around the rim, the kite form is stabilized by dimerization (so-called "velcrands" forming "velcraplexes"), which is driven by intermolecular hydrogen-

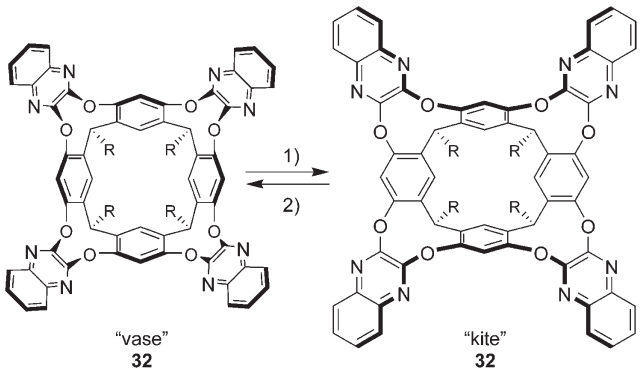

Scheme 12. Conformational bistability in resorcin[4]arene cavitands **32**. Reversible switching between the two forms can be achieved with a number of stimuli: a) by changing the temperature; for example, for R = Me in $CDCl_3/CS_2$: 1) $T < 211$ K; 2) $T > 318$ K;[114] b) by changing the pH value; for example, for R = 3,5-di(*tert*-butyl)phenylmethyl in $CDCl_3$ at $T = 298$ K: 1) CF_3COOH; 2) K_2CO_3;[115] c) by adding metal ions; for example, for R = *n*-Hex in $CDCl_3$ at 295 K: 1) ZnI_2 in [D_4]methanol; 2) excess [D_4]methanol.[116]

bonding, van der Waals, and solvophobic forces. Increasing the temperature or solvent polarity, as well as the introduction of suitable guest species, can induce switching to the monomeric vase forms.[117] Conversely, the use of amide substituents that are able to stabilize the vase form through intramolecular hydrogen bonding results in kinetically stable inclusion complexes in the presence of a suitable guest.[118] Incorporation of metal-ligating carboxymethylphosphonate groups into these structures allows switching of the preferred conformation from vase to kite, along with concomitant release of any encapsulated guest, on addition of lanthanum ions.[119] The reverse process occurs on addition of a competing ligand for the metal ion. The calixarene family, in general, clearly share this potential for interesting conformational dynamics,[120] and in certain cases significant degrees of control over these can be achieved, thus resulting in a number of induced-fit and allosteric receptor systems.[121]

Rather than adding an external species to induce a conformational change on binding, intramolecular interactions between two parts of the same molecule can be controlled remotely to bring about changes in the geometry. Macrocyclic compound $\mathbf{33}^{4+}$ preferentially adopts the self-complexed conformation shown in Scheme 13, which is stabilized both by π–π charge-transfer interactions and by hydrogen bonds.[122] Electrochemical reduction of the cyclophane, however, "switches off" these interactions and the molecule adopts a (poorly defined) conformation in which the dioxynaphthalene unit is no longer encapsulated by the macrocycle.[123]

The formation of excimers or exciplexes between two chromophores in the same molecule is another way by which intramolecular interactions may be remotely controlled so as to effect a conformational change. Most examples, however, involve flexible, linear ground states with poorly defined geometries.[124] In certain donor–bridge–acceptor systems, a conformational change does not occur in the initial photochemically excited state, rather, electron transfer occurs to give an "extended charge transfer" species. Depending on the

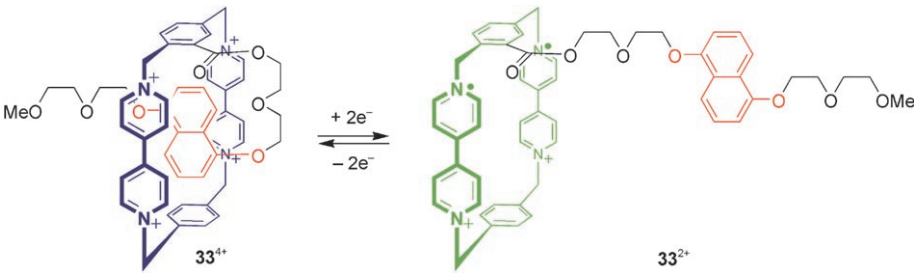

Scheme 13. Electrochemically induced conformational motion based on remote control of intramolecular interactions.[122]

rigidity of the structure, electrostatic attraction can then drive a conformational change to a "compact charge transfer" state. Such systems are often referred to as "molecular harpoons".[125]

In recent years, a number of oligomeric synthetic systems have been investigated in solution for their ability to adopt well-defined conformations with interesting and tunable secondary and tertiary structures, particularly those of a helical nature.[126] Oligomeric phenylacetylenes, for example, form helical structures in polar solvents as a result of solvophobic interactions and thus exhibit solvent- and temperature-sensitive secondary structures.[127,128] Aromatic oligoamide foldamers, on the other hand, adopt helical conformations in nonpolar solutions, and in the solid state, given suitably arranged hydrogen-bonding substituents.[126h-j] For heptamer **34**, helix formation is driven by intramolecular hydrogen bonding between the amide groups and pyridine units (Figure 16a).[129] Under certain conditions, double helices (in which two strands of the same oligomeric monomer are intertwined) are formed. This structure is mainly stabilized through intermolecular π–π stacking interactions, with hydrogen bonding determining the helical conformation of each strand. The double-helix structure is asymmetric, with each end of a strand in different environments. Interconversion of two equivalent forms occurs by a rotational corkscrew motion of one strand relative to the other. Significant heating is required to cause the much larger conformational changes required to bring the system into the single-helix regime (Figure 16b).[129a,c]

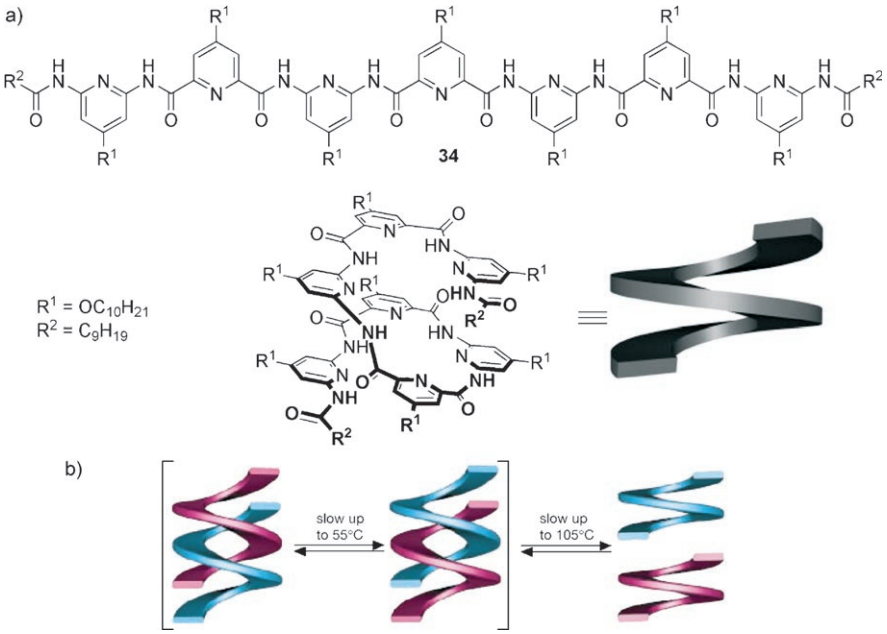

Figure 16. a) Chemical structure and folding of heptameric aromatic polyamide **34** (see Scheme 14 for representation of the hydrogen-bonding arrangement responsible for the folding).[129] b) In concentrated solutions, **34** dimerizes to form double helices. The double-helix structure is dissymmetrical and interconversion between the two equivalent forms occurs through a relative corkscrew motion of the two monomers. Exchange with the monomeric species is slow, as dissociation of the dimer involves unwinding of the helix structure. The ribbon representations are reprinted with permission from Ref. [129a].

In closely related heptamer, **35**, the single-helix secondary structure is disrupted upon protonation of the four diaminopyridine units, thus giving an extended linear conformation (**35**·$(H^+)_4$, Scheme 14).[130] Further protonation of the three remaining dicarboxypyridine moieties yields a second helical arrangement (**35**·$(H^+)_7$), which on deprotonation can be returned through the linear tetraprotonated form back to the neutral helix. A pentadecamer analogue has recently been shown to undergo a similar reversible uncoiling/coiling transformation, which results in a remarkable change in the overall length from 12.5 to 57 Å.[131] Using the same principles of altering hydrogen-bonding arrangements, conformational switching can be achieved in a different aromatic oligoamide system in which the protonation state of a repeating phenol functionality is controlled.[132]

Oligoheterocyclic strands consisting of alternating α,α′-connected pyridine and pyrimidine subunits adopt coiled structures because of the preferred transoid conformation at each heterocycle linkage.[133] However, the binding of a metal cation stabilizes the cisoid arrangement of the terpyridine-like coordination sites. In the presence of Pb^{II} ions, for example, helix **36** is converted into an extended linear arrangement (a "[5]-rack" complex, Scheme 15). Again this process results in an enormous change in the molecular length, from 7.5 to 38 Å, and can be carried out reversibly and repeatedly by employing cryptand **37** to sequester and release Pb^{II} ions depending on the pH value of the environment.[134] By contrast, α,α′-linked pyridine units naturally form linear arrangements. Although oligomers of this type are challenging to prepare, hydrazones can be used as isosteric replacements for alternate pyridine units, thus allowing preparation of linear pyridine–hydrazone sequences. These systems undergo the reverse process to that

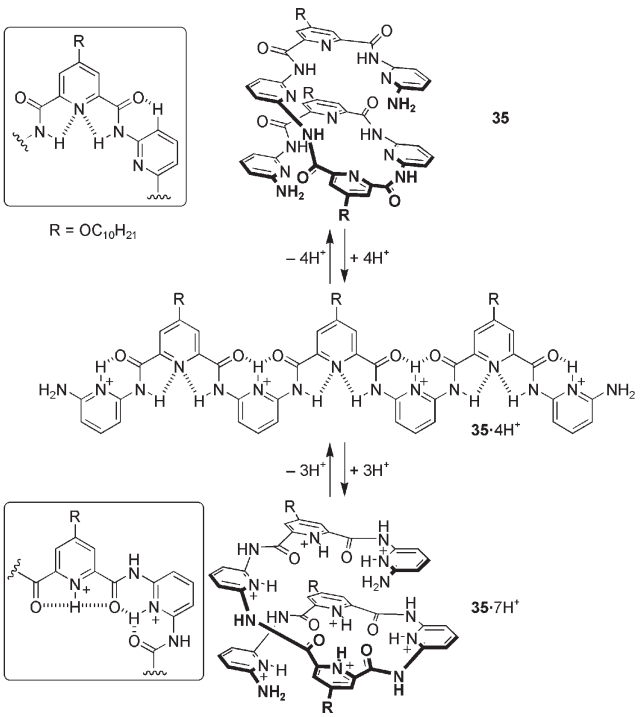

Scheme 14. pH-controlled helix formation for aromatic polyamide heptamer **35**. The insets show the hydrogen-bonding arrangements responsible for the helical structures.[130]

illustrated for **36**, namely, they form linear chains in solution which can be reversibly coiled around divalent metal ions.[135]

Oligoheterocyclic systems such as **36** can also form double-helix structures. Whereas single/double helix interconversion for the aromatic oligoamide systems in Figure 16 is controlled by the solvent, concentration, and temperature, pyrimidine–pyridine oligomers can be made to form double helices by complexation to metal ions. Addition of Ag^{I} ions to helical compound **38**, for example, results in the formation of double-helical dimers of formula $[(Ag^{I})_2(\mathbf{38})_2]^{2+}$, with the two metal ions bound at opposite ends of the chain and extensive intermolecular π–π stacking between the intertwined strands (Figure 17).[136] The single/double helix interconversion process can be achieved reversibly in a manner analogous to that in Scheme 15.

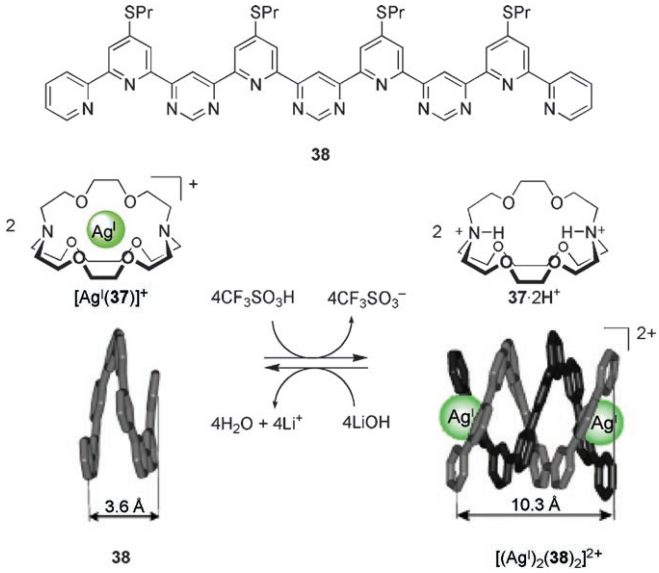

Figure 17. pH-switched contraction and extension by metal ion triggered single/double helix interconversion.[136] On models of **38** and $[(Ag^{I})_2(\mathbf{38})_2]^{2+}$, SPr substituents have been omitted for clarity. The model structures are reprinted with permission from Ref. [136].

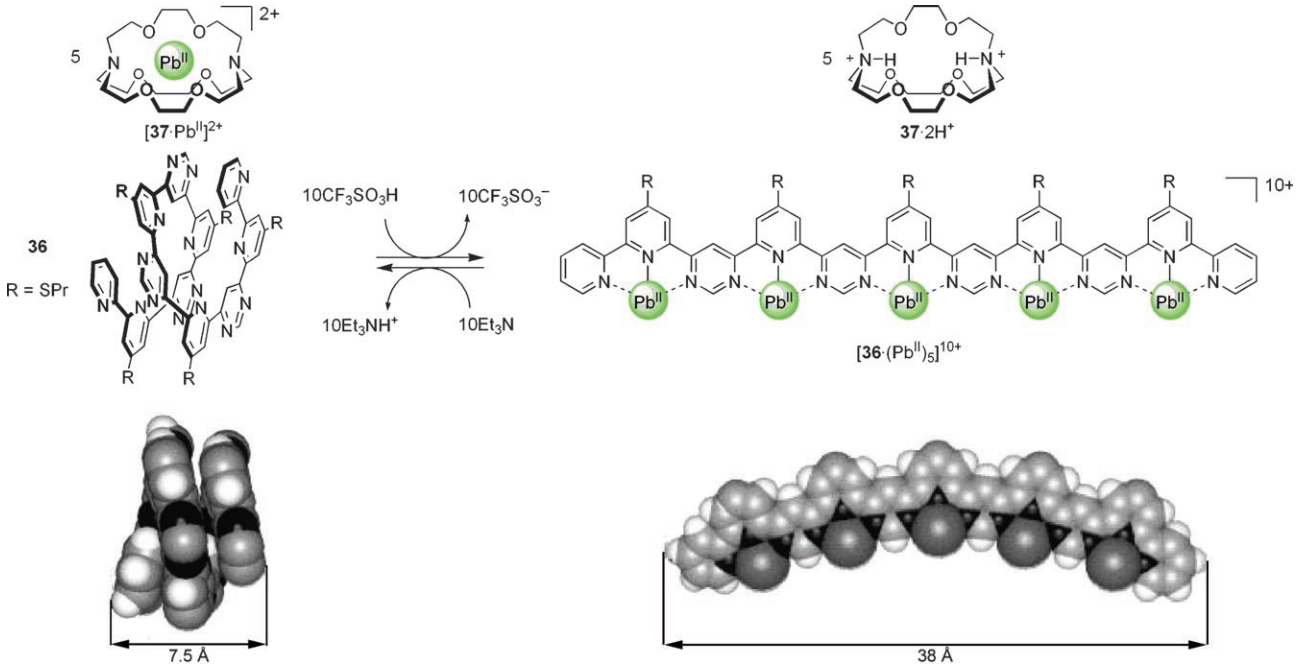

Scheme 15. pH-switched helix formation using a metal-ion template.[134] Counterions ($CF_3SO_3^-$) and solvent (CH_3CN), which complete the Pb^{II} coordination sphere in the [5]-rack complex $[(Pb^{II})_5(\mathbf{36})]^{10+}$, are omitted for clarity, as have the SPr substituents in the space-filling models. The space-filling representations are reprinted with permission from Ref. [134].

A similar mechanism applies to **39**, in which the two anthracene groups are held in a parallel arrangement, thereby creating a molecular tweezerlike cavity in which electron-poor guests such as 2,4,7-trinitro-9-fluorenone (TNF) can be bound (Scheme 16a).[137] Addition of cuprous ions, however, results in a cisoid–cisoid arrangement of the triheterocyclic unit so as to provide bipyridyl-like ligand environments for the metal ions. This separates the tweezer arms and releases the bound guest. Conversely, in **40**, the oligoheterocyclic portion is designed so that the electron-rich binding cavity is only set up on ion binding (Zn^{II} is used in this case, Scheme 16b).

Salen/salophen ligand **41** is not intrinsically helical, but it forms helical structures on coordination to tetradentate metal ions such as Cu^{II} or Ni^{II}.[138] Electrochemical reduction of the Cu^{II}-templated helix in a coordinating environment causes a reversible disruption of the helical secondary structure as the Cu^{I} center prefers to adopt a pentacoordinate geometry in the absence of any tetrahedral ligand (Scheme 17).

Finally, significant stimuli-induced conformational changes have also been achieved in a number of truly polymeric systems. More often than not, these are accompanied by detectable macroscopic changes in the material and will be discussed further in Section 8.3.3.

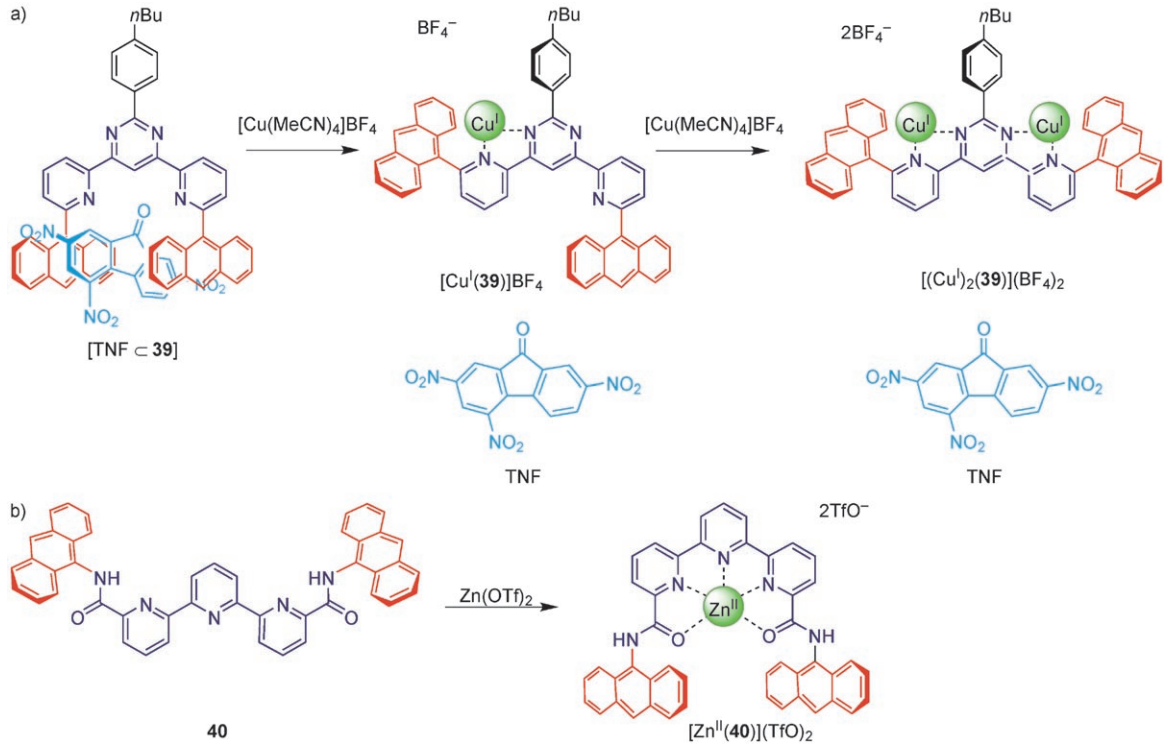

Scheme 16. Cation-induced substrate release and binding as a result of large-amplitude conformational changes.[137] a) On binding cuprous ions, U-shaped tweezerlike receptor **39** is forced to adopt a cisoid conformation at the pyridyl–pyrimidine linkages, thus separating the electron-rich tweezer "arms" and releasing the electron-poor guest. Dicuprous W-shaped derivative $[(Cu^{I})_2(\mathbf{39})]^{2+}$ is only formed on addition of large excesses of $[Cu(MeCN)_4]^{+}$ (>8 equiv). b) On binding zinc ions, W-shaped terpyridine **40** adopts a U shape, thus aligning the electron-rich anthracene moieties so that electron-poor guests can be intercalated in the cavity.

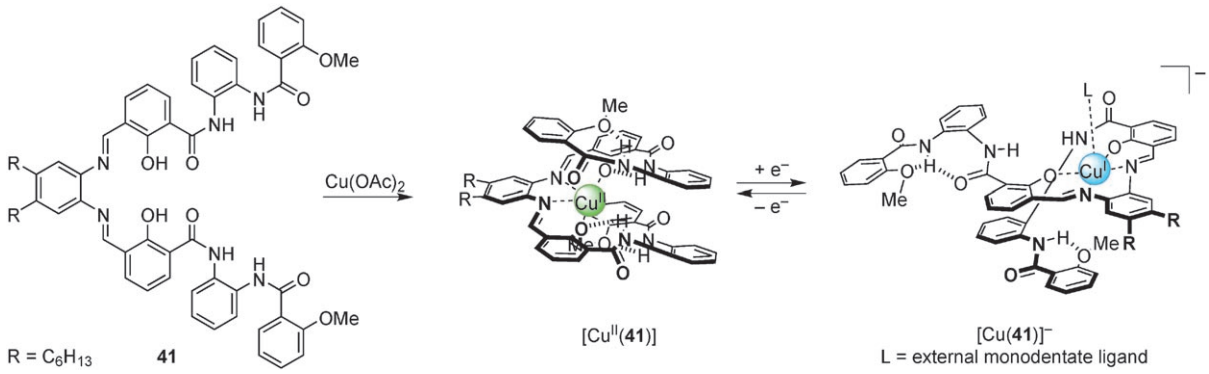

Scheme 17. Formation of a helical complex ($[Cu^{II}(\mathbf{41})]$) from a nonhelical ligand and electrochemically induced reversible unfolding of the helix.[138]

2.1.5. Torsional Control Arising from Molecular Orbital Symmetry

The stereochemical outcome of many chemical reactions arises from the relative movements of groups, which are determined by orbital symmetry considerations, most famously those governed by the Woodward–Hoffmann rules.[139] A full discussion of this area is beyond the scope of the current Review, but it is worth noting that such mechanisms for controlling submolecular motions in molecular-machine systems have been particularly underexploited to date. However, a purely electronically driven correlated rotational process has been observed in carbonium ion tricobalt complexes, driven by maintaining favorable overlaps between a molecular orbital centered on the three metal centers and an orbital belonging to the organic fragment as it moves between three degenerate conformational positions.[140] Recently, an interesting molecular dynamics study on 5-methyltropolone (**42**, Scheme 18), showed that proton transfer at the α-hydroxyketone should directly result in rotation of the methyl group at the 5-position.[141] This is explained by a coupling of the π system to the methyl group through hyperconjugation (involving two of the three methyl hydrogen 1s orbitals). Overlap of the HOMO of the methyl group with the LUMO of the ring is therefore strongest when the two out-of-plane hydrogen atoms straddle a single bond in the ring. As proton transfer results in tautomerization and bond alternation round the ring, this flips the preferred orientation of the methyl group and a 60° rotation occurs.

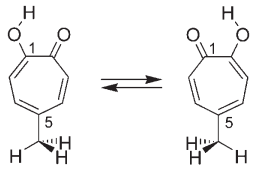

42

Scheme 18. Coupling of proton transfer to rotation of a methyl group in 5-methyltropolone (**42**).[141]

As a prototypical example of this type of system, the photoisomerization of stilbenes has been extensively studied for well over 50 years.[144] As organic photochemistry developed, other important photochromic systems were discovered (Scheme 19):[145] the photoisomerization of azobenzenes,[146] the reversible electrocyclization of diarylethenes,[147] the photochromic reactions of fulgides,[148] the interconversion of spiropyrans with merocyanine (and the associated spirooxazine/merocyanine system),[149] as well as chiroptical switching in overcrowded alkenes (for example, **45**, Scheme 21).[150] All these processes are accompanied by marked changes in both physical and chemical properties, such as color, charge, and stereochemistry, and a wide range of applications based on their switching properties have both been proposed and, in some cases, realized, from liquid crystal display technology to

2.2. Controlling Configurational Changes

Changes in configuration,[142] in particular *cis–trans* isomerization of double bonds, have been widely studied from theoretical, chemical, and biological perspectives.[107,143] Although the small amplitude motion involved is not generally sufficient for direct exploitation as a machine, it can provide an extremely useful photoswitchable control mechanism for more complex systems (see below) and, in some cases, can even be harnessed to perform a significant mechanical task. Such systems represent some of the first examples of molecular-level motion which can be controlled by the application of an external stimulus.

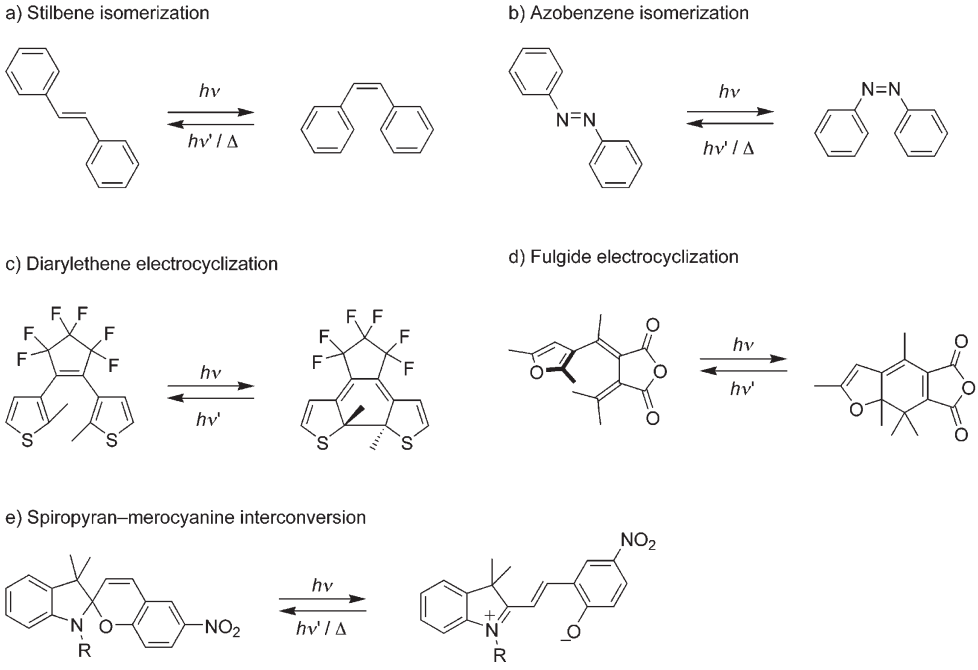

Scheme 19. Archetypical examples of photochromic systems that give a mechanical response. a), b) The *cis–trans* isomerization of stilbenes[144] and azobenzenes,[146] respectively. c) The reversible photochemical electrocyclization of a diarylethene.[147] This can be a competing process in the *cis–trans* isomerization of stilbenes (a) and is observed for a number of heterocyclic and non-heterocyclic aromatic compounds joined through a C=C bond. The methyl groups shown prevent irreversible loss of H_2 to give a tricyclic aromatic compound, while substitution of the double bond prevents *cis*→*trans* isomerization. d) The reversible photochemical electrocyclization of a fulgide.[148] Again, a number of substitution patterns are tolerated (*cis–trans* isomerization around either double bond may occur, but is undesirable). e) The photochemical interconversion of spiropyrans with their ring-open, zwitterionic merocyanine forms.[149] Analogues in which the benzylic carbon atom of the double bond is replaced with a nitrogen atom (spirooxazines) undergo a similar transition.

variable-tint spectacles and optical recording media.[151] Most of these applications simply rely on the intrinsic electronic and spectroscopic changes on interconversion between the two species. There are some cases, however, in which small configurational changes can be harnessed in a more mechanical fashion and the resulting devices can be considered to be like molecular machines.

Various configurational changes (in particular, photoisomerization of azobenzene) have been employed to alter peptide structures, thereby creating semisynthetic biomaterials whose activity can be controlled photonically.[97n–u] These systems, which amplify the small configurational change of the synthetic unit to cause a significant change in the peptide secondary structure, mimic to some extent the role of proline and peptidylprolyl *cis–trans* isomerases[152] in controlling protein activity in cells. Recently, it has been shown that the effective helix length can be controlled by photoisomerization in synthetic oligomers similar to those discussed in Section 2.1.4 but composed of alternating 2,6-dicarboxamide and *m*-(phenylazo)azobenzene units.[153] Incorporation of azobenzene or stilbene chromophores into dendritic molecules can result in interesting photochemical effects, as well as allowing amplification of the configurational change into large amplitude changes in molecular conformation or other properties.[154] These strategies are somewhat similar to the use of azobenzene units as phototriggers in polymeric synthetic materials (see Section 8.3.3).

In small-molecule systems, converting a configurational change around a double bond into significant mechanical motion requires considerable ingenuity. Combining the reversible photoisomerization of an azobenzene with the "molecular-bearing" attributes of metallocene complexes (see Section 2.1.3), Aida and co-workers have created a pair of "molecular scissors" **43** (Scheme 20a).[155] The optically triggered change in the double-bond configuration brings about an angular change of position about the ferrocene "pivot" (green) and results in an opening and closing of the phenyl "blades" (red). Reversible switching is possible over a number of cycles, with the bite angle between the blades

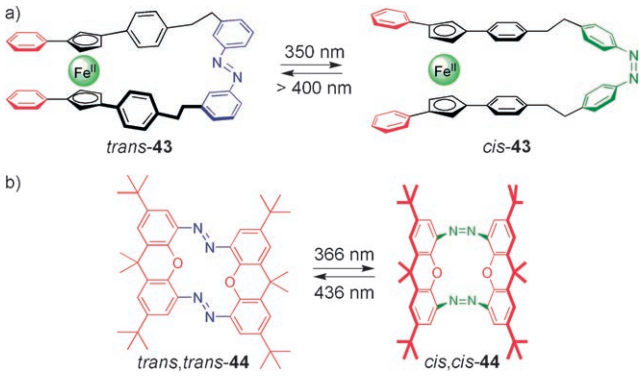

Scheme 20. a) "Molecular scissors" **43**, in which photoisomerization of an azobenzene is converted into a 49° rotary motion around a metallocene bearing.[155] b) "Molecular hinge" **44**, in which concerted configurational change of the two azobenzene units results in a change of approximately 90° in the angle between the planar xanthene units.[157]

altered from approximately 9° when closed to more than 58° when open.

The concerted action of two azobenzene configurational switches[156] has been used to alter the angle between two planar moieties in a so-called "molecular hinge" **44** (Scheme 20b).[157] In *trans,trans*-**44**, the two xanthene units are virtually coplanar. Photoisomerization to the *cis,cis* isomer occurs upon irradiation at 366 nm, thus resulting in an angle of almost 90° between the two aromatic ring systems. The high energy of the strained *trans,cis* form renders *cis,cis*-**44** remarkably thermally stable, but reisomerization can be achieved by irradiation at 436 nm.

While investigating the use of overcrowded alkenes as chiroptical molecular switches,[150] Feringa et al. created a molecular brake, **45**, in which the speed of rotation around an arene–arene single bond can be varied by changing the alkene configuration (Scheme 21).[158] Counterintuitively from the

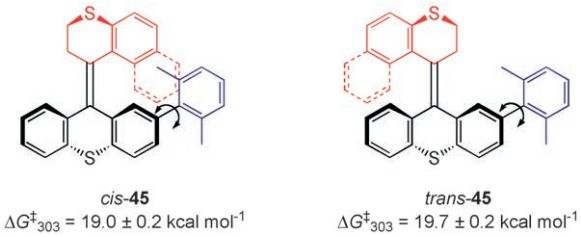

Scheme 21. Counterintuitive variation of kinetic barrier to rotation around an aryl–aryl bond by isomerization of the double bond in an overcrowded alkene.[158] Values for the free energy of activation ($\Delta G^{\ddagger}$) for the rotary motion in each configuration are shown.

two-dimensional representations in Scheme 21, the rate of rotation around the indicated bond is actually faster in *cis*-**45** than in *trans*-**45** (demonstrated by ^{1}H NMR spectroscopy)—the naphthalene unit is flexible enough to bend away from the phenyl rotator unit, while the methylene protons on the other side of the double bond are rigidly held in equatorial and axial positions and present a significant steric barrier to the rotator. Unfortunately, the photochemical interconversion between the *cis* and *trans* forms is not efficient for this molecule, although the system stands as proof (see also rotaxanes **87**–**89**, Scheme 51) that a change in configuration can alter not just the optical properties or bulk orientations, but can also control aspects of large amplitude submolecular motions.

The chiral helicity in molecules such as **45** causes the photochemically induced *trans–cis* isomerization to occur unidirectionally according to the handedness of the helix. Accordingly, this system already possesses some of the features necessary for a unidirectional rotor and, indeed, the incorporation of one further chiral element[159] allowed the realization of the first synthetic molecular rotor capable of achieving a full and repetitive 360° unidirectional rotation (Figure 18a).[160,161] Irradiation ($\lambda > 280$ nm) of this extraordinary molecule, (3*R*,3′*R*)-(*P*,*P*)-*trans*-**46**, causes chiral helicity-directed clockwise rotation of the upper half relative to the lower portion (as drawn), at the same time switching the configuration of the double bond and inverting the helicity to give (3*R*,3′*R*)-(*M*,*M*)-*cis*-**46**. However, this form is not stable

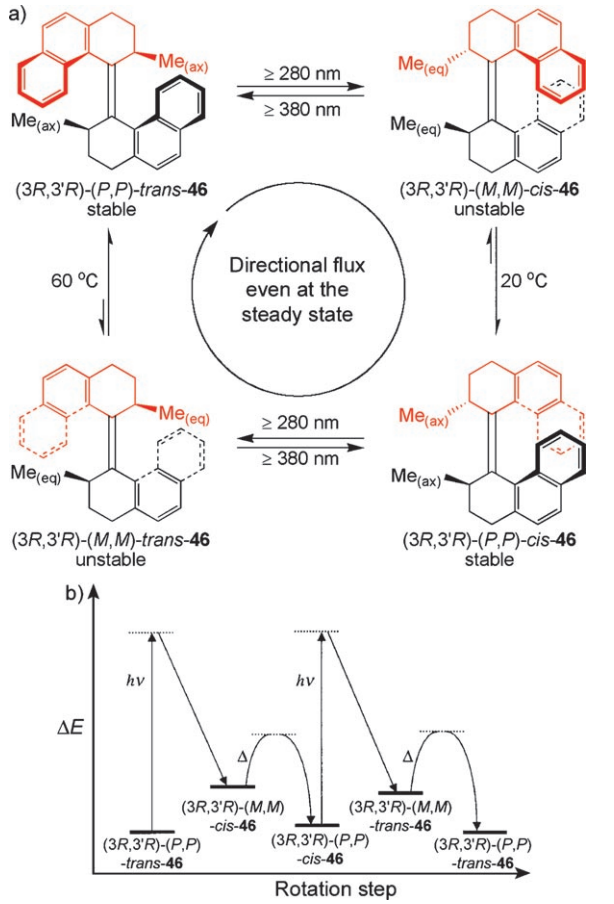

Figure 18. Operational sequence (a) and potential energy profile (b) of the first light-driven unidirectional 360° molecular rotary motor, (3*R*,3′*R*)-**46**.[160] Note, the labels "stable" and "unstable" in (a) refer to thermodynamic stability, and the reaction coordinate in (b) does not correspond directly to the angle of rotation around the central bond. Even at the steady state (> 280 nm and > 60 °C), net fluxes occur in each of the isomer interconversions that make up the reaction cycle. The energy profile is adapted with permission from Ref. [161b].

at temperatures above −55 °C as the methyl substituents on the cyclohexyl ring are placed in unfavorable equatorial positions. At ambient temperatures, therefore, the system relaxes through a second, thermally activated helix inversion to give (3*R*,3′*R*)-(*P*,*P*)-*cis*-**46**, with the substituents at either end of the double bond continuing to rotate in the same direction with respect to each other. Irradiation of (3*R*,3′*R*)-(*P*,*P*)-*cis*-**46** ($\lambda > 280$ nm) results in a second photoisomerization and helix inversion to give (3*R*,3′*R*)-(*M*,*M*)-*trans*-**46**. Again, the methyl substituents are placed in an energetically unfavorable position by the photoisomerization reaction and thermal relaxation (this time temperatures > 60 °C are required[162]) completes the 360° rotation of the olefin substituents, thereby regenerating the starting species (3*R*,3′*R*)-(*P*,*P*)-*trans*-**46**. As each different step in the cycle involves a change in helicity, the directionality of the process can be monitored through the change in the circular dichroism spectrum at each stage. The four states can be differently populated depending on the precise choice of wavelength and temperatures used, while irradiation at 280 nm at > 60 °C results in continuous 360° rotation.[160] Figure 18b shows the overall potential-energy changes during a full 360° rotation. In terms of mechanism, the process essentially involves switching between two asymmetric potential energy surfaces (one each for the *cis* and *trans* diastereomers) which are spatially separated (in terms of their position along the reaction coordinate for rotation around the central bond). Furthermore, this switching process is directional (see above) and so this system bears many of the hallmarks of a dichotomous, stepwise traveling-wave ratchet (see Section 1.4.2.1). The potential-energy minima and maxima on the *cis* and *trans* surfaces are of course actually slightly different, and so elements of a flashing ratchet are also present—such hybrids are perfectly acceptable under Brownian ratchet theory.[39f]

Note that if **46** is irradiated at wavelengths greater than 280 nm and at temperatures above 60 °C the system will reach a steady state at which point the bulk distribution of diastereomers no longer changes. Crucially, however, this steady state is not an adiabatic equilibrium. The steady state is maintained by a process (Figure 18) that features nonzero fluxes (corresponding to directional rotation of one component with respect to the other) between various pairs of diastereomers. In other words, as long as an external source of light and heat is supplied, the steady state in Figure 18 is effectively maintained by a cyclic process A→B→C→D→A (see Section 1.4.1), with the arrow indicating a net flux. Thus, even at the steady state, **46**, and other molecules of this type, behave as directional rotary motors.

As the photoisomerization process in such systems is extremely fast (< 300 ps),[163] the rate-limiting step in the operation of **46** is the slowest of the thermally activated isomerization reactions. The effect of molecular structure on this rate has been investigated in a series of derivatives. An ethyl substituent at the two stereogenic centers results in a moderate increase in the rates of thermal relaxation, probably because of greater steric hindrance when these groups occupy the unfavorable equatorial positions.[164] The isopropyl-substituted homologue showed a further increase in the rate for the thermal relaxation step between the *cis* diastereomers (fast even at −60 °C), but this trend was not followed for the equivalent step between the two *trans* diastereomers, which was very significantly retarded. This situation allowed the isolation of an intermediate *meso*-like isomer of the form (*P*,*M*)-*trans*, thus demonstrating that the thermal relaxation step in fact comprises two consecutive helix inversions,[164] inline with an earlier theoretical prediction.[162b] A second generation of motors (**47**–**49**, Scheme 22) was created in which "rotator" and "stator" sections of the molecule are differentiated (with a view to future applications; see Section 8.1) and in which only one stereogenic center is sufficient to direct the rotation.[165] For all the second generation motors shown in Scheme 22, the slowest thermal isomerization step has a lower kinetic barrier than in **46**; in general, smaller bridging groups at Y and, in particular, at X result in the lowest activation barriers. Not all the kinetic effects of the structural changes turned out to be intuitive, however. Motor **48** contains an even smaller upper portion, yet the free energy of activation for the thermal isomerization

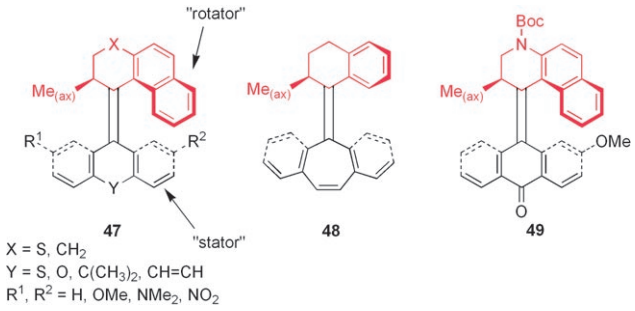

Scheme 22. General structure of second-generation light-driven unidirectional rotors **47**, **48**, and the fastest member of this series, **49**.[165] Boc = *tert*-butyloxycarbonyl.

process in this molecule is actually higher than its phenanthrene analogue (that is, **47**; X = CH_2, Y = CH=CH, $R^1 = R^2 =$ H).[165c] The decreased steric hindrance in **48** lowers the ground-state energy of the "unstable" isomer more than it lowers the transition-state energy for the thermal isomerization process. Conversely, a derivative bearing donor and acceptor substituents (**47**; X = S, Y = S, $R^1 = NMe_2$, $R^2 = NO_2$) exhibited thermal relaxation rates more comparable with less sterically encumbered examples.[165d] Furthermore, this molecule can operate using visible light, while protonation of the amine substituent led to slightly improved ratios for the photostationary state, which were reached in shorter irradiation times, but were then followed by slower thermal relaxation steps. It appears, therefore, that electronic effects also play an important role in the mechanism of these systems. This was further emphasized by derivative **49**, in which an amine in the upper half of the molecule is directly conjugated with a ketone in the lower half. The consequent increase in single-bond character of the central olefin results in greatly increased rates for the thermal isomerization steps.[165e]

Fast rotation rates have also been achieved with cyclopentane analogue **50** which can be accessed in higher synthetic yields than the six-membered ring compounds (Scheme 23).[166] Despite the greater conformational flexibility of the five-membered ring, a significant difference in the energies between the pseudoequatorial and pseudoaxial positions of the appended methyl groups still exists, and unidirectional rotation occurs. Both **49** and **50** suffer from lower photostationary state ratios,[167] while the thermal relaxation steps for **49** are accompanied by a small amount of thermal back-isomerization.[165e,166a] However, neither of these factors affects the integrity of the process, as in all cases the thermal relaxation steps are entirely unidirectional, thus ensuring the motion is ratcheted. Only the overall photon efficiency for rotation (a combination of quantum yield for the isomerization and the photostationary state ratio) is reduced.

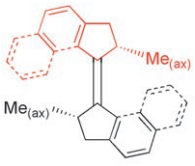

(2*S*,2'*S*)-(*M*,*M*)-*trans*-**50**

Scheme 23. Third-generation unidirectional rotor **50**.[166] In this case "ax" refers to the pseudoaxial orientation for substituents on the cyclopentyl ring.

Recently, Feringa and co-workers have returned to the theme of using isomerization around the central olefin to control the rate of rotation of an aryl group in motor molecule **51** (Scheme 24).[168] Although **51** displays more complex photochemistry than the previous motor molecules, it still exhibits unidirectional rotation around the olefinic bond. The

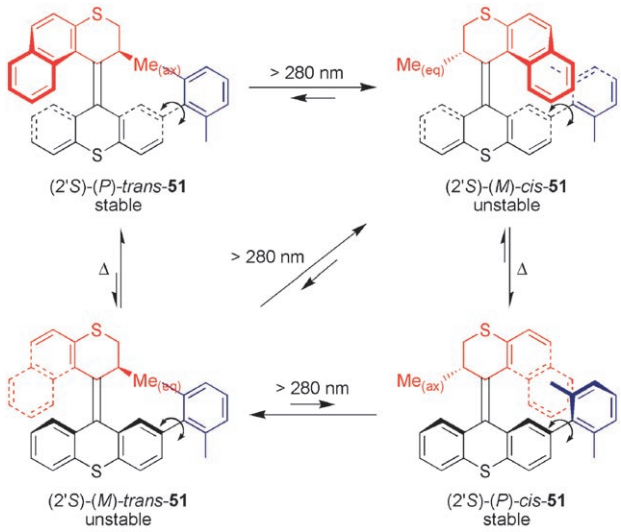

Scheme 24. Rotational scheme for molecular motor **51** in which each diastereoisomer has a different barrier to rotation around the aryl–aryl bond indicated.[168] The terms "stable" and "unstable" refer to the thermodynamic stabilities of each isomer.

rate of rotation around the aryl–aryl single bond was determined experimentally for each diastereoisomer and found to follow the order $cis_{stable} > cis_{unstable} > trans_{stable} > trans_{unstable}$. Similar to switch **45** (Scheme 21), therefore, the sp^3-hybridized side of the dihydronaphthothiopyran part exerts the greater steric hindrance on the aryl rotator, particularly when the methyl substituent is in the less-favored equatorial position. Of course, the unidirectionality of the conversions between the four isomers is immaterial to the switching of the rotation rates.

3. Controlling Motion in Supramolecular Systems

Using an external stimulus to modulate the binding affinity of a host for a guest is the simplest expression of controllable molecular recognition.[169] A wide variety of stimuli can be employed to bring about changes, not just in geometric configuration, but also in electronic arrangement and environmental influences to modulate noncovalent interactions. Switchable host–guest systems teach us much about the nature of noncovalent interactions and how to manipulate them, although the requirement for kinetic association of components in a molecular machine rules out simple host–guest complexation where binding does not bring about a change in the conformation of either species or where transport of the guest between sites within the host is slow with respect to exchange with the bulk. For example, myosin must move along a track to which it is kinetically associated through a series of sequential binding events to bring about

muscle contraction; no mechanical task occurs through simple "on"/"off" binding to the track by myosin molecules from the bulk.[170] In other words, simple host–guest/supramolecular systems cannot function as nanoscale mechanical machines unless restrictions on the motion of the unbound species apply or the binding event causes a mechanical (that is, conformational) change in one of the molecular components. A stimuli-induced molecular recognition event is neither a sufficient nor necessary condition for the construction of a molecular-level machine.

3.1. Switchable Host–Guest Systems

Whilst the requirement for kinetic association during the operation of the machine means that many switchable host–guest systems do not have the potential to act as mechanical machines, many still do. We have already seen that certain synthetic allosteric systems transmit binding at one site to a remote receptor through binding-induced conformational motions (see Sections 2.1.3 and 2.1.4). In other conformation-switching molecular machines, intermolecular binding events are both the stimulus and outcome of the molecular-level motion. An early example of a switchable host–guest system which demonstrates molecular-machine-like characteristics is (*E*)/(*Z*)-**52** (Scheme 25a) developed by Shinkai et al.[171] These photoresponsive "molecular tweezers" exhibit high selectivity for binding large cations such as Rb^+ when in the *cis* form and selectivity for small cations such as Na^+ in the *trans* form. Furthermore, the presence of Rb^+ ions in solution increases the proportion of (*Z*)-**52** at the photostationary state and decreases the rate of the thermal $Z \rightarrow E$ transformation. Subsequently, the same research group developed the "tail-biting" crown ether switchable receptor (*E*)/(*Z*)-**53**·H^+ (Scheme 25b).[172] In the (*Z*)-**53**·H^+ form, intramolecular binding of the ammonium ion to the crown ether prevents recognition of other cations in the medium, while thermal isomerization to give (*E*)-**53**·H^+ restores the properties of the crown ether necessary for binding alkali metal cations. It is also observed that the rate of $Z \rightarrow E$ isomerization is lowered (by 1.6–2.2 fold) for (*Z*)-**53**·H^+ relative to the deprotonated control compound (*Z*)-**53**. Crucially, the rate of this reaction increases as the concentration of K^+ ions in solution increases. Both these systems can therefore be viewed as primitive molecular machines in which a binding event at the crown ether unit(s) affects the isomerization processes of the azobenzene moiety with which it is kinetically associated.

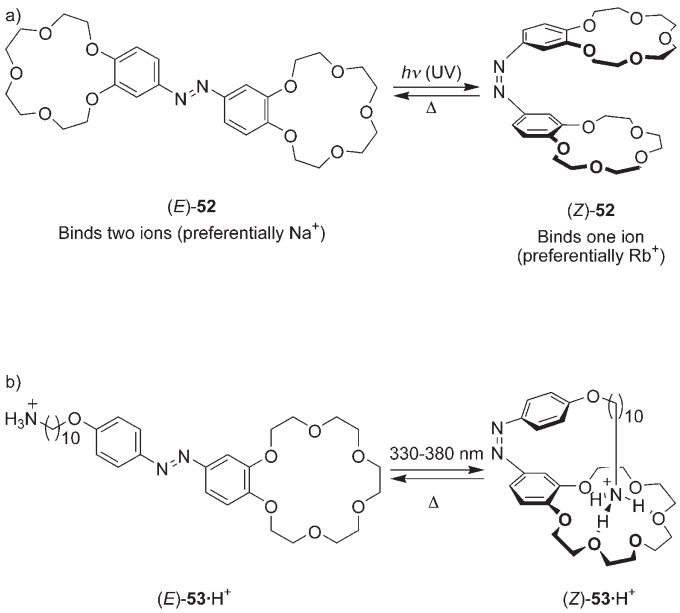

Scheme 25. Two of the earliest molecular machines. a) Photoresponsive molecular tweezers (*E*)/(*Z*)-**52**.[171] b) "Tail-biting" crown ether (*E*)/(*Z*)-**53**.[172]

3.2. Intramachine Ion Translocation

Metal–ligand binding interactions are often relatively kinetically inert and careful structural design has produced systems in which intramolecular motions are significantly favored over intermolecular exchange.[173] System $\mathbf{54}^{4+}$ (Scheme 26) consists of a coordinatively unsaturated Cu^{II} center covalently linked to a redox-active Ni^{II}–cyclam unit.[174] In this form, chloride anions bind strongly to the copper center, filling the vacant coordination site ($[\mathbf{54}(Cl)]^{3+}$). Electrochemical oxidation of the nickel center to Ni^{III} dramatically increases its affinity for anions so that the chloride translocates to this new, more energetically favorable site. The motion is completely reversible on reduction of the nickel ion. In principle, the switching of the anion position could be an intermolecular process involving either free anions in solution or more than one molecule of **54**. However, the anion translocation was demonstrated experimentally not to be concentration-dependent, in contrast to an analogous three-component system (Cu receptor + Ni receptor + Cl^-) which exhibited strongly concentration-dependent behavior. Thermodynamic comparisons of the two systems suggest that the dominant mechanism in **54** is an intramolecular translocation, brought about by folding of the ditopic receptor.[175]

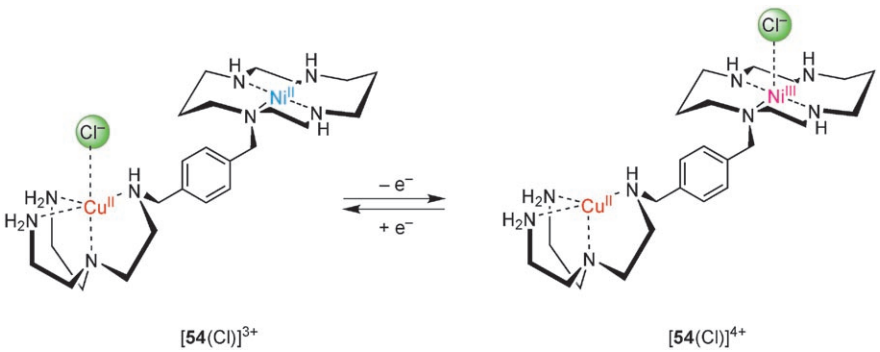

Scheme 26. Redox-driven intramolecular anion translocation.[174]

Calix[4]arene **55** reversibly translocates metal cations through protonation of the tertiary nitrogen atom (Scheme 27).[176] Dynamic ^{1}H NMR experiments indicate a high kinetic barrier to dissociation of the metal ion from the

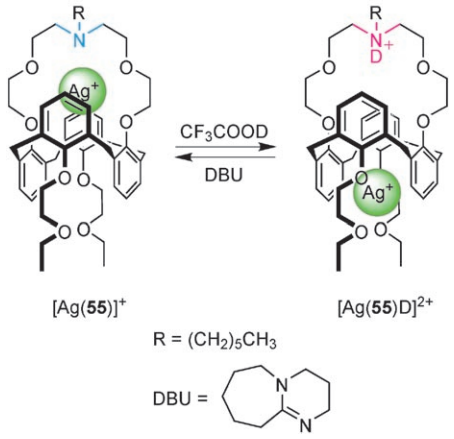

Scheme 27. Translocation of a silver cation between two sites in a calix[4]arene cavity: a "molecular syringe".[176]

neutral receptor, thus suggesting that upon protonation, translocation occurs intramolecularly through the cavity defined by the aromatic rings in a manner reminiscent of the action of a syringe. However, the protonated form exhibits much faster cation exchange with the bulk so the integrity of the stimuli-induced return stroke is probably less well maintained.[176]

The first redox-driven cation-translocation system was reported by Shanzer and co-workers in helical complex [Fe^{III}·**56**], which exhibits strong evidence for a fully intramolecular process (Scheme 28).[177] The system exploits the preference of Fe^{III} and Fe^{II} ions for hard and soft ligands, respectively. Reduction of [Fe^{III}(**56**)] with ascorbic acid

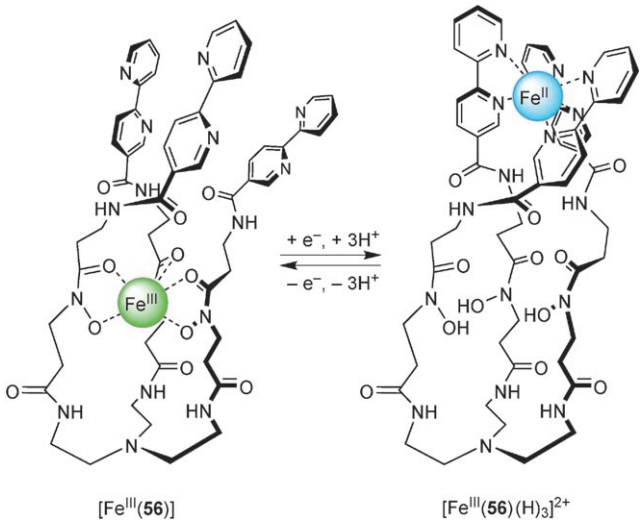

Scheme 28. Redox-switched intramolecular cation translocation in a triple-stranded helical complex.[177] Reductant: ascorbic acid; oxidant: $(NH_4)_2S_2O_8$.

generates [Fe^{II}(**56**)$(H)_3$]$^{2+}$ which has spectral properties characteristic of the [Fe^{II}(bipyridyl)$_3$] coordination sphere. Subsequent reoxidation ($(NH_4)_2S_2O_8$) returns the system to its original state. The equivalent intermolecular process between two monotopic ligands does not occur under the same conditions, while even the translocation of the cation in **56** is relatively kinetically slow, thus suggesting an intramolecular process.[178]

Pseudorotaxanes—supramolecular complexes in which a macrocyclic host encapsulates a linear, threadlike guest—are subject to the same issues regarding kinetic stability as other host–guest complexes.[179–181] While these complexes are model systems for kinetically locked analogues (rotaxanes,[182] see Section 4), their dynamic properties are similar to other supramolecular systems. Many interesting pseudorotaxane devices have been created[183] with functions including: reversible formation and dethreading by using a number of stimuli;[122,123d,184] switching between different preferred guests;[185] shuttling between two binding sites within the same guest;[186] and control of intracomplex electron-transfer reactions.[187] However, only in the case of kinetically stable pseudorotaxanes—systems where the components do not exchange with the bulk during the operation of the machine—are there sufficient restrictions on the motions of the unbound species for them to feature controlled mechanical behavior and they are otherwise best considered as supramolecular devices not mechanical machines.[188]

4. Controlling Motion in Mechanically Bonded Molecular Systems

4.1. Basic Features

Catenanes are chemical structures in which two or more macrocycles are interlocked, while in rotaxanes one or more macrocycles are mechanically prevented from dethreading from a linear unit by bulky "stoppers" (Figure 19).[189] Even though their components are not covalently connected, catenanes and rotaxanes are molecules (not supramolecular complexes) as covalent bonds must be broken to separate the constituent parts. In these structures,[190] the mechanical bond severely restricts the relative degrees of freedom of the

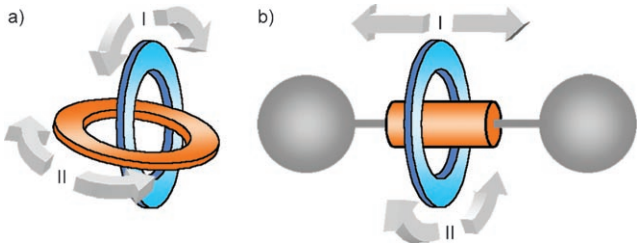

Figure 19. Schematic representations of: a) a [2]catenane and b) a [2]rotaxane.[192] The arrows show possible large-amplitude modes of movement for one component relative to another. In a [2]rotaxane (b), these are defined as I: translation and II: pirouetting. In a [2]catenane, (a), however, motion I can be considered as pirouetting of the blue ring around the orange one or, equally, translation of the orange ring around the blue one.

components in several directions, while often permitting motion of extraordinarily large amplitude in an allowed vector. This situation is in many ways analogous to the restriction of movement imposed on biological motors by a track[170] and is one reason interlocked structures continue to play a central role in the development of synthetic molecular machines.[191]

The large-amplitude submolecular motions particular to catenanes and rotaxanes can be divided into two classes (Figure 19): pirouetting of the macrocycle around the thread (rotaxanes) or the other ring (catenanes) and translation of the macrocycle along the thread (rotaxanes) or around the other ring (catenanes). By analogy to the stereochemical term "conformation", which refers to geometries that can formally be interconverted by rotating about covalent bonds, the relative positioning of the components in interlocked molecules (and supramolecular complexes) is often referred to as a "co-conformation".[142]

For a long time, synthetic approaches to mechanically interlocked structures relied on statistical or lengthy covalent-directed approaches.[193] The development of supramolecular chemistry, however, allowed chemists to apply noncovalent interactions to synthesis, thus resulting in many template methods ("clipping" and "threading")[194] to catenanes and rotaxanes being developed.[195] In such syntheses, noncovalent binding interactions between the components often "live-on" in the interlocked products. These can ultimately be manipulated to effect positional displacements of one component with respect to another. Much attention has been given to the submolecular motions within these structures at equilibrium. We shall briefly cover the inherent large amplitude motion in rotaxanes as it is instructive for the consideration of stimuli-induced control of motion in these structures (see Sections 4.3–4.6).

4.2. Shuttling in Rotaxanes: Inherent Dynamics

Shuttling is the movement of a macrocycle along the linear thread component of a rotaxane. This motion takes the form of a random walk powered by Brownian motion that is constrained to one dimension by the thread and to translational displacement boundaries by the bulky stoppers. By virtue of the template methods employed in interlocked molecule synthesis,[195] rotaxanes without sites of attractive interaction between the macrocycle and thread are relatively rare.[196] It is more common that the thread consists of one or more recognition elements, or "stations", for the macrocycle(s); shuttling therefore becomes the movement on, off, and between such stations, with rates dependent on the strength of the intercomponent interactions.

4.2.1. Observation of Shuttling in Degenerate, Two Binding Site Molecular Shuttles

Stoddart and co-workers demonstrated that $\mathbf{57}^{4+}$, the first [2]rotaxane to be constructed with two well-defined noncovalent binding sites, exhibits shuttling behavior (Scheme 29a).[197] ^{1}H NMR experiments were consistent with the macrocycle moving between the two hydroquinol stations in a temperature-dependent fashion. Directly analogous situations have subsequently been demonstrated for many rotaxanes bearing the same, or similar, macrocycles and multiple electron-rich aromatic rings on the thread.[198]

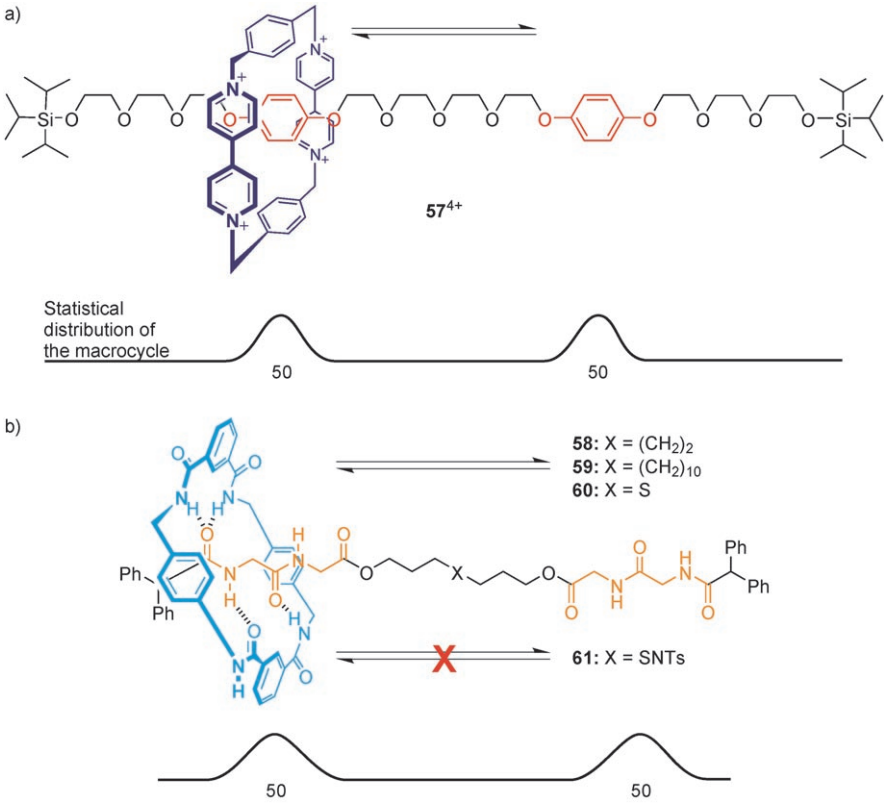

Scheme 29. a) The first "molecular shuttle" $\mathbf{57}^{4+}$.[197] b) Peptide-based degenerate molecular shuttles **58**–**61**.[199]

Similar effects are seen with other multistation rotaxane systems. Shuttling dynamics have been systematically studied for a series of peptide-based molecular shuttles in which two glycylglycine stations are separated by aliphatic linkers.[199] In $CDCl_3$, the macrocycle in **58**–**60** shuttles between the two degenerate peptide stations rapidly at room temperature (Scheme 29b). The shuttling mechanism—a simplified profile is shown in Figure 20—requires at least partial rupture of the intercomponent interactions at one station before formation

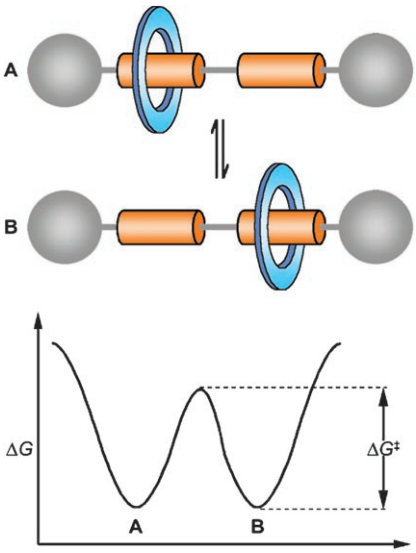

Figure 20. Idealized free-energy profile for movement between two identical stations in a degenerate molecular shuttle. The height of the barrier ΔG^{+} contains two components: the energy required to break the noncovalent interactions holding it to the station and a distance-dependent diffusional component.

of new interactions at a second station. If the kinetic barrier can be made to be significantly larger than the available thermal energy, the shuttling will stop. This can be achieved for **60** by introduction of a bulky *N*-tosyl (NTs) moiety (giving **61**, Scheme 29b). Shuttling is restored upon removal of the *N*-tosyl barrier. In single binding site rotaxanes, hydrogen-bond-disrupting solvents such as [D_6]DMSO break up the interactions between the benzylic amide macrocycle and peptide units,[200] and solvent composition indeed has a profound effect on the shuttling rate in **58**–**60**. As little as 5% [D_4]methanol increases the shuttling rate by more than two orders of magnitude in halogenated solvents.[199,201] In a different hydrogen-bonded system, the shuttling rate could be controlled by deprotonation of a phenol moiety located between two degenerate stations.[202] Noncovalent interaction between the phenolate and counterion was found to significantly slow—but not prevent—shuttling, while the precise rate could again be fine-tuned by variation of the solvent composition.

The reversible introduction of large kinetic barriers to shuttling has also been achieved without formation of covalent bonds.[203] In rotaxane **62**, the crown ether normally shuttles between the two bipyridinium stations (Scheme 30). The introduction of Cu^{I} ions, however, forms a kinetically stable dimeric complex, thus blocking movement of the ring. An ion-exchange resin can be used to sequester the metal and restore shuttling.[204]

4.2.2. *A Physical Model of Degenerate, Two Binding Site Molecular Shuttles*

An interesting structural effect is observed on increasing the length of the spacer in degenerate shuttles. Although ostensibly not involved in any interactions with the macrocycle, extension of the alkyl chain from **58** to **59** (Scheme 29b) reduces the rate of shuttling by a factor corresponding to an increase in activation energy of 1.2 kcal mol^{-1}—an effect solely of the increased distance the macrocycle must

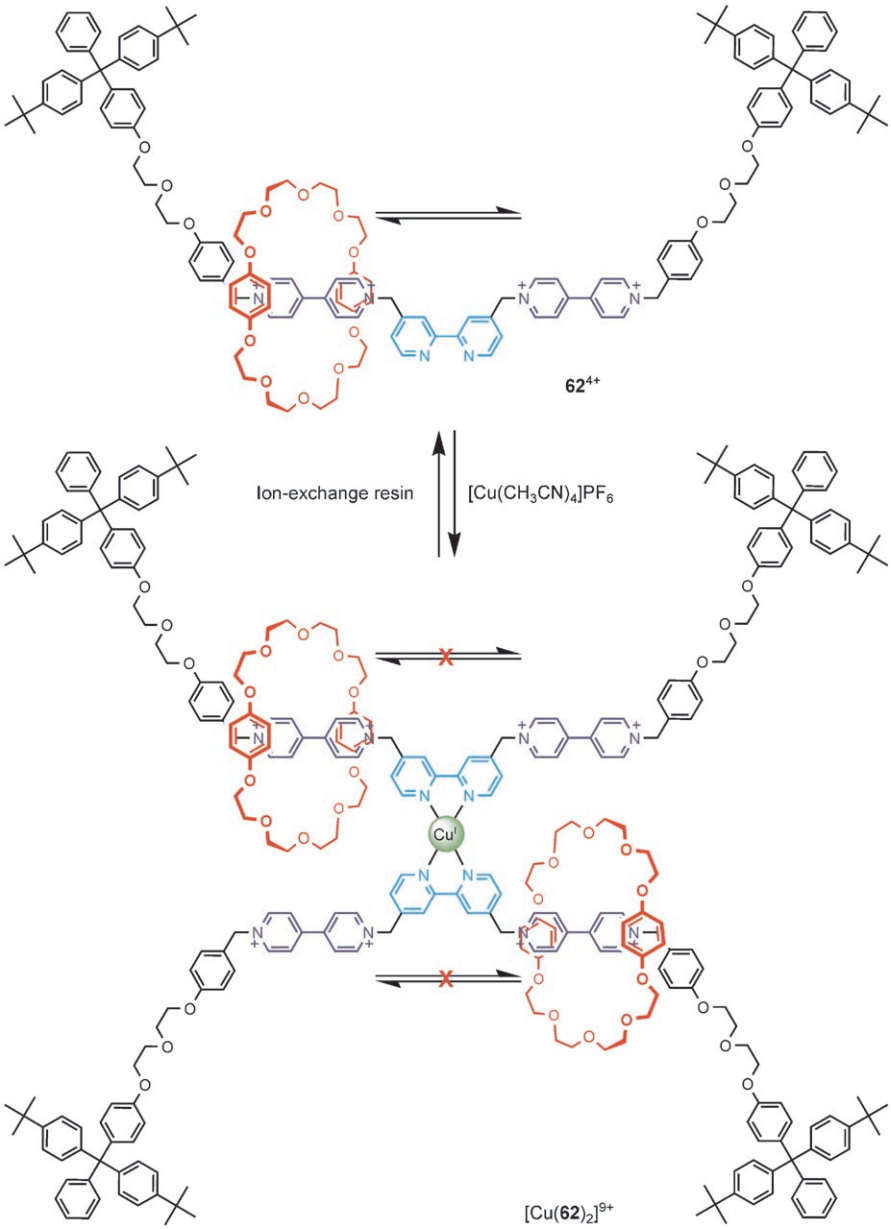

Scheme 30. Switchable degenerate shuttling through reversible formation of kinetically stable dimeric complexes.[204a]

travel.[199] This effect is most clearly understood by considering the macrocycle as a particle moving along a one-dimensional potential energy (rather than free-energy) surface (Figure 21). At any point on the potential-energy surface, the gradient of the line gives the force exerted on the macrocycle by the thread. When the macrocycle is in the vicinity of a station, hydrogen bonds and/or other attractive noncovalent interactions exert large forces (typically varying as a high power of the inverse distance r^{-n}) on the macrocycle, opposing its motion. When the macrocycle is on the thread between the stations, the hydrogen bonds and other noncovalent binding interactions are broken and no forces are exerted on the macrocycle by the thread (that is, the gradient of the line is zero). The rate at which the macrocycles escape from each station is given by a standard Arrhenius equation, which depends on the depth of the energy well and the temperature. However, this is not the only factor involved in determining the rate at which macrocycles move between the two stations; there must also be some distance-dependent diffusional factor in the function describing rate of shuttling (Figure 21).

The experimentally determined values of $\Delta G^{\ddagger}$ for **58** and **59** have also been reconciled with a quantum-mechanical description of the shuttling process.[205] Calculation of the wavefunctions for the system shows that an increase in distance between the stations does not, of course, change the activation energy for cleavage of hydrogen bonds but rather the effect is to widen the free-energy potential well (Figure 20). As the well widens, it possesses a higher density of states per unit energy (just like the simple "particle-in-a-box" model). The closer the levels are to one another, the more readily thermally populated they are or, in other words, the larger is the partition function and therefore also the $\Delta G^{\ddagger}$ value.

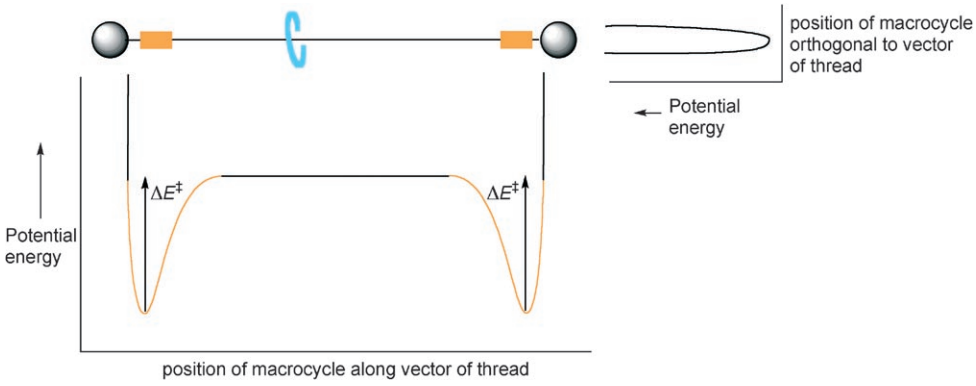

Figure 21. Idealized potential energy of the macrocycle in a two-station, degenerate molecular shuttle. The potential-energy surface shows the effect of the interaction between the macrocycle and thread on the energy of the macrocycle (ignoring any complicating factors such as folding). Chemical potential energies (ΔE values) generally follow similar trends to free energies (ΔG values, Figure 20) but there are some important differences; for example, the activation free energy of shuttling $\Delta G^{\ddagger}$ corresponds to the energy required for the macrocycle to move all the way to the new binding site (that is, it includes a contribution for the distance the ring has to move along the track to reach the other station) whereas $\Delta E^{\ddagger}$ (shown here) represents the energy required for the macrocycle to escape the forces exerted through noncovalent binding interactions at a station. The main plot shows the ΔE value in terms of the position of the macrocycle along the vector of the thread; the minor plot shows the ΔE value in terms of the position of the macrocycle orthogonal to the vector of the thread, thus illustrating that the thread genuinely behaves as a one-dimensional potential-energy surface for the macrocycle.

The nature of the wavefunctions at energies close to the top of the barrier is intriguing, as under this energy regime the maximum probability of finding the macrocycle is over the aliphatic spacer. The shuttling process can therefore be thought of in terms of a function of free energy (Figure 20) as long as we remember that the height of the $\Delta G^{\ddagger}$ barrier is affected by both binding strength and distance between the stations. The behavior of the macrocycle is similar to a cart moving along a roller coaster track shaped like the double potential minima in Figure 20. At low temperatures, the cart mostly resides on the stations (oscillating with small amplitude in the troughs). As energy approaches the value of the barrier, the cart spends most of its time passing over the barrier (occupying co-conformations close to the transition state for movement between the stations). At higher energies still, the cart is most likely to be found at the extremes of its translational motion (once again occupying ground-state co-conformations at the stations).

4.3. Stimuli-Responsive Molecular Shuttles: Translational Molecular Switches

As we have seen, the rate at which the macrocycle moves between the stations by Brownian motion in molecular shuttles can be regulated by temperature and, in some cases, solvent composition or binding events. However, the principle of detailed balance (Section 1.4.1) tells us that no useful task can be performed by such a process, even if the two stations are different. A more important kind of control is one in which the net location of the macrocycle is changed in response to an applied stimulus. This breaks detailed balance and, as the system relaxes back to equilibrium, the biased Brownian motion of the macrocycle can be used to perform a mechanical task.[206]

4.3.1. Single Binding Site, Stimuli-Responsive Molecular Shuttles

A limited amount of control over the position of the macrocycle can be introduced into single recognition site rotaxanes if the binding affinity can be affected by a stimulus. An important first step towards photoswitchable molecular shuttles was [2]rotaxane $\mathbf{63}^{4+}$ (Scheme 31).[207] This rotaxane is closely related to $\mathbf{57}^{4+}$, but in $\mathbf{63}^{4+}$ there is only one electron-rich station for the macrocycle and the bulky stoppers are redox-active ferrocene groups. A laser flash photolysis pulse within the charge transfer band of $\mathbf{63}^{4+}$ induces electron transfer from the dioxyarene to the cyclophane, thereby generating an intimate radical ion pair. Charge recombination is normally fast compared with any competing processes such as solvent

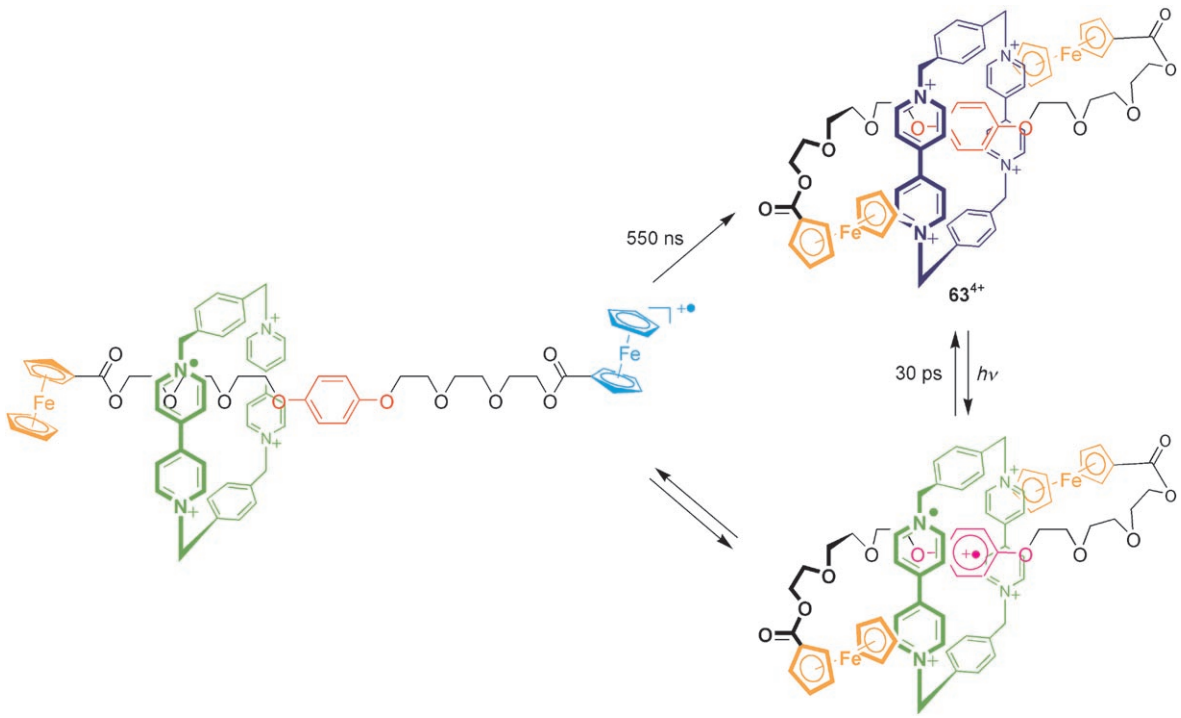

Scheme 31. Conformational dynamics and electron-transfer processes possible in [2]rotaxane $\mathbf{63}^{4+}$: a "single-station" molecular shuttle.[207]

penetration or spatial separation of the radical ions. The flexible thread, however, allows close contact of the electron-rich ferrocenyl stoppers with the cyclophane through a secondary π-stacking interaction (also observed in the solid state). This electronic coupling allows some of the radical ion pairs (ca. 25%) to undergo a secondary electron-transfer step in which the electron hole is transferred to one of the ferrocenyl stoppers. The interactions between the cyclophane and the stopper are therefore "switched off" and the molecule unravels. This spatially remote charge-separated state is relatively long-lived, so that some shuttling of the cyclophane away from the oxidized stopper may occur, driven by electrostatic repulsion. However, there is no direct evidence for this transient shuttling, or means to control the position of the cyclophane in the spatially remote charge-separated state.

The environment-sensitive nature of the intercomponent hydrogen bonds in peptidic [2]rotaxanes allows control over effects arising from communication between the thread and macrocycle (Scheme 32a). Unlike the free sarcoglycine thread, rotaxane **64** exhibits only one (*E*) tertiary amide rotamer in apolar solvents, as the *Z* rotamer allows the formation of fewer favorable intercomponent hydrogen bonds (Scheme 32a). In hydrogen-bond-competing solvents, however, the interactions between the thread and macrocycle are "switched off" and both rotamers are observed.[208] It was found that a similar effect could switch on and off an induced circular dichroism (ICD) response between the intrinsically achiral benzylic amide macrocycle and the chiral center in the thread in chiral dipeptide [2]rotaxane **65** (Scheme 32b).[209]

In two related systems, it has been possible to control the position of a cyclodextrin (CD) macrocycle on threads containing azobenzene and stilbene units (Scheme 33).[210,211] The cyclodextrin spends most of its time over the central aromatic units in the *E* isomers of [2]rotaxanes **66** and **67** in aqueous media. Irradiation at suitable wavelengths results in photoisomerization of the N=N and C=C bonds in **66** and **67**, respectively, to the *Z* forms. The steric demands of the "kinked" thread require the cyclodextrin to be positioned away from the central unit. Even in the *E* isomers, however, the cyclodextrin does not sit exclusively over the central unit. This is in fact crucial for allowing photoisomerization to occur—an analogue of **66** which lacks the ethylene spacer (light blue) between the azobenzene and viologen units undergoes no photoisomerization as the *trans* chromophore is fully encapsulated by the ring.[210b,212] Interestingly, in **67**, despite having a symmetrical thread, the displacement has been shown to be unidirectional, with the narrower 6-rim of the cyclodextrin always closest to the *Z* olefin.[211,213] It has been noted in a variety of studies that the asymmetry of cyclodextrins can result in the selective formation of orientational isomers when constructing pseudorotaxane or rotaxane architectures.[214] Although the observation of such isomers requires nonsymmetrical thread portions, an asymmetric substrate, such as a cyclodextrin ring, should itself satisfy the requirement of symmetry breaking for the creation of a full ratchet mechanism even on a symmetric track (see Section 1.4.2).

4.3.2. A Physical Model of Two Binding Site, Stimuli-Responsive Molecular Shuttles

Rotaxanes in which the macrocycle can be translocated between two or more well-separated stations in response to an external signal should, in principle, provide a greater level

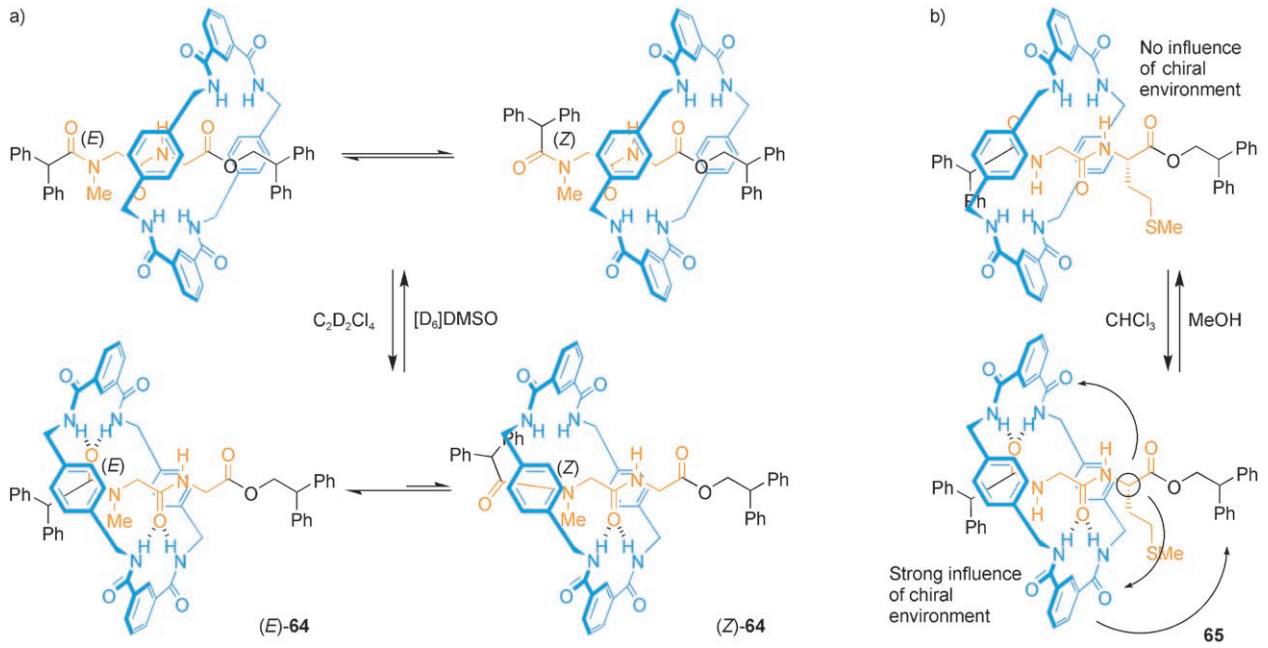

Scheme 32. Environment-sensitive communication between interlocked components in single-station dipeptide [2]rotaxanes. a) In $C_2D_2Cl_4$, hydrogen bonding between the thread and macrocycle stabilizes the *E* rotamer so that this is the sole conformation observed by NMR spectroscopy. In [D_6]DMSO, the hydrogen bonding is switched off and both rotamers are observed, as they are for the free thread in all solvents.[208] b) In $CHCl_3$, the achiral macrocycle is held close to the chiral center, thereby conferring a chiral nature on its conformation which, in turn, affects the conformation of the C-terminal diphenylmethyl moiety, thus resulting in an ICD response. In MeOH, the hydrogen bonding is switched off and the communication between the components is lost.[209]

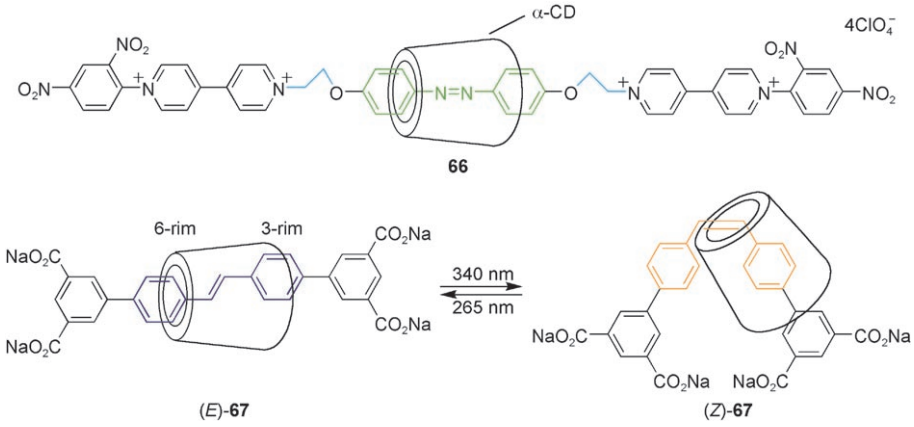

Scheme 33. Photoresponsive single-station shuttles **66**[210] and **67**,[211] based on azobenzene and stilbene units, respectively.

of positional control. As seen in Section 4.2.2, in any rotaxane the macrocycle distributes itself between the available binding sites according to the difference in the macrocycle binding energies and the temperature. If a suitably large difference in macrocycle affinity exists between two stations, the macrocycle resides overwhelmingly in one positional isomer or co-conformation.[142] In stimuli-responsive molecular shuttles, an external trigger is used to chemically modify the system and alter the noncovalent intercomponent interactions such that the second macrocycle binding site becomes energetically more favored, thus causing translocation of the macrocycle along the thread to the second station (Figure 22). This may be achieved by addressing either of the stations (destabilizing the initially preferred site or increasing the binding affinity of the originally weaker station). The system can be returned to its original state by using a second chemical modification to restore the initial order of station binding affinities. Performed consecutively, these two steps allow the "machine" to carry out a complete cycle of shuttling motion.

The physical basis for this motion is again best understood by consideration of the potential energy of the macrocycle as a function of its position along the thread (Figure 23). It is important to appreciate that the external stimulus does not actually induce directional motion of the macrocycle, rather the system is put out of co-conformational equilibrium by increasing the binding strength of the less-populated station and/or destabilizing the initially preferred binding site.[215] Relaxation towards the new global energy minimum subsequently occurs by thermally activated motion of the components, a phenomenon which is recognized as biased Brownian motion. This effect can be envisaged as a net directional transport (a directional flux) of macrocycles towards the newly preferred station.

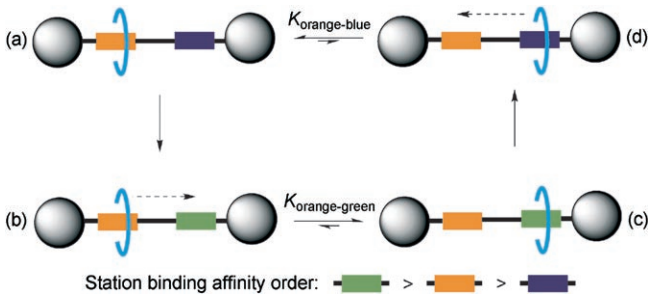

Figure 22. Translational submolecular motion in a stimuli-responsive molecular shuttle: a) the macrocycle initially resides on the preferred station (orange); b) a reaction occurs (blue→green) which changes the relative binding potentials of the two stations such that, c) the macrocycle "shuttles" to the now-preferred station (green). If the reverse reaction (green→blue) now occurs (d), the components return to their original positions.

Figure 23. Idealized potential energy of the macrocycle in a stimuli-responsive molecular shuttle in which one station changes (A'→A) in response to the stimulus and complicating factors such as folding are ignored. As before (Figure 21), the potential-energy surface shows the effect of the interaction between the macrocycle and thread on the energy of the macrocycle. The main plot shows the potential energy in terms of the position of the macrocycle along the vector of the thread; the minor plot shows the potential energy in terms of the position of the macrocycle orthogonal to the vector of the thread.

Given this mode of action, a key requirement is finding ways of generating large long-lived binding energy differences between pairs of positional isomers. A Boltzmann distribution at 298 K requires a $\Delta\Delta E$ (or $\Delta\Delta G$) value between translational co-conformers of about 2 kcal mol^{-1} for 95% occupancy of one station. Achieving such discrimination in two states to form a positionally bistable shuttle (that is, both $\Delta\Delta E_{A'\text{-}B}$ and $\Delta\Delta E_{B\text{-}A} \geq 2$ kcal mol^{-1}) by modifying only intrinsically weak, noncovalent binding modes thus presents a significant challenge.

4.3.3. *Adding and Removing Protons to Induce Net Positional Change*

The first bistable switchable molecular shuttle, reported by Stoddart, Kaifer, and co-workers in 1994 and arguably the first true example of a molecular Brownian motion machine, employed a two-station design (Scheme 34).[216] The biphenol and benzidine units in the thread of [2]rotaxane **68**$^{4+}$ are both potential π-electron-donor stations for the cyclobis(paraquat-p-phenylene) (CBPQT^{4+}) cyclophane, and at room temperature rapid shuttling of the macrocycle occurs as in related degenerate shuttles (Section 4.2.1). Cooling the solution to 229 K allowed observation (by NMR and UV/Vis absorption spectroscopy) of the two translational isomers in a ratio of 21:4 in favor of encapsulation of the benzidine station. Protonation of the benzidine residue with CF_3CO_2D destabilizes its interaction with the macrocycle so that it now resides overwhelmingly on the biphenol station. The system can be restored to its original state by neutralization with [D_5]pyridine.[217]

Although this system is a controllable molecular shuttle, it exhibits modest positional integrity in the nonprotonated state—a much larger binding difference between the two stations is required. Inspired by the complexation of ammonium ions by crown ethers, a new series of rotaxanes based on threads containing secondary alkylammonium species and crown ether macrocycles was developed.[218] [2]Rotaxane [**69**·H]$^{3+}$ (Scheme 35) was the first switchable molecular shuttle reported using these units.[219] The dibenzo-crown ether is bound to the ammonium cation by means of N$^+$–H···O hydrogen bonds as well as weaker C–H···O bonds from methylene groups in the α position to the nitrogen atom. ^{1}H NMR spectroscopic analysis of the rotaxane in [D_6]acetone at room temperature shows (to the limits of detection of this experimental technique) the crown ether to be sitting mainly (but not exclusively[220]) over the ammonium ion. Deprotonation of the ammonium center with diisopropylethylamine turns off the interactions holding the macrocycle to this station so it resides on the alternative bipyridinium station (**69**$^{2+}$).[221] A kinetic study of the shuttling in a closely related rotaxane revealed that the base-induced step is significantly slower than the return motion. This occurs despite a lower enthalpy of activation for the forward step and is due to entropic factors arising from the rearrangement of counterions in the transition state.[219c,222]

While this example exhibits good macrocycle positional integrity in both chemical states, the low binding constant between the crown ether and bipyridinium moieties in the deprotonated state might be a limitation in more complex systems, especially if the macrocycle is afforded a greater degree of translational freedom (the distance between the

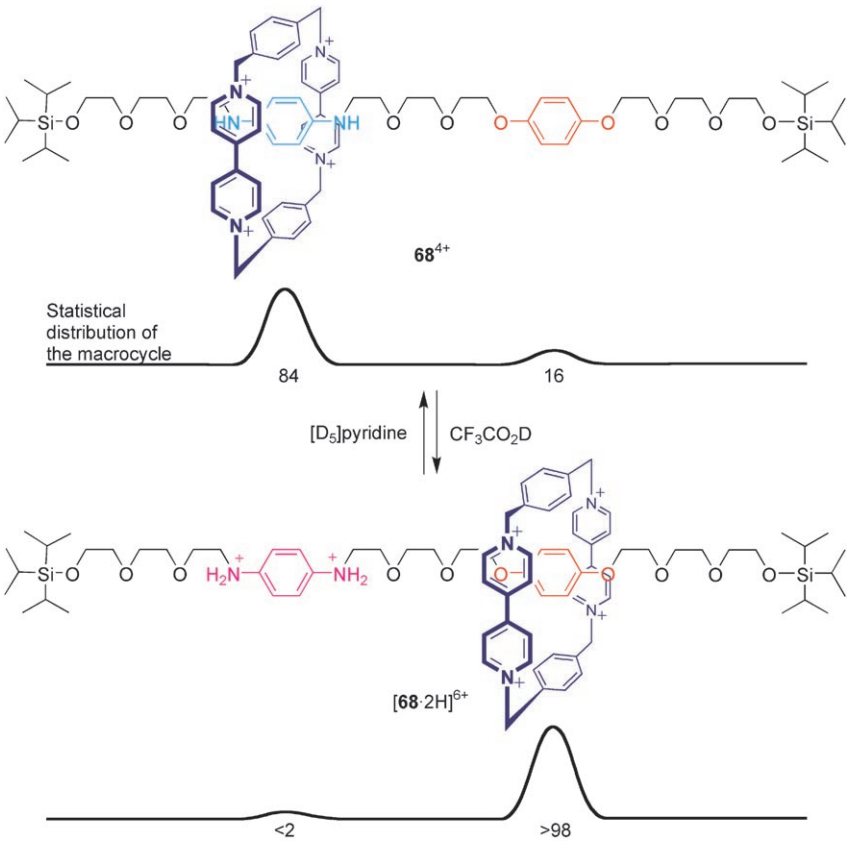

Scheme 34. The first switchable molecular shuttle $\mathbf{68}^{4+}$/$[\mathbf{68}\cdot 2\,H]^{6+}$.[216] The macrocycle distribution in $\mathbf{68}^{4+}$ was determined by ^{1}H NMR spectroscopy at 229 K in CD_3CN. The macrocycle distribution in $[\mathbf{68}\cdot 2\,H]^{6+}$ is based on the lack of observation of the other translational isomer by ^{1}H NMR spectroscopy at a number of temperatures in the range 193–304 K in [D_6]acetone

stations in the current system is ca. 7 Å). Accordingly, Stoddart, Balzani, and co-workers prepared a combination of three shuttle units in parallel by using this system.[223] The molecule ($[\mathbf{70}\cdot 3\,H]^{9+}$, Scheme 36) consists of three threadlike components connected at one end and encircled by three catechol-polyether macrocycles connected in a platformlike fashion. Essentially, the shuttling action works as in **69**; just over three equivalents of base are required to move the platform from the ammonium ("top") to the bipyridinium ("bottom") positions. Titration experiments and molecular-modeling studies indicate that the shuttling motion proceeds in a stepwise fashion with each polyether macrocycle stepping individually from station to station. The effect of combining the three binding sites is excellent positional integrity in both the fully protonated and fully deprotonated states, while a further analogue utilizing a dioxynaphthalene trismacrocyclic platform exhibits even stronger interactions when on the bipyridyl station.[223b]

The first pH-switchable shuttle to exploit hydrogen-bonding interactions to anions was recently reported.[224] In [2]rotaxane **71**·H (Scheme 37) formation of the benzylic amide macrocycle is templated by a succinamide station in the thread. However, the thread also contains a cinnamate derivative. In the neutral form the macrocycle resides on the succinamide station more than 95% of the time because the phenol ring is a poor hydrogen-bonding group. Deprotonation in [D_7]DMF to give $\mathbf{71}^-$ results in the macrocycle changing position to bind to the strongly hydrogen-bond-basic phenolate anion. Reprotonation returns the system to its original state and the macrocycle to its original position. However, the shuttling is extremely solvent-dependent. Hydrogen-bonding molecular shuttles usually perform best in "non-competing" solvents. However, when the deprotonation of **71**·H is carried out in $CDCl_3$ or CD_2Cl_2, a change of position of the macrocycle does not occur. Instead, intramolecular folding occurs to allow the phenolate group to hydrogen bond with the macrocycle while it remains on the succinamide station. This solvent dependence is explained by the fact that the phenolate group can only satisfy the hydrogen-bonding requirements of one isophthalamide unit of the macrocycle. The DMF facilitates shuttling by hydrogen bonding to the remaining amide groups of the macrocycle. Shuttling is unaffected by the nature of the accompanying cation or the addition of up to ten equivalents of other anions.

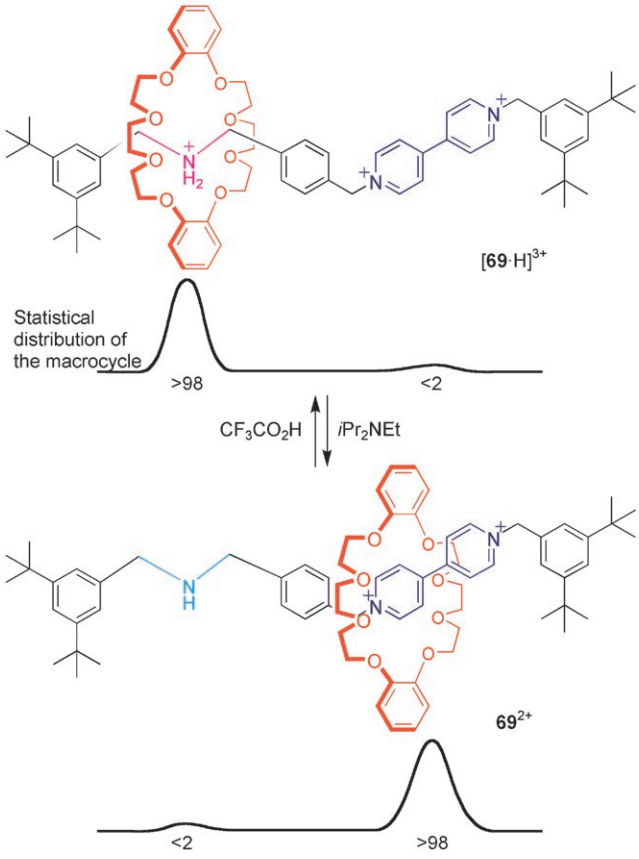

Scheme 35. A pH-responsive bistable molecular shuttle displaying good positional integrity in both chemical states.[219] Statistical distributions of the macrocycle were determined at a number of temperatures in the range 193–304 K in [D_6]acetone.

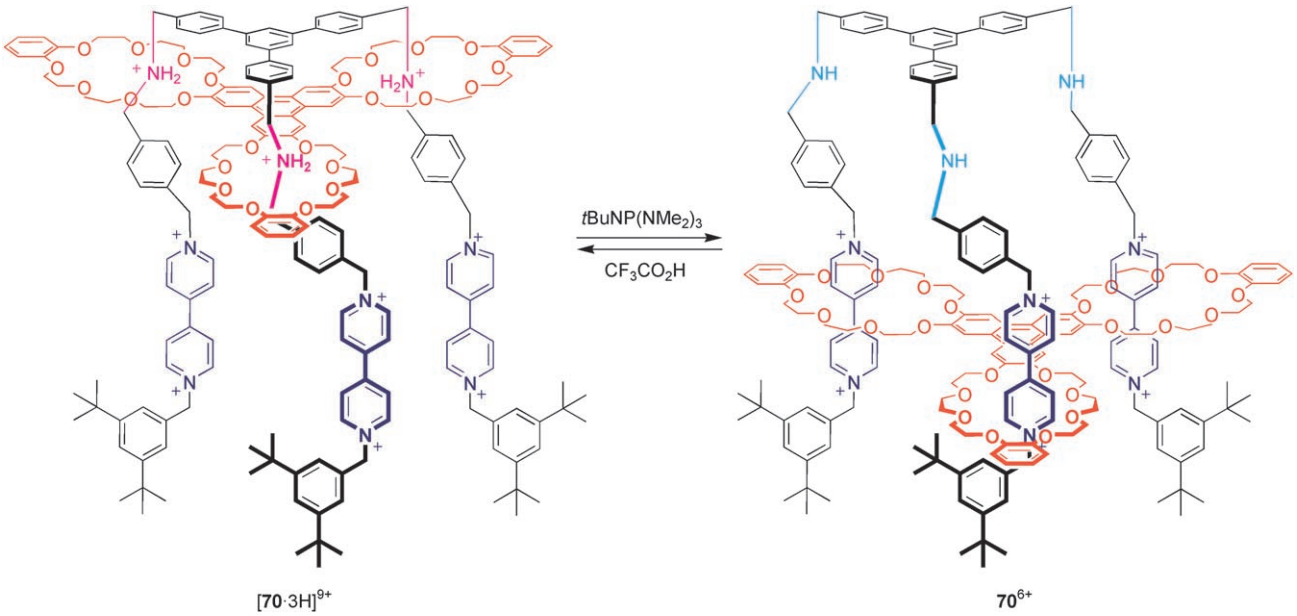

Scheme 36. Chemical structure of a "molecular elevator" $[\mathbf{70}\cdot 3H]^{9+}/\mathbf{70}^{6+}$.[223]

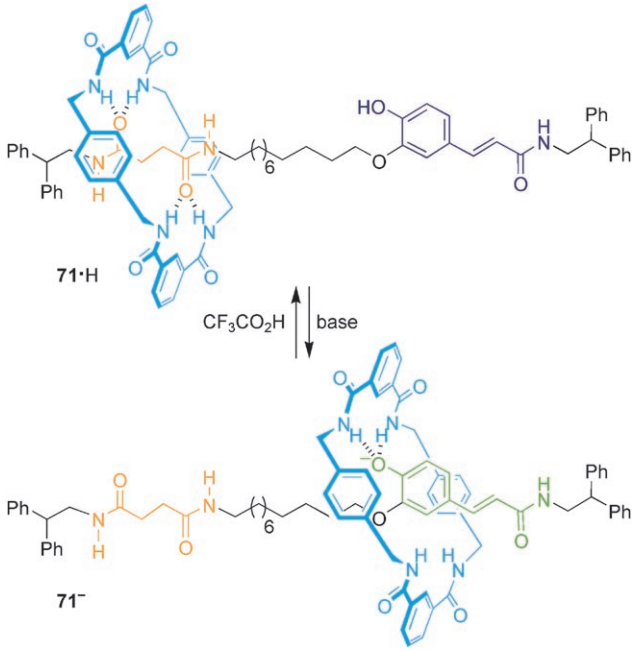

Scheme 37. pH-switched anion-induced shuttling in hydrogen-bonded [2]rotaxane $\mathbf{71}\cdot H/\mathbf{71}^{-}$ in $[D_7]$DMF at RT.[224] Bases that are effective include LiOH, NaOH, KOH, CsOH, Bu_4NOH, *t*BuOK, DBU, and Schwesinger's phosphazine P_1 base, thus illustrating the lack of influence of the accompanying cation on shuttling.

4.3.4. *Adding and Removing Electrons To Induce Net Positional Change*

In the original switchable shuttle $\mathbf{68}^{4+}$ (Scheme 34), the change of position could also be achieved in a reagent-free manner by electrochemical oxidation of the benzidine station; the macrocycle shuttles away from this station after oxidation to the radical cation.[216] A number of attempts to create related redox-switched shuttles with greater positional integrity failed to give an improved distribution of translational isomers in the ground state.[225,226] Incorporation of redox-active stations based on tetrathiafulvalene (TTF), however, has given rise to a whole series of redox-active shuttles, a typical example of which ($\mathbf{72}^{4+}/\mathbf{72}^{6+}$) is illustrated in Scheme 38.[227] Switching of the $CBPQT^{4+}$ cyclophane between TTF (or closely related derivatives) and dioxyarene units has since been extensively studied in both rotaxane and catenane (see Section 4.6.1) architectures (as well as a number of model systems) to fully understand the relationship between chemical structure and performance characteristics with a view to incorporate these shuttles in various condensed-phase devices (see Section 8.3).[180c,184l,u,186c,227,228] One of the key findings to emerge from these studies is that there is a significant activation barrier for the shuttling of the ring back onto the TTF unit when it is reduced from the oxidized state. This is in contrast to movement away from the freshly oxidized TTF unit which involves a very low kinetic barrier on account of the unfavorable interaction between the two positively charged components. The metastable state can be observed in solution at low temperature,[228f] and its characterization has been crucial in determining the mechanism of operation of the solid-state electronic devices constructed from molecules of this type (see Section 8.3.1).

An electrochemical switch with one of the highest positional fidelities (ca. 10^6:1 in one state; ca. 1:500 in the other) has been demonstrated with amide-based molecular shuttles.[229] [2]Rotaxane **73** contains two potential hydrogen-bonding stations (a succinamide (succ) station and a redox-active 3,6-di-*tert*-butyl-1,8-naphthalimide (ni) station) for the benzylic amide macrocycle that are separated by a C_{12} aliphatic spacer (Scheme 39).[229]

While the ability of the succ station to template formation of the macrocycle is well established, the neutral naphthalimide moiety is a poor hydrogen-bond acceptor. In fact, the

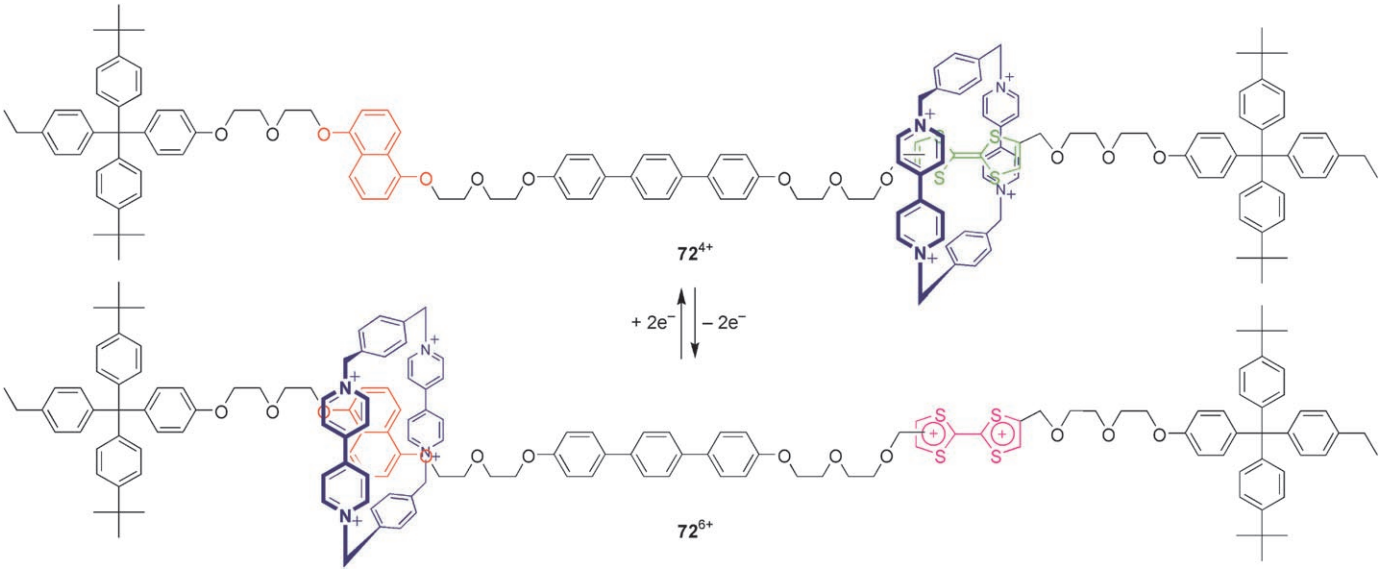

Scheme 38. Redox-switchable molecular shuttle **72**$^{4+}$/**72**$^{6+}$.[227] The redox reactions may be carried out either chemically or electrochemically.

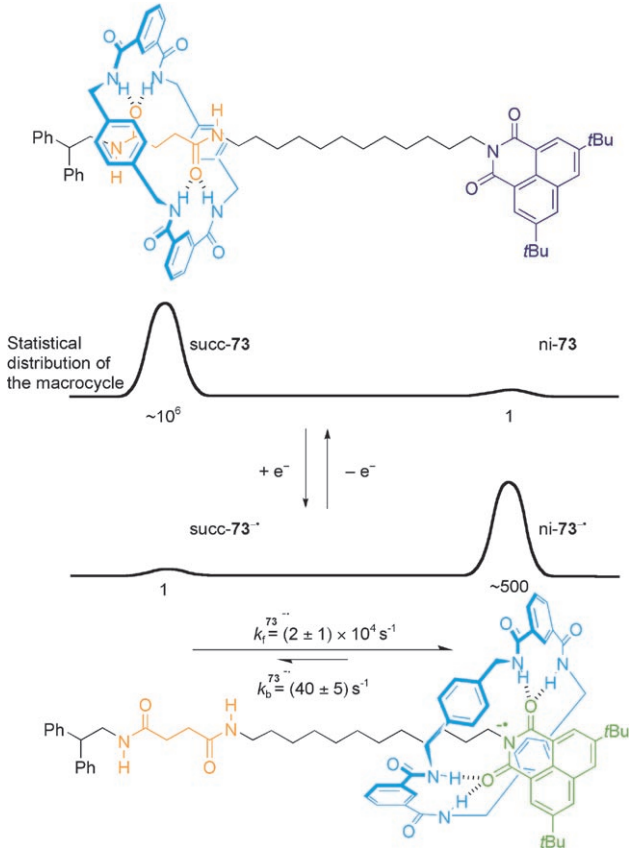

Scheme 39. A photochemically and electrochemically switchable, hydrogen-bonded molecular shuttle **73**.[229] In the neutral state, the translational co-conformation succ-**73** is predominant as the ni station is a poor hydrogen-bond acceptor ($K_n = (1.2 \pm 1) \times 10^{-6}$). Upon reduction, the equilibrium between succ-**73**$^{-\bullet}$ and ni-**73**$^{-\bullet}$ is altered ($K_{red} = (5 \pm 1) \times 10^2$) because ni$^{-\bullet}$ is a powerful hydrogen-bond acceptor and the macrocycle moves through biased Brownian motion. Upon reoxidation, the macrocycle shuttles back to the succinamide station. Repeated reduction and oxidation causes the macrocycle to shuttle forwards and backwards between the two stations. All the values shown refer to cyclic voltammetry experiments in anhydrous THF at 298 K with tetrabutylammonium hexafluorophosphate as the supporting electrolyte. Similar values were determined on photoexcitation and reduction of the ensuing triplet excited state by an external electron donor.

difference in macrocycle binding affinities is so great that succ-**73** is the only translational isomer detectable by ^{1}H NMR specroscopy in $CDCl_3$, CD_3CN, and [D_8]THF (an equilibrium constant of $(1.2 \pm 1) \times 10^{-6}$ for the two translational isomers was determined by electrochemistry in THF containing Bu_4NPF_6 as a supporting electrolyte); even in the strongly hydrogen-bond-disrupting [D_6]DMSO, the macrocycle resides over the succ station about half of the time. One-electron reduction of naphthalimide to the corresponding radical anion, however, results in a substantial increase in electron charge density on the imide carbonyl groups and a concomitant increase in hydrogen-bond-accepting ability. In **73**, this reverses the relative hydrogen-bonding abilities of the two thread stations so that co-conformation ni-**73**$^{-\bullet}$ is preferred over succ-**73**$^{-\bullet}$ to the extent of approximately 500:1. Subsequent reoxidation to the neutral state restores the original binding affinities and the shuttle returns to its initial state. The process can be observed in cyclic voltammetry experiments,[229b] or alternatively photochemistry can be employed to initiate (through excitation of the naphthalimide group by a nanosecond laser pulse at 355 nm followed by electron transfer from an external electron donor) and observe (by using transient absorption spectroscopy) the change of position.[229a] Importantly, a number of control experiments involving the incorporation of steric barriers to shuttling were carried out to prove unequivocally that the dynamic process observed in this rotaxane system is a reversible shuttling of the macrocycle between the stations rather than any other conformational or co-conformational changes.[229b,230]

Although many metal–ligand interactions can be rather kinetically stable, the difference in preferred coordination geometries of different oxidation states can be exploited to bring about redox-induced shuttling in transition-metal-based systems. The preference of Cu^{I} ions for four-coordinate tetrahedral complexes has been widely employed in the synthesis of interlocked architectures,[189-

[g,195a,e–g,j,af] as it enforces the orthogonal arrangement of two bidentate ligands which can be further elaborated to give rotaxanes or catenanes. In [Cu^{I}(**74**)] (Scheme 40), a macrocycle containing a bidentate 2,9-diphenyl-1,10-phenanthroline (dpp) unit, is locked onto a thread which contains one bidentate phenanthroline (phen) and one tridentate 2,2′:6′,2″-terpyridine (terpy) unit.[231] Chelation of Cu^{I} ions ensures that the macrocycle is positioned over the phenanthroline station in the thread, phen-[Cu^{I}(**74**)]. Electrochemical oxidation initially generates phen-[Cu^{II}(**74**)]. However, as Cu^{II} ions prefer higher coordination numbers, a thermally activated relaxation to the thermodynamically preferred terpy-[Cu^{II}(**74**)] occurs. The metastable phen-[Cu^{II}(**74**)] state is relatively kinetically inert, however, and this shuttling step takes several hours at room temperature ($k = 1.5 \times 10^{-4}\ s^{-1}$). Electrochemical reduction of the divalent species gives terpy-[Cu^{I}(**74**)] which slowly converts into the original translational isomer phen-[Cu^{I}(**74**)] ($10^{-4} \le k \le 10^{-2}\ s^{-1}$, which is slightly faster than the first step because of the smaller charge on the metal center). The same shuttling process can also be accomplished by a photochemically triggered oxidation. The reverse reduction step cannot be carried out photochemically but proceeds successfully with a chemical reductant (ascorbic acid).[232]

4.3.5. *Adding and Removing Metal Ions To Induce Net Positional Change*

The research groups of Sanders and Stoddart have collaborated to produce another class of molecular shuttles that can be switched in several ways (Scheme 41). In the ground state, the co-conformation of kinetically stable [2]pseudorotaxane **75** with the macrocycle sitting over the naphthaldiimide station (blue) is dominant, as observed by ^{1}H NMR spectroscopy and one-electron reduction of this station (which has the lower reduction potential) results in shuttling of the ring onto the pyromellitic diimide station (green). Somewhat unexpectedly, however, the change in position of the macrocycle can also be induced by adding lithium ions. Two of the small metal ions can be complexed between the crown ether macrocycle and the carbonyl groups of the diimide moieties and this interaction is significantly stronger at the pyromellitic station (Scheme 41). Addition of a large excess of [18]crown-6 sequesters the lithium ions, thereby returning the system to its initial state.[233]

Rather than serving to enhance intercomponent interactions at a specific station, metal-ion binding can be used to destabilize the binding of the macrocycle at one site, thus causing it to translocate to another, unaffected unit. This is

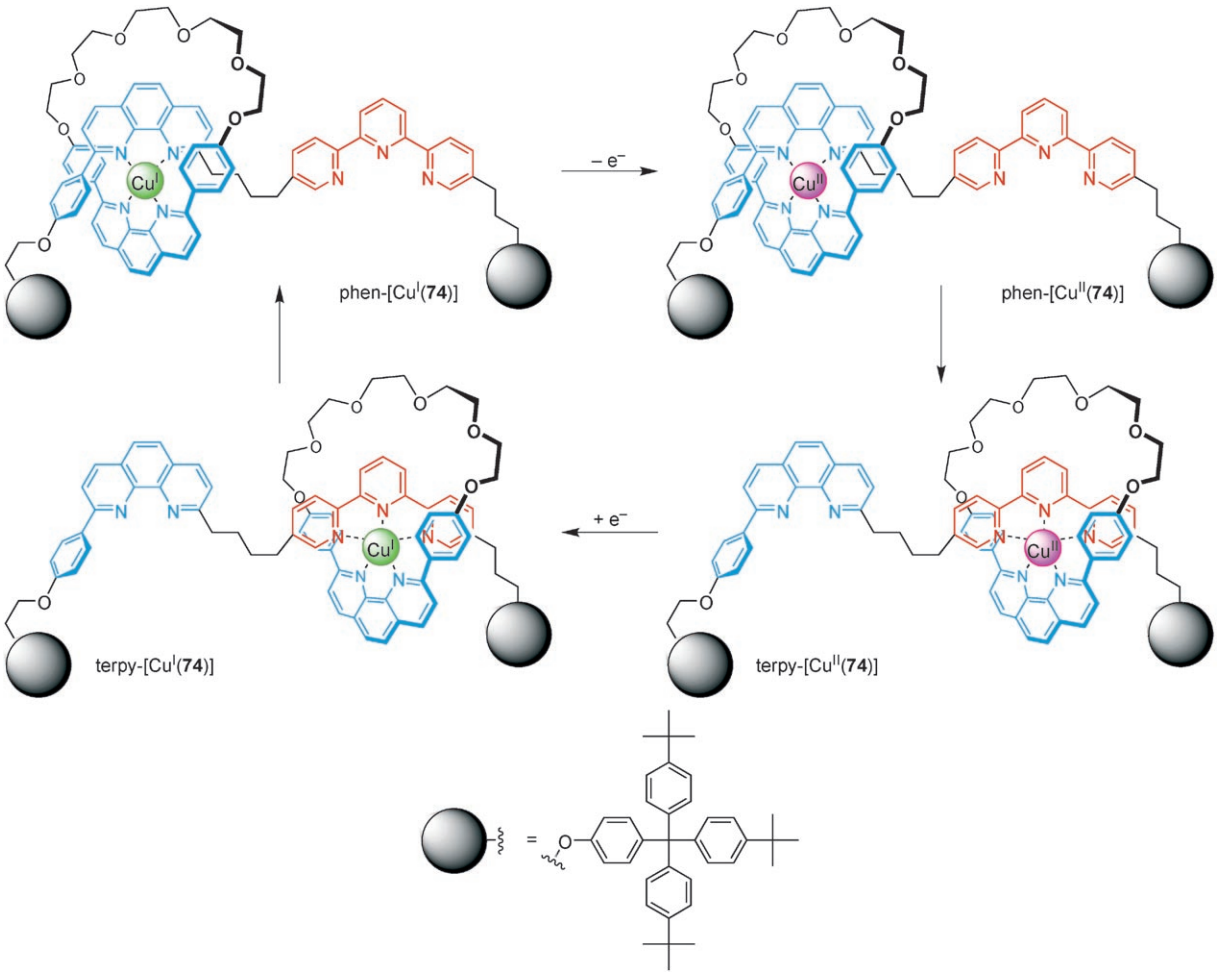

Scheme 40. Redox-switched shuttling in the metal-templated [2]rotaxane **74**.[231]

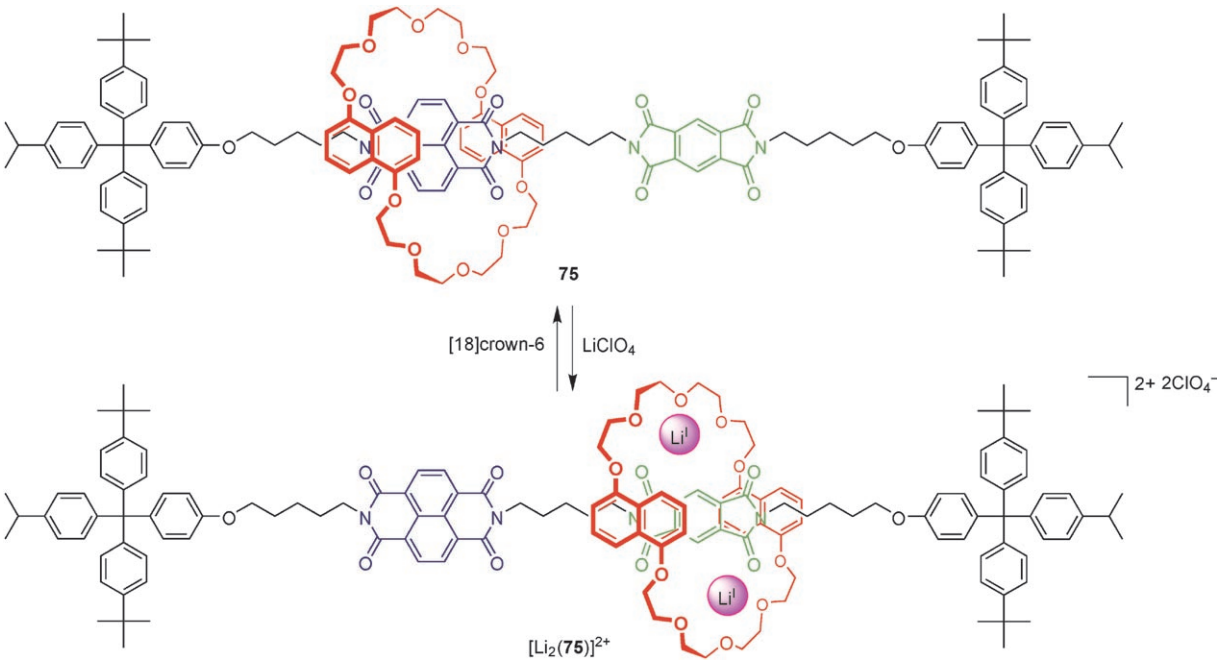

Scheme 41. Cation-induced shuttling based on complexation and decomplexation of lithium ions.[233]

possible through two distinct mechanisms (Scheme 42).[234,235] In [2]rotaxane **76** the macrocycle preferentially sits over the glycylglycine station derivatized with a bis(2-picolyl)amino (BPA) stopper. The addition of one equivalent of $Cd(NO_3)_2 \cdot 4H_2O$ generates a complex in which the metal ion is bound to the first carboxamide carbonyl oxygen atom as well as the three nitrogen donors of the BPA ligand, and the preferred postion of the macrocycle remains essentially unchanged. However, deprotonation of the first carboxamide moiety[236] results in coordination of the nitrogen anion, as well as the carbonyl oxygen atom of the second carboxamide group. The cadmium ion essentially wraps itself up in the deprotonated glycylglycine residue, thus switching off any intercomponent interactions with the macrocycle which now occupies the succinic amide ester station. The shuttling process is fully reversible: removal of the Cd^{II} ion with excess cyanide and reprotonation of the amide nitrogen atom with NH_4Cl quantitatively regenerates **76**.[234] In [2]rotaxane **77**, again the macrocycle preferentially resides on the carboxamide-based station adjacent to a BPA ligand. In this case, divalent metal ions such as Cd^{II} are only able to chelate to the three BPA nitrogen atoms. To accommodate such a binding mode, however, the two pyridyl arms must adopt a coplanar conformation, which sterically destabilizes macrocycle binding to the succinamide station, thus causing it to move to the inherently weaker succinic amide ester unit. Rather than competing for the same donor atoms, as in **76**, the metal- and macrocycle-binding modes in **77** compete for the same 3D space so that this mechanism corresponds to a negative heterotropic allosteric binding event. The shuttling is fully reversible on demetalation of $[Cd(NO_3)_2(\mathbf{77})]$ with cyanide.[235]

4.3.6. Adding and Removing Covalent Bonds To Induce Net Positional Change

Perhaps surprisingly, the use of covalent-bond-forming reactions to bring about positional change in molecular shuttles has not yet been explored extensively. In one successful example, the formation (and breaking) of C–C bonds through Diels–Alder and retro-Diels–Alder reactions of rotaxane **78** (Scheme 43) can control shuttling with excellent positional discrimination: the steric bulk of the Diels–Alder adduct displaces the macrocycle to the succinic amide ester station in Cp-**78**.[237]

A transient shuttling system involving photoinduced cleavage of a covalent bond and subsequent recombination has recently been reported. Diaryl cycloheptatrienes can act as π-electron-donor binding sites in rotaxanes containing $CBPQT^{4+}$ macrocycles.[180b,d] In [2]rotaxane $\mathbf{79}^{4+}$, the cationic cyclophane resides over the diarylcycloheptatriene station (green) with additional "alongside" interactions with the anisole unit (red). Photoheterolysis of the C–OMe bond under conventional flash photolysis conditions at 360 nm generates the diaryl tropylium cation and displaces the ring to the anisole station (Scheme 44). The lifetime of this species at room temperature is 15 s, before the thermal back reaction returns the system to $\mathbf{79}^{4+}$ (or a regioisomer resulting from nucleophilic attack of the methoxide at a different site on the seven-membered ring). The shuttling motion was inferred by comparison of the transient absorption spectrum of $\mathbf{79}^{5+} \cdot MeO^-$ with the spectral characteristics of $\mathbf{79}^{5+}$ generated by electrochemical oxidation.[238] Recently, modifications to the inactive thread components have allowed preparation of an analogue which adopts a linear conformation in the ground

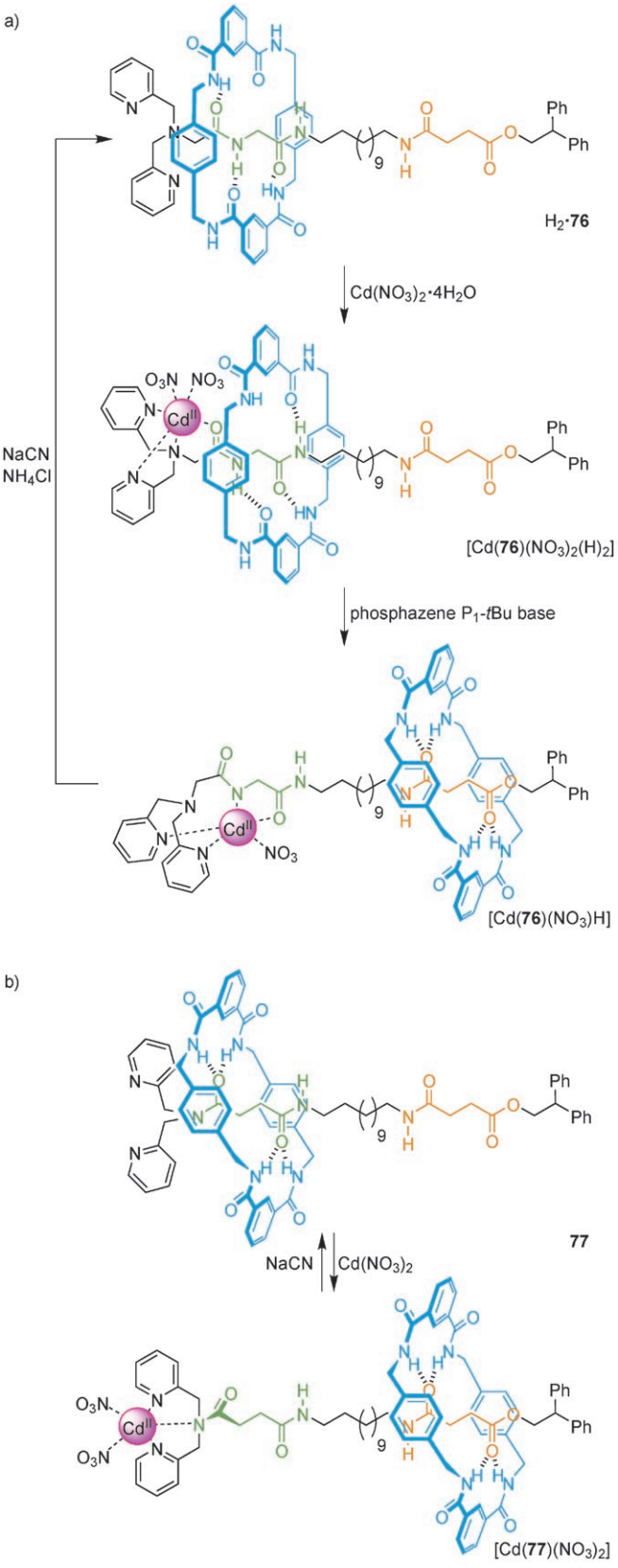

Scheme 42. a) Shuttling through stepwise competitive binding.[234] A similar shuttling mechanism can be observed with Cu^{II} ions, where the deprotonation results in a color change. b) An allosterically regulated molecular shuttle.[235]

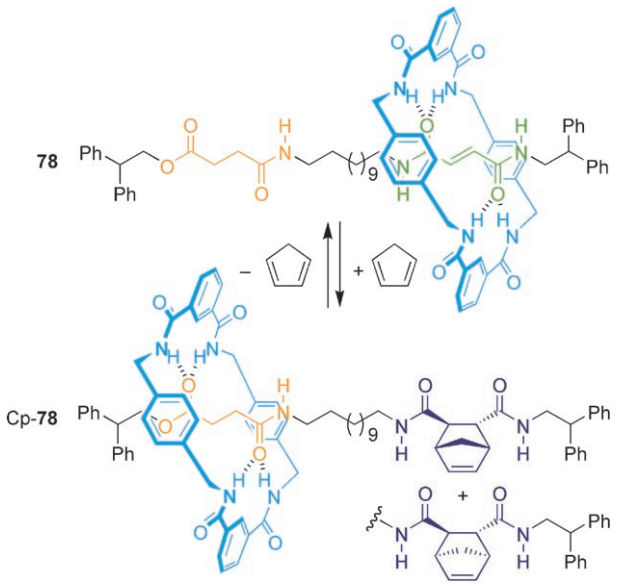

Scheme 43. Shuttling through reversible formation of covalent bonds.[237] The absolute stereochemistry for Cp-**78** is depicted arbitrarily.

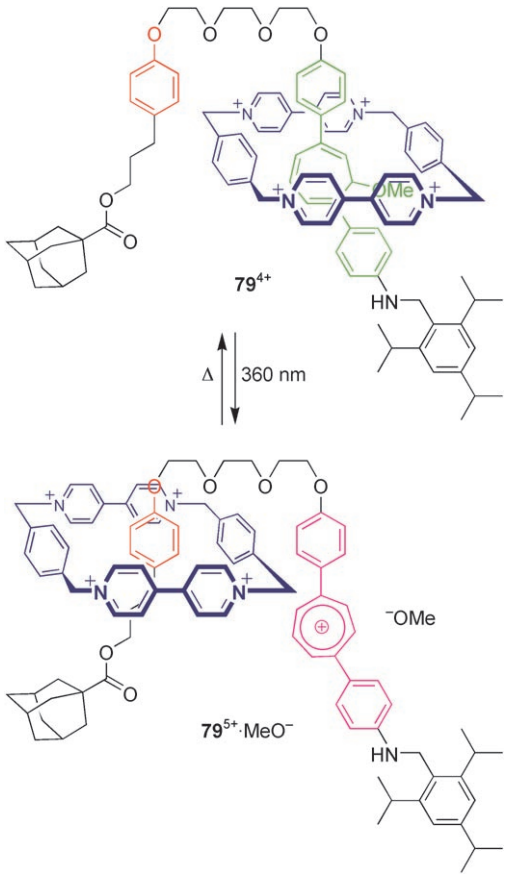

Scheme 44. Photoheterolysis-induced reversible shuttling through formation of a tropylium cation.[238]

state and for which formation of the tropylium cation can be achieved with acids, as well as through the photoheterolysis mechanism.[239]

4.3.7. Changing Configuration To Induce Net Positional Change

As with controlling motion in covalently bonded systems, isomerization processes, particularly photoisomerization processes, are a very attractive means of inducing shuttling in rotaxanes. Shuttle (*E*)/(*Z*)-**80** (Scheme 45) utilizes the inter-

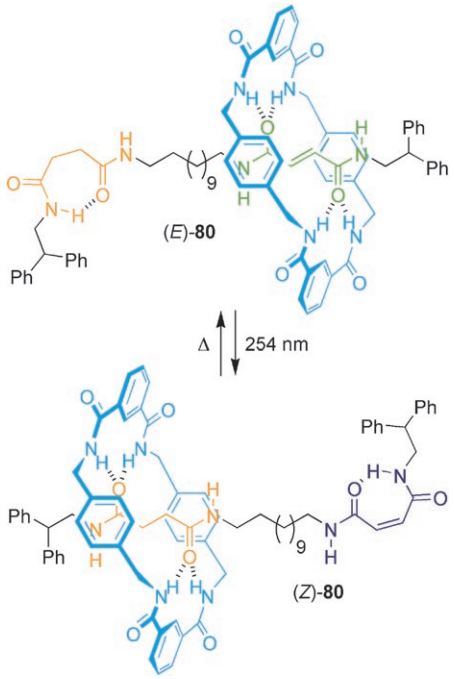

Scheme 45. Bistable molecular shuttle (*E*)/(*Z*)-**80** in which self-binding of the low affinity station in each state is a major factor in producing excellent positional discrimination.[240] Similar results are achieved when the intermediate affinity station (orange) is a succinic amide ester.

conversion of fumaramide (*trans*) and maleamide (*cis*) isomers of the olefinic unit.[240] Fumaramide groups are excellent binding sites for benzylic amide macrocycles:[241] the *trans* olefin holds the two strongly hydrogen bond accepting amide carbonyl groups in a preorganized close-to-ideal spatial arrangement for interaction with the amide groups of the macrocycle. Although a similar hydrogen-bonding surface is presented to the host, binding of the macrocycle to the succinamide station in (*E*)-**80** would result in a loss in entropy (loss of bond rotation in the succinamide group) as well as one less intracomponent hydrogen bond than would be present in the fumaramide-occupied positional isomer. The result is that only one major positional isomer of (*E*)-**80** (shown in Scheme 45) is observed at room temperature in $CDCl_3$. Photoisomerization (254 nm) reduces the number of possible intercomponent hydrogen bonds at the olefin station from four to two and so the macrocycle changes position to the succinamide station ((*Z*)-**80**, Scheme 45). Unlike many other light-switchable shuttles, this new state is essentially indefinitely stable until a further stimulus is applied to reisomerize the maleamide unit back to fumaramide.

4.3.8. Shuttling through Excited States

When operating in the light-stimulated mode, [2]rotaxane **73** (Section 4.3.4) employs a highly oxidizing photochemically excited state to trigger the electron-transfer process which results in macrocycle shuttling. After about 100 μs, the reduced rotaxane undergoes charge recombination with the radical cation of the external electron donor to regenerate the starting state. As long as photons of a suitable wavelength are supplied, this process will continue to occur indefinitely; the photochemical process can be said to be autonomous. The same principle is also true of shuttle **79** (Section 4.3.6). Attempts to induce shuttling using intramolecular electron transfer from photoexcited states have in the past been plagued by the problem of back electron transfer being fast compared to the desired nuclear motion.[207,232b] Recently, however, it has been demonstrated that a previously studied [2]rotaxane, $\mathbf{81}^{6+}$,[232b] does indeed undergo shuttling in an intramolecular charge-separated state (Figure 24).[242,3] Irradiation of the ruthenium–trisbipyridine complex (green) generates a highly reducing excited state. An intramolecular electron transfer then occurs between the excited metal center and the most easily reduced bipyridinium station (blue), on which the macrocycle prefers to sit. The result is destabilization of the macrocycle–station interactions so that the alternative bipyridinium unit (pink) is now preferred. Remarkably, in this system the back electron-transfer process is slow enough to allow shuttling of the ring towards the other station in approximately 10% of the molecules. Naturally, charge recombination quickly restores the initial state, but if photons are continually supplied, this cycle is followed indefinitely.

In another example, shuttling has been observed simply as a result of the altered electron density in a photoexcited state, without any subsequent electron-transfer reactions. The nonplanarity of the anthracene-9-carboxamide unit in [2]rotaxane **82** means the macrocycle can only form hydrogen bonds with one of the amide carbonyl groups (Scheme 46).[243] Photoexcitation of the anthracene system causes a planar conformation to be adopted in which some charge is transferred onto the adjacent carbonyl group, thus increasing its hydrogen-bond basicity. Subsequent translocation of the macrocycle occurs on a nanosecond timescale and is reflected in a change in the anthracene fluorescence spectrum, before decay of the excited state restores the original co-conformation.

These shuttles operate without the consumption of chemical fuels or the formation of waste products and they automatically reset so that they operate autonomously. It must be noted, however, that if a continuous supply of photons is provided the distribution of the rings between the two stations would reach a steady state (the exact ratio depending on the intensity of the light) within a few milliseconds. For an autonomous molecular motor (for example, **46**; see Section 2.2) a steady state of isomer populations can still correspond to a net flux in a particular direction through these forms. In switches such as these shuttles, however, after the steady state has been reached, there is no subsequent net flux of rings between the two stations at any point in time. The

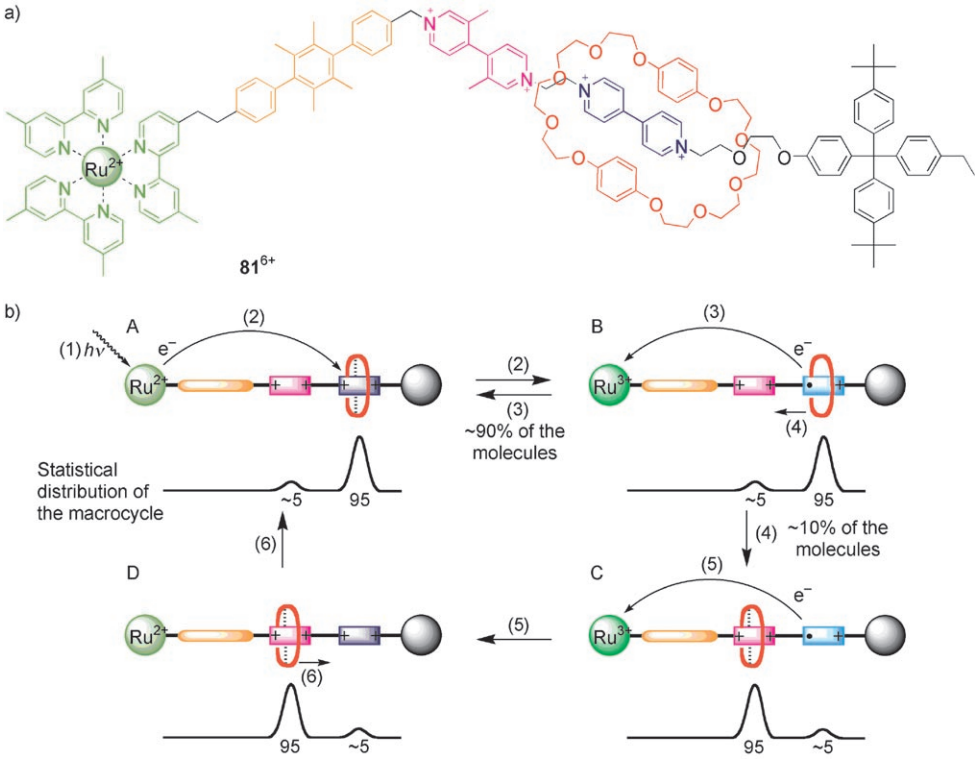

Figure 24. Chemical structure (a) and operating cycle in a schematic form (b) of a molecular shuttle $\mathbf{81}^{6+}$ operating through a photoinduced internal charge-separated state.[242,3] At equilibrium in the ground state, the ring spends most of the time over the unsubstituted bipyridinium station (blue, A). Irradiation (1) of the ruthenium complex (green) generates a highly reducing excited state, which results in electron transfer (2) to the blue station, thus weakening its electrostatic interactions with the ring (B). Normally charge recombination processes such as (3) are fast in comparison with nuclear motions, but here it is slow enough to allow approximately 10% of the molecules to undergo significant Brownian motion (4), thereby shifting the statistical distribution in this portion of the ensemble to favor the dimethylbipyridinium station (pink, C). When charge recombination (5) eventually does take place, the higher binding affinity of the blue station is restored (D). The system relaxes (6) to restore the original statistical distribution of rings (A).

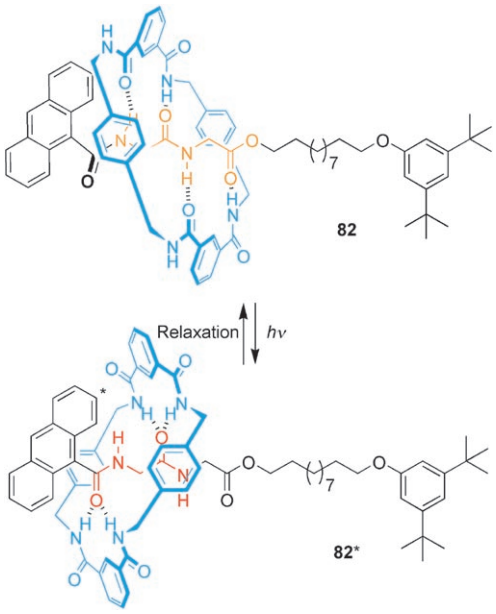

Scheme 46. Photoinduced shuttling in the singlet excited state of benzylic amide [2]rotaxane **82**.[243] The shuttling amplitude is approximately 3 Å and the lifetime of **82*** is 4.3 ns.

only way to generate net fluxes of macrocycles between the stations in these types of systems would be to rapidly switch the photon source on and off.[3]

4.3.9. *Entropy-Driven Shuttling*

Most of the shuttles which exhibit excellent positional discrimination between two stations are switched using stimuli to modify the enthalpy of the macrocycle binding to one or both stations. Generally, the effect of temperature is only to alter the degree of discrimination, not to alter the station preference.[244] In [2]rotaxane **83**, however, the macrocycle can be switched between stations simply by changing the temperature.[245] In fact, **83** is a tristable molecular shuttle: the ring can be switched between three different positions on the thread (Scheme 47).

Structurally, **83** is closely related to **80**, the differences being substitution of the isophthaloyl unit in the macrocycle for pyridine-2,6-dicarbonyl groups and replacement of the succinamide station with a succinic amide ester. In the (*E*)-**83** form, the macrocycle resides over the fumaramide station in $CDCl_3$ at all temperatures investigated. However, although the ^{1}H NMR spectrum of the maleamide isomer ((*Z*)-**83**) in $CDCl_3$ showed that the macrocycle was no longer positioned over the olefin station, the spectrum was highly temperature-dependent. At elevated temperatures (308 K) the expected succ-(*Z*)-**83** co-conformation was observed, but at lower temperatures it is the alkyl chain which exhibits the spectroscopic shifts indicative of encapsulation by the macrocycle (dodec-(*Z*)-**83**, Scheme 47). The origin of this temperature-switchable effect is the large difference in the entropy of binding ($\Delta S_{binding}$) to the succinamide and alkyl chain stations which allows the $T\Delta S_{binding}$ term to have a significant impact on the $\Delta G_{binding}$ value as the temperature is varied.[246] In the succ-(*Z*)-**83** co-conformation, the macrocycle forms two strong hydrogen bonds with an amide carbonyl group and two, significantly weaker, bonds to the ester carbonyl group. The dodec-(*Z*)-**83** co-conformation allows the formation of four strong hydrogen bonds to amide carbonyl groups, thus making it enthalpically favored by about 2 kcal mol^{-1}. At

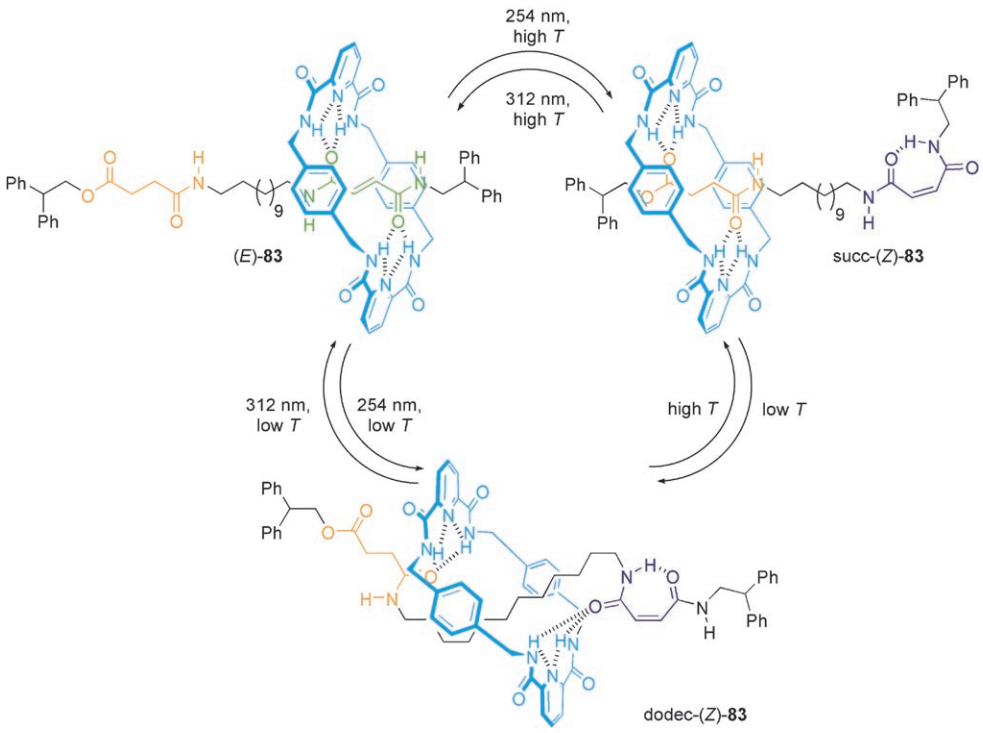

Scheme 47. A tristable molecular shuttle **83**.[245]

low temperatures, where the effects of entropy are less significant, the molecule adopts the dodec-(*Z*)-**83** co-conformation. At higher temperatures, the increased contribution from the $T\Delta S_{binding}$ term favors the entropically preferred succ-(*Z*)-**83** co-conformation.[247]

4.3.10. *Shuttling through a Change in the Nature of the Environment*

A significant advantage[248] of using temperature to induce a change in net position of the macrocycle in a molecular shuttle is that no chemical reaction is involved and any property change associated with the new state cannot arise from a change in the covalent structure of the molecule. The same holds true for switching induced by a change in the nature (solvation or polarity) of the environment of the shuttle. The benzylic amide macrocycle in amphiphilic rotaxanes (including those discussed in Section 4.2.1) can be shuttled between various hydrogen-bonding stations ($CDCl_3$ and most nonpolar solvents) and an alkyl chain ([D_6]DMSO, H_2NCHO).[199,249] A similar effect has been observed in a range of poly(urethane/crown ether rotaxane)s.[250]

Many of the examples of stimuli-induced shuttling described in Sections 4.3.1–4.3.9 display remarkable degrees of control over the positioning and dynamics of submolecular fragments. They utilize a number of different stimuli-induced processes to trigger changes in the net position of macrocycles over large distances (up to ca. 15 Å in the case of **71**, **73**, and **80**) and operate over a range of timescales (a complete switching cycle in **73** is over in ca. 100 μs while, in **80**, both states are effectively indefinitely stable). Note, however, that all these shuttles exist as an equilibrium of co-conformations and it is just the position of the equilibrium that is being varied.[220] As the position of equilibrium changes, detailed balance is broken and it is this that can allow a useful mechanical task to be performed by Brownian motion of the macrocycle.

4.4. *Compartmentalized Molecular Machines*

We discussed in Section 4.3.2 how stimuli-responsive molecular shuttles can be considered in terms of a machine (the thread) which transports a particle (the interlocked macrocycle) between two sites (compartments) on a one-dimensional potential-energy surface. This approach provides a basic framework with which to explore some of the ideas to create, control, order, and manipulate non-equilibrium conformations and co-conformations raised at the end of Section 1.4.2. In all of the examples in Section 4.3, an external stimulus alters the relative binding affinities of the stations for the macrocycle by placing the system momentarily out of co-conformational equilibrium. Detailed balance is broken and the system acts to restore balance through biased Brownian motion of the macrocycles towards the new global minimum. Detailed balance, however, can be considered to result from two separate properties of the system (Section 1.4.1): the statistical distribution of a quantity (an imbalance which provides the thermodynamic impetus for net transport) and the ability of that quantity to be dynamically exchanged (which provides the communication necessary for transport to occur).[51] In the switchable shuttles of Section 4.3, the macrocycle is at all times able to seek its equilibrium statistical distribution along the full length of the thread, and the position of the substrate is always indicated by the state of the machine. To create artificial Brownian machines which are more sophisticated than simple positional switches, control over the kinetics for exchange of the substrate between two sites of the machine must be introduced.

Rotaxane system **84** is able to change the average position of the macrocycle irreversibly through a fundamentally different mechanism to previous shuttles (Scheme 48).[32] In **84** the two stations are structurally identical (but distinguishable: note the different stoppers) and a bulky silyl ether acts as a barrier which prevents the ring from moving between them. The system starts out statistically unbalanced (succ1-**84**, because of the synthetic route used to access it). The stimulus that leads to the net change in position of the macrocycle is a "linking" operation—removal of the silyl ether—which switches "on" dynamic exchange of the macrocycle between the two stations and allows the system to move towards equilibrium, which results in an average displacement of the

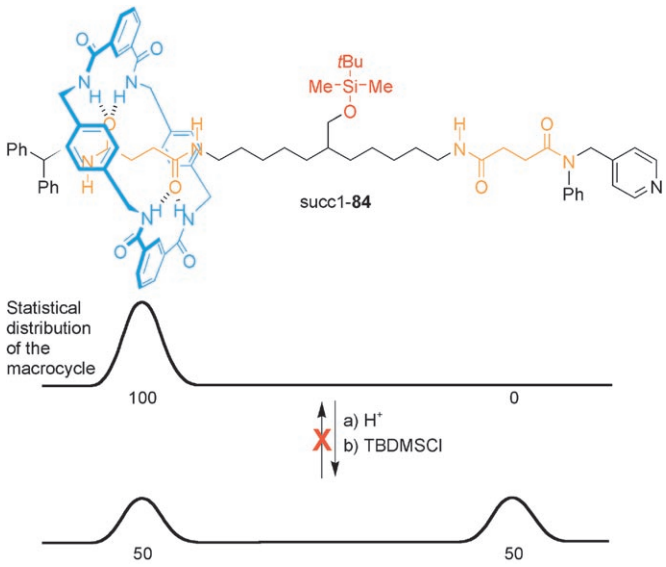

Scheme 48. Operation of a compartmentalized Brownian molecular machine that acts as an irreversible switch.[32] As the macrocycle distributions on the thread are determined when the two compartments are unlinked, they are independent of factors such as temperature or solvent. TBDMS = *tert*-butyldimethylsilyl.

macrocycle half the distance separating the two stations. This is a molecular-level form of "escapement", the element of the mechanism that controls the release of potential energy to drive mechanical motion in clocks and other macroscopic mechanical devices. Raising the barrier by applying an "unlinking stimulus" resets the machine (the thread) without undoing the task just performed. However, applying the linking stimulus again after the machine is reset, does not change the average position of the macrocycle a second time, because the system is now statistically balanced. This stimuli-induced irreversible net change in the position of the macrocycle represents a new type of molecular shuttle in phenomenological terms: its operation is irreversible and the state of the machine (the thread) does not determine the position of the substrate.

Combining control over exchange between the two stations (kinetics) with the ability to modulate their relative binding affinities (thermodynamics) led to the creation of another novel type of simple molecular machine system, namely **85** (Scheme 49).[32] Here, the machine is statistically balanced (85% of the macrocycles on the fumaramide (green) station, 15% on the succinamide (orange) station), and unlinked (and therefore not in equilibrium) by simply removing and reattaching the silyl group (Scheme 49, steps a and c). From this balanced state, a balance-breaking stimulus is applied (irradiation at 312 nm, generating a 49:51 ± 2% E:Z photostationary state), followed by removal of the kinetic barrier ("linking stimulus") which allows balance to be restored by biased Brownian motion of the ring towards the new equilibrium distribution. Restoring the barrier ("unlinking stimulus") makes the system unlinked and not in equilibrium, although statistically balanced. The resetting step (a different balance-breaking stimulus, to promote the $Z \rightarrow E$ olefin isomerization), makes the system statistically unbalanced, unlinked, and not in equilibrium. After the operational cycle of the machine, approximately 56% of the macrocycles are located on the succinamide station. The transportation of the macrocycle in **85** is repeatedly reversible between the statistically balanced (85:15) and statistically unbalanced (44:56) ratios of fum-(E)-**85** to succ-(E)-**85**.

In this rotaxane the thread performs the task of directionally changing the net position of the macrocycle—and since the succinamide station binds the macrocycle more weakly than the fumaramide station, the thread moves the macrocycle energetically uphill—while itself returning to its

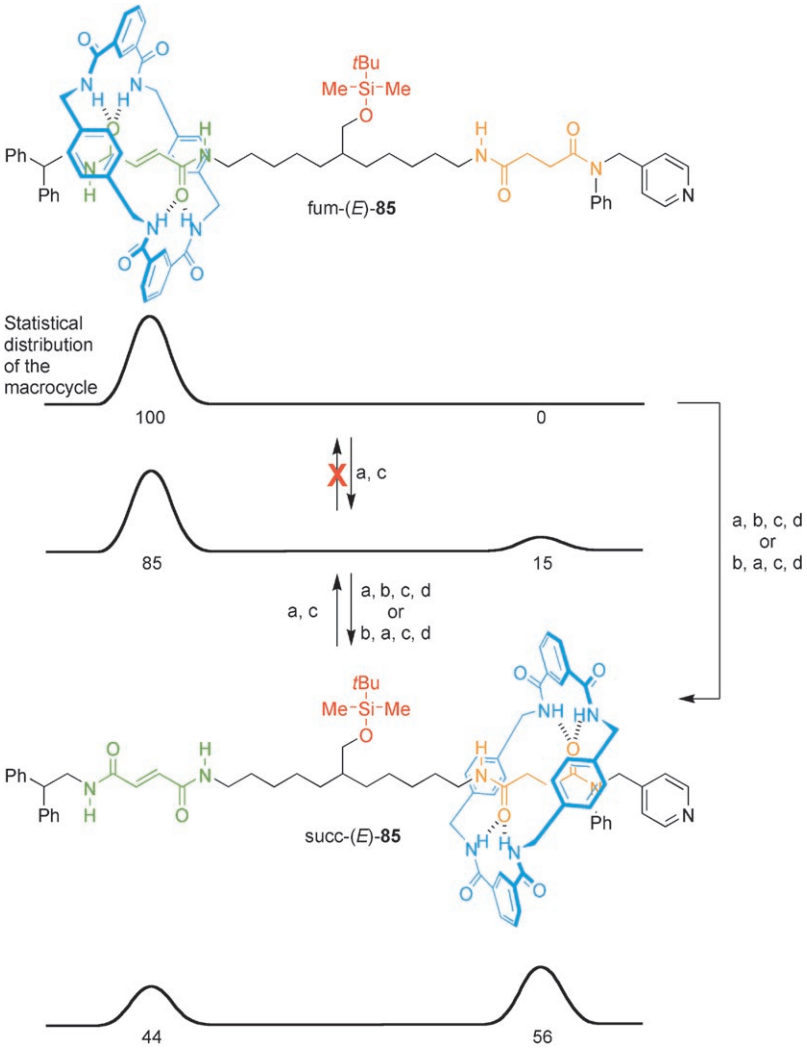

Scheme 49. Operation of compartmentalized molecular machine **85** which corresponds to a two-state Brownian flip-flop.[32] Operation steps: a) Desilylation (80% aqueous acetic acid); b) $E \rightarrow Z$ photoisomerization ($h\nu$ at 312 nm); c) resilylation (TBDMSCl); and d) $Z \rightarrow E$ thermal isomerization (catalytic piperidine). As the macrocycle distributions on the thread are determined when the two compartments are unlinked, they are independent of factors such as temperature or solvent.

initial state. This behavior amounts to "ratcheting", a characteristic feature of the operating mechanisms of many biological molecular machines. A thermodynamically unfavorable concentration gradient of the macrocycle between the compartments is the result, which is precisely the function envisaged for the thought-machine pressure demons discussed in Section 1.2.1. Unlike the thought machines, however, the position of the Brownian particle in **85** has no role in the mechanism.[251] Rather the rotaxane machine carries out a sequence of four steps (independent of the position of the particle) which govern in turn the thermodynamics and the kinetics for transport between the two stations (Figure 25): balance-breaking 1, linking, unlinking, balance-breaking 2 (resetting, of the machine not the substrate).

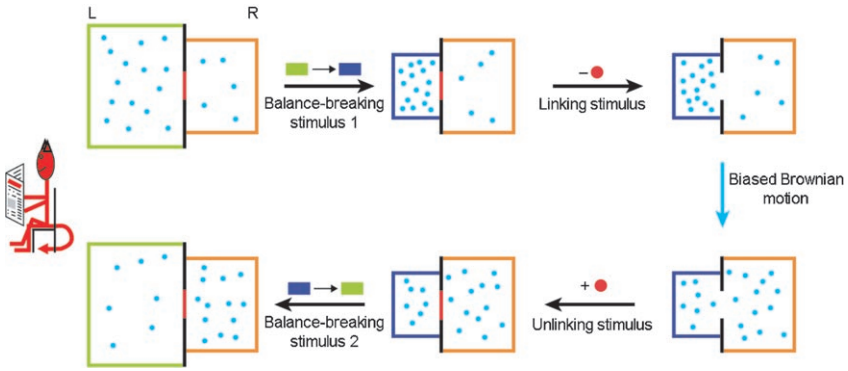

Figure 25. The operation[32] of machine–substrate system **85** in Scheme 49 is the experimental realization (albeit in non-adiabatic form) of the transportation task required of Smoluchowski's trapdoor[16] (Figure 4a) and Maxwell's pressure demon[15c] (Figure 2b). The mechanistic equivalent of the schematic representations from Section 1.4.2 is shown above. The colors of the compartments, particles, and door are the same as the corresponding elements of **85**. The initially balanced (in proportion to the sizes of the two compartments) distribution of the Brownian particles between the left (L) and right (R) compartments becomes statistically unbalanced by a change in the volume of the left-hand compartment. Opening the door allows the particles to redistribute themselves according to the new size ratio of the compartments. Closing the door ratchets the new distribution of particles. Restoring the left-hand compartment to its original size then results in a concentration gradient of the Brownian particles across the two compartments. There is no role for an information-gathering demon in this mechanism.

Significantly, examining the state of the machine (the rotaxane thread) in **85** does not provide information regarding the state (distribution) of the substrate. It is only from the history of the machine's operations that the distribution of the substrate can be known; in other words, the net position of the macrocycle in rotaxane **85** is a consequence of a form of sequential logic.[252] The behavior of **85** is characteristic of a two-state (one-bit) memory or "flip-flop" component in electronics[253] and therefore **85** is the first example of a new class of simple molecular machine: a two-state Brownian flip-flop. A flip-flop maintains its effect on a system indefinitely until an input pulse operates on it that causes its output to change to a new indefinitely stable state according to defined rules.[254]

From the analysis of the behavior of these rotaxanes, and the analysis of the workings of the fluctuation-driven transport mechanisms discussed in Section 1.4.2, there appear to be four phenomenological terms (ratcheting, escapement, balance, and linkage) that are crucial for controlling the non-equilibrium distribution of Brownian substrates with compartmentalized molecular-level machines:

1) "Ratcheting"[32] is an often used, but previously ill-defined, process in chemical terms. Unfortunately, this vagueness has led to the term sometimes being applied to describe phenomena that are unrelated to Brownian ratchet mechanisms. Ratcheting is the capturing of a positional displacement of a substrate through the imposition of a kinetic energy barrier which prevents the displacement being reversed when the thermodynamic driving force is removed. The key feature of ratcheting is that the ratcheted part of the system is not linked with (that is, not allowed to exchange the substrate with) any part of the system that it is ratcheted from. Ratcheting is a crucial requirement for allowing a Brownian machine to be reset without undoing the task it has performed;
2) "Escapement"[32] is the counterpart to ratcheting and consists of the (directional) release of a ratcheted substrate in a statistically unbalanced system by lowering a kinetic energy barrier (by linking). The key feature of escapement is that it requires the linking of two unbalanced parts of a system that were previously unlinked. An escapement step must be subsequently ratcheted for a machine to be able to do work repetitively on a substrate;
3) "Balance"[32,51] is the thermodynamically preferred distribution of a substrate over a machine or parts of a machine. The impetus for net transportation of a substrate between two parts of a machine comes from the balance being broken (note that balance being broken is not the same as detailed balance being broken, balance is the thermodynamic driving force for detailed balance);
4) "Linkage"[32,51] is the communication necessary for transportation of a substrate to occur between parts of a machine. However, the ability to exchange the substrate between the linked parts is not in itself enough for a task to be performed, there must also be a driving force for it to occur (see above). Linking and unlinking operations are purely kinetic parameters and so can be accomplished by simply changing the rate of reactions rather than introducing or removing physical barriers.

The statistical balance of a dynamic substrate and whether the parts of the machine acting on the substrate allow exchange of the substrate or not appear to be key factors that determine whether the machine can perform a useful task or not. In fact, it appears that the behavior of a molecular machine towards a substrate can be defined by the changing relationship (linked/unlinked, balanced/unbalanced) between the parts of machine interacting with the substrate.

We can see that there are three fundamental types of Brownian machine that act through various combinations of

balance-breaking, linking/unlinking, ratcheting, and escapement steps: Brownian switches (for example, the switchable molecular shuttles in Section 4.3), Brownian flip-flops (for example, rotaxane **85**), and Brownian motors (for example, **17** or **46**, see Sections 2.1.2 and 2.2). By combining these simple Brownian machine types with other combinational and/or sequential operations based on Boolean logic, machines of increasing complexity can be envisaged (Figure 28).

1) A "Two-state (or multistate) Brownian switch"[32] is a machine that can reversibly change the distribution or position of a Brownian substrate between two (or more) distinguishable sites as a function of the state of the machine. It does this by biasing the Brownian motion of the substrate (Figure 26a). Classic stimuli-responsive molecular shuttles, such as those discussed in Section 4.3, are examples of two-state (or three-state, Section 4.3.9) Brownian switches. An "irreversible Brownian switch" is a "once only" machine, such as succ1-**84** (Scheme 48), which irreversibly changes the distribution or position of a Brownian substrate in response to an external stimulus (Figure 26b).

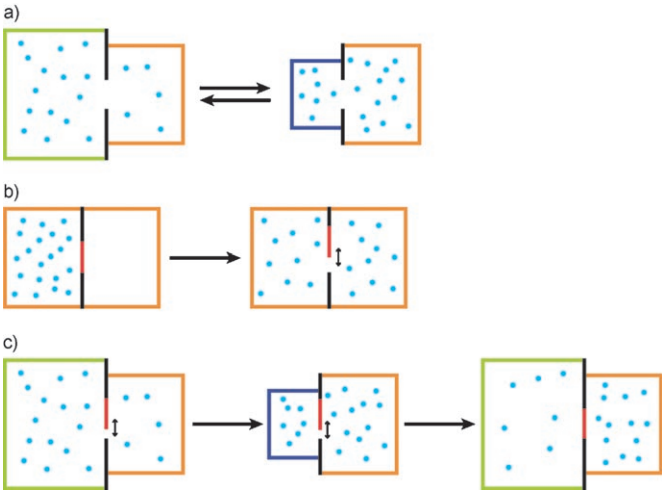

Figure 26. Schematic representations of some simple compartmentalized molecular-level machines. a) Two-state Brownian switch. b) Irreversible Brownian switch. c) A two-state Brownian flip-flop (shown operating through a partial energy ratchet mechanism; other mechanisms can achieve the same machine function).[32]

2) A "Two-state (or multistate) Brownian flip-flop"[32] is a machine that can reversibly change the distribution or position of a Brownian substrate between two (or more) distinguishable sites and can be reset without restoring the original distribution of the substrate (Figure 26c). The statistical distribution of the substrate cannot be determined from the state of the flip-flop but rather is determined by the history of operation of the machine. Rotaxane **85** is an example of a two-state Brownian flip-flop.
3) A "Brownian motor"[32,255] is a machine that can repetitively and progressively change the distribution or position of a Brownian substrate, during which the machine is reset without restoring the original distribution or position of the substrate (Figure 27). Like a flip-flop, a Brownian motor affects a system as a function of the pathway that the machine takes, not as a function of state.[6] Indeed, even at the machine's steady state it can produce a net flux of a substrate in a given direction. The rotary motors designed by Feringa and co-workers (see Section 2.2) are examples of this category of machines. A catenane-based two-stroke rotary Brownian motor in which the substrate is repetitively transported between two sites through two alternating pathways is given in Section 4.6.3.

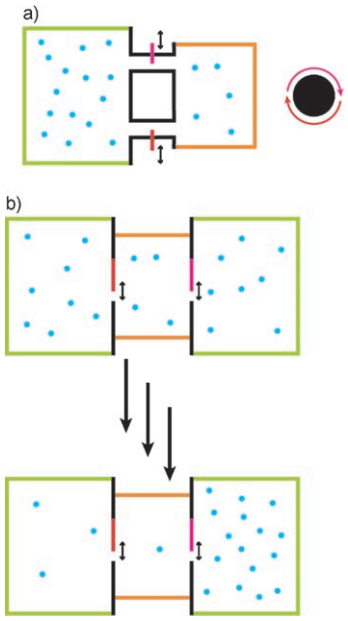

Figure 27. Schematic representations of two types of Brownian motors: a) a two-stroke rotary motor and b) a three-compartment translational motor or pump.[32]

4) In addition to switches, flip-flops, and motors, other machines can be envisaged that exploit selective, controlled manipulation of Brownian moieties (parts of the machine molecule or a substrate) far from equilibrium. By combining balance-breaking and linking/unlinking steps with Boolean logic functions, machines that can move a substrate (or itself) in different directions (Figure 28a) or sort and separate different ions (Figure 28b) can be invented. We have little doubt that many other types of machines that exploit and control non-equilibrium distributions of conformations and co-conformations will be designed and realized in the future.

The requirements for linking and unlinking, for example, can also be achieved by using a substrate that has two or more sites that can interact with the track. In its simplest form, this requires a "walker" with at least two "feet" (similar to biological molecular motors such as kinesin) and directional motion along the track can then occur by several different categories of energy ratchet-based mechanisms, for example,

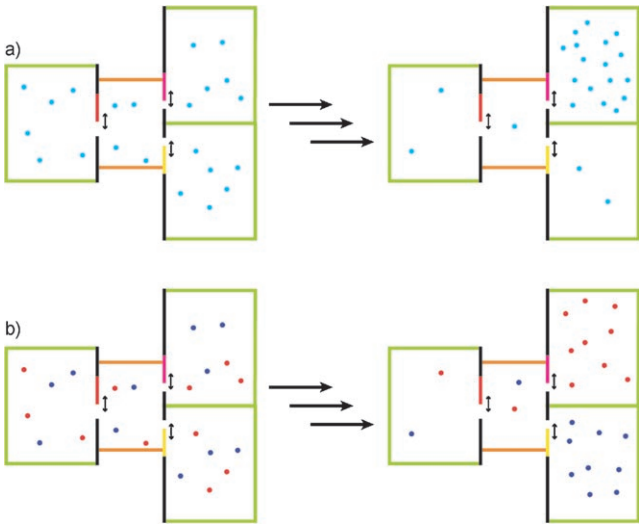

Figure 28. Schematic representations of some compartmentalized molecular-level machines that combine ratcheting and escapement with Boolean logic operations: a) a four-compartment Brownian machine that pumps a substrate in a given (variable) direction. Deciding which one of the purple or yellow gates is used for ratcheting determines whether the substrate is transported to the top compartment or the bottom. b) A four-compartment Brownian machine that sorts and separates different ions (for example, red = Na^+, blue = K^+). A logic operation providing selective access through each of the purple and yellow gates ensures one type of ion is pumped into each compartment.[32]

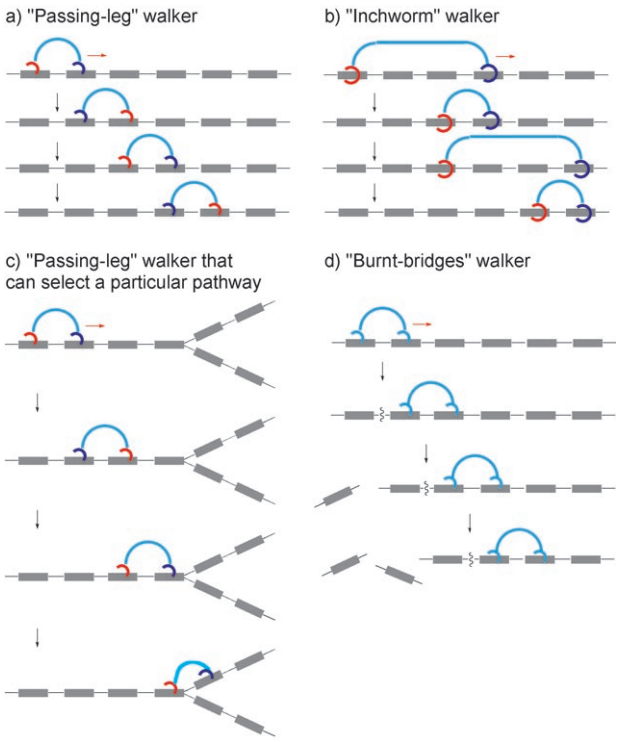

Figure 29. Schematic representations of compartmentalized molecular machines which use attachment of the substrate to a track to prevent a Brownian substrate from adopting a statistical thermodynamic equilibrium distribution. a) A "passing-leg" walker is ratcheted by fixing the "front" foot to the track while the rearmost foot swings forward to bind at a site further down the track in the direction of travel. b) In an "inchworm" walker, the order of the feet is prevented from changing (for example, by using rings to mechanically link to the track as illustrated here) and ratcheting occurs by first fixing the rear foot to the track while the front moves, then fixing this foot in place while the rear one moves. c) These mechanisms can be combined with more complex functions such as Boolean logic operations to allow a passing-leg walker to choose between different pathways. d) Information ratchet mechanisms can also be employed by walker compartmentalized machines, such as a "burnt-bridges" walker which destroys the track to the rear whenever a step is taken in the intended direction of travel.

"passing-leg" (Figure 29a) and "inchworm" (Figure 29b). Using the ideas outlined above (and in Section 1.4.3) it appears to us that each of these mechanisms can be realized through several different permutations of binding sites on the track (which may be active or passive) and on the walker "feet" (which may also be active or passive), but the key elements of the mechanism are the same. Compartmentalization is achieved by having, at all times, at least one foot kinetically associated with a particular site on the track, while a free foot seeks out the most preferable binding site for itself by Brownian motion. Directionality is achieved by the relative arrangement of stations in the region of space that the free foot can explore—controlled by the mode of walking (stepping or inchworm) and the length of linker between the feet (which could also be varied in some mechanisms). In Section 4.6.2 we will see that an inchworm-type mechanism around a cyclic track can be achieved in a [3]catenane where the two "walking" rings are not joined, although it would not be possible to extend this to a repetitive linear track without connecting them together. Such systems which operate solely through changes in the walker itself may be regarded as "self-propelled" walkers (see Section 6.2).

Just like compartmentalized molecular machines in which linking/unlinking is controlled by changes in the track (Figures 26–28), one can also envisage walkers which incorporate more complex functions, such as Boolean logic operations to select between a choice of pathways (Figure 29c). Furthermore, an information ratchet mechanism may also be used to control the directionality of a walker, for example a walker that irreversibly destroys its track when making a step in one direction, but not the other (Figure 29d).

4.5. Controlling Rotational Motion in Rotaxanes

Macrocycle pirouetting in rotaxanes presents two challenges in terms of control: the frequency of the random motion and its directionality. The former can be achieved through temperature, structure, electric fields, light, and solvent effects; the latter has yet to be demonstrated.[256]

Alternating current (a.c.) electric fields represent an ideal stimulus with which to control submolecular dynamics in many applications. In the two [2]rotaxanes **86** and (*E*)-**87** (Scheme 50), it was observed that application of a.c. fields of around 50 Hz resulted in unusual Kerr effect responses which are unique to the interlocked architecture (they are not observed for either of the components alone).[257] Increasing

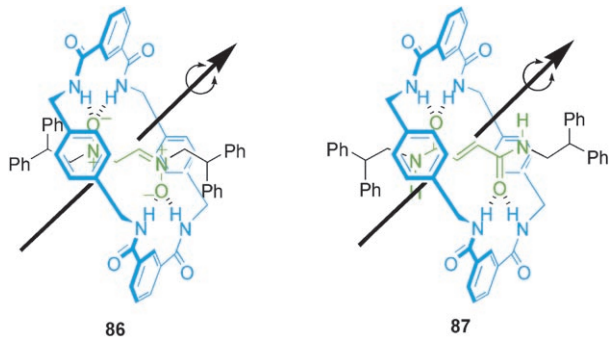

Scheme 50. [2]Rotaxanes **86** and **87** in which the rate of pirouetting can be controlled by application of an alternating current electric field.[257]

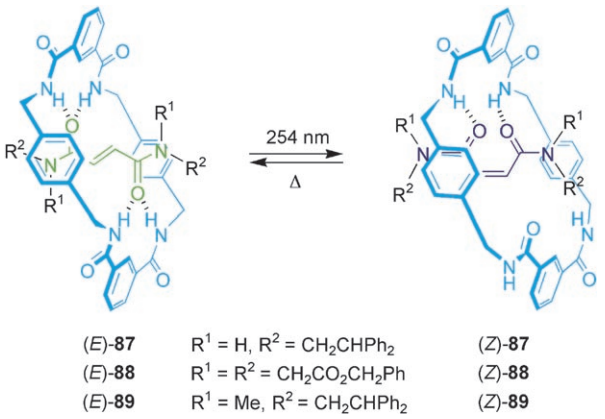

Scheme 51. Photoisomerization of [2]rotaxanes (*E*)-**87**–**89** which results in pirouetting rate enhancements of up to six orders of magnitude.[259] The reverse process (*Z*→*E* isomerization) can be effected by heating a 0.02 M solution of the *Z* rotaxanes at 400 K, generating bromine radicals (cat. Br_2, *hν* 400 nm), or through reversible Michael addition of piperidine (RT, 1 h).

the temperature had the same effect as decreasing the field strength, namely, enhancement of the response. The same sort of Kerr effects have previously been seen with rigid-rod polymers and correlated with the dynamics of the polymer backbones.[258] Variable temperature (VT) ^{1}H NMR experiments and molecular-modeling studies confirmed that macrocycle pirouetting is the only dynamic process in the rotaxanes on this timescale. The experimental and theoretical studies also predict the slightly more complex Kerr effect response observed experimentally for **87** relative to that of **86**. It was concluded that application of an a.c. electric field attenuates macrocycle pirouetting in **86** and **87**, probably by polarizing and strengthening intercomponent hydrogen bonding. The extent of the dampening can be varied with the strength of the applied field; even modest fields of about 1 V cm^{-1} produce pirouetting rate reductions of two to three orders of magnitude.

An alternative strategy for affecting pirouetting rates is to apply a stimulus which directly alters the structure of the thread or macrocycle. This has been demonstrated to great effect for olefin-containing [2]rotaxanes (*E*)/(*Z*)-**87**–**89** (Scheme 51).[259] The decrease in intercomponent binding affinity on photoisomerization of the fumaramide units in (*E*)-**87**–**89** to the *cis*-maleamide isomers gives a huge increase in the rate of pirouetting of more than six orders of magnitude. The switching process is reversible: subjecting the maleamide rotaxanes to heat or a suitable catalyst results in reisomerization to the more thermally stable *trans*-olefin isomers, with accompanying reinstatement of the strong hydrogen-bonding network.

Binding of sodium or potassium cations to a crown ether embedded in a rotaxane macrocycle has been shown experimentally to retard co-conformational Brownian motion, particularly pirouetting.[260] Removal of the metal template from a rotaxane can induce rotation of the ring relative to the thread,[261] while incorporating two different coordination sites into a macrocycle can be used to control the rotational orientation of components in a manner analogous to the translational shuttling modes discussed in Section 4.3.4.[262] This pirouetting motion, however, tends to be faster than the analogous shuttling modes and in the particular example illustrated in Scheme 52 for [Cu(**90**)], the pirouetting rate is further enhanced by using an unhindered bipyridine ligand in the thread, from which the bulky stoppers are well separated.[262e]

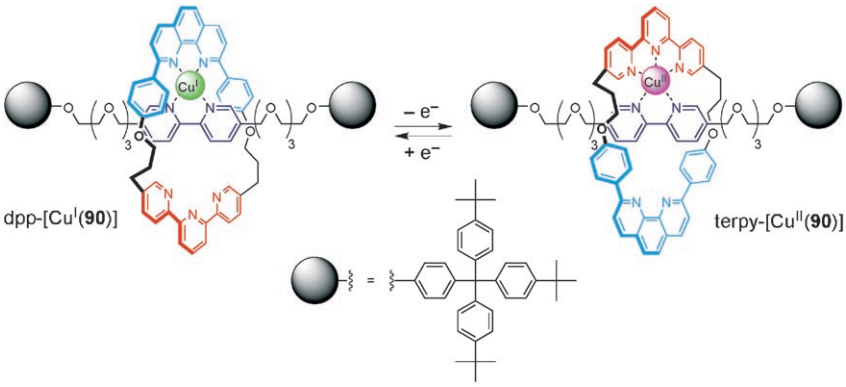

Scheme 52. Electrochemically triggered rapid pirouetting motion in metal-templated [2]rotaxane [Cu(**90**)].[262e]

4.6. Controlling Rotational Motion in Catenanes

4.6.1. Two-Way and Three-Way Catenane Positional Switches

As with rotaxanes, stimuli-induced structural changes can be used to alter the rates of the thermal intercomponent motions in catenanes. For example, photoisomerization of an azobenzene unit in a π-donor/acceptor [2]catenane was found to influence the rate of dynamic processes, presumably by altering the size of the macrocycle cavity.[263] Electrochemical reduction of a homocircuit benzylic amide [2]catenane completely halts the circumrotational process as a result of the formation of an intercomponent covalent bond between the macrocycles.[264] Protonation of a porphyrin free base in a catenane was found to result in a rearrangement to minimize

repulsive electrostatic interactions, thus altering the rate of pirouetting of a tetracationic cyclophane.[191w,265] Electrochemical studies suggest similar conformational and dynamic changes can occur on reduction of the cyclophane.[266]

The fundamental principles for controlling the position of a macrocycle on a thread in a rotaxane and the relative positions and orientations of the rings in a catenane are the same. For example, the behavior of amphiphilic homocircuit [2]catenane **91** is governed by the same driving forces that cause solvent-induced shuttling in amphiphilic shuttle **58** (see Sections 4.2.1 and 4.3.10).[267] In halogenated solvents such as $CDCl_3$, the two macrocycles of **91** interact through hydrogen bonds (amido-**91**, Scheme 53, also the structure observed in the solid state) whereby each constitutionally identical ring adopts a different conformation, one effectively acting as the host (convergent H-bonding sites) and the other the guest (divergent H-bonding sites). Pirouetting of the two rings interconverts the host–guest relationship rapidly on the NMR timescale in $CDCl_3$ at RT. In a hydrogen-bond-disrupting solvent such as $[D_6]$DMSO, however, the preferred co-conformation has the amide groups exposed on the surface where they can interact with the surrounding medium, while the hydrophobic alkyl chains are buried in the middle of the molecule to avoid disrupting the structure of the polar solvent (alkyl-**91**, Scheme 53).[268]

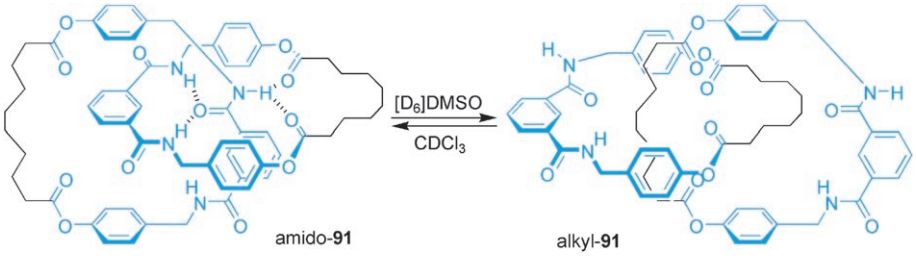

Scheme 53. Translational isomerism in an amphiphilic benzylic amide [2]catenane **91**.[267]

In heterocircuit [2]catenanes such as $\mathbf{92}^{4+}$ the change in the position of one macrocycle with respect to the other is even more reminiscent of shuttling in [2]rotaxanes (Scheme 54).[184l,228a] In the ground state ($\mathbf{92}^{4+}$) the tetracationic cyclophane (blue) mostly sits over the more electron rich TTF station (green). Oxidation of the TTF (green→pink) to either its radical cation or dication ($\mathbf{92}^{5+}$ or $\mathbf{92}^{6+}$) can be achieved chemically or electrochemically and results in the cyclophane being positioned over the dihydroxynaphthalene unit (DNP, red). The movement can be reversed by reduction of the TTF unit back to its neutral state. Just as for the rotaxane derivatives in this series (Section 4.3.4), [2]catenane $\mathbf{92}^{4+}$ exhibits rapid shuttling away from the TTF station and slower kinetics for the return step.[228f,269] There is, of course, no control over the direction in which the motion occurs; the cyclophane has a choice of two routes between the stations in both directions and half the molecules will change position in one direction and the other half in the other.[270,271]

Electrochemical co-conformational switching has also been observed for [2]catenane **93**, which features a crown ether threaded onto a large macrocycle containing two cyclen rings containing different metal ions (Scheme 55).[272] In both the solution and solid states, the crown ether sits over the

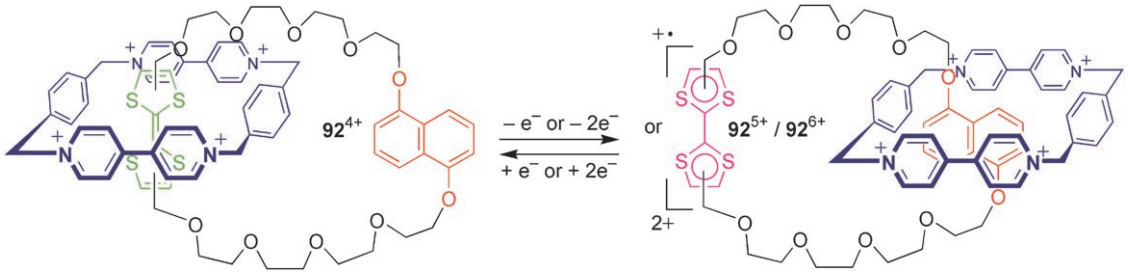

Scheme 54. Chemically and/or electrochemically driven translational isomer switching of [2]catenane $\mathbf{92}^{4+}$ to $\mathbf{92}^{5+}$/$\mathbf{92}^{6+}$.[184l,228a]

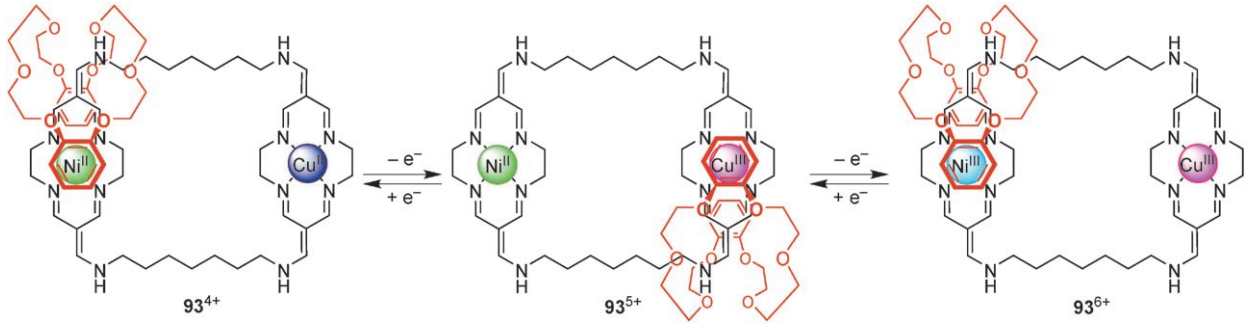

Scheme 55. Electrochemically induced co-conformational changes in a heterodinuclear [2]catenane.[272]

Ni^{II} center. However, the Cu^{II} ion is more easily oxidized than Ni^{II} ion, and the resulting Cu^{III} center provides an effective electron-poor station for the π-donor macrocycle. Subsequent oxidation of the nickel ion moves the crown ether back to its original site.

In the classical metal-templated [2]catenates pioneered by the Sauvage group (for example, [Cu^{I}(**94**)], Scheme 56),[273]

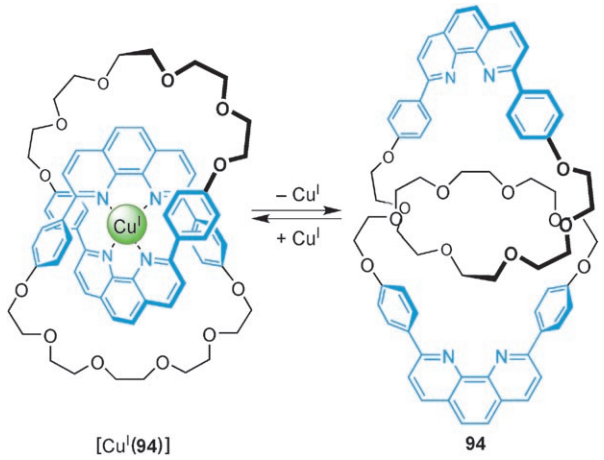

Scheme 56. The original metal-templated [2]catenate, [Cu^{I}(**94**)].[273] Removal of the Cu^{I} ion results in reorganization of the organic ligands to present the diphenylphenanthroline units (light blue) on the outer surface.[274] The resultant [2]catenand free ligand can complex a wide range of metal ions.[275,276]

removal of the metal template to give the corresponding [2]catenand often results in significant co-conformational changes. In nonpolar solvents and the solid state, the polyether chains are buried in the center of the molecule, thus presenting the heterocyclic ligands to the outside.[274] The process is often fully reversible—indeed, complexation of a variety of cations can be achieved with the [2]catenand (including Li^{+}, Fe^{2+}, Co^{2+}, Ni^{2+}, Cu^{+}, Zn^{2+}, Ag^{+}, Cd^{2+}, and even H^{+}), in each case restoring the original complexed co-conformation shown in Scheme 56.[275,276]

Introducing a second, orthogonal, set of possible interactions between the two rings can make the co-conformational changes better defined. The presence of π-electron-donor (red) and π-electron-acceptor (dark blue) units on the two macrocycles in [2]catenate [Cu^{I}(**95**)]$^{5+}$ (Scheme 57)[277] means that a precisely defined co-conformation ensues on demetalation to give [2]catenand **95**$^{4+}$, which is stabilized by π–π charge-transfer interactions. A similar switching process can also be achieved reversibly simply by protonation and deprotonation (Scheme 57). Anion binding has been shown to result in an alteration of the co-conformational arrangement of a bipyrrole-based [2]catenane templated by hydrogen-bonding interactions.[278]

In a series of [2]catenates formed around square-planar templates, demetalation does not result in a significant co-conformational change.[279] [2]Catenane **96** was generated in this fashion, but it was then found that the templating metal (Pd^{II}) can either be reinserted along with concomitant deprotonation of two amide nitrogen atoms to give the original catenate or else complexation to only one ring can be achieved, thereby producing a half-turn in the relative orientation of the components.[280] All three forms are fully interconvertible (Scheme 58) and can be observed in both solution and the solid state.

Steps towards photochemical switching in metal-templated catenates have also recently been taken, by making use of the ready access of dissociative d-d* excited states in ruthenium(II) complexes with distorted octahedral geome-

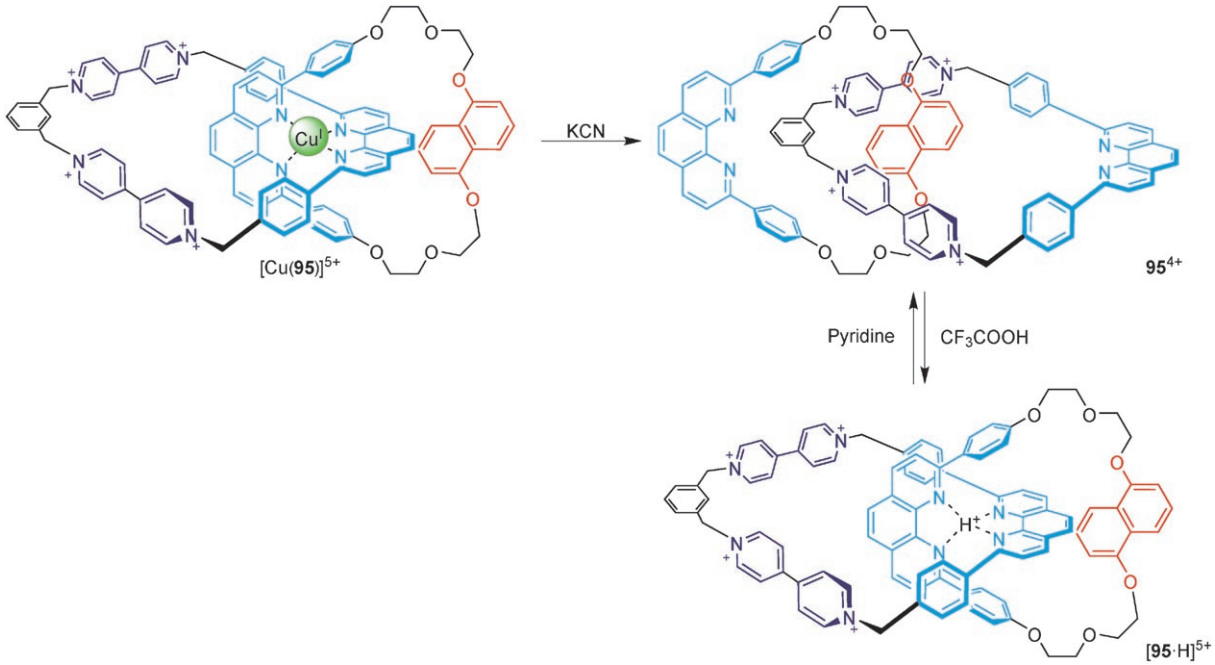

Scheme 57. Reversible co-conformational switching in a hybrid coordination/charge transfer [2]catenane.[277]

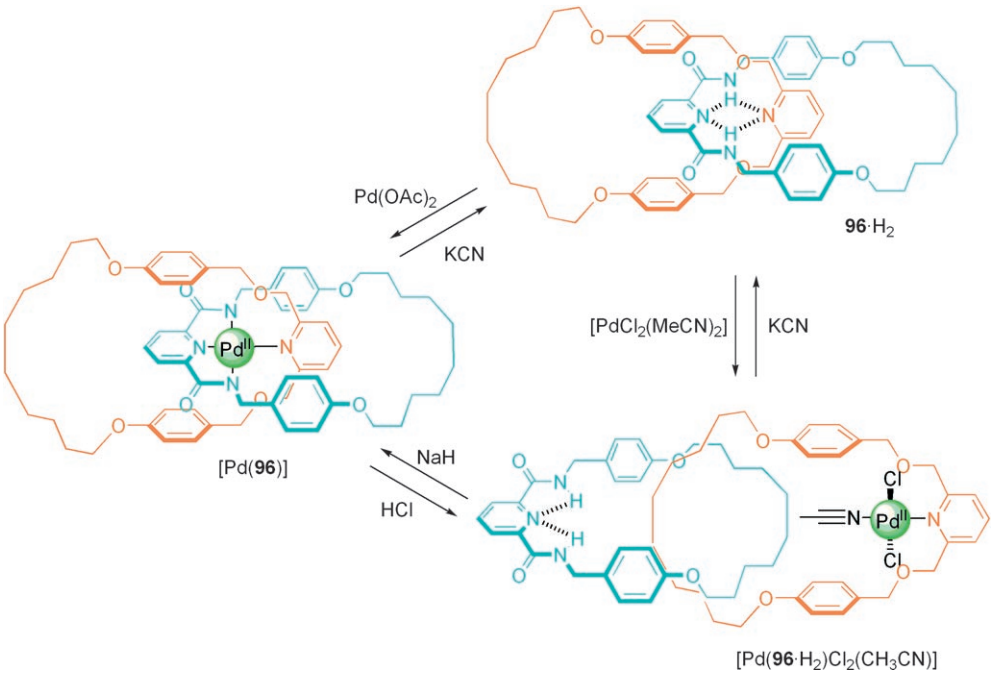

Scheme 58. Half-rotation in a [2]catenane through interconvertible Pd^{II} coordination modes.[280]

tries.[281] Irradiation ($\lambda > 300$ nm) of [2]catenate **97** results in dissociation of the bipyridyl unit (red), which allows free movement of the two rings (Scheme 59). The vacant coordination sites on the metal ion are filled by chloride ions added to the reaction mixture (shown) or by a coordinating solvent such as acetonitrile (not shown).[282] The recomplexation reaction is achieved simply by heating.[283]

Sauvage and co-workers have also demonstrated both electrochemical and photochemical control over ring motions in hetero-[2]catenate **98** (Scheme 60a) which is closely related to molecular shuttle **74** (see Section 4.3.4).[284] The behavior observed for the catenate is essentially the same as its rotaxane analogue. The kinetics for the intercomponent motions are again slow relative to other molecular machines, although some differences are observed between the catenane and rotaxane on account of easier access of the solvent or ionic species to the metal center in the rotaxane, thus stabilizing transition states on the way to species with higher coordination numbers.

The related homocircuit [2]catenate [Cu(**99**)] (Scheme 60b), in which each ring contains a bidentate dpp unit and tridentate terpy site, exhibits more complicated behavior.[285] In dpp,dpp-[Cu^{I}(**99**)], the copper ion coordinates to the two dpp units in the usual tetrahedral arrangement. Oxidation of the metal center (by either chemical or electrochemical means) reverses the order of preference for coordination numbers (the preferred order for Cu^{II} is $6 > 5 > 4$). The result is circumvolution of the rings to give the preferred hexacoordinated species terpy,terpy-[Cu^{II}(**99**)]. It was demonstrated that this process occurs by revolution of one ring to give an intermediate five-coordinate species (dpp,terpy-[Cu^{II}(**99**)]).[285] In comparison to many related transition-metal-coordinated systems, the process is relatively fast, with the ligand rearrangement occurring on the timescale of tens of seconds. The process is completely reversible, via the same five-coordinate geometry, on reduction to Cu^{I} (that is, via dpp,terpy-[Cu^{I}(**99**)]).

Accordingly, this catenate adopts three different translational isomeric forms (six different states when the oxidation state of the metal ion is considered). The intermediate five-coordinate states are only transient, however, and could not be isolated. A system which displays three distinct, stable states is [2]catenane **100** (Scheme 61). This catenane, and the related [3]catenane **101**, extend the olefin photoisomerization strategy utilized in [2]rotaxanes **80**, **83**, and **87**–**89** to create the first examples of stimuli-driven sequential and unidirectional rotation in interlocked molecules, thereby addressing the key

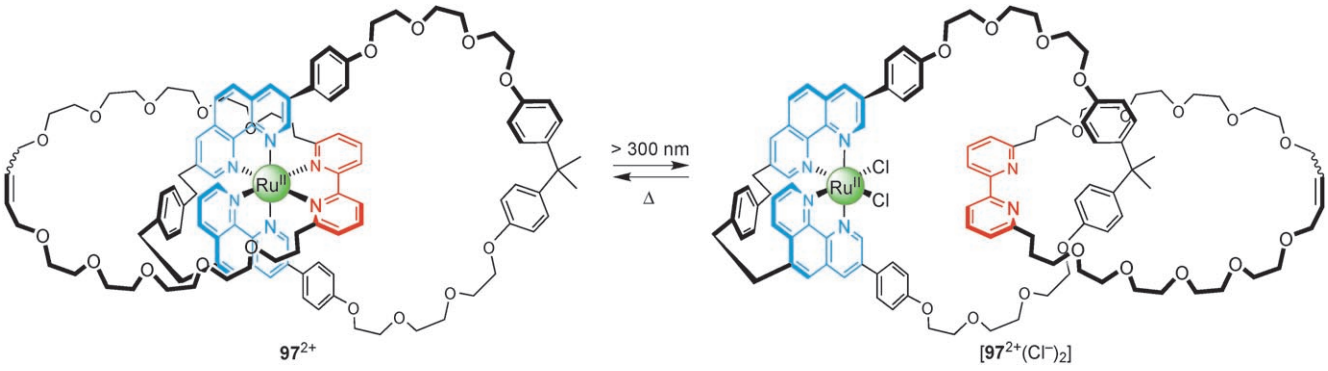

Scheme 59. Photoinduced selective decomplexation in a ruthenium(II) [2]catenate.[282] In the decomplexed form [$\mathbf{97}^{2+}\cdot 2\,Cl^{-}$], no bonding interactions exist between the two rings and free rotation occurs. The co-conformation shown is purely illustrative and does not indicate a preferred arrangement.

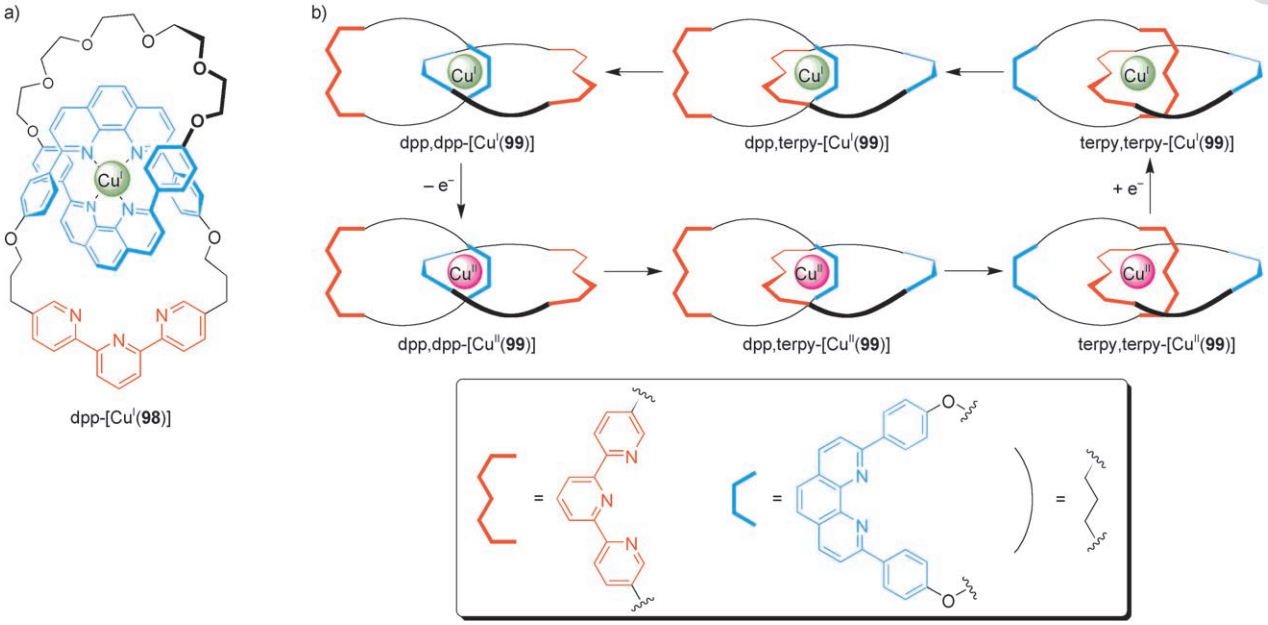

Scheme 60. a) Heterocircuit switchable catenate [Cu(**98**)].[284] b) Oxidation-state-controlled switching of [2]catenate [Cu(**99**)] between three distinct co-conformations.[285]

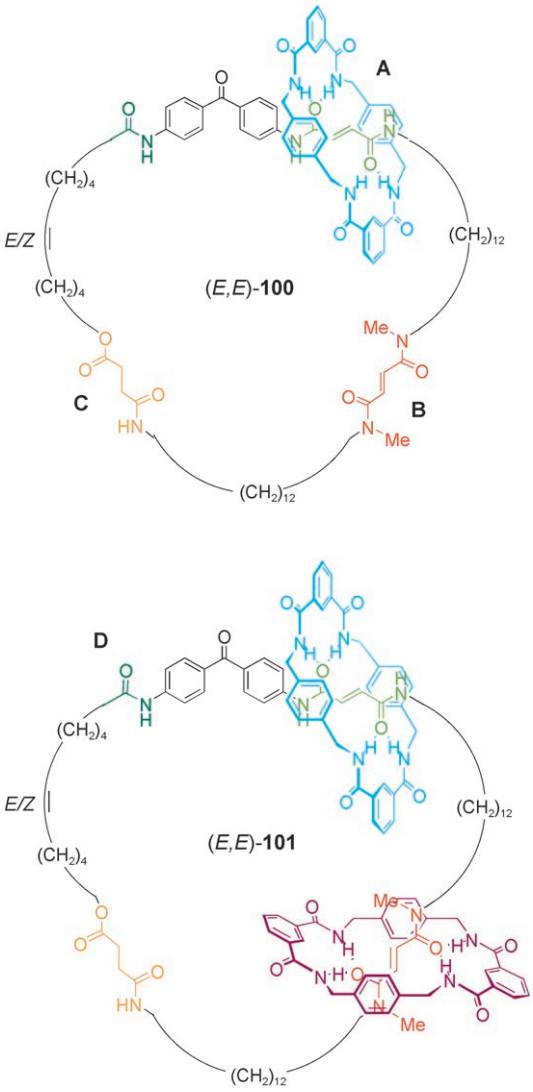

Scheme 61. [2]Catenane **100** and [3]catenane **101**, shown as their *E*,*E* isomers.[286]

difference between shuttling in two-station rotaxanes and rotation in catenanes (closely related to the difference between a switch and a motor, see Section 1.1): the issue of directionality.[286]

Sequential movement of one macrocycle between three stations on a second ring requires independent switching of the affinities for two of the units so as to change the relative order of binding affinities, as shown schematically in Figure 30.[286] In **100** this is achieved (Scheme 61) by employing two fumaramide stations with differing macrocycle binding affinities (steric mismatching of some tertiary amide rotamers disfavor the methylated station B), one of which (station A, green) is located next to a benzophenone unit. This allows selective photosensitized isomerization of station A at 350 nm, before photoisomerization of the other fumaramide station (station B, red) at 254 nm. The third station (station C, orange), a succinic amide ester, is not photoactive and is intermediate in macrocycle binding affinity

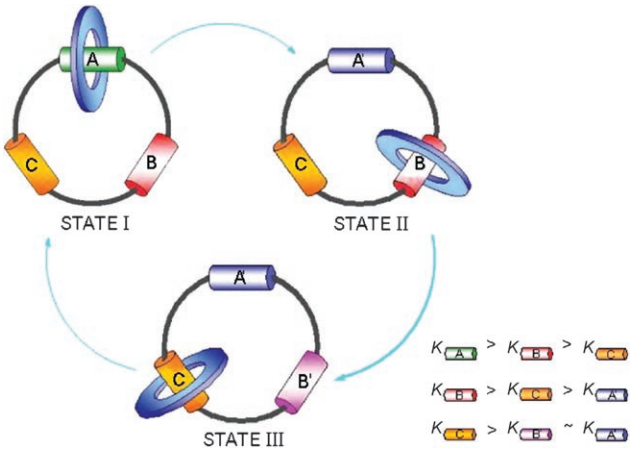

Figure 30. Stimuli-induced sequential movement of a macrocycle between three different binding sites in a [2]catenane.[286]

between the two fumaramide stations and their maleamide counterparts. A fourth station, an isolated amide group (shown as D in (*E*,*E*)-**101**) which can make fewer intercomponent hydrogen bonding contacts than A, B, or C, is also present but only plays a significant role in the behavior of the [3]catenane.

Consequently, in the initial state (state I, Figure 30), the small macrocycle resides on the green, nonmethylated fumaramide station of [2]catenane **100**. Isomerization of this station (irradiation at 350 nm, green→blue) puts the system out of co-conformational equilibrium and the macrocycle changes its net position to the new energy minimum on the red station (state II). Subsequent photoisomerization of this station (irradiation at 254 nm, red→purple) displaces the macrocycle to the succinic amide ester unit (orange, state III). Finally, heating the catenane (or treating it with photogenerated bromine radicals or piperidine) results in isomerization of both the *Z* olefins back to their *E* forms (purple→red and blue→green) so that the original order of binding affinities is restored and the macrocycle returns to its original position on the green station (state I).

The ^{1}H NMR spectra of each diastereomer show excellent positional integrity of the small macrocycle at all stages of the process, but the rotation is not directional—over the complete sequence of reactions, an equal number of macrocycles go from A, through B and C, back to A again in each direction.

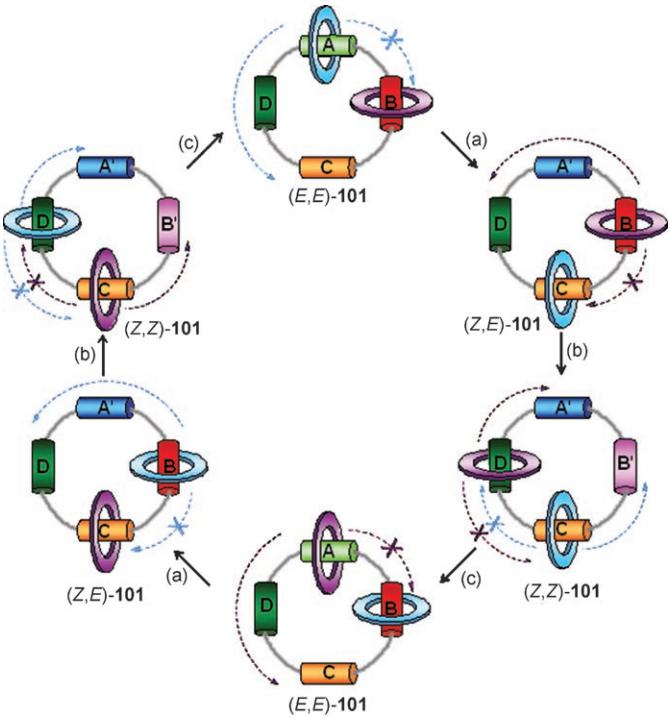

Figure 31. Stimuli-induced unidirectional rotation in a four-station [3]catenane, **101**.[286] Conditions: a) irradiation at 350 nm; b) irradiation at 254 nm; and c) Δ; or catalytic ethylenediamine, Δ; or catalytic Br_2, irradiation at 400–670 nm.

4.6.2. *Directional Circumrotation: A [3]Catenane Rotary Motor*

To bias the direction the macrocycle takes from station to station in a catenane such as **100**, kinetic barriers are required to restrict Brownian motion in one direction at each stage and bias the path taken by the macrocycle. Such a situation is intrinsically present in [3]catenane **101** (Scheme 61).[286] Irradiation of (*E*,*E*)-**101** at 350 nm causes counterclockwise (as drawn) rotation of the light blue macrocycle to the succinic amide ester (orange) station to give (*Z*,*E*)-**101**. Isomerization (254 nm) of the remaining fumaramide group causes the other (purple) macrocycle to relocate to the single amide (dark green) station ((*Z*,*Z*)-**101**) and, again, this occurs counterclockwise because the clockwise route is blocked by the other (light blue) macrocycle. This "follow-the-leader" process, in which each macrocycle in turn moves and then blocks a direction of passage for the other macrocycle, is repeated throughout the sequence of transformations shown in Figure 31. After three diastereomer interconversions, (*E*,*E*)-**101** is again formed, but 360° rotation of each of the small rings has not yet occurred, they have only swapped places. Complete unidirectional rotation of both small rings occurs only after the synthetic sequence (a)–(c) has been completed twice.

The directionality of the movement of the small macrocycles in Figure 31 could only be inferred from dynamic studies on related rotaxane-based molecular shuttles.[286] Nevertheless, these imply that stimuli-induced rotation carried out at 195 K occurs with extremely high (>99%) directional fidelity. The $\Delta G^{\ddagger}$ value for background rotation of the small rings in (*E*,*E*)-**101** is greater than 23 kcal mol^{-1}, which means that the half-life for random circumrotation at 195 K is over 1.5 years. This design could only be used to do a limited amount of progressive mechanical work since the only way that the ring movements are ratcheted is the relatively modest $\Delta G^{\ddagger}$ value for background rotation. The efficiency of this motor is either poor (<1% based on irradiated photons) or modest (ca. 17%, based on molecules that unidirectionally rotate during one sequence of reactions). Unlike the directionally rotating systems introduced by the research groups of Kelly (Section 2.1.2) and Feringa (Sections 2.1.2 and 2.2), [3]catenane **101** is achiral.

It seems likely that the designs (and modes of operation) of synthetic molecular machines will provide significant feedback for the understanding and development of new fluctuation-driven transport mechanisms. If we compare [2]catenane **100** with [3]catenane **101**, for example, we can see that they share a common track or potential-energy surface that is manipulated by the same set of chemical reactions. However, in [3]catenane **101** the Brownian particle (macrocycle) is transported directionally while in [2]catenane **100** it is not. The only difference between the two machines is the "concentration" of the Brownian particles on the potential-energy surface. It seems possible that such a mechanism could account for the dependence of some biological pumps on the substrate concentration.

4.6.3. *Selective Rotation in Either Direction: A [2]Catenane Reversible Rotary Motor*

Clearly, just like their rotaxane analogues, catenanes such as **101** can be viewed as one macrocycle (the machine) which

provides a potential-energy surface over which one (or more) smaller ring(s) (the Brownian substrate(s)) can be transported. By considering a flashing ratchet mechanism (Section 1.4.2), it is possible to design a [2]catenane which is able to directionally rotate the smaller ring about the larger one in either direction in response to a series of chemical reactions (shown schematically in Figure 32).[51,287]

This concept was realized in chemical terms through the synthesis and operation of catenane fum-(*E*)-**102** (Scheme 62).[51] Net changes in the position or potential energy of the smaller ring were sequentially achieved by: a) photoisomerization to maleamide (→mal-(*Z*)-**102**); b) desilylation/resilylation (→succ-(*Z*)-**102**); c) reisomerization to fumaramide (→succ-(*E*)-**102**); and finally, d) detritylation/retritylation to regenerate fum-(*E*)-**102**, the whole reaction sequence producing a net clockwise (as drawn in Scheme 62) circumrotation of the small ring about the larger one. Exchanging the order of steps (b) and (d) produced an equivalent counterclockwise rotation of the small ring.

The simplicity of **102**, together with the minimalist nature of its design, allows insight into the fundamental role each part of the structure plays in the operation of the rotary machine. [2]Catenane **102** is easily understood as an example of a compartmentalized molecular machine (see Section 4.4). The various chemical transformations perform linking/unlinking reactions (silylation/desilylation and tritylation/detritylation) and balance-breaking reactions (olefin isomerization (*E*→*Z* and *Z*→*E*)). As with other compartmentalized molecular machines, the balance-breaking reactions control the thermodynamics and impetus for net transport; the linking/unlinking reactions control the relative kinetics and ability to exchange. Raising the kinetic barriers ratchets transportation (see Section 4.4), thus allowing the statistical balance of the small ring to be subsequently broken without reversing the preceding net transportation sequence. Lowering the kinetic barrier allows escapement (see Section 4.4) of a ratcheted quantity of rings in a particular direction—the element missing from rotaxane **85**, which prevents it being a molecular motor.

To obtain 360° rotation of the small ring about the large ring, the four sets of reactions must be applied in one of two sequences, each taking the form: first a balance-breaking reaction; then a linking/unlinking step; then the second balance-breaking reaction; and finally, the second linking/unlinking step. This is the same manipulation of the potential-energy surface shown for the flashing

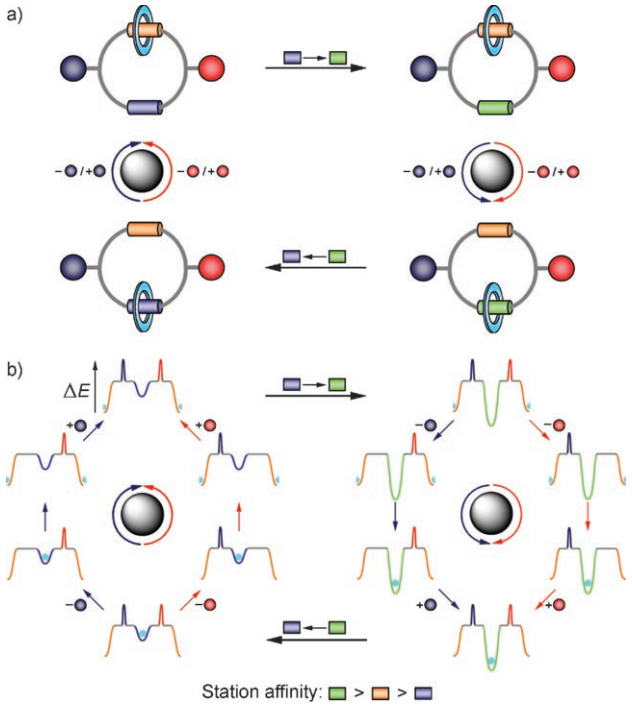

Figure 32. a) Schematic illustration and b) potential-energy surface for the blue ring in a minimalist [2]catenane rotary molecular motor.[51]

Scheme 62. Reversible [2]catenane rotary motor **102**.[51]

ratchet in Figure 7 (Section 1.4.2). The direction of net rotation is determined solely by the way the balance-breaking and linking/unlinking steps are paired: an input of information. The efficiency or yields of the reactions—or the position of the ring at any stage (even if the machine makes a "mistake")—are immaterial to the direction in which net motion occurs, as long as the reactions continue to be applied in the same sequence. Changing the pairings rotates the small ring in the opposite direction.

The analysis of this deceptively simple molecule, particularly the separation of the kinetic and thermodynamic requirements for detailed balance, provides experimental insight into how an energy input is essential for directional rotation of a submolecular fragment by Brownian motion. Even though no net energy is used to power the motion, there has to be some processing of chemical energy for net rotation to be directional over a statistically significant number of molecules, a requirement that is absent if the equivalent motion is nondirectional. The amount of energy conversion required to induce directionality has an intrinsic lower limit, which corresponds to the difference in the binding energy of the fumaramide and maleamide binding sites, the same value that determines the directional efficiency of rotation and the maximum amount of work the motor can theoretically perform in a single cycle.

5. Molecular-Level Motion Driven by External Fields

In most of the synthetic molecular machines described so far, control over motion arises from the selective restriction of Brownian fluctuations through the manipulation of chemical structure, composition, and electronics to influence steric and noncovalent bonding interactions. Common to all these approaches is that the forces exerted are short range—steric interactions are only felt over van der Waals distances, while bonding interactions (hydrogen bonds, charge-transfer interactions, or metal–ligand coordination) also operate over very short distances—and it is almost always thermal energy that powers the large-amplitude motions. It is well known that the application of external fields can cause bulk motion or orientation of molecular species, the most important technological application being the electric-field-directed alignment of liquid crystals. In addition to their more well-known applications, electrophoresis,[44l–n,q,v] dielectrophoresis,[44a,d,f,h,t] and photon pressure[44b,c] have been shown to provide potentials in which the motion of microscopic particles and macromolecules can be manipulated through Brownian ratchet mechanisms. An emerging field of research, however, aims to use the long-range forces that can be applied by external electric and electromagnetic fields to influence submolecular motions. The effect of alternating current electric fields on the rate of random pirouetting in rotaxanes, which has already been discussed (Section 4.5), is just one example.

Electric-field-controlled conformational switches have been proposed to create switchable molecular junctions for use in molecular electronics.[288] Computational investigations of **103** chemisorbed between two electrodes (Scheme 63) have suggested that an electric-field-induced conformational change (arising from interaction of the field with the dipolar rotator, red) could result in a significant change in the conductance of the tunnel junction, thus resulting in a "conformational molecular rectifier".[289] From a molecular electronics perspective, in both single-molecule junctions and STM-contacted molecules (see Section 7), the ability of the electric current to induce dynamic motion of a molecule after transient electronic excitation is becoming a matter of both theoretical and practical investigation.[290]

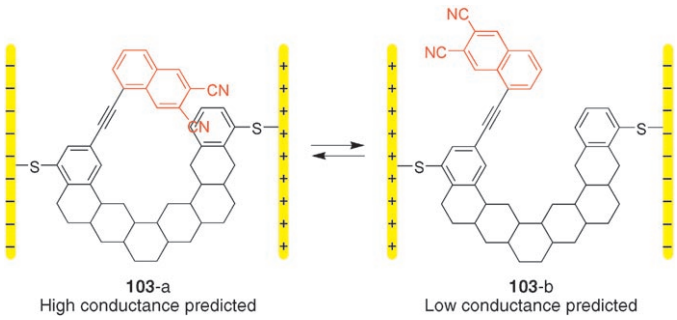

Scheme 63. A proposed molecular rectifier based on field-driven conformational switching.[289]

In terms of using long-range fields to drive the motions of a collection of molecular machines, the main challenge which has been addressed is the generation of submolecular rotary motion.[1k] The 360° rotation of any rotor involves passage over a torsional potential-energy surface, with its particular series of minima and maxima. The effect of an external field could be to: 1) promote the system to an excited state where the torsional potential-energy surface is different, or 2) interact with a permanent, or induced, molecular dipole so as to force orientation in a particular direction. The interaction between the field and the rotor provides the energy to surmount kinetic barriers and overcome energy dissipation and thermal randomization, so the field strength may need to be relatively large. With these intended systems, random thermal noise and dissipative effects such as friction would need to be minimized to maximize efficiency (for the problems in doing so, see Section 1.2). However, the requirements for generating unidirectional motion are no different from those under the thermally driven regime: asymmetry in the potential-energy surface and an energy input which can drive the system away from equilibrium.

This type of rotary device is likely to require orientation of the rotational axis along a fixed direction by using surface-mounted, solid-state, or liquid-crystal rotors. However, the consideration of small molecules in the gas phase as models has allowed high-level quantum dynamics simulations of such a process. Fujimura and co-workers have studied the internal rotation in the single enantiomeric forms of chiral aldehyde **104**, driven by an intense linearly polarized infrared laser pulse on the picosecond timescale (Scheme 64).[291,292] The chiral-

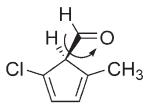

(*R*)-**104**

Scheme 64. One enantiomer of chiral molecule **104** in which electric-field-driven rotation around the C–CHO bond was studied by quantum and classical mechanical simulations.[291,293,295,326]

ity of **104** means that it has an asymmetric potential-energy surface for rotation about the C–CHO bond, while energy sufficient to surmount the highest potential-energy barrier is provided by interaction between the electric field of the laser pulse and the permanent dipole of the aldehyde. The process is reminiscent of a rocking Brownian ratchet (Section 1.4.2.2), although here thermal energy is not required to surmount the kinetic barriers. The system can also be modeled as an ensemble of randomly oriented rotors, but in either case the result is unidirectional motion and the two enantiomers rotate with equal magnitudes but in opposite directions (within the molecular frame of reference).

In the above calculations dissipative effects were ignored. Inertia therefore plays a significant role and rotation is seen to continue even after the driving field is removed. As discussed in Section 1.2.2, it is somewhat debatable how applicable such conditions are to practical situations in which molecular machines might operate. Fujimura and co-workers have subsequently taken energy dissipation into account, and have shown that, as one might expect, rotation only occurs under these conditions while the field is applied.[293] It was also found that on reducing the field intensity so that the field–dipole interaction falls below the maximum kinetic-barrier height, rotation occurs in the opposite direction, with barrier crossings mediated by quantum effects. Such behavior bears a striking resemblance to rocked quantum-tunneling ratchets designed to pump electrons. In such cases, the direction of electron transport has been shown (both experimentally and theoretically) to switch with rising temperature, depending on whether quantum tunneling though the kinetic barriers (low temperatures) or thermally activated barrier crossing (high temperatures) is the dominant process.[294] The quantum control of rotational direction in enantiomerically pure **104** was further elucidated by studies in which the time- and frequency-resolved spectra of the laser electric field were examined and the conditions for generating rotation in each direction were optimized.[295]

A number of computational studies of idealized graphite nanotube dynamics have been undertaken[296] in structures reminiscent of some of the futuristic "hard" nanotechnology machine components envisioned by Drexler.[297] The interactions between concentric nanotubes (that is, in double-walled nanotubes (DWNTs) and multiwalled nanotubes (MWNTs)) have received considerable attention with regard to their predicted low friction for relative sliding and rotational motions.[298] So-called "molecular bearings" in which the inner tube can be rotated within an outer sleeve have been studied,[299] as have "nanodrills" in which the interaction between the tubes is such that a rotational torque on one tube is converted into translation relative to the other.[300] Also proposed is the possibility of a gear effect for two parallel single-walled nanotubes (SWNTs) functionalized with benzyne-derived "teeth" along their length.[301] Potential methods for powering motions in all these systems clearly need to be considered. Attaching opposite charges to the inner tube of a DWNT molecular bearing in a molecular dynamics study enabled the coupling of the energy from a linearly polarized laser field with rotational modes of the system to be simulated.[302] A similar approach was used to study the theoretical motion of a SWNT gear system.[303] When the simulated gearing effect was used to transmit angular momentum to a noncharged nanotube, periods of induced directional rotation grew longer.[304] A further class of proposed nanotube-based mechanical devices are oscillators, in which the inner tube should be able to shuttle back and forth inside an open-ended outer tube at gigahertz frequencies.[305] Again the problems of powering the proposed motions and providing environments in which they could be effective must be tackled. One scenario has been modeled in which the inner tube encapsulates potassium ions and its oscillatory motion is driven by an external electric field,[306] while another has proposed thermal expansion of gases to power the motion.[307] However, the arrival of the experimental techniques required to produce or operate any of these systems in practice appears to be distant. The chemical functionalization of nanotubes is, however, a rapidly developing field,[308] while improved manipulation techniques have allowed the telescoping of inner tubes from a MWNT, and have demonstrated extremely low friction and a large driving force for the retraction of the extended structure.[309,310]

Rotors driven by circularly or linearly polarized electric fields[311] have been investigated by Michl and co-workers. Their approach closely follows an experimental effort to create surface-mounted dipolar rotors and so their calculations had to tackle technologically relevant conditions and complex structures. Dipolar chiral rhenium complex rotor **105**, was attached to a molecular grid constructed from [2]staffanedicarboxylate edges and dirhodium tetracarboxylate vertices (Scheme 65).[312,313] The theoretical rotational

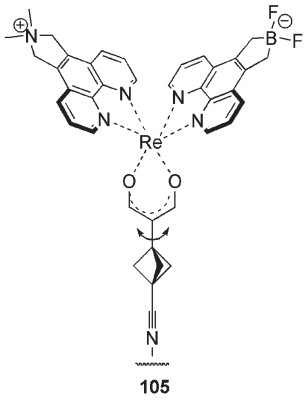

105

Scheme 65. Chiral dipolar rotor **105** which was studied computationally mounted on a 2D supramolecular framework and driven by a rotating electric field.[312]

motion, driven by a circularly polarized electric field in a vacuum and at low temperature, was studied by molecular dynamics over a range of field frequencies and field strengths. At low field frequencies, the simulations suggest that the average lag angle (the position of the rotator in the rotating field coordinate system) depends only on the field strength, as the major restriction to unidirectional rotation is thermal energy. At higher frequencies, friction is the dominant hindrance to directional motion and appears to be linearly proportional to the driving frequency. Five different rota-

tional regimes were characterized, depending on the interplay of the field–dipole interaction, thermal energy, friction, and intrinsic torsional barrier height. These range from synchronous motion, where the rotator slavishly follows the field, to situations where thermal energy or the torsional barrier dominates the behavior.[312,314]

Michl and co-workers have synthesized nonpolar and dipolar altitudinal rotors (that is, rotors with axles parallel to the surface) **106** and **107** (Scheme 66).[315] ^{19}F NMR spectroscopy showed that the barriers to rotation in **107** were extremely low in solution. Both systems have also been adsorbed on Au(111) and the surfaces studied by X-ray photoelectron spectroscopy (XPS), scanning tunneling microscopy (STM), and grazing incidence IR spectroscopy. It was found that, for a fraction of the molecules, the static electric field from the STM tip could induce an orientational change in the dipolar rotor but not the nonpolar analogue.[316] The propeller-like conformation of the tetraarylcyclobutadienes means that **107** can exist as three pairs (residual diastereomers) of helical enantiomers. Approximate molecular dynamics simulations have predicted an asymmetric rotational potential energy surface for at least one out of the three diastereomers, so that unidirectional rotation can be predicted for this isomer on application of an alternating current electric field.[317,318] The Michl research group has also reported initial synthetic investigations of an alternative, self-assembled, altitudinal rotor design, although no functional studies have yet been reported.[319] Jian and Tour have reported the synthesis of dipolar rotors such as **108** and their monolayer formation on gold (Scheme 67), but have yet to communicate any results on its field-driven motion.[320]

The above examples all consist of either permanent molecular dipole moments within a chiral structure, driven by achiral fields or else by a chiral field and therefore not requiring a chiral structure. Permanent molecular dipoles are not necessarily required however. If the rotator has a strongly anisotropic molecular polarizability, a dipole can be induced and rotated by an applied circularly polarized field. This has been proposed,[321] and experimentally achieved,[322] by subjecting chlorine molecules to an intense linearly polarized laser pulse, the polarization of which is rotating. In this "optical centrifuge" extremely high rotational energy levels can be accessed in very short time periods and the centrifugal force can induce bond dissociation.

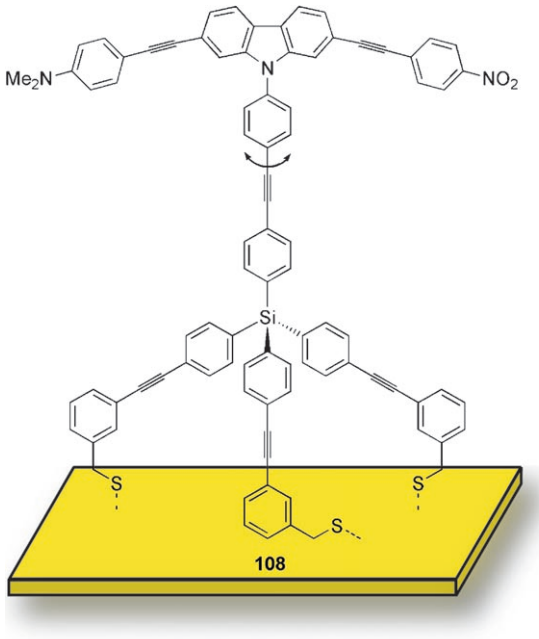

Scheme 67. Dipolar rotor **108** designed to be attached to gold surfaces.[320]

An approach which has yet to be investigated experimentally[323] is the transfer of momentum from a directional stream of atoms or molecules to bias the rotation of components of molecules fixed to a surface. Three possible arrangements can be envisaged:[1k] 1) fluid flow parallel to the rotor axle, combined with a chiral propeller-like rotator (windmill-like operation); 2) fluid flow perpendicular to the rotor axle, with faster flow on one side of the axis of rotation than the other (waterwheel-like operation); and 3) fluid flow perpendicular to the rotor axle, combined with rotator blades which interact with the fluid particles differently on either side (operating somewhat like an anemometer). Vacek and Michl have modeled the second of these possibilities for chiral rotor **105** (Scheme 65) as well as an analogue bearing larger blades.[324] The molecular dynamics simulations, in which a supersonic jet of noble gas atoms was directed parallel to the rotor axis through the open grid structure on which it was mounted, suggested that high-density beams of lighter atoms (He or Ne, but not Ar or Xe) might indeed be able to induce

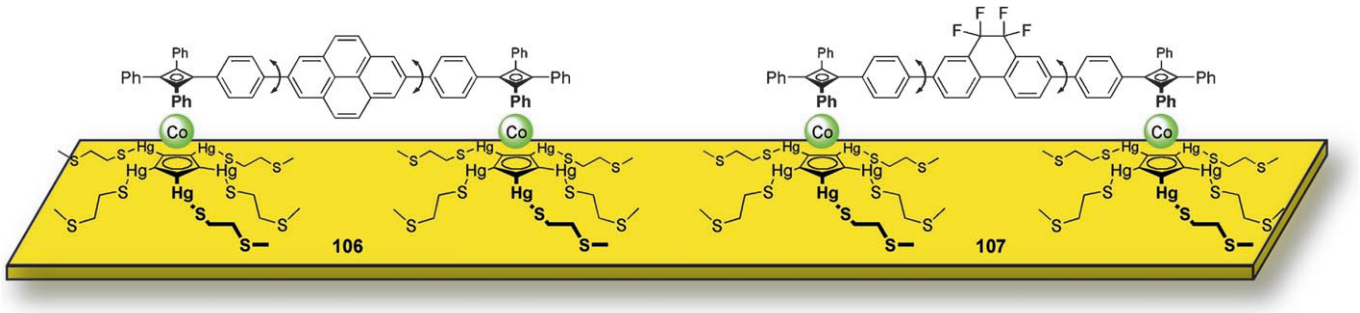

Scheme 66. Nonpolar (**106**) and dipolar (**107**) altitudinal rotors which have been studied on Au(111) surfaces. Note that the rotator and flanking aryl rings are arbitrarily shown perpendicular to the surface for clarity. Interaction with the surface is through several atoms in the cyclopentadienyl "tentacle" substituents.[315,317]

directional rotation, albeit at low temperatures and in competition with deformation of the rotor.[325]

Fujimura and co-workers performed calculations that consider exploiting the different torsional potential-energy surfaces in the electronic ground and excited states of **104** (Scheme 64) to achieve unidirectional rotation.[326] A femtosecond, UV-frequency pulse was used to excite the molecule to its first excited state. As a vertical transition does not correspond to a minimum in the excited-state potential-energy surface, rotation is induced, the direction of which is governed by the gradient of the potential-energy surface in the Franck–Condon region (opposite in each enantiomer). In theory, if the molecules are returned to the electronic ground state by a second femtosecond pulse before the excited-state minimum is reached, then the angular momentum can be preserved and rotation continues in the same direction. Of course, Brownian thermal and frictional effects will very quickly degrade such motion and relaxation must next be taken into account to ascertain if sequential such "pump–dump" cycles would be able to maintain unidirectional rotation. A related approach was applied to theoretically consider rotation around the double bond in **109** (Scheme 68).[327] In this case, an IR-frequency pulse would be used to excite vibrational motion in the deep torsional potential well of the double bond. In the first electronic excited state, the double-bond character is significantly reduced and kinetic barriers to rotation are much smaller. On excitation to this state by using a UV laser, all the kinetic barriers could, in principle, be overcome and the instantaneous angular momentum at the moment of excitation preserved. A well-timed excitation pulse should therefore be able to select the direction in which rotation will continue in the excited state. Once again, if relaxation effects are taken into account, this rotation will soon be retarded and will certainly stop on return to the ground state. A timely return to a repulsive region on the ground-state surface, however, may be able to maintain the motion and allow a second cycle of excitation to be applied. The use of two electronic states of a double bond to generate unidirectional rotation can be related back to the directional motors from the Feringa research group, discussed in Section 2.2.

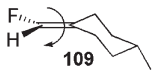

Scheme 68. Axially chiral 1-(fluoromethylene)-4-methylcyclohexane (**109**), in which rotational motion around the double bond, initiated by an IR frequency followed by a UV-frequency laser pulse, has been studied computationally.[327]

As shall be discussed extensively in Section 8, the incorporation of molecular machines into ordered phases, such as at interfaces or in liquid crystals, is an important goal in current research. Crystalline solids, however, present a very different environment within which to explore submolecular motions.[328] The combination of crystalline order with addressable molecular motions, to yield so-called "amphidynamic" crystals, provides a novel and challenging situation for the operation of artificial molecular machines. To this end, Garcia-Garibay and co-workers have initiated a detailed investigation of the gas-phase and solution-phase dynamics as well as the solid-state packing and dynamics of a series of molecules such as **110**–**113** (Scheme 69).[329,330] It is intended that the bulky trityl- (**110**, **112**, or **113**) or triptycyl-derived (**111**) portions (blue) should form the lattice framework and remain static, while rotation of the phenylene (**110**, **111**, or **113**) or diamantane (**112**) rotator (red) is the single internal degree of freedom. The arrangement of a central rotator spinning within a framework which shields it from external contracts can be compared to a macroscopic gyroscope.[331] Key to the desired dynamics is the volume-conserving nature of the conformational process, together with the ability of the bulky framework to force packing arrangements which allow free volume around the rotator unit. The construction of analogues in which the central rotator contains a dipole is intended to create systems in which the motion can be controlled by an external electric field.[329d] The thermal solid-state dynamics of one such example, **113** ($\Delta G^{\ddagger} \approx 13$ kcal mol^{-1} for fluoroarene spinning), have been studied by both NMR and dielectric spectroscopies,[329j] while dynamic studies of the nonpolar analogues suggest that significantly lower barriers to rotation are obtainable on suitable functionaliza-

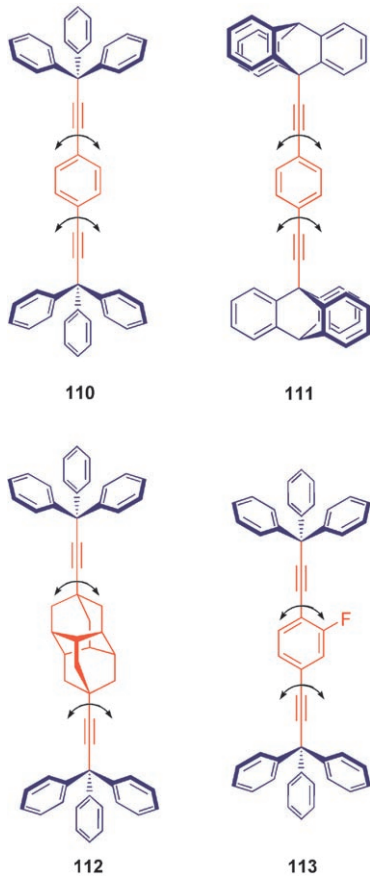

Scheme 69. Molecular "gyroscopes".[329,330] A selection of rotor structures constructed with the intention of demonstrating controllable molecular-level motion in crystalline solids. The bulky components colored blue are intended to direct the formation of ordered crystalline arrays in which free volume around the rotator section (red) results in low barriers to rotation.

tion of the static framework,[329e,330a] or on incorporation of rotators with higher symmetry, as in **112**.[329i,332]

A series of fully encapsulated gyroscope structures have been prepared and studied in solution by Gladysz and co-workers.[333] The crystal structure of **114** indicates that sufficient free volume around the rotator should exist to permit a low barrier to rotation in the solid state (Scheme 70).

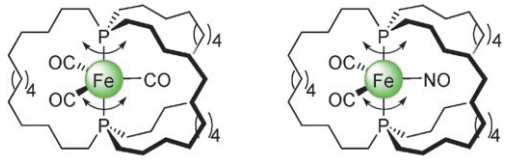

114 **115**

Scheme 70. Fully encapsulated "gyroscope" structures **114** and **115**.[333]

Reduced-symmetry derivative **115**, which also possesses a dipole moment as a possible handle to externally control the motion, allowed the rotational motion to be observed in solution. However, the activation barrier for the process was found to be not insignificant ($\Delta G^{\ddagger} \approx 11$ kcal mol^{-1}).[333] As was noted in Section 1.2.2, the effects of friction and thermal noise are extremely important on the molecular scale, but it is proposed that conditions may ultimately be found in which they are reduced to the extent that inertia in encapsulated or solid-state rotors becomes significant.

Supramolecular crystalline structures offer a different approach to solid-state rotors. The crown ethers in the triple-decker supramolecular cation $[Cs_2([18]crown\text{-}6)_3]^{2+}$ undergo rotational motion above 220 K in a crystalline environment with paramagnetic $[Ni(dmit)_2]^-$ counterions ($dmit^{2-}$ = 2-thioxo-1,3-dithiole-4,5-dithiolate).[334] Furthermore, the motion is strongly coupled with the magnetic properties of the crystal, thus suggesting one potential control mechanism. It has already been demonstrated that the application of pressure to the crystal can retard or even stop the thermally driven motion.[334]

6. Self-Propelled "Nanostructures"

The self-propulsion of microscopic objects has fascinated scientists from a range of backgrounds for well over a century. Spontaneous physical phenomena such as "tears of wine" and the motion of "camphor boats" engaged the minds of many eminent 19th century scientists, while the advent of microscopy revealed the deterministic motion of microorganisms to the biological community. Two distinct mechanisms—interfacial and mechanical—can be discerned in these natural phenomena and attention has recently turned to artificial devices, ultimately of molecular size, which can achieve the same results.[335] Just like the machines in Section 5, nanoscale self-propulsion devices are not powered by thermal energy. Field-driven mechanisms, however, address ensembles of molecules, whereas here we look at structures whose movements are driven by forces generated between each individual machine and the surrounding medium or track. Such machines can either operate autonomously—where the energy for movement is constantly present—or non-autonomously—where the energy must be applied in a series of stimuli given in a particular order.

6.1. Propulsion by Manipulating Surface Tension

A difference in surface tensions on either side of a liquid droplet or gas bubble can cause its directional transport through a second liquid or over a solid substrate.[336] This phenomenon is known as the Marangoni effect and is responsible for a number of naturally observed spontaneous processes.[337] In artificial systems, Marangoni flows are usually associated with a temperature gradient[336a,338] and have been proposed as a means of microfluidic pumping.[339] A similar effect can be achieved for a droplet sitting on a homogeneous surface if the droplet contains a species which adsorbs onto the surface.[340] Droplet motion is then driven by the irreversible modification of the surface free energy which affects the interfacial energy on either side of the droplet (see also Section 8.3.4)—a so-called "chemical" Marangoni effect.[341]

Whitesides and co-workers have reported the autonomous movement of millimeter-scale metallic objects at the liquid/air interface.[342] On one side, the objects feature a small area of platinum metal which catalyzes the decomposition of hydrogen peroxide to water and dioxygen. In an aqueous solution of hydrogen peroxide, the metallic plates are propelled by the recoil force of the oxygen bubbles. Subsequently, Sen, Mallouk, Crespi, and co-workers created smaller rod-shaped particles consisting of 1-μm-long platinum and gold segments.[343] These were suspended within an aqueous solution of hydrogen peroxide and again showed propulsion which is directly linked to the production of oxygen. In contrast to the system developed by Whitesides and co-workers, however, movement was found to be towards the oxygen-producing platinum region. It appears that the oxygen produced adheres to the hydrophobic gold surface in the form of nanobubbles, thus setting up a concentration gradient along the gold segment as the oxygen diffuses away from the platinum regions. It has been proposed that the resulting interfacial energy gradient causes motion of the rod towards the platinum end. However, the precise details of the propulsion mechanism are still a matter of investigation.[335,344] The driven and random thermal components of the motion could be distinguished at various viscosities for rods operating near an aqueous/organic interface.[345] The same technology has been used to create a rotational device,[346] while incorporation of a ferromagnetic metal into the nanorod design has allowed control over the directionality of movement by using an external magnetic field.[347] Independently, a nanorod system composed of nickel and gold regions has been developed by Ozin, Manners, and co-workers which undergoes both linear and rotational self-propelled motions in hydrogen peroxide (Figure 33), the latter seemingly a consequence of the tethering of one end of a rod to a surface impurity or defect.[348]

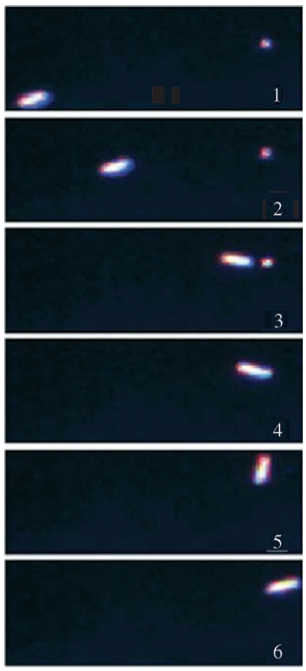

Figure 33. Optical microscope snapshots of a nickel/gold nanorod moving in a linear fashion (1→3) before becoming attached to a surface impurity and rotating counterclockwise (4→6).[348] Reprinted with permission from Ref. [348].

All these devices are both autonomous and catalyst-based, which means that, unlike a camphor boat or a chemical Marangoni droplet, they do not have to carry a finite supply of "fuel" onboard. Clearly, however, they are not yet molecular in nature. Recently Feringa and co-workers tethered a synthetic dinuclear manganese catalase mimic to a silica microparticle and again observed motion powered by the decomposition of hydrogen peroxide.[349] Although functionalization of the microparticle is theoretically homogeneous, defects result in inhomogeneous bubble nucleation, thus providing the asymmetry that gives rise to directional powered movement. Even though the mechanism of propulsion in this case is not yet clear, it demonstrates that the catalytic domain of a self-propelled motor can be scaled down to a molecular size. It remains to be seen if there is a lower limit to the particle size for which these types of strategies are practical (in all current systems, the movement of particles less than a micrometer in length is indistinguishable from Brownwin motion), what fidelity of directionality is possible (particularly for small particles where Brownian motion becomes significant), and whether or not it is possible to constrain the medium to a track along which the particle moves (for example, by confining the fluid to a microscopic capillary).

6.2. Mechanical Self-Propulsion—Molecules that Can Swim?

Most microorganisms use a different mechanistic approach to self-propulsion which is more akin to the mechanical swimming of an animal or propulsion of a macroscopic boat. However, the low Reynolds number at small length scales (see Section 1.2.2) puts constraints on the nature of productive swimming mechanisms.[350] This was probably first considered from a physical perspective by Purcell, who deduced that any useful mechanical mechanism must involve a nonreciprocal motion which breaks the time-reversal symmetry.[27] Since the mechanism needs to be repetitive, this effectively corresponds to the requirements of a molecular-level motor in which the substrate is the components of the machine itself (Sections 1.4.2 and 4.4). Purcell proposed a simple way in which this could be achieved: utilization of a "swimmer" composed of three rigid parts, linked by two hinges (Figure 34a). This device has recently been examined quantitatively[351] and reduced to a simpler one-dimensional problem by replacement of the hinges by simple springs (Figure 34b).[352] A number of other

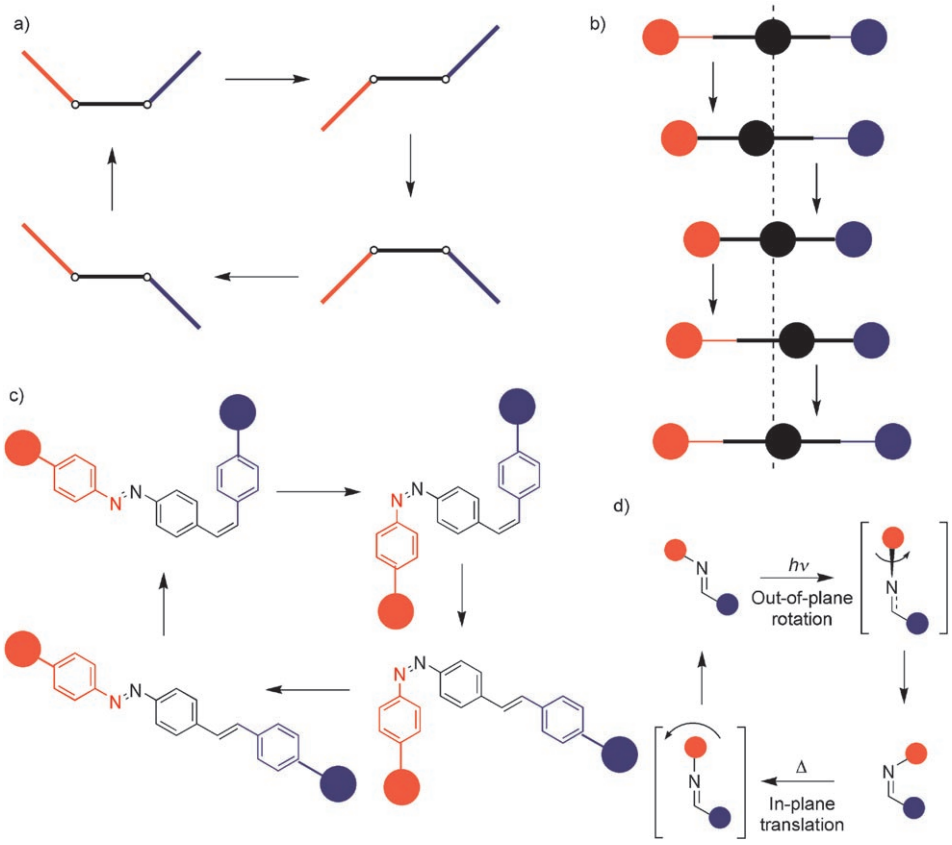

Figure 34. a) Nonreciprocal sequence of configurations for Purcell's three-link swimmer, which could result in propulsion at low Reynolds number.[27,351] b) A one-dimensional relative of Purcell's three-link swimmer.[352] c) Possible nonreciprocal motion in a three-part, two-hinge molecule. d) Possible nonreciprocal motion in a two-part, one-hinge molecule: *cis–trans* isomerization of an imine.[356]

swimming mechanisms involving nonreciprocal motion have also been investigated theoretically from the dual perspectives of modeling biological phenomena and designing microscopic devices.[353] Somewhat surprisingly (and perhaps analogous to the lack of molecular designs based on fluctuation-driven transport mechanisms), despite a recent success in creating a microscopic swimmer which operates by nonreciprocal motion,[354] there appears to have as yet been no investigation of such mechanisms at the molecular level. Incorporating two orthogonally addressable switches into a molecule would give a Purcell-like three-part-two-hinge/spring structure (Figure 34c). Adding bulk, the cyclodextrin in a known rotaxane system,[355] for example, would increase the net change in the position of the mass. However, the requirements of stimuli-induced nonreciprocal nanoscale motion for a low Reynolds number swimmer could also potentially be fulfilled by a two-part-one-hinge/spring molecule, by using a chemical reaction that can be reversed by a different nuclear pathway to the original transformation; for example, the photoisomerization and thermal reisomerization of certain imines[356] (Figure 34d). Other mechanical molecular switches discussed elsewhere in this Review are plausible candidates for linear mechanisms of the type shown in Figure 34b. The major problem with the realization of any of these systems in a working molecular form will be carrying out the stimuli-fueled motions fast and frequently enough so that they are not swamped by the background Brownian motion.

Repetitive directional rotation of any chiral object is, of course, also a nonreciprocal motion. Field-driven unidirectional rotation of a chiral molecular rotor (Section 5) which is not confined to a surface through any stator unit could result in its propulsion through a liquid in direct analogy to a screw propeller on a boat or the bacterial flagellar system. This situation has been studied theoretically with a view to using circularly polarized microwaves to spatially resolve a racemic mixture of "propeller-shaped" molecules.[357] It has been postulated that anchoring such rotors at a fixed location within a fluid could theoretically create a microfluidic pumping system.[312]

7. Molecular-Level Motion Driven by Atomically Sharp Tools

The development of STM[358] and AFM[359] has dramatically shifted the goalposts for what it is possible to see, and potentially do, with synthetic molecular machines. For the first time these instruments offer scientists the opportunity to both observe and manipulate atomic and molecular events that operate not on ensemble-averaged populations of species but on single chemical entities.[360,361]

The early STM manipulations of single atoms and molecules had to be carried out at extremely low temperatures to suppress thermal motion. In one famous example, a single-atom electronic switch was created by using STM, with its operation based on changing the position of a xenon atom relative to two electrodes.[362] The manipulation of organic molecules requires careful balancing of adsorbant–adsorbate interactions: molecule–substrate binding must be strong enough to prevent thermal motion at the temperature used, but not so strong that rupture of covalent bonds results instead of translation across the surface.[360e,f] These criteria were first met at room temperature in 1996 with porphyrin **116** (Figure 35).[363] In the gas phase, and on a Cu(100) surface,

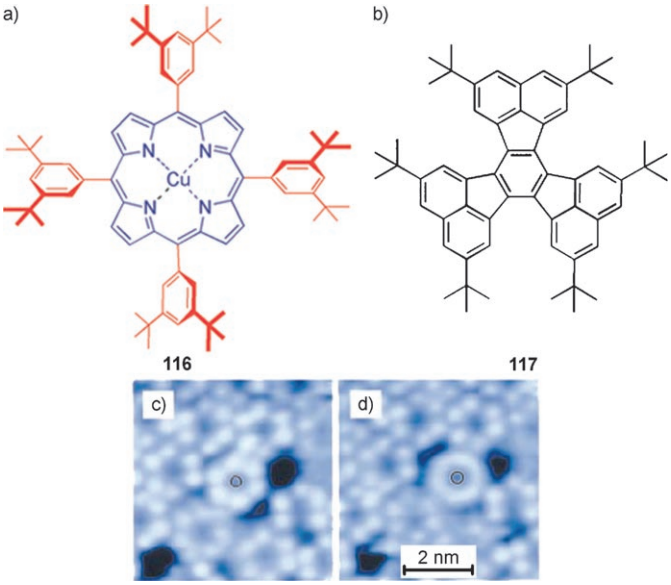

Figure 35. a) Porphyrin **116** for which positioning was induced at room temperature on a Cu(100) surface by the STM tip.[363,364,366] b) Decacyclene **117**, for which STM-tip-switched, thermally driven rotations are observed on a Cu(100) surface at coverages just below one monolayer (c and d).[374] Both molecules adsorb on the surface through the appended *tert*-butyl groups, with the main planar skeletons in the plane of the substrate. c) and d) Constant-current STM images of a clean Cu(100) surface with a submonolayer coverage of **117**. Stationary molecules appear as a circular arrangement of six lobes (arising from the six *tert*-butyl groups) and gaps in the monolayer appear as dark regions. In (c), the marked molecule is at a gap in the monolayer but it is aligned with the lattice and therefore stationary. In (d), the same molecule has been moved a distance of 0.25 nm by the STM tip and is no longer bound tightly by its neighbors and it therefore rotates, which is observed as a blurring of the lobed structure. The STM images are reprinted with permission from Ref. [374].

the di-*tert*-butylphenylene substituents are oriented perpendicular to the porphyrin unit and act as relatively sticky "legs" which separate the polyaromatic core from the surface, thereby fixing the molecules securely in place while modulating the extremely strong interaction of the planar central core with the substrate.[364] Pushing with an STM tip causes translational motion, which is facilitated by accompanying random rotations or "chattering" of the phenyl rings, which lowers the barrier to movement.[363,365,366]

Interlocked architectures provide another means through which the correct balance of forces can be achieved, ultimately enabling submolecular co-conformational changes to be made in a single molecule. An early report on STM imaging of a benzylic amide [2]catenane deposited from solution onto highly oriented pyrolitic graphite (HOPG) showed rather weak adsorption on the surface.[367] A much

larger [2]catenane was subsequently shown to form a tightly packed polycrystalline arrangement on the same surface, with the larger number of aromatic functionalities and greater flexibility leading to stronger adsorption.[368] Co-conformational motion in an interlocked architecture was achieved when an STM tip was used to reversibly move one or two adjacent cyclodextrin rings along the polyethylene glycol derived thread in a polyrotaxane adsorbed on MoS_2 (Figure 36).[369] This abacus-like motion is reminiscent of an earlier report on the positional manipulation of C_{60} molecules on Cu(111) surfaces, where the thermal motion of these rather poorly adsorbed species is restricted by confinement to a monatomic step edge.[370]

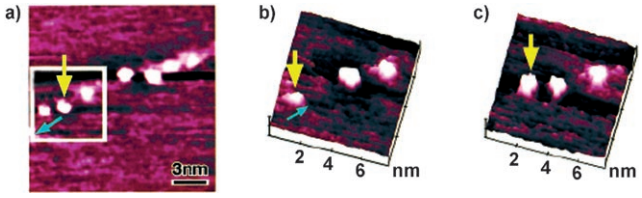

Figure 36. Translocation of a cyclodextrin ring in a polyrotaxane induced by a scanning probe.[369] The ring (indicated by a yellow arrow) is moved first towards the left (a→b) then back to the right (b→c). The white box on image (a) indicates the region of detail which is magnified in (b) and (c). Reprinted with permission from Ref. [369].

An STM tip has been used to apply a localized voltage to a thin film of bistable [2]rotaxanes which has resulted in conductance switching.[371] Based on the behavior of similar molecules in other solid-state experiments (see Section 8.3.1) it is proposed this effect is due to macrocycle shuttling triggered by tip-induced oxidation of the thread. A similar single-molecule switching phenomenon has been observed for an oligopeptide organized in a self-assembled monolayer. The peptide adopts one of two helical conformations depending on the polarization of the STM tip and the two states are characterized by different molecular heights and conductances.[372,373]

STM-induced single-molecule positional switching has been employed to reversibly control thermally driven motions on surfaces.[374] At monolayer coverage on Cu(100), decacyclene **117** forms a two-dimensional van der Waals crystal, while at coverages significantly below one monolayer, random thermal motions are extremely fast and not observable by STM. When coverage is a little less than a full monolayer, however, the 2D lattice has small gaps or "nanocavities" (Figure 35 c,d). The molecules at the borders of these free spaces can sit in one of two positions: a highly symmetrical one, following the order of the adjacent lattice, or a less symmetrical one. Movement between these two sites can be effected by the STM tip. In the less symmetrical site, the molecule is still constrained by its neighbors, but is disengaged from some of the intermolecular interactions, so that it freely rotates in a random fashion at high speeds (Figure 35 d).[374,375] It has been noted that in the "engaged" state the potential-energy profile for rotation is asymmetric, thus suggesting that such a system could be a starting point for a unidirectional rotor. To date, however, there have been no further reports on the incorporation of the remaining features necessary for such a system.[376]

While STM permits the manipulation and observation of complex molecular species adsorbed on conducting surfaces, AFM can be used to image nonconducting surfaces and can operate under ambient conditions, even on samples in solution. The use of an AFM cantilever as a force sensor or applicator (so-called "force spectroscopy") has facilitated some remarkable single-molecule investigations of receptor–ligand interactions, of the entropic and enthalpic factors involved in biopolymer folding, and of the mechanical elasticity of biopolymers.[360j–p] Synthetic polymers are also amenable to this approach, although nonspecific forces at small tip–substrate separations and the physical size of available tips have impeded the application of AFM to small-molecule perturbations and measurements to date.[360g,i,377] It has recently been discovered that an AFM tip can be used to initiate the formation of regular arrays of deformations in thin films of simple rotaxanes (Figure 37).[378] The effect is unique to films made from interlocked molecules (it does not happen to films of the non-interlocked components, for example) and is a result of coupled nucleation recrystallization being favored by the ease of intercomponent mobility for these molecules. The features of the nanoscale dot arrays are easily varied by changing the thickness of the film, and show potential for application in information storage technology.

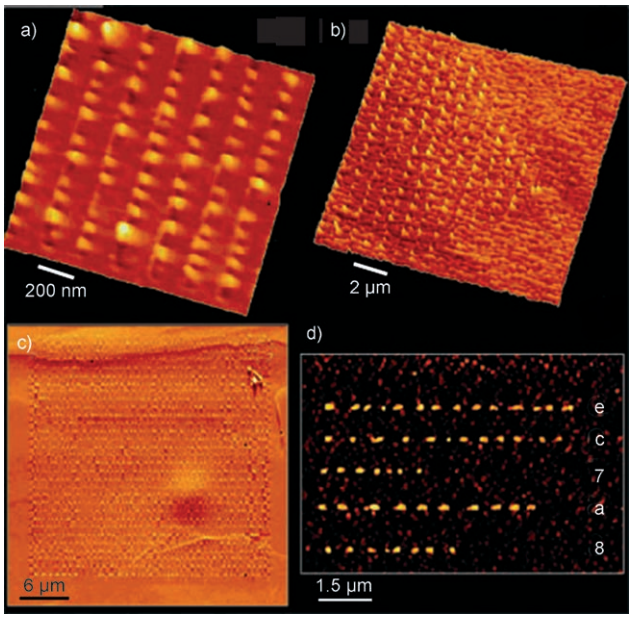

Figure 37. a) Array of dots fabricated by individual line scans of the AFM tip on a 5-nm-thick film of a benzylic amide [2]rotaxane **89** (Scheme 51) deposited on HOPG.[378] b) For a given thickness (here 20 nm), the number of dots is linearly proportional to the scan length. The film thickness controls the characteristic size. c) A pattern made up of 31 lines with 45 dots each on an approximately $30 \times 30\ \mu m^2$ area of a thicker film. d) Proof-of-concept for information storage. The sequence "ec7a8" in the hexadecimal base corresponds to the number 968616.

Despite the advances in the observation and manipulation of single-molecule dynamics, it is only recently that potential structural precursors for molecular machines specifically designed to be actuated at the single-molecule level by probe techniques have been investigated. Variations in conductance on deformation by atomically sharp probes have been reported for a number of molecular species, in particular fullerenes.[360s] For example, the angle between the porphyrin core and an individual di-*tert*-butylphenyl leg in **116** can be reversibly manipulated by either STM or AFM, thereby leading to an order of magnitude switching of the STM tunneling current between the tip and substrate.[379] The low energy requirements of such manipulations make them inherently attractive for exploitation in future nanoelectronic devices[360t] but they have also inspired the design of structures specifically designed to exhibit mechanical switching of electrical properties induced by an STM tip. Molecules such as **118** (Scheme 71 a) have been proposed in which two polyaromatic regions (blue) are connected by an aryl rotator (red).[380] In analogy to a series of rigid predecessors,[360t,381] the polyaromatic core of these molecular "landers" is intended to act as a single molecular wire, which is raised and insulated from the surface by the di-*tert*-butylphenyl legs (similar to **116**). If variation in the angle of the central rotator can significantly affect conductance through the molecule it would constitute a single-molecule nanomechanical electrical switch. A clear challenge here is achieving a system where thermal rotations of the central rotator do not erase the state of the switch while still allowing tip-induced rotation. A recent study of simple triphenyl **119** (Scheme 71 b), chemisorbed through the oxygen atoms to a Si(100)-2×1 surface has highlighted some of the problems facing such delicate manipulations of intramolecular conformation with an STM tip.[382] However, reversible conformational switching of biphenyl molecules adsorbed on a Si(100) surface, has been successfully realized through electronic excitation using an STM tip.[383] Remarkably, two different dynamic processes could be initiated simply by positioning the tip at slightly different locations over the molecule.

Investigations into the correlation and manipulation of mechanical modes within single molecules on surfaces has begun. These early studies highlight the exciting potential for successful working systems together with the difficulties involved in balancing the forces necessary for a molecule to overcome thermal motion while still allowing reversibly addressable internal modes. Pushing the 4-*tert*-butyl "handles" (dark blue) with an STM tip was intended to rotate the triptycene "wheels" (red) and roll "molecular wheelbarrow" **120** (Scheme 72) across a surface.[384,385] Simulations of early designs did not result in the intended motion on account of a flattening of the rear legs on the surface.[384a] If this effect was eliminated from the simulations, rotation of the wheels still did not occur, they simply glided across the surface. On the other hand, when second-generation system **120** was adsorbed on Cu(100), contact with the STM tip fragmented the molecule, thus suggesting strong interactions between the molecule and the surface even at room temperature.[386]

Clearly a macroscopic wheelbarrow operates on the principle that friction between the wheel and the ground is greater than resistance to rotation around the axle. Friction is a function of the nature of the surfaces in contact and the weight of the barrow. At the molecular level, however, the concept of friction is less easily understood:[387] the resistance to sliding motion arises from individual short-range attractive and repulsive forces, as well as longer-range attractive van der Waals interactions, while the effect of gravity is negligible. Rolling translation on surfaces and the role of friction have

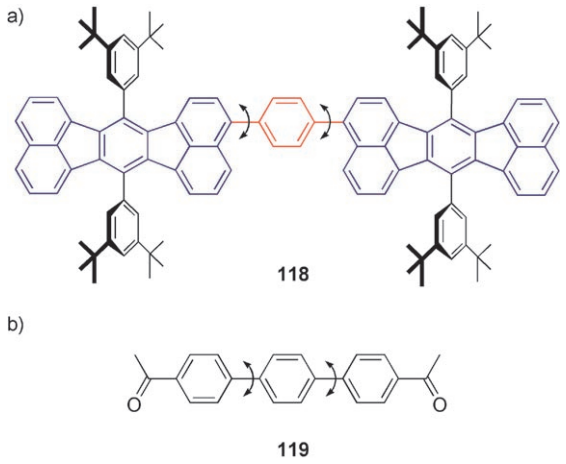

Scheme 71. a) Structure of "lander" molecule **118** in which it is intended that manipulation of the angle between the phenyl rotator (red) and polyaromatic boards (blue) will control conductance through the molecule.[380] As for previous structures, interaction with the surface is through the orthogonally oriented di-*tert*-butyl "legs" (black). b) 1,4″-Paratriphenyldimethylacetone (**119**) has been chemisorbed on a Si(100)-2×1 surface through the oxygen atoms and the manipulation of the phenyl rings investigated by STM.[382] The arrows indicate the degrees of freedom which were probed with the tip.

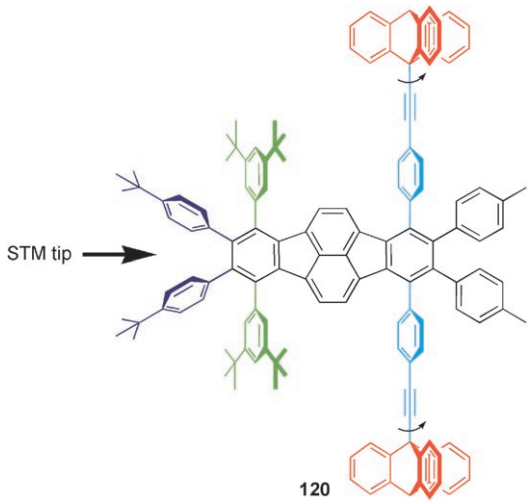

Scheme 72. Structure of "molecular wheelbarrow" **120**, designed to convert a directional translational stimulus applied by the STM tip at the "handles" (dark blue) into directional rotation of the "wheels" (red).[384–386]

been considered more extensively in relation to fullerenes and carbon nanotubes (see also Section 5) on account of their spherical and cylindrical shapes.[388] It has now been demonstrated experimentally that both carbon nanotubes[389] and C_{60}[390] can undergo tip-induced surface translations through a rolling mechanism in preference to sliding motions. This has recently been exploited by Tour and co-workers in a remarkable demonstration of what they term a single-molecule "nanocar", **121** (Figure 38a).[391] The molecule consists of an oligo(phenylethylene) "chassis" supporting four C_{60}-derived "wheels". These molecules can be imaged on Au(111) by STM as four bright lobes that are stationary at room temperature. Increasing the substrate temperature results in 2D movement of the molecules, observed through sequential STM images (Figure 38c–g). The orientation of the molecules can be determined because of the difference in the length and width dimensions, and translational motion clearly occurs perpendicular to the axles, with pivoting around one wheel accounting for changes in direction. This orientation strongly suggests a thermally driven rolling mechanism, and was confirmed by the behavior of two three-wheeled analogues, one of which (**122**, Figure 38b) was designed only to undergo pivoting, the other of which could not sustain any motions involving concerted rolling of all the wheels (not shown). Movement of **121** could also be achieved by manipulation with the STM tip, but again only motion perpendicular to the axles was facile. Intriguingly, this motion was generated with the tip in front of the molecule, pulling it along, in contrast to most other examples of tip-induced molecular movements. The authors propose that

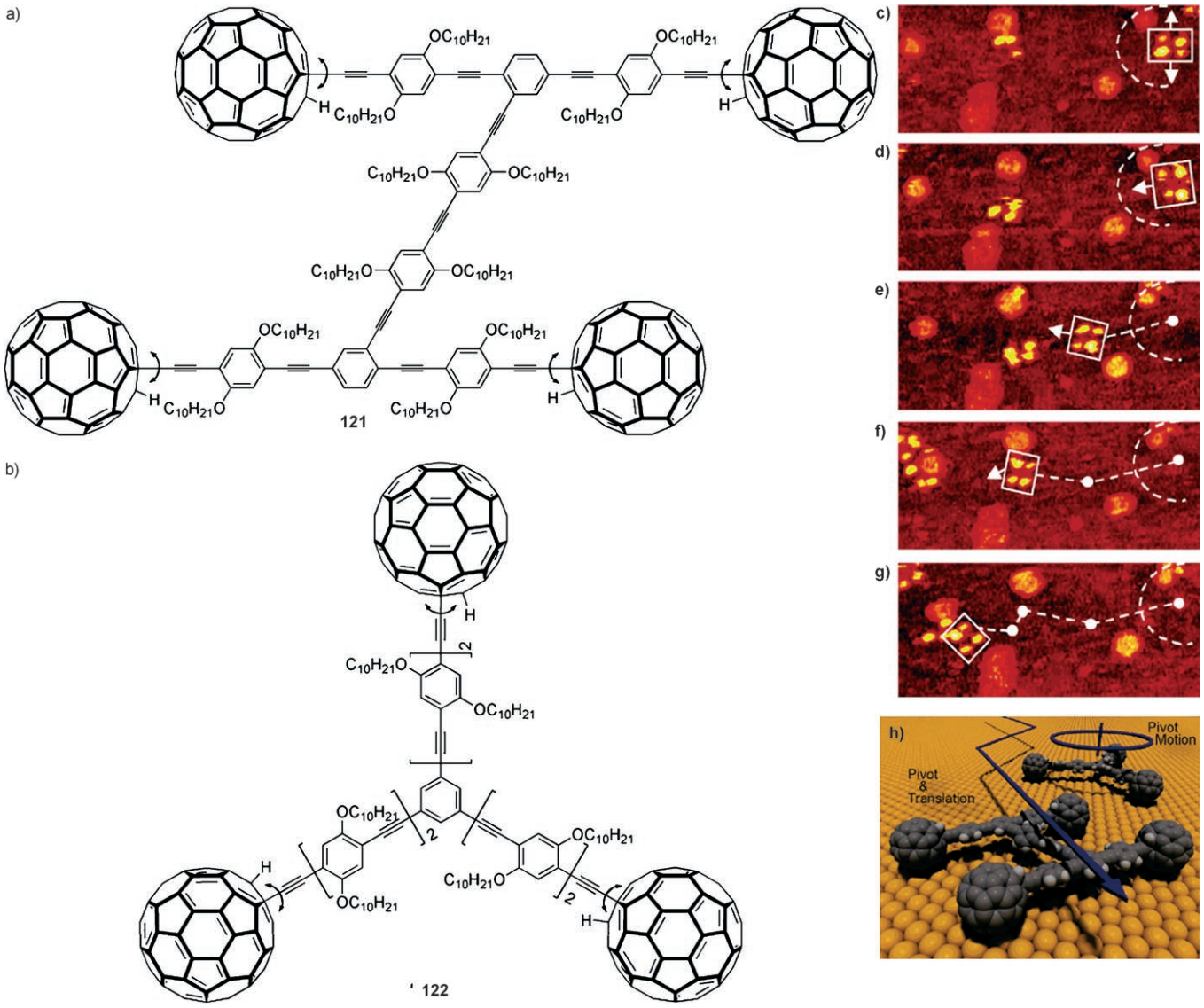

Figure 38. a) Chemical structure of four-wheeled "nanocar" **121**.[391] b) Chemical structure of the three-wheeled analogue **122** with an axle arrangement designed to allow only pivoting motion through correlated rolling of the fullerene wheels. c)–g) STM images of **121** rolling on Au(111) at 200 °C. The orientation of **121** can be determined by the wheel separation. Images (c)–(g) were selected from a series spanning 10 min. h) Schematic representation of the motions of **121** and **122**. For clarity the alkoxy substituents have been omitted. The STM images (c)–(g) and the schematic representation (h) are reprinted with permission from Ref. [391].

ultimately ensembles of such molecules could be propelled by external fields (see Section 5).[391]

Cyclic molecules in which a position of unsaturation moves around equivalent positions through sigmatropic rearrangements (see Section 2.1.5) have been proposed as being able to roll across surfaces, powered by the breaking and formation of substrate–molecule bonds around the ring.[392] A related phenomenon has been observed experimentally by STM when a fluorinated C_{60} derivative was deposited on Si(111)-(7×7). The fullerenes were observed to move across the surface leaving a trail of fluorine atoms in their wake—presumably the result of a rolling motion powered by chemisorption of fluorine to the surface (somewhat reminiscent of the "chemical" Marangoni motion of droplets containing surface-active species, Section 6.1).[393] Random surface motions of adsorbates can be directed along specific directions on low-symmetry surfaces.[394] Recently, however, STM was employed to observe the directional diffusion of a chemisorbed molecule (9,10-dithioanthracene) on a high symmetry Cu(111) surface.[395] A size mismatch between the molecular dimensions and surface periodicity results in sequential motion of the thiol "legs" so that the molecule's orientation is always maintained.

Scanning probe microscopies also open up opportunities to design machines that operate and generate an output at the single-molecule level without being powered by direct manipulation by the probe tip. Electroactive organometallic rotor **123** (Figure 39) has been designed to function on a surface, attached through derivatization of the hydrotris(indazolyl)borate ligand (red) leaving the cyclopentadienyl ligand (blue) free to rotate.[385,396] The proposed mechanism for driven directional rotation envisages a single-molecule electronic junction through which selective oxidation of one ferrocene moiety occurs. Anodic repulsion of the resulting cation moves the charge towards the cathode where it is reduced, the rotation bringing the next ferrocene unit close to the positive terminal for oxidation. It is not yet clear if such an experimental set-up is achievable or whether direct electron tunneling from the cathode to the anode would result instead or even whether thermal motion would scramble the rotor's position. Indeed, the low-energy barrier demonstrated for rotation around the ruthenium–cyclopentadienyl bond[397] requires that the electrostatic driving forces be significant at all times during the mechanism to avoid thermal scrambling. An alternative approach may be to bias rotation using a perpendicularly aligned electric field.

Other techniques besides scanning probe microscopies allow the application of external fields (Section 5) for both imaging and manipulation with molecular-scale precision. Magnetic tweezers, glass microneedles, and, perhaps most prominently, optical tweezers have been used to investigate the mechanical behavior of biomolecules.[398] Many of the most significant advances with optical tweezers have been in the study of molecular motor proteins, the optical trap allowing monitoring and application of forces to motors and their subunits at various stages in their operation. This technique has also been applied to protein folding and unfolding, binding events, and DNA transcription. One of the most striking demonstrations of the capabilities of this tool is the tying of a knot in an actin strand, thereby determining significant mechanical properties of the filament.[399] Recently, a light pattern incident on an photoconductive surface was used to set up non-uniform electric fields which allow parallel trapping and manipulation of multiple particles over a large area—essentially a molecular-level example of dielectrophoresis.[400] Various methods for detecting single fluorophore molecules have been developed, thus leading to new insights in many biophysical investigations.[401] Together, all these tools for probing dynamic events, interactions, and processes at the single-molecule level have had a profound effect on the understanding of many biological systems. The ability to examine single entities as opposed to ensemble

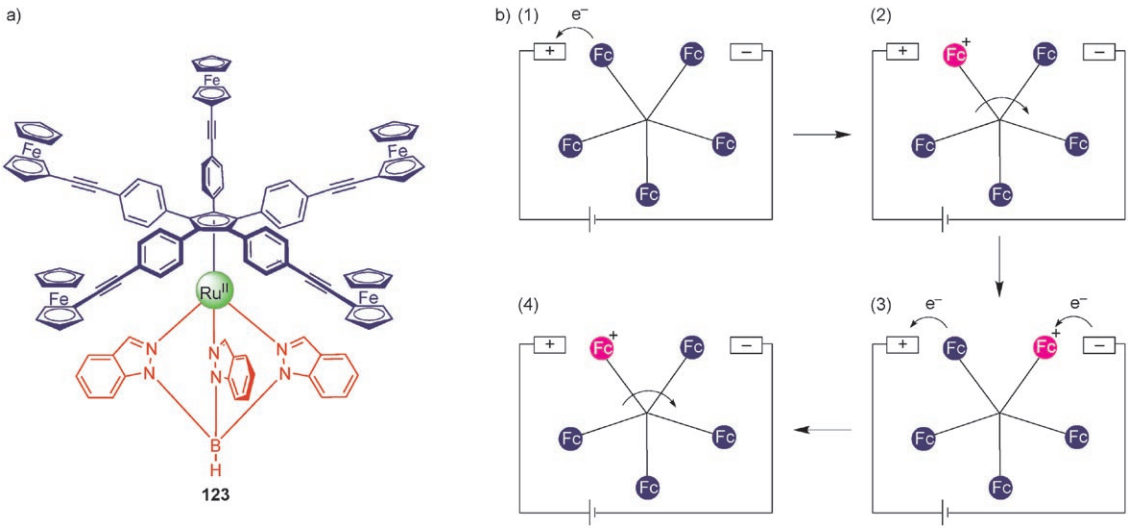

Figure 39. a) Chemical structure of a potential molecular motor designed to operate at the single-molecule level.[385,396] b) Proposed mechanism of operation: 1) a potential difference applied across a nanojunction results in oxidation of the ferrocene group nearest the anode (2); electrostatic repulsion results in rotation so as to bring the ferrocenium cation towards the cathode where it can be reduced (3); simultaneously a new ferrocene unit is brought close to the anode where it is oxidized (4), to generate a rotational isomer of (2). Fc = ferrocene; Fc^+ = ferrocenium.

averages has allowed the study of phenomena in a manner not possible with a nonsynchronized population of molecules. We look forward to the increased application of these powerful techniques to synthetic molecular motors and machines over the next few years. On the other hand, as the design and mechanistic complexity of synthetic devices grows, so more demanding questions will be asked of analytical techniques. Accordingly, the quest for new techniques for addressing and analysis on the nanoscale continues apace. Very recently, for example, the creation of an optical "superlens" was reported which breaks the diffraction limit in optical microscopy and allows imaging of objects significantly smaller than the wavelength of light used.[402] The resolution of the new lens is 60 nm, but this work points the way for progression towards truly nanoscale optical microscopy.

8. From Laboratory to Technology: Towards Useful Molecular Machines

8.1. The Current Challenges: Constraining, Communicating, Correlating

Although the development of reaction-driven, field-driven, self-propelled, and scanning-probe-controlled submolecular motion is rapidly gathering pace, it is the design and synthesis of molecular structures—both classical covalent and mechanically interlocked—which restrict the thermal movements of various submolecular components that has been central to the major advancements in molecular-level machines to date. These structural constraints have been successfully combined with external switching of molecular and/or electronic structure to create systems which exhibit a remarkable level of control over both the relative position of units as well as the frequency and even directionality of their motion. Whatever the application or the precise mode of action, however, it is clear any practical device requires that the molecular machine is able to interact with the outside world, either directly through macroscopic or nanoscopic property changes or through further interactions with other molecular-scale devices. The problem of how to "wire" molecular machines together and to the outside world also has implications for the physical construction of the devices which, in turn, puts further demands on the fidelity of the molecular-level mechanical processes over a range of conditions. In the following sections, we examine research that addresses these challenges by focusing on using molecular-level motion to produce a functional property change or perform a physical task.

Nature's motors and machines generally work at interfaces or on surfaces and the transfer of molecular-machine technology onto solid substrates is a key step in the development of many potential applications. Not only do solution-phase systems pose problems in terms of integration with current technologies, directly transmitting mechanical changes at the molecular level to the macroscopic world will generally require organization and cooperation of many molecular-level machines. There are already several examples of switchable and detectable supramolecular recognition events (including threading and dethreading of pseudorotaxanes) which occur at surfaces.[403,404] The current state-of-the-art in this regard is well represented by Stoddart, Zink, and co-workers, who have harnessed the photochemically triggered dethreading of a surface-mounted pseudorotaxane to release molecules trapped in nanoscopic pores on the same surface.[405]

The problem of achieving controlled movement within surface-mounted or solid-state interlocked molecules is more demanding, however, with both components constrained to the solid support or interface at all times. The first evidence for externally stimulated submolecular motions of a catenane in the solid state was observed when a vacuum-evaporated thin film of a benzylic amide [2]catenane was subjected to oscillating electric fields and produced an unexpected second-order nonlinear optical effect.[406,407] In earlier studies, thin films of a metal-templated polyrotaxane were deposited on a carbon electrode by electropolymerization of pyrrole rings.[408] Each rotaxane monomer contained the three binding motifs present in [2]catenate [Cu(**98**)] (Scheme 60a, Section 4.6.1). Electrochemical reduction of the pentacoordinate Cu^{II} species resulted in pirouetting of the macrocycle around the thread to give the Cu^{I} co-conformer in its lower energy tetrahedral geometry. The motion was slow, however, taking 24 h to go to completion, and oxidation back to Cu^{II} did not result in any detectable submolecular motion (the dpp-Cu^{II}→terpy-Cu^{II} transition is known to be slower in solution, see above). The same kind of motion was attempted in a catenate attached to a gold surface through S–Au bonds. However, in this case no motion could be observed at all.[409]

Electrochemically induced shuttling has been carried out on self-assembled monolayers (SAMs) of [2]rotaxane **124** on gold wire immersed in an electrolyte solution (Scheme 73).[410] The shuttle features TTF (green) and DNP (red) stations, and voltammetry measurements consistent with reversible translation of the macrocycle were observed on oxidation and subsequent reduction of the TTF unit. A related [2]rotaxane organized in Langmuir films undergoes shuttling induced by adding a chemical oxidant to the aqueous subphase.[411] Evidence for the submolecular motion was garnered from comparison of the π-A isotherms of the shuttle film with those of control compounds. X-ray photoelectron spectroscopy (XPS) of the initial and the oxidized films transferred onto solid substrates as Langmuir–Blodgett (LB) monolayers also confirmed a change in the position of the ring which was consistent with shuttling.

A different redox-active molecular shuttle was successfully oriented perpendicular to the surface of a titanium dioxide nanoparticle through attachment to a tripodal phosphonate unit at one end of the thread.[412] The use of nanoparticles as a support allowed characterization of the dynamic processes in the surface-mounted species by both ^{1}H NMR spectroscopy and cyclic voltammetry. Redox-triggered shuttling of the macrocycle was observed, although not with the expected switching characteristics. Paramagnetic suppression spectroscopy (PASSY), a novel NMR technique, suggests that the shuttling process, at least in solution, in these examples is complicated by various folded conformations of the thread.[413]

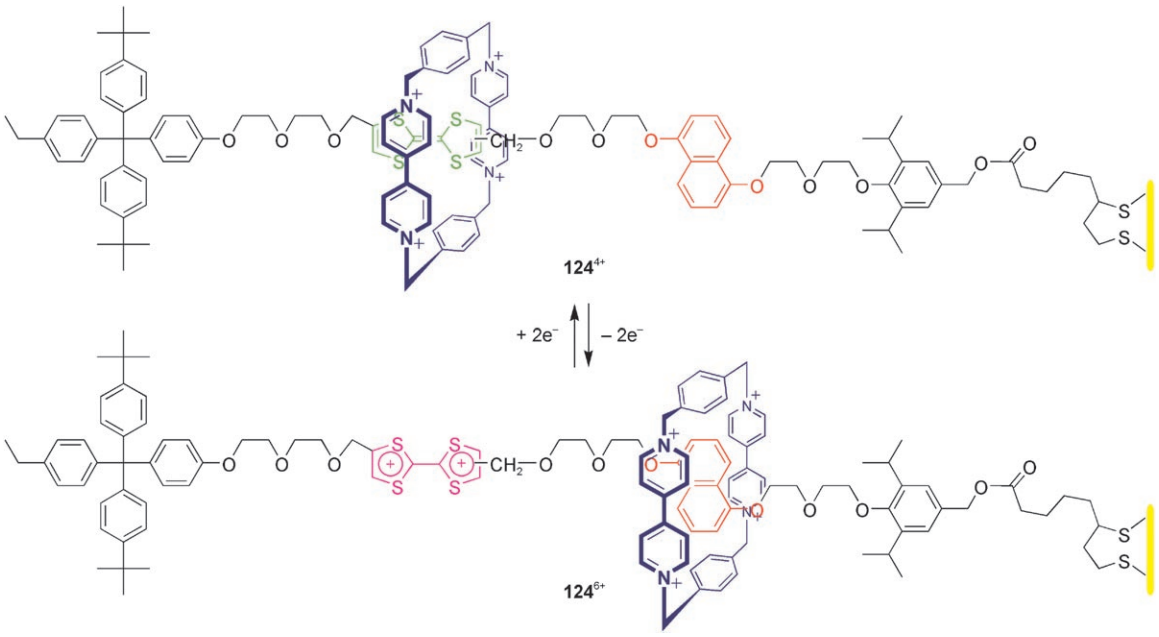

Scheme 73. An electrochemically switchable [2]rotaxane immobilized as a SAM on a gold wire.[410]

Taking advantage of the distinct "rotator" and "stator" design of the second-generation overcrowded alkene rotary motors (Scheme 22, Section 2.2), Feringa and co-workers have anchored these molecules on gold nanoparticles through two thioalkyl substituents appended to the base unit.[414] The photochemical and thermal rotation was monitored by CD spectroscopy and also by differentiation of the two thioalkane tethers with an isotopic label, followed by cleavage of the motor molecules from the surface at various stages and analysis in solution by NMR spectroscopy.[415]

8.2. Reporting Controlled Motion in Solution

Like other types of molecular switch,[151] a change in property induced by submolecular motion in a molecular machine could potentially be used in an information-storage or other switching device. The fundamental requirements for mechanical systems are the same as their nonmechanical counterparts and include: 1) a useful and detectable difference between two states; 2) fatigue resistance; 3) stability of each state under the operating conditions; 4) fast response times; and, particularly for memory applications, 5) nondestructive read-out.[151] The first of these is rather open to interpretation. A change in the chemical shift of an NMR signal, for example, may be considered by a chemist to be both easily detectable and useful—and there is no reason why such outputs might not be technologically relevant in certain applications one day. However, most of the examples highlighted in this section are chosen in view of the technological advantages of particular output modes: optical, electronic, and mechanical. This indeed reflects the research direction of the field of molecular machines over the past five years, in which the interaction of the machine with the outside world has become an increasingly important design element.

8.2.1. Conformational Switches in Solution

The stimuli-induced cessation of conformational motions ("molecular brakes", discussed in Sections 2.1.2 and 2.1.3) can be employed for switching applications. Glass and Raker have developed sensors by using a "molecular pinwheel" architecture (for example, **125**, Scheme 74) which exploits positive allosteric binding effects achieved in molecular brakes with multiple binding sites (for example, metal porphyrinate sandwich compound **22**, Scheme 7, Section 2.1.3).[416] Each trityl unit has one blade functionalized with a fluorophore and the other two with suitable binding sites. The binding of an analyte which can bridge between the two trityl moieties freezes the rotational motion of the trityl groups with respect to each other. The remaining binding sites are now preorganized, thus favoring a second, cooperative, binding of the substrate. The mode of binding holds the two fluorophores in proximity so that an increase in the ratio of the excimer:monomer fluorescence can be measured. Pinwheel receptor **125** is therefore able to detect short dicarboxylates selectively over monocarboxylates in aqueous media.[416d] It is proposed that this strategy could provide a general means to create cooperative sensors through tailoring the binding sites and distance between them to be specific for a particular analyte. A different approach to mechanically operated sensors is to append linear or macrocyclic polyethers to polythiophenes or oligothiophenes. In some cases binding can result in a significant perturbation to the conformation of the π-conjugated system, which results in changes to the molecular electronic properties.[417–419]

The possibility of conformational changes being transmitted over relatively long distances through fused cyclic frameworks was first noted by Barton in his seminal work on the conformational analysis of steroids.[420] An impressive example was recently reported by Clayden et al., who

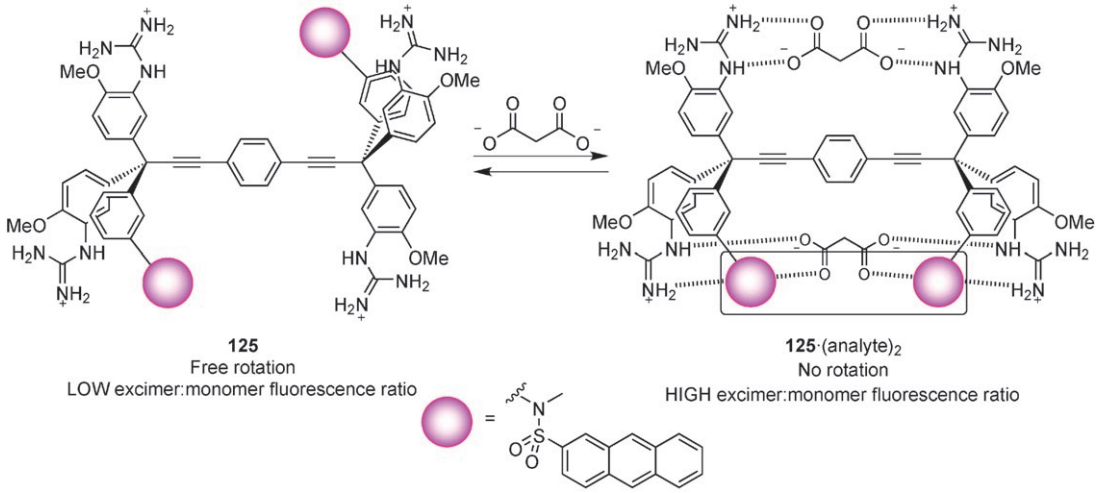

Scheme 74. An example of a molecular pinwheel receptor, **125**.[416d] Cooperative binding between pairs of convergent binding sites freezes internal rotation, thereby bringing the fluorophores into proximity so that the ratio of excimer:monomer fluorescence increases. The combination of cooperative binding and a mechanically transmitted binding-induced change in the fluorescence spectrum allows the sensing of short dicarboxylates at low concentrations in aqueous solution.

employed the conformational interactions of aromatic amides in **126** to transmit stereochemical information from a chiral group to a prochiral reaction site over 25 Å and a minimum of 23 covalent bonds (Scheme 75).[421]

Such conformational communication also presents opportunities to relay a stimuli-induced conformational change—triggered by a stimulus at some receptor site—through some structural framework so as to produce a detectable and reversible signal at a remote reporter unit. Pyranose-based conformational switch **31**, for example, (Scheme 11, Section 2.1.4) has been adapted to bring together two fluorophores through a chelation-induced ring-flip, therefore altering the optical properties.[422] Similarly, the W-shaped transoid–transoid to U-shaped cisoid–cisoid switching of terpyridine derivatives (see Scheme 16, Section 2.1.4) has been utilized to create another cation-triggered optomechanical switch **127** (Scheme 76).[423] This same strategy has also been used to switch the distance between two appended porphyrins, thus controlling energy- and electron-transfer processes between them.[424]

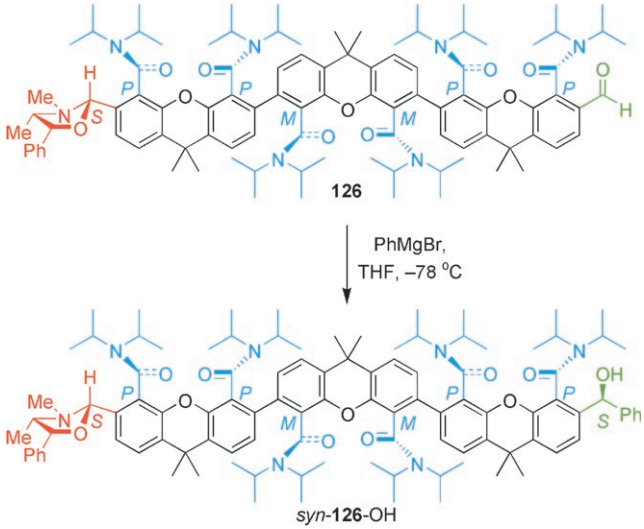

Scheme 75. Ultra-remote stereocontrol by conformational communication in the reaction of trisxanthene **126**.[421] The chiral oxazolidine ring (red) imposes a right-handed (*P*) twist on the adjacent amide as a result of both electronic and steric interactions. As the amides in such xanthene derivatives strongly prefer all-*anti* conformations, the effect of the enantiopure unit is transmitted throughout the molecule as a strongly preferred conformation for all the amide groups. The result is that Grignard addition to the aldehyde (green) proceeds with >95:5 diastereofacialselectivity. Subsequent cleavage of the oxazolidine affords an almost enantiomerically pure (>90% *ee*) alcohol.

One challenge, however, is to transduce a signal over longer distances, and for that purpose, 2,3,6,7-tetrasubstituted perhydroanthracene **128** was designed and constructed.[425] Conformational switching is triggered by metal-ion binding to the bipyridyl receptor units (red). The resultant three-ring flip separates the pyrene reporter units (blue), thus causing a change in fluorescence (Scheme 77). The binding signal is relayed over a distance of about 2 nm, while an analogous system based on 2,3,6,7-tetrasubstituted *cis*-decalins operates over a shorter distance of 1.5 nm.[426] In a first step towards transmitting signals over longer distances, the coupling of two such *cis*-decalin switches has been reported: the conformational change in one unit precipitates flipping of the remote ring system.[427]

The conformational bistability of resorcin[4]arene cavitands (Scheme 12, Section 2.1.4) has been exploited to create a well-defined mechanical switch, **129**, in which the distance between the extremities of the two "arms" is varied from approximately 0.7 nm to about 7 nm by a pH change (Scheme 78).[428] The conformational change is used to alter the distance between a donor–acceptor dye pair, thereby eliciting a major difference in the fluorescence resonance energy transfer (FRET) response.

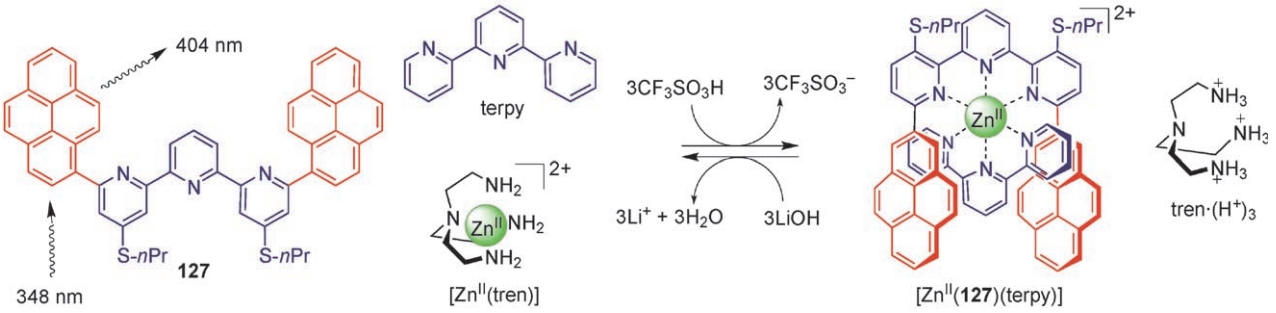

Scheme 76. A cation-triggered optomechanical switch.[423] When in the U-shape conformation, charge transfer from the pyrene fluorophores to the electron-poor complexed terpyridine (terpy) ligand effectively quenches fluorescence. Pulses of Zn^{II} ions are provided by protonation and deprotonation of the *N*,*N*-bis(2-aminoethyl)ethane-1,2-diamine (tren) ligand, so that, overall, the system is switched by alternate acid (CF_3SO_3H) and base (LiOH) stimuli.

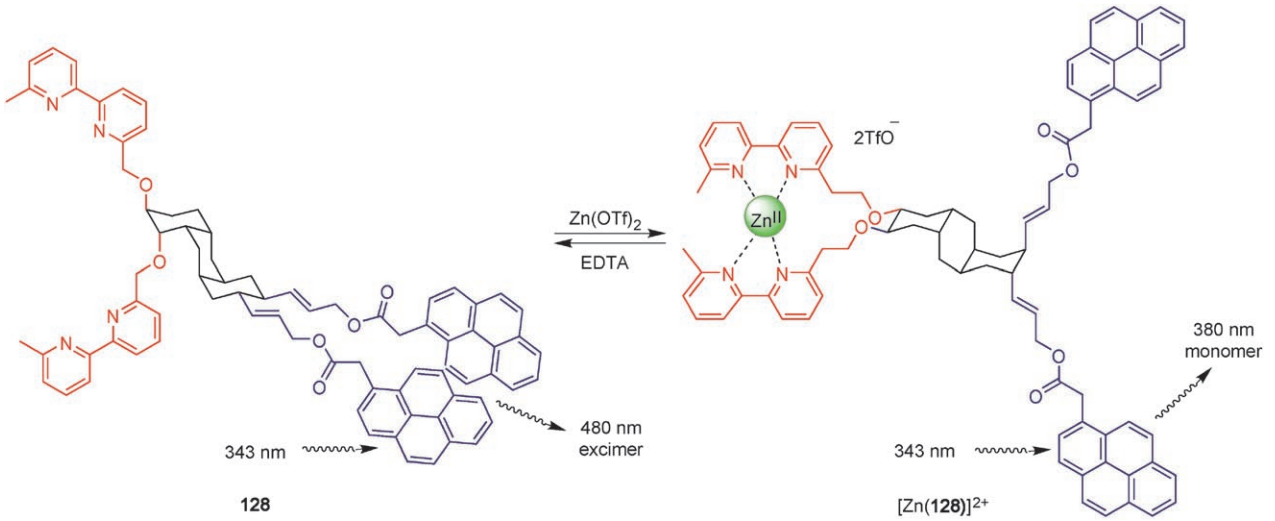

Scheme 77. Signal transduction by transmission of a conformational change from a receptor unit (red) to a reporter (blue).[425]

8.2.2. ***Co-conformational Switches in Solution***

The principles of shuttling in metal-templated rotaxanes have been extended to create a dimeric system in which the submolecular motion results in lengthening and contraction of the molecule in a manner reminiscent of the operation of the actin–myosin complex, which is the basis of natural muscle.[191v,429] Each monomer (**130**, Figure 40) consists of a bidentate dpp site incorporated in a macrocycle (see **98**, Section 4.6.1) connected to a thread which also contains a 2,9-dimethylphenanthroline (dmp) ligand and a tridentate terpyridine (terpy) site. The Cu^{I} ions used to template formation of the dimer coordinate to the dpp unit of one monomer and the dmp moiety of the other to give the threaded structure $[Cu_2(\mathbf{130})_2]^{2+}$ (Figure 41). Unfortunately, electrochemical oxidation to the Cu^{II} species did not trigger a change in co-conformation; even this unfavorable geometry for divalent copper ions is too kinetically stable. However, demetalation (excess KCN, room temperature, 3 h) to give the free ligand system $\mathbf{130}_2$, followed by insertion of Zn^{II} ions ($Zn(NO_3)_2$, room temperature, 1 h) generated the contracted form $[Zn_2(\mathbf{130})_2]^{4+}$, a length change of approximately 85 Å to 65 Å (a reduction of 24%). The molecule could be returned to its original length simply by treatment with excess $[Cu(CH_3CN)_4]PF_6$.

Simple monomeric stimuli-responsive molecular shuttles offer a generic approach to mechanical molecular switches for distance-dependant properties through suitable functionalization of the macrocycle and one end of the thread (Figure 42).[430]

Following the observation that the positioning of an intrinsically achiral benzylic amide macrocycle in relation to a chiral center can result in an induced circular dichroism (ICD) effect (Section 4.3.1), chiroptical molecular shuttle (*E*)/(*Z*)-**131** was prepared (Figure 43).[431] Unlike chiroptical switches in which the presence of, or handedness of, chirality is intrinsically altered,[150] (*E*)/(*Z*)-**131** remains chiral and nonracemic with the same handedness throughout; it is the expression of chirality that is altered. In the (*E*)-**131** form, the macrocycle is held over the fumaramide template and thus far from the chiral center of the peptidic station. Correspondingly the circular dichroism response is zero, as observed for the free thread. In the (*Z*)-**131** maleamide isomer, however, the olefin hydrogen-bonding station is "switched off", the macrocycle resides on the chiral peptide station, and a strong ($-13\,000\,deg\,cm^2\,dmol^{-1}$) negative ICD response is observed.

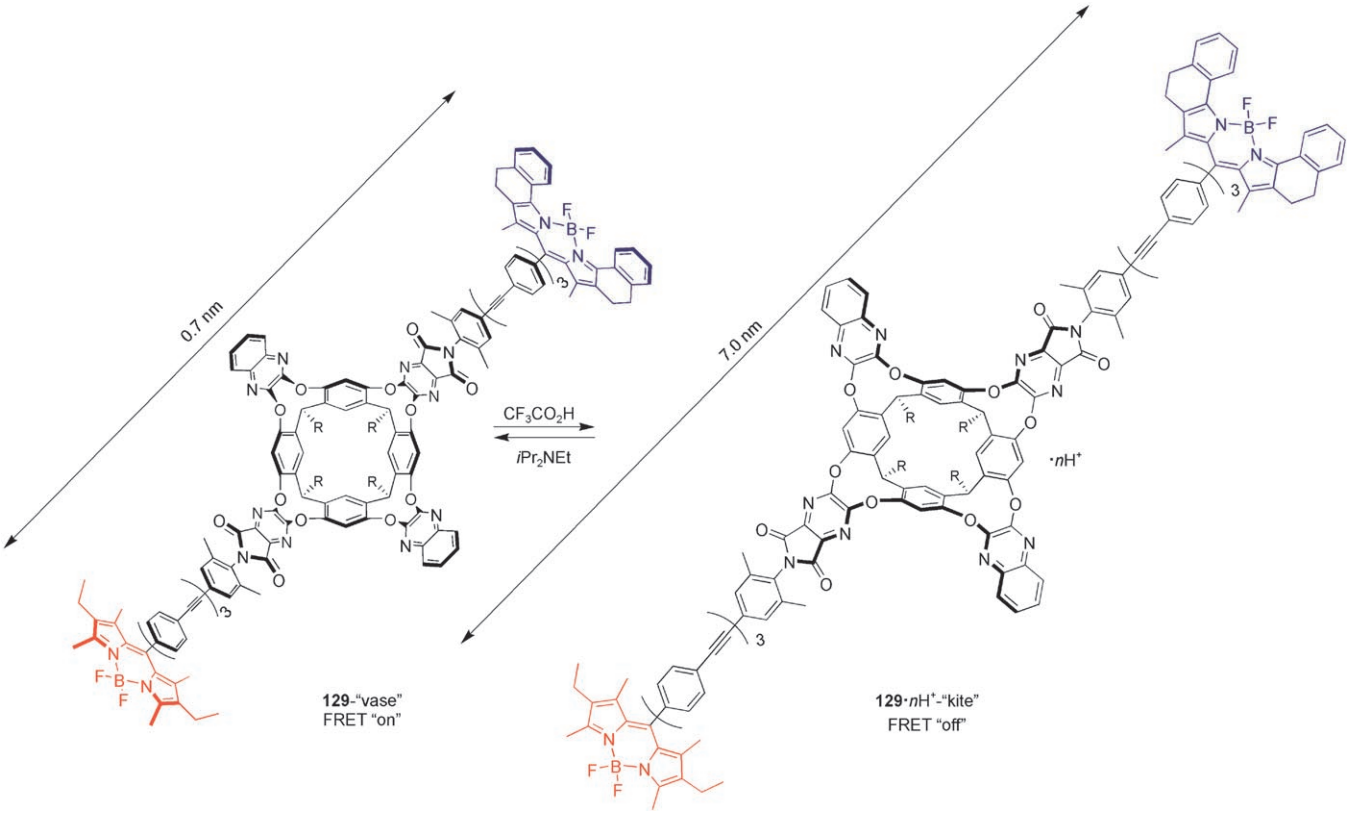

Scheme 78. pH-Governed conformational switching to control a FRET response in resorcin[4]arene cavitand **129**.[428] R = *n*-Hex.

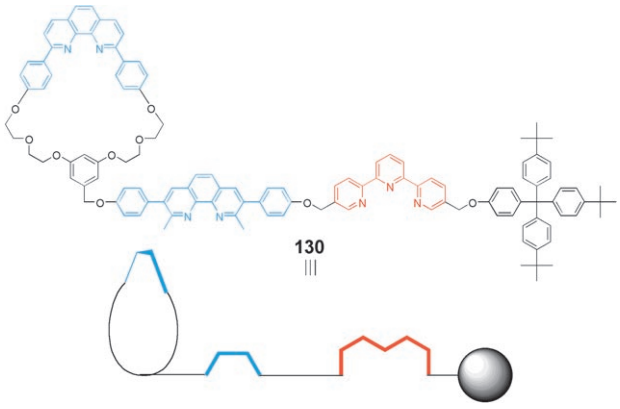

Figure 40. Monomer unit **130** for the construction of an artificial molecular muscle rotaxane dimer.[429]

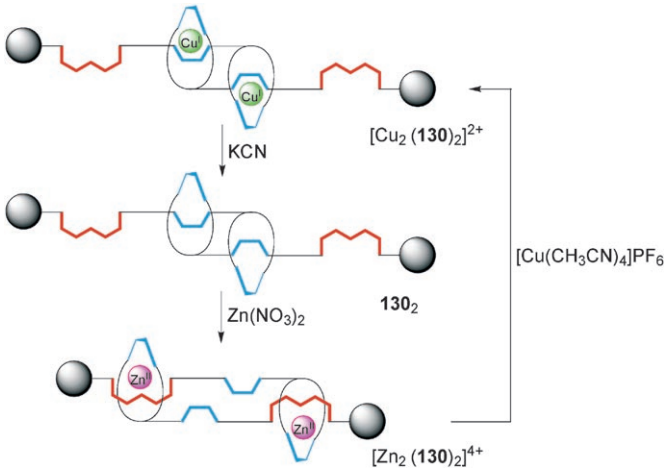

Figure 41. Reversible switching between extended ($[Cu_2(\mathbf{130})_2]^{2+}$) and contracted ($[Zn_2(\mathbf{130})_2]^{4+}$) forms in a chemically switched artificial molecular muscle.[429]

The $E \rightarrow Z$ isomerization is most efficiently carried out by irradiation at 350 nm in the presence of a benzophenone sensitizer (photostationary state 70:30 Z/E), while the $Z \rightarrow E$ transformation can be achieved almost quantitatively by irradiation at 400–670 nm in the presence of catalytic Br_2. Although a more modest difference in photostationary states is achieved by irradiation at 254 nm (photostationary state 56:44 Z/E) and 312 nm (photostationary state 49:51 Z/E), a large net change (> 1500 deg cm^2 dmol^{-1}) in the elliptical polarization response is still observed (Figure 43b) and this is reproducible over several cycles without addition of any external chemical reagents.[431]

A similar approach has been used to create a molecular shuttle switch for fluorescence, namely, $(E)/(Z)$-**132** (Figure 44).[430] This system also relies on the photoswitchable fumaramide/maleamide station, but attached to the intermediate-strength dipeptide station is an anthracene fluorophore while the macrocycle now contains pyridinium units, which are known to quench anthracene fluorescence by electron transfer. Strong fluorescence ($\lambda_{exc} = 365$ nm) is observed in both the free thread and (E)-**132**, while shuttling

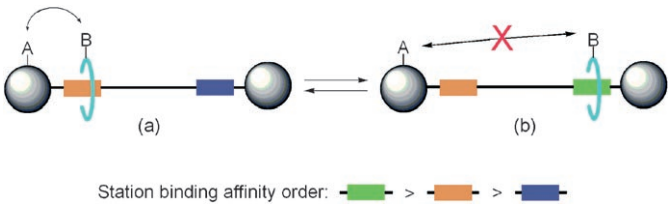

Figure 42. Exploiting a well-defined, large amplitude positional change to trigger property changes.[430] a) A and B interact to produce a physical response (fluorescence quenching, specific dipole or magnetic moment, nonlinear optical properties, color, creation/concealment of a binding site or reactive/catalytic group, hydrophobic/hydrophilic region, etc.); b) moving A and B far apart mechanically switches off the interaction and the corresponding property effect.

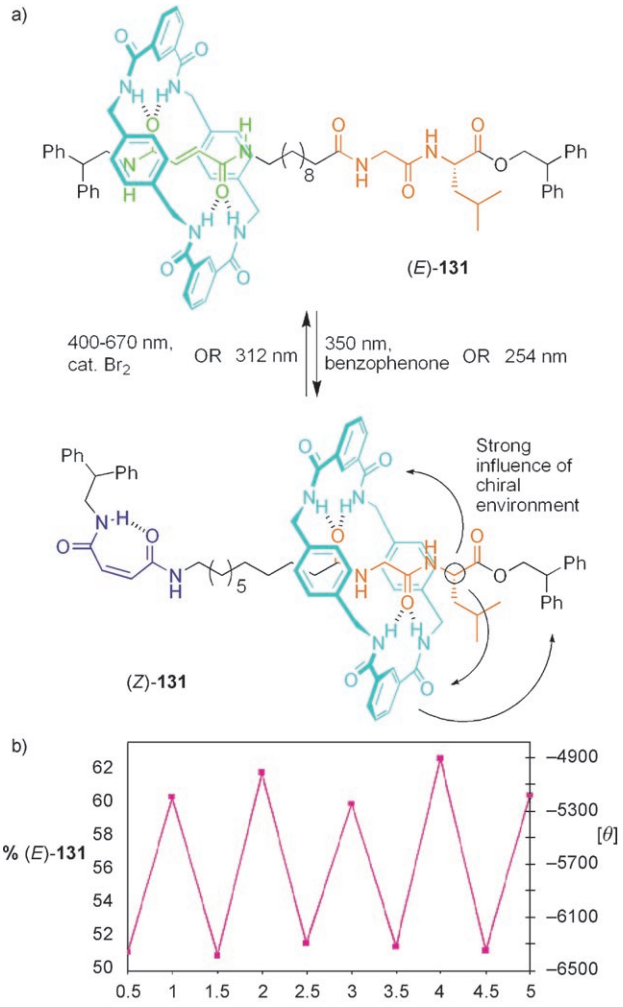

Figure 43. a) Chiroptical switching in the [2]rotaxane-based molecular shuttle (*E*)/(*Z*)-**131**.[431] b) Percentage of (*E*)-**131** in the photostationary state (from ^{1}H NMR data) after alternating the irradiation between 254 nm (half integers) and 312 nm (integers) for five complete cycles. The right-hand *y*-axis shows the CD absorption at 246 nm.

of the macrocycle onto the glycylglycine station in (*Z*)-**132** almost completely quenches this emission. At the wavelength of maximum emission from (*E*)-**132** ($\lambda_{max} = 417$ nm) there is a remarkable 200:1 difference in intensity between the two

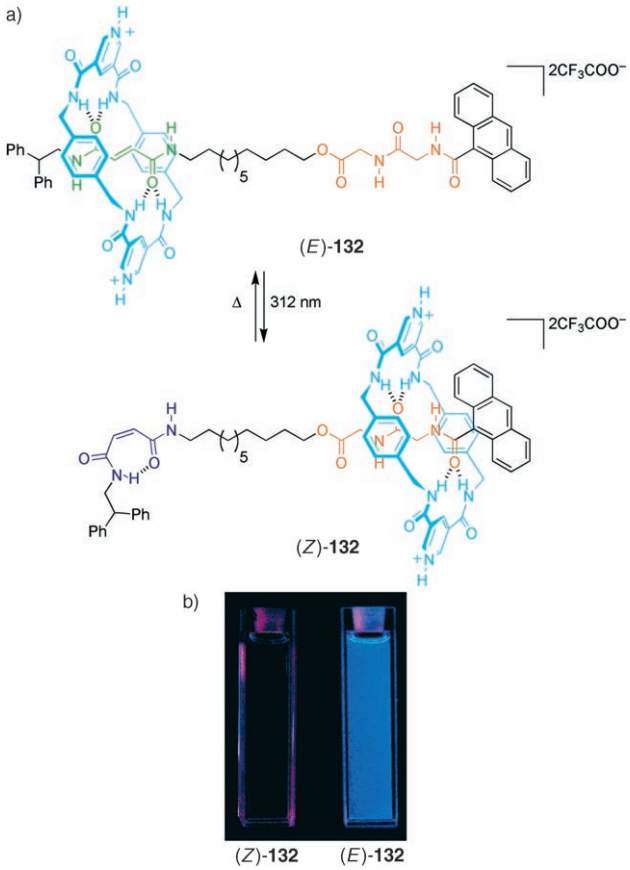

Figure 44. A fluorescent molecular switch based on [2]rotaxane molecular shuttle (*E*)/(*Z*)-**132**.[430] a) Interconversion between fluorescent (*E*)-**132** and nonfluorescent (*Z*)-**132**; b) images of cuvettes containing solutions of (*Z*)-**132** and (*E*)-**132**, respectively (0.8 μM, CH_2Cl_2), illustrating the clearly visible difference in fluorescence intensity. The photograph was taken while illuminating the samples with UV light (365 nm).

states which is strikingly visible to the naked eye (Figure 44b).[432]

A related strategy has been applied by Tian and coworkers to achieve fluorescence switching in a different type of [2]rotaxane system, (*E*)/(*Z*)-**133** (Scheme 79).[433] In (*E*)-**133**·2H, the α-cyclodextrin ring sits preferentially over the *trans*-stilbene unit and this co-conformation is apparently further stabilized by strong hydrogen-bonding interactions between hydroxy groups on the cyclodextrin 3-rim and the isophthaloyl stopper group.[434] As for previous α-CD-based rotaxanes (Scheme 33, Section 4.3.1), photoisomerization of the stilbene unit can only occur when thermal motion has moved the ring away from the binding site. However, the strength of the combined hydrophobic and hydrogen-bonding interactions (even in water) for (*E*)-**133**·2H means that the shuttle is effectively conformationally locked: irradiation at 355 nm, which should isomerize the stilbene moiety, results in no change to the system. Formation of the disodium salt of the isophthaloyl group (giving (*E*)-**133**·2Na) breaks the hydrogen-bonding network and although NMR studies show that the cyclodextrin continues to sit over the stilbene station, enough thermal motion is now present to allow photoisome-

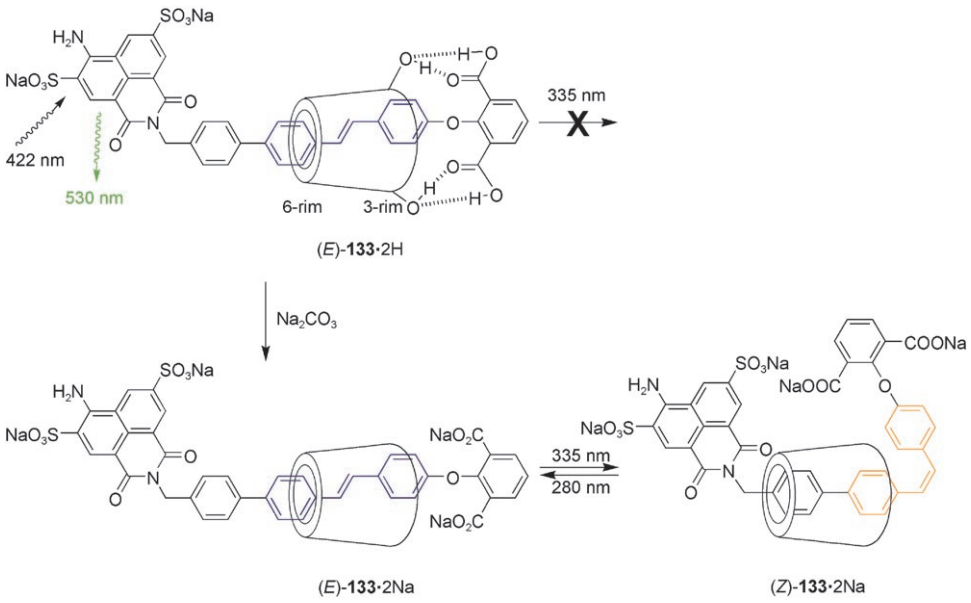

Scheme 79. Photoswitched shuttling in [2]rotaxane (*E*)/(*Z*)-**133**·2 Na which results in fluorescence enhancement of the 4-aminonaphthalimide group.[433] The photoisomerization process is prevented when the free carboxylic acids of the isophthaloyl stopper are present ((*E*)-**133**·2H).

rization to give (*Z*)-**133**·2 Na (photostationary state 63:37 *Z*/*E*). In the *Z* isomer the cyclodextrin ring is forced to reside over the biphenyl group. The translocation of the ring is accompanied by a 46% increase in fluorescence intensity of the 4-aminonaphthalimide stopper ($\lambda_{max} = 530$ nm). This change is attributed to a restriction of the vibrational and rotational movement of the methylene and biaryl linkages thus disfavoring nonradiative relaxation processes. The shuttling and fluorescence changes are reversible on reisomerization to (*E*)-**133**·2 Na at 280 nm.

Using either a stilbene[50k] or an azobenzene[435] configurational switch, the same research group have extended this concept to [2]rotaxanes in which the fluorescence of either one of two different fluorophores can be enhanced depending on the position of the ring.[436] Incorporating two different configurational switches into such a rotaxane has allowed the creation of a molecular system capable of carrying out the function of a half-adder—a two-input, two-output device which combines AND and XOR logic functions and which can perform binary addition.[355] [2]Rotaxane **134** can be reversibly switched between four different configurational isomers through selective photochemical and thermal stimuli (Scheme 80). For operation as a logic gate, UV irradiation at 380 nm and 313 nm can be considered as two input signals (I1 and I2). In both ($Z_{N=N}$,$E_{C=C}$)-**134** and ($E_{N=N}$,$Z_{C=C}$)-**134**, the proximity of the ring to one or other stopper increases its fluorescence by an appreciable amount, while in both (*E*,*E*)-**134** and (*Z*,*Z*)-**134** the cyclodextrin is not held close to either fluorescent stopper (because of rapid shuttling in the former case and trapping on the biphenyl unit in the latter). Therefore, if the change in fluorescence intensity relative to (*E*,*E*)-**134** (ΔF) is taken as an output (O1), this can be interpreted as an XOR gate (see truth table in Scheme 80). All four states exhibit absorbance maxima at 270 nm, which is found to increase in intensity on successive $E \rightarrow Z$ isomerization of the double bonds, and at 350 nm, which decreases as $E \rightarrow Z$ for each configurational switch. The result is that the difference in the absorption at these two wavelengths, expressed as a fraction of the absorption at the isobestic point (301 nm), is relatively small for all but the (*Z*,*Z*)-**134** isomer and, thus, this value can be considered the output of an AND gate (O2). As these two functions operate in parallel, are based on the same two inputs, and give two distinct outputs, this system represents monomolecular realization of a half-adder function operating purely through photonic stimuli.[252,355] It is also possible to construct a [3]rotaxane analogue of **134**.[437] The resulting shuttle exhibits three stable states (*E*,*E*-, *Z*,*E*-, and *E*,*Z*-) each of which exhibits a different fluorescent response as a consequence of the position of the rings.

The nature of interlocked architectures—in which certain functional groups are encapsulated by the binding cavity of a separate unit—suggests that their dynamic attributes may allow the development of novel applications in catalysis. As a first step towards creating a fully processive catalyst, Rowan and co-workers have created a macrocyclic unit incorporating a manganese porphyrin, which can catalyze the epoxidation of an olefin bound in the inner cavity when an external oxidant and a bulky ligand are also present.[438] Threading this unit onto a polybutadiene chain and stoppering to create a rotaxane architecture creates a mechanically linked catalyst–substrate system; when the external reagents are added, the macrocycle promotes epoxidation at multiple positions on the thread, although at present the movement and action of the macrocycle is presumably random and nondirectional between thread sites.[439] The mechanically linked nature of such catalyst–substrate complexes could lead to processive catalysts for the post-polymerization modification of polymers and provide insight into the operation of the processive enzymes which are so central to fundamental processes in the cell.

8.3. Reporting Controlled Motion on Surfaces, in Solids, and Other Condensed Phases

Early successes at operating molecular machines on surfaces and at interfaces were discussed in Section 8.1. Incorporation of mechanical switches (Section 8.2) into such environments can lead to switchable solids and interfaces in which stimuli-induced molecular-level motions can be communicated to the macroscopic world as changes in the

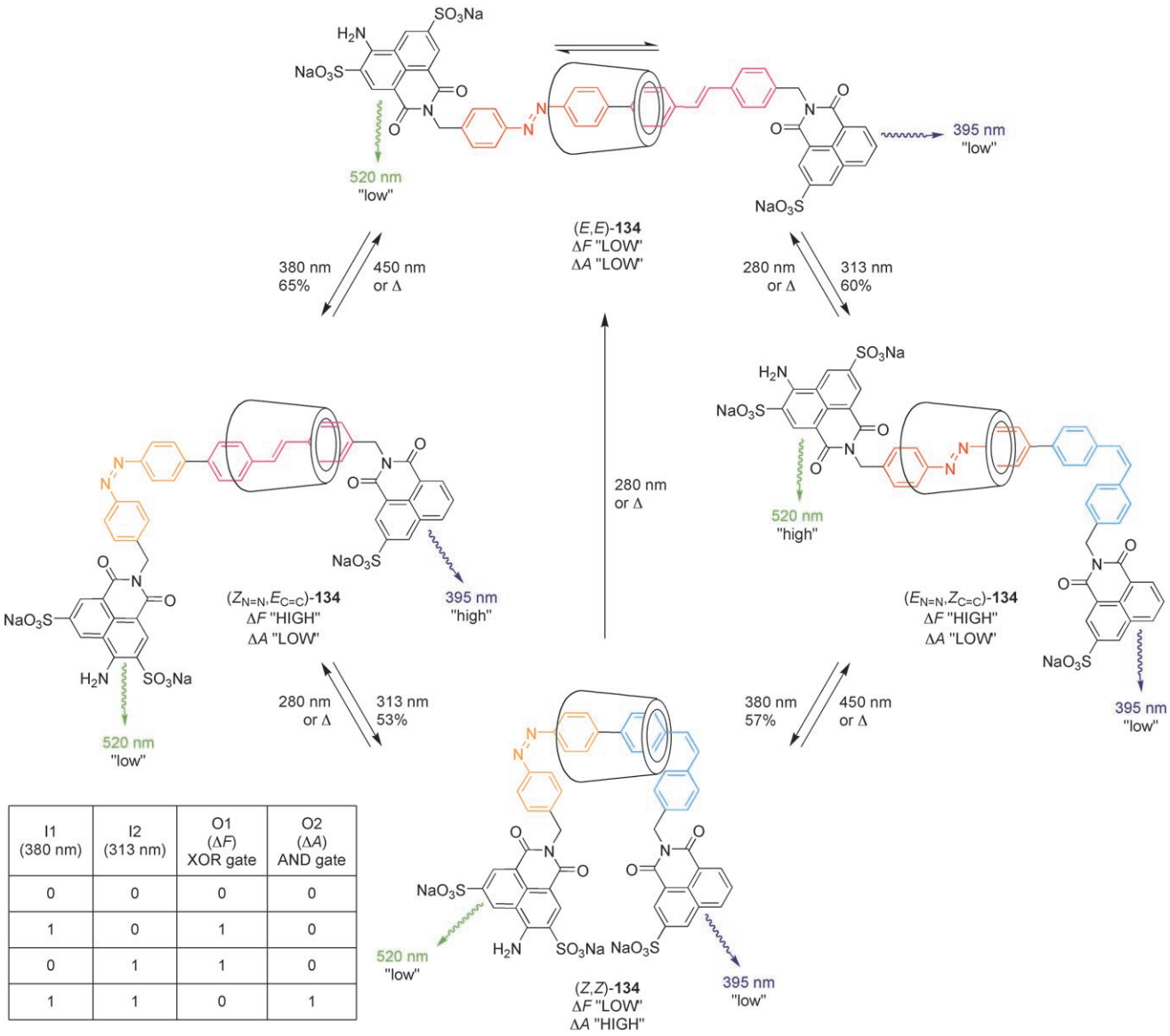

I1 (380 nm)	I2 (313 nm)	O1 (ΔF) XOR gate	O2 (ΔA) AND gate
0	0	0	0
1	0	1	0
0	1	1	0
1	1	0	1

Scheme 80. Operation and truth table for a molecular half-adder based on a fluorescent molecular shuttle.[355] Note, the $E \rightarrow Z$ photoisomerizations reached photostationary states, shown here as percentages of the major isomer over the reaction arrows. All the fluorescence and absorption measurements were carried out on these photostationary state compositions and the differences in the ΔF and ΔA values were sufficient to discern "high" (1) and "low" (0) responses.

properties of the material. At the very least, this requires the combined mechanical switching of an ensemble of molecules and, in the most sophisticated cases, coordinated coherent motions of a population of molecular machines is required.

8.3.1. Solid-State Molecular Electronic Devices

In a series of ground-breaking experiments that interface molecular-level machines with silicon-based electronics, molecular shuttles (Sections 4.2 and 4.3) have been employed as an active molecular component in solid-state molecular electronic devices.[440] In the first example of such devices to utilize interlocked molecules, a monolayer of redox-active degenerate two-station rotaxanes (**135**$^{4+}$, Scheme 81) was sandwiched between electrodes made from titanium and aluminum oxide.[441] The resulting junctions exhibited a strongly nonlinear current–voltage response at small negative biases. Application of an oxidizing voltage however resulted in an irreversible reduction in conductance. Connection of these fuselike switches in linear arrays created wired-logic gates performing OR and AND functions that displayed more pronounced voltage responses compared to resistor-based circuits, and thus demonstrating the defect-tolerance of this architecture for generating logic functions.

In a second generation of devices, bistable interlocked molecules were employed and reversible switching achieved. Structures containing the tetracationic cyclophane CBPQT^{4+} can be ordered in Langmuir films by using an amphiphilic counterion and the monolayers subsequently transferred onto solid substrates by using the LB technique.[442] The process

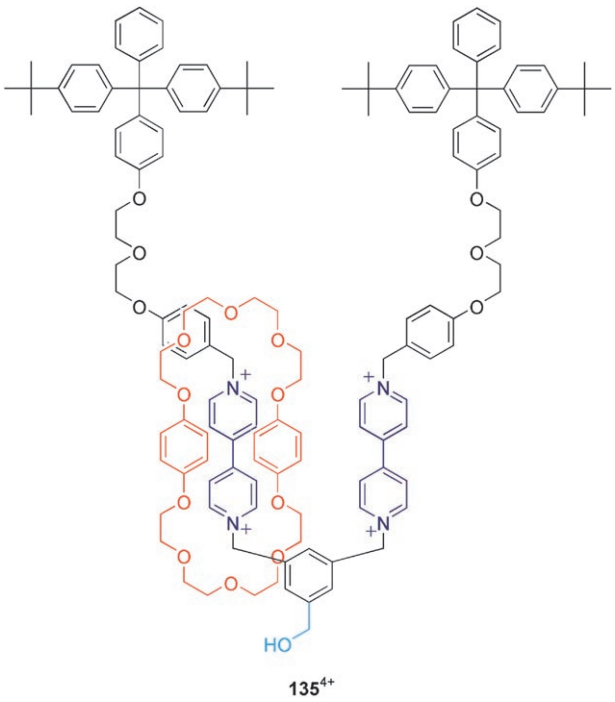

Scheme 81. Chemical structure of amphiphilic [2]rotaxane $\mathbf{135}^{4+}$ employed in the first electronic switches based on an interlocked molecule.[441] Alignment of the molecules was achieved by exploiting the hydrophobic (black stoppers) and hydrophilic (light blue hydroxymethyl moiety) portions at the top and bottom of the molecule as drawn.

was used to create a molecular switch tunnel junction (MSTJ) in which a monolayer of bistable [2]catenane $\mathbf{92}^{4+}$ (Scheme 54, Section 4.6.1) was sandwiched between silicon and titanium/aluminum electrodes.[443] These devices exhibited a moderate (ca. 2×) increase in conductance after application of an oxidizing potential, while recovery of the initial state occurred after a reducing voltage was applied. The "read" voltage was in the region 0.1 to 0.3 V and did not interfere with the switch configuration, while the devices withstood many switching cycles. A rational design process then led to devices made from a related [2]pseudorotaxane ($\mathbf{136}^{4+}$, Scheme 82) in which hydrophobic and hydrophilic regions are now directly incorporated into the molecular structure to allow self-organization.[444] Although larger on/off current ratios and absolute currents were observed, the device characteristics were found to vary widely between both cycles and devices. On further investigation, these problems were attributed to the formation of molecular domains, which means that the device characteristics were no longer determined by single-molecule properties.

Further refinements of this shuttle structure produced amphiphilic bistable [2]rotaxanes $\mathbf{137}^{4+}$ and $\mathbf{138}^{4+}$. Molecular switch tunnel junctions of these rotaxanes possessed stable switching voltages around −2 and +2 V with reasonable on/off ratios and switch-closed currents.[445] These favorable characteristics allowed preparation of nanometer-scale devices which displayed properties similar to the original micrometer-sized analogues, thus suggesting a molecular-level mechanism for the MSTJ operation. Furthermore, these

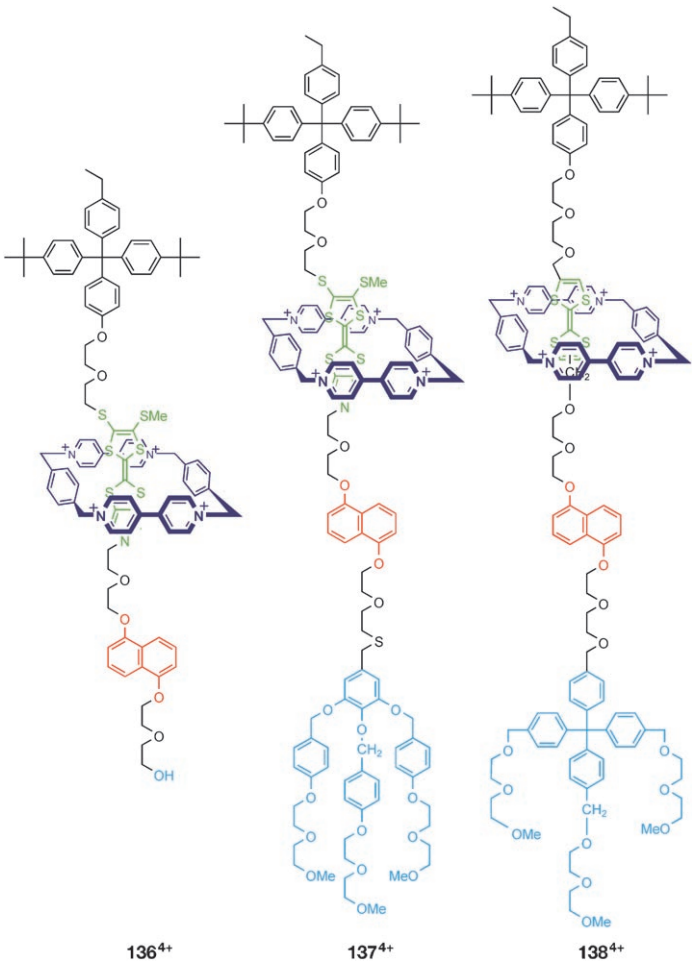

Scheme 82. Chemical structures of amphiphilic bistable [2]pseudorotaxane $\mathbf{136}^{4+}$ and [2]rotaxanes $\mathbf{137}^{4+}$ and $\mathbf{138}^{4+}$ used as the active components MSTJs.[444,445] Hydrophobic (black) and hydrophilic (light blue) regions are incorporated directly into the structures to allow self-assembly in Langmuir films without requiring additives.

devices could be successfully connected to form a 2D crossbar circuit architecture. The circuit could be used as a reliable 64-bit random access memory (RAM). The more demanding task of creating a logic circuit was also demonstrated by hard-wiring 1D circuits. A genuine 2D MSTJ-based crossbar logic circuit, however, will require junctions with features yet to be attained by using molecular systems, such as diode character and gain.

A limited number of non-interlocked and nonswitchable control molecules (for example, a simple alkyl chain carboxylic acid, the free CBPQT^{4+} ring, and related degenerate catenanes) have been tested in similar settings to provide supporting evidence that a molecular-level electromechanical mechanism is responsible for the switching observed in the rotaxane-based devices.[442c,443–445] The studies suggest that some form of bistability, together with the presence of the macrocycle, are necessary for the switching properties and are therefore consistent with a mechanism whereby electronically stimulated shuttling alters the junction conductance. However, devices made from a single station [2]rotaxane still exhibit conductance switching, albeit with a significantly

lower on/off ratio than the two-station analogues **137**$^{4+}$ and **138**$^{4+}$.[444] Crucially, all the solid-state devices exhibit marked temperature dependence, which showed that at least one thermally activated step is involved in their operation. This is in line with the observation of a metastable state for shuttling in solution at low temperature (Section 4.3.4),[228f] as well in similar interlocked systems aligned in SAMs,[410] Langmuir films, and Langmuir–Blodgett monolayers (Section 8.1),[411] and dispersed in a solid-state polymer electrolyte (Section 8.3.2).[446] By comparison of these systems, together with the performance of a different rotaxane analogue in solution, in a polymer electrolyte, and in MSTJs,[228i] it has been demonstrated that the ground-state thermodynamics of these shuttles are controllable by manipulation of chemical structure and are qualitatively independent of the surrounding medium. However, the nature of the environment does strongly affect the kinetics for relaxation of the non-equilibrium state as one would expect, and the experimentally determined values from each environment quantitatively support a common molecular-level switching mechanism based on shuttling motion.[191ad,228f,i] The proposed mechanism for operation of the solid-state electronic devices is summarized in Figure 45.

Identification of the high conductance state as that with the cyclophane encircling DNP (state (d), Figure 45) is supported by quantum mechanical computational studies in which the I–V response was simulated for a model pseudorotaxane in each of the two co-conformations (that is, corresponding to (a) and (d) in Figure 45).[447] The picture presented in Figure 45 is not entirely accurate, however, particularly with regard to the conformation of the rotaxane molecules. Analysis of the structures of Langmuir and LB films composed of various amphiphilic [2]rotaxanes indicates that unless high surface pressures or larger hydrophilic stoppers are employed, a very acute angle to the interface is adopted, probably as a result of the hydrophilicity of the tetracationic cyclophane.[448] These experimental results were recently reproduced by a molecular dynamics study of the Langmuir films, in which similar tilted arrangements were observed for both co-conformations.[449] The overall conformation of the thread portion is folded and dependent on the position of the macrocycle. Folded conformations resulting from "alongside" interactions between the CBPQT^{4+} moiety and the vacant π-donor station are often observed in solution,[191ad,217j,225e,228c,d,h,238] so it seems likely that such arrangements are also present at surfaces and in the solid state. The importance of conformation on electronic properties was highlighted in a computational study in which density functional theory was used to calculate the electronic structure of various functional components of the rotaxanes and from which a description of the rotaxane frontier molecular orbitals could be derived.[450] It was found that the ring-on-DNP co-conformation was only the most conductive if the cyclophane participates directly in electron tunneling by providing low-lying LUMO orbitals. Such a situation is most plausible for a folded conformation with direct interactions between the ring and the unoccupied station. The molecular dynamics simulation of Langmuir films,[449] as well as a similar treatment of thiol-anchored SAMs on Au(111),[451] suggest that such folded conformations form thermodynamically favored superstructures, while the added intra- and intermolecular interactions do not alter the relative stabilities of the two co-conformations. Such arrangements actually place the rotaxane functional units in relative orientations comparable to the analogous [2]catenane which originally displayed very similar device characteristics. Density functional calculations for optimized monolayers of [2]catenane **92**$^{4+}$ sandwiched between two gold electrodes demonstrated again that the ring-on-DNP co-conformation exhibits the higher conductance at small applied read bias, with the conduction involving HOMOs from TTF as well as DNP and LUMOs from CBPQT^{4+}.[452]

Clearly the most convincing verification of an electromechanical mechanism for conductance switching

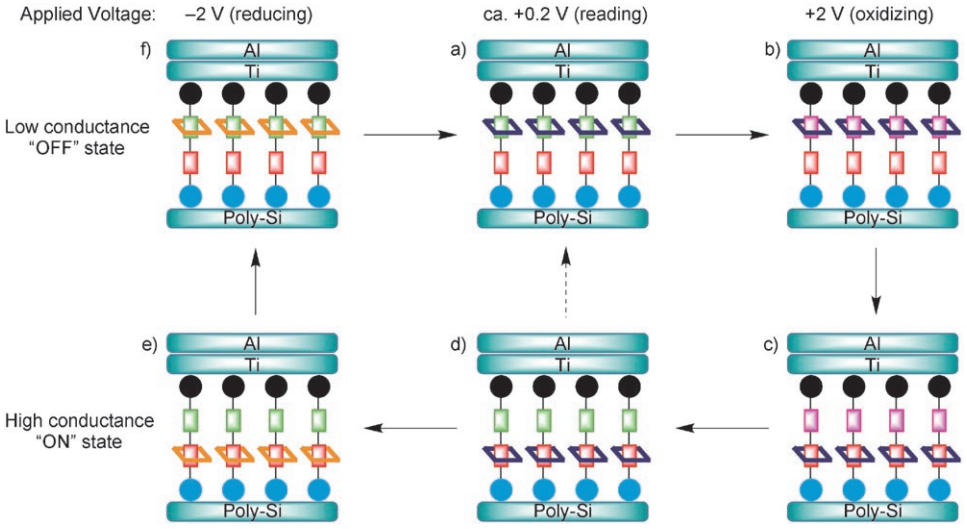

Figure 45. Proposed mechanism for the operation of rotaxane-based MSTJs.[191x,y,ad,228f] The coloring of functional units corresponds to that used for structural diagrams in Scheme 82. a) In the ground state, the tetracationic cyclophane (dark blue) mainly encircles the TTF station (green) and the junction exhibits low conductance (the precise ratio of co-conformers in this state is dependent on the exact chemical structure of the [2]rotaxane and in some cases can also be temperature dependent). b) Application of a positive bias results in one- or two-electron oxidation of the TTF units (green→pink) and the resulting electrostatic repulsion causes shuttling of the ring onto the DNP station (red, c). d) Returning the bias to near 0 V reveals a high conductance state in which the TTF units have been returned to neutral, but translocation of the cyclophane has not yet occurred, because of a significant activation barrier. Thermally activated decay of this metastable state ((d)→(a)) may occur slowly, over time (dependant on temperature) or can be triggered by application of a negative voltage (e) which temporarily reduces the cyclophane to its diradiacal dication form (dark blue→orange), thus allowing facile recovery of the thermodynamically favored co-conformation (f). A similar mechanism is applicable in the operation of devices based on analogous [2]catenanes.

would be direct real-time observation of the shuttles in an operating solid-state device. Probing a single molecular monolayer confined between two electrodes is a challenge which cannot yet be routinely met by modern-day analytical methods, and preliminary attempts at using grazing-angle refection-absorption infrared spectroscopy (RAIRS) to study mechanical movements in such scenarios have proven unsuccessful.[453] Following on from indirectly observed shuttling in Langmuir monolayers[411] (see Section 8.1), the first direct evidence for shuttling in such a condensed phase was recently obtained by using X-ray reflectometry.[454] These results have also confirmed the considerably tilted and folded rotaxane conformations which were previously inferred (see above).

Although these devices show potential as possible components for genuine single-molecule electromechanical switches, a significant barrier to achieving this goal is the nature of the physical connections used to wire the device. At very small dimensions, it is expected that metal wires will exhibit the best conductance characteristics, but unfortunately a range of molecular shuttle devices with two metal electrodes failed to demonstrate switching properties that were dependent on the nature of the organic monolayer.[455] Indeed, the polarity of molecule–metal interfaces and the potential for the formation of metal filaments within molecular monolayers are emerging as recurring issues in metal-contacted organic molecular electronics.[456] However, catenane-based MSTJs which utilize single-walled carbon nanotubes in place of the silicon electrode have been successfully created and this may provide a valuable alternative in the creation of real-world devices.[457] Whether the philosophy of using thermally activated nuclear motions which occur on timescales many orders of magnitude slower than electron motions is the right one for a practical molecular computer or not is not necessarily the most valuable aspect of this work. The interfacing of molecular machines with electronics opens up the possibility of many types of practical hybrid devices and will doubtless prove seminal in getting molecular motors and machines out of solutions in laboratories and into technological devices.

8.3.2. Using Mechanical Switches to Affect the Optical Properties of Materials

The configurational changes that occur in photochromic dopants have been used for a number of years to initiate changes in a number of liquid-crystal properties.[458] The *trans*→*cis* photoisomerization of stilbene or azobenzene dopants, for example, can cause reversible disruption of the nematic mesophase, effectively "turning off" liquid crystallinity. However, a more subtle form of mechanical molecular-level control is achievable in systems where the mesophase structure is maintained throughout. It is possible to orient photochromic dopants in a liquid-crystalline phase through axis-selective photoconversion by applying plane-polarized light to stimulate repeated photoisomerization. This directional orientation triggers alignment of the whole liquid-crystal phase. A second vector of polarization can then be used to produce a differently aligned state. This type of process has recently been modeled as a Brownian ratchet—each of the interconverting forms of the dopant molecule move over a different potential energy surface as a result of different interactions with the liquid-crystalline phase, while transitions between them are fueled by the optical stimulus.[459] Such systems clearly exhibit remarkable amplification of a relatively small photoinduced configurational change which causes a global orientation change in the bulk. It is even possible to create surface-controlled systems where a monolayer of photochromic species (a so-called "command surface") controls the alignment of a whole liquid-crystal layer in contact with it. Potential applications of this photoinduced mechanical molecular-level motion include optical recording media and light-addressable displays.[458]

Chiral dopants can induce the formation of chiral nematic (cholesteric) phases. If the dopants contain photoswitchable units, variations in the expression of chirality can be achieved. Recently a dopant of fixed chirality bound to an azobenzene photoswitch was used to reverse the screw sense of the cholestric phase.[460] Some chiroptical switches, such as the overcrowded alkenes discussed in Section 2.2, have a change in helicity associated with their photochromic switching and so are well-suited to switching the cholesteric liquid-crystal chirality.[461] Unidirectional molecular motor **46** (Figure 18, Section 2.2) has also been shown to play such a role.[462] Of the three isomers which can be isolated at room temperature, each exerts a different helical twisting power on the liquid-crystalline matrix, with opposite dopant helical handedness inducing contrary screw senses in the liquid crystal. Photochemical and thermal unidirectional rotation of the motor was shown to occur within the liquid-crystal matrix, albeit with reduced efficiency and rates compared to solution studies. Liquid-crystal films doped with (*P*,*P*)-*trans*-**46** gave a cholesteric phase with right-handed helicity and displayed a violet color. Photoirradiation ($\lambda > 280$ nm) at room temperature leads to a decrease in the proportion of this isomer and concomitant increases in the amount of (*P*,*P*)-*cis*-**46** (which has a much weaker right-handed helical-twisting power) and (*M*,*M*)-*trans*-**46** (which exerts a left-handed helical twist). The combined effect of the change in dopant isomer composition is to progressively change the color of reflected light from violet through to red (Figure 46). A blue shift of the reflected wavelength could also be achieved on heating the film to 60 °C which converts any (*M*,*M*)-*trans*-**46** present back into (*P*,*P*)-*trans*-**46**.[462] As a consequence of the induced helicity in the liquid-crystal phase, it seems likely that the reorganizational motions triggered by isomerization of the dopant molecule are directional in nature. The color change, however, is not a result of the unidirectional trajectory of the motor; rather it is an expression of the system's state at

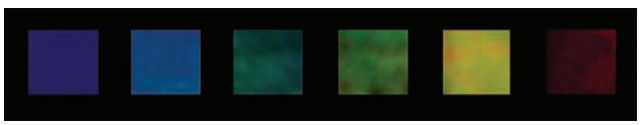

Figure 46. Color changes in a liquid-crystal film doped with **46** (6.16 wt%).[462] Starting from 100% (*P*,*P*)-*trans*-**46**, the sample is irradiated with light of $\lambda > 280$ nm at room temperature. The pictures of the film shown from left to right were taken at 0, 10, 20, 30, 40, and 80 s. Reprinted with permission from Ref. [462].

any particular moment in time, a function of the different populations of a three- (or four-) state switch (see also Section 8.3.3). In other words, in this situation the motor molecule is simply acting as a switch and the directionality of the rotation of its components probably plays no role in changing the liquid-crystal color.

The use of controlled molecular motion in polymer films to generate patterns visible to the naked eye (Figure 47) has been demonstrated with a molecular shuttle based fluorescent switch derivatized with poly(methyl methacrylate) (**139**, Scheme 83).[463] A polymer film INHIBIT logic gate based on a combination of stimuli-controlled submolecular positioning of the ring and protonation was also demonstrated (**140**/**140**·2 H^+, Scheme 83, Figure 48).[463]

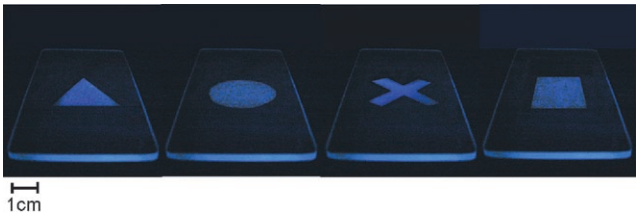

Figure 47. Images obtained by casting films of polymer **139** on quartz slides, covering them with an aluminum mask, and exposing the unmasked area to dimethyl sulfoxide vapors for 5 min.[463] The photographs were taken while illuminating the slides with UV light (254–350 nm). The symbols of Sony Playstation are illustrative of the types of patterns that can be created.

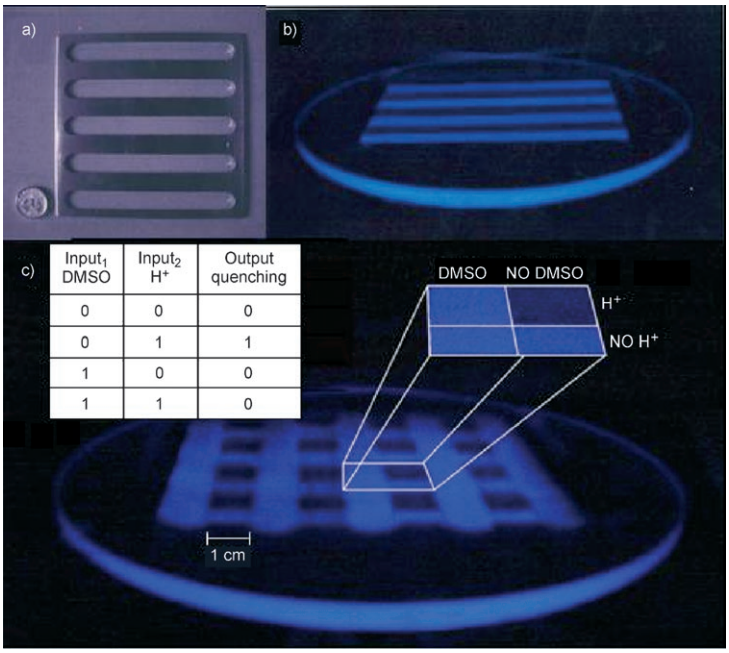

Figure 48. A molecular-shuttle Boolean logic gate that functions in a polymer film.[463] a) The aluminum grid used in the experiment. The coin shown for scale is a UK 5p piece. b) The pattern generated when films of **140** were exposed to trifluoroacetic acid vapor for 5 min through the aluminum grid mask. c) The criss-cross pattern obtained by rotating the aluminum grid 90° and exposing the film shown in (b) to DMSO vapor for a further 5 min. Only regions exposed to trifluoroacetic acid but not to DMSO are quenched. The truth table for an INHIBIT logic gate is shown in the inset. The photographs of the slides were taken in the dark while illuminating with UV light (254–350 nm).

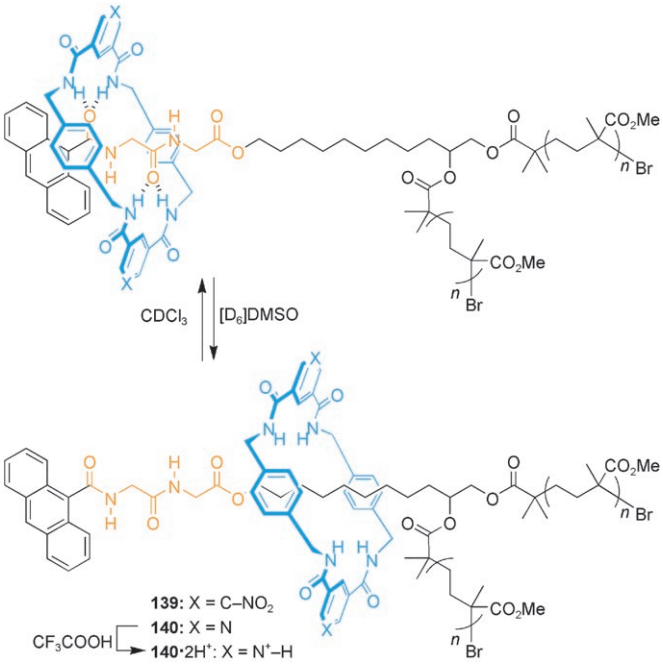

Scheme 83. Polymeric environment-switchable molecular shuttles **139** and **140**/**140**·2 H^+.[463]

Many of the switchable rotaxane and catenane systems which employ charge-transfer interactions between the components intrinsically involve changes in absorption profiles—and therefore color—concomitant with shuttling. Incorporation of a rotaxane similar to **124**$^{4+}$ (Scheme 73) into a solid-state polymer electrolyte gives an electrochromic device in which a color change occurs on application of an oxidizing potential.[446] The observed color change is consistent with that seen on shuttling in solution for this family of catenanes and rotaxanes (for example, [2]catenane **92**$^{4+}$, Scheme 54, Section 4.6.1), while on subsequent reduction, the reverse color change occurs slowly, and is indicative of the slow relaxation of the non-equilibrium system in the solid state. Both these observations serve as strong evidence for shuttling in the condensed phase (as discussed in Section 8.3.1). Stoddart, Goddard, and co-workers have recently proposed an extension of this concept, based on [2]catenane **92**$^{4+}$, but incorporating a third, intermediate and electroactive, station to create a three-state switchable catenane in which each of the states should be characterized by a different color arising from the intercomponent charge-transfer interactions.[464]

8.3.3. Using Mechanical Switches To Affect the Mechanical Properties of Materials

Materials which can transduce an external stimulus into a mechanical response are at present probably best exemplified by piezoelectrics, but the development of molecular materials

which exhibit similar—or potentially even more sophisticated—properties is an area of intense interest.[465] It is well established that conformational changes in polymers can result in mechanical changes at the macroscopic level. Such effects have been extensively studied for over half a century in stimuli-responsive hydrogels. These water-swollen 3D-cross-linked networks of neutral or ionic (also known as polyelectrolytes in this case) amphiphilic polymers can undergo reversible phase transitions in response to a number of stimuli, including pH, temperature, solvent composition, electric fields, and light. The phase changes result from altering the balance between hydrophilic and hydrophobic forces and can be accompanied by volume changes of up to two orders of magnitude.[466] These were perhaps the first synthetic chemomechanical systems to be investigated and their significance was recognized early on by Katchalsky and co-workers, who developed a number of remarkable macroscopic devices for directly and continuously transducing chemical potential into mechanical work.[467,468] Recent developments include using photons to induce phase transitions,[469] the use of oscillating chemical reactions to control the environment for pH-responsive gels to produce autonomously fluctuating chemomechanical systems,[470] and "core–shell" architectures to give materials with multistep volume changes.[471] Synthesis and optimization of such systems in the future may also be expedited by a supramolecular approach to their construction.[472] A wide range of technologically relevant devices have been proposed and are under development using such materials, with functions including the binding and release of guests,[473] flow control valves for microfluidic devices,[474] a macroscopic walking device,[475] control of enzyme activity,[476] as well as a number of biomedical applications.[477] Incorporation of molecular recognition units into the gel network can lead to volume changes—and, in turn, other effects—upon binding of a specific guest molecule or ion.[478] This approach has not only been successful for relatively simple host–guest systems, but with redox-active enzymes, such as glucose oxidase. Binding to, and subsequent oxidation of, the substrate produces the charged form of the enzyme cofactor which initiates the gel phase transition.[478c,d]

Another emerging area of molecular-level mechanical motion in which hydrogels and other responsive polymeric materials have been applied, is the development of shape-memory materials, in particular ones which are biologically compatible.[479] While most systems use a temperature change to induce recovery of the "memorized" shape, light-induced shape-memory effects have recently been reported in which a photoinitiated radical reaction has been used to rearrange covalent cross-links[480] or the reversible formation of cross-links through a [2+2] cycloaddition which can be induced and reversed by irradiation with light of different wavelengths.[481]

Stimuli-induced mechanical changes can also be induced in conducting polymers. Electrochemical oxidation and reduction of polypyrrole, polythiophene, or polyaniline films induces counterion transport into or out of the polymer matrix, thus resulting in volume changes.[482] Such effects were first demonstrated for macroscopic devices immersed in aqueous electrolytes, but the long reaction times and the small forces generated are practical limitations of such systems. More recently, solid-state,[483] gel,[484] and ionic-liquid[485] electrolytes have been employed, while the development of microfabricated devices has been successful in realizing quite complex and potentially technologically relevant electrochemomechanical actuators.[482c] The combination of the conducting polymer technology with a hydrogel material has been used to overcome some of the problems associated with each individual approach to demonstrate a novel drug-delivery system,[486] while similar processes are now being investigated in conductive supramolecular crystalline materials.[487] A related but novel mechanism for electromechanical actuation, which avoids many of the drawbacks associated with redox-induced dopant diffusion, has been realized in sheets of entangled nanotube bundles[488] and in porous films of gold nanoparticles.[489] The process (termed double-layer charging) does not involve any redox reaction, but rather the injection of charge into these high surface area materials attracts electrolyte ions to the surfaces, thus resulting in surface-stress-induced deformation.

In the preceding examples a macroscopic mechanical change is produced by the combined effect of a number of nonspecific conformational changes in the polymeric network. Even if in some cases this is the result of a specific recognition event, the mechanical change is not an intrinsic feature of the molecular components. There are a number of systems, however, in which particular submolecular conformational, co-conformational, and/or configurational switches can be used to directly trigger macroscopic motion. These approaches circumvent the problems of diffusion-limited rates and uniformity of response throughout the material. The incorporation of configurational switches, especially azobenzenes, to reversibly control secondary and tertiary structure in biopolymers and synthetic oligomers (Section 2.2) or to control long-range order in liquid-crystalline phases (Section 8.3.2) has already been discussed. A similar approach can be used for synthetic polymers, where the effect is often a macroscopically detectable response.

Several types of azobenzene-containing polymer films undergo contraction–extension cycles on photoisomerization,[490] while other physical properties such as viscosity and solubility can be similarly controlled.[491] Length changes in an azobenzene-containing polymer have recently been observed at the single-molecule level using AFM.[492] One end of a polyazopeptide (a polymer of azobenzene units linked by dipeptide spacers) was isolated on a glass slide while the other was attached to a gold-coated AFM tip through a thioether–gold bond (Scheme 84). At zero applied force, the polymer showed repeated shortening and lengthening on photoisomerization of the azobenzene units to *cis* and *trans*, respectively. Furthermore, this experimental arrangement was used to demonstrate the transduction of light energy into mechanical work. A "load" was applied to one of the polyazopeptides—in its fully *trans* form—by increasing the force applied by the AFM tip from 80 pN to 200 pN, thus resulting in a stretching of the polymer. Photoisomerization to increase the percentage of *cis* linkages in the polymer strand resulted in contraction, even against the externally applied force ("raising the load"). Removal of the "load" (reducing the applied

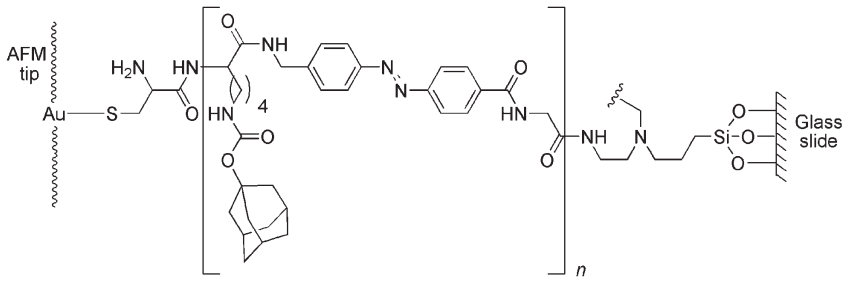

Scheme 84. Experimental set-up for the observation of single-molecule extension and contraction using AFM (the azobenzene unit is shown as the extended *Z* isomer).[492]

force) followed by reisomerization to the *trans* form, restored the polymer to its original length, ready to lift another load. The work done in this way by the single-molecule optomechanical device was approximately 5×10^{-20} J.

Analogous to controlling the chirality of liquid-crystal phases, and following the observation of environment-sensitive screw-sense inversion in certain biopolymers, there is considerable interest in remotely controlling the handedness of synthetic helical polymer systems.[493] While this has been achieved in a number of nonspecific ways (for example, by changing the solvent or temperature) molecular switches can also be employed. Chiral azobenzene side chains permit reversible switching between *P* and *M* helices by controlling the proximity of the chiral center to the polymer backbone.[494] Circularly polarized light has been used to generate an enantiomeric excess in an axially chiral alkene pendant group.[495] As observed for the liquid-crystal examples, even a very small enantiomeric excess is amplified into a bulk chiral rearrangement of the polymer. Thin films of liquid-crystalline or amorphous azobenzene side-chain polymers can also be reoriented on the nanoscale level with linearly polarized light.[496] The photoinduced anisotropy confers dichroism and birefringence on the material, thus suggesting potential for application in holographic data storage.[497] Intriguingly, such optically induced birefringence gratings are created in a process which can also involve mass transport to give surface relief features detectable by AFM or even the naked eye.[498,499] Indeed, the properties of liquid crystals and polymers can be combined in liquid–crystal elastomers—polymers constructed from mesogenic monomers which can become oriented in an ordered manner. The nematic to isotropic phase transition can result in a macroscopic response.[500] If an azobenzene configurational switch is also incorporated, switching between nematic and isotropic phases, or reorientation of the chromophores, can be achieved on irradiation with linearly polarized light, and quite specific changes in the elastomer film can be induced.[501] This has even been demonstrated in a system where the azobenzene photoswitch is not covalently attached to the main polymer backbone and, in this case, the light-triggered deformation can also propel the elastomer across a water surface.[501g,502]

On doping a nonpolymeric liquid-crystal film with light-driven unidirectional rotor **141** (Figure 49a, a member of the "third generation" series discussed in Section 2.2), the helical organization induced by the dopant results in a fingerprint-like structure to the surface of the film.[503] Both thermal relaxation steps can occur at room temperature with this motor molecule. Irradiation of the film with light alters the distribution of the isomers present and, as they have different helical twisting powers, the organization of the liquid crystal is changed. This results in a rotational reorganizaton of the surface structure, which can be followed by a glass rod sitting on the film (Figure 49b). After irradiation of the sample for ten minutes, however, the rod's rotary motion ceases, which is indicative of the photostationary state being reached. Although there continues to be a directional flux

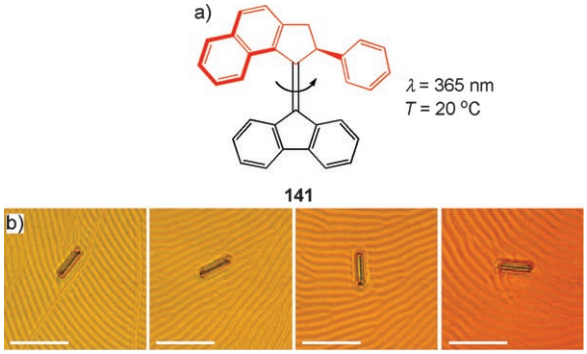

Figure 49. a) Chemical structure of light-driven unidirectional molecular rotor **141**.[503] b) Rotation of a glass rod (5×28 μm) on a liquid-crystal film doped with **141** (1 wt%). Pictures (from left to right) were taken at 0, 15, 30, and 45 s and show clockwise rotations of 0, 28, 141, and 226°, respectively. Scale bars: 50 μm. The pictures are reprinted with permission from Ref. [503].

of motor molecules between the different isomers, the net distribution of the isomers is no longer changing (see Section 2.2) and so the reorganization of the liquid-crystal matrix ceases. Removing the light stimulus allows the population of the "unstable" isomer to decay, returning the system to its starting state, accompanied by rotation of the rod in the opposite direction. Similar to the color switching discussed in Section 8.3.2 (Figure 46), this effect is not a product of the directional trajectory of a motor. The liquid-crystal organization reflects the distribution of dopant isomers at any particular moment in time, while the directionality of the rod's movement is due to the original chirality of the liquid-crystalline phase and dopant.

In terms of conducting polymers, it is possible that an intrinsic molecular-level change of length is a contributing factor to the mechanism of operation of polyaniline-based electrochemomechanical actuators.[504] However, new systems are being developed in which a designed molecular-level conformational change is responsible for inducing mechanical motion. These include a thiophene-fused [8]annulene which switches between puckered and planar forms depending on the oxidation state.[505] The conformational flexibility of calix[4]arenes has led them to be incorporated as hinge elements into conducting polymers based on oligothiophenes.[506] It has been proposed that electrochemical switching of π–π interactions between adjacent oligothiophene units

should lead to microscopic and macroscopic mechanical motions, although there is some debate over the precise mechanism.[507]

Although the metal-templated rotaxane dimer illustrated in Figure 41 (Section 8.2.2) exhibits reversible switching of its molecular length, cooperative coherent motion in a population of $\mathbf{130}_2$ to generate a macroscopic response has yet to be achieved. The first demonstration of macroscopic mechanical motion triggered by shuttling in a rotaxane was recently demonstrated using electroactive [3]rotaxane $\mathbf{142}^{8+}$.[508] Oxidation of the TTF stations (green→pink) results in shuttling of the cyclophanes onto the hydroxynaphthalene units (red), significantly shortening the inter-ring separation (Scheme 85). A self-assembled monolayer of $\mathbf{142}^{8+}$ was deposited on an array of microcantilever beams which had been coated on one side with a gold film and the set-up then inserted in a fluid cell. The chemical oxidant $Fe(ClO_4)_3$ was added to the solution and the combined effect of co-conformational change in approximately six billion randomly oriented rotaxanes on each cantilever was an upward bending of the beam by about 35 nm. Reduction with ascorbic acid returned the cantilever to its starting position. The process could be repeated over several cycles, albeit with gradually decreasing amplitude.[509]

8.3.4. Using Mechanical Switches To Affect Interfacial Properties

The surface properties of an object are crucial in determining many aspects of its behavior and the ability to remotely change these characteristics could have a significantly impact on both current and future technologies. Many of the stimuli-switchable surfaces developed to date rely on induced submolecular motions to bring about the change in properties.[510]

Anchoring stimuli-responsive polymers to solid substrates has allowed the creation of switchable surfaces based on

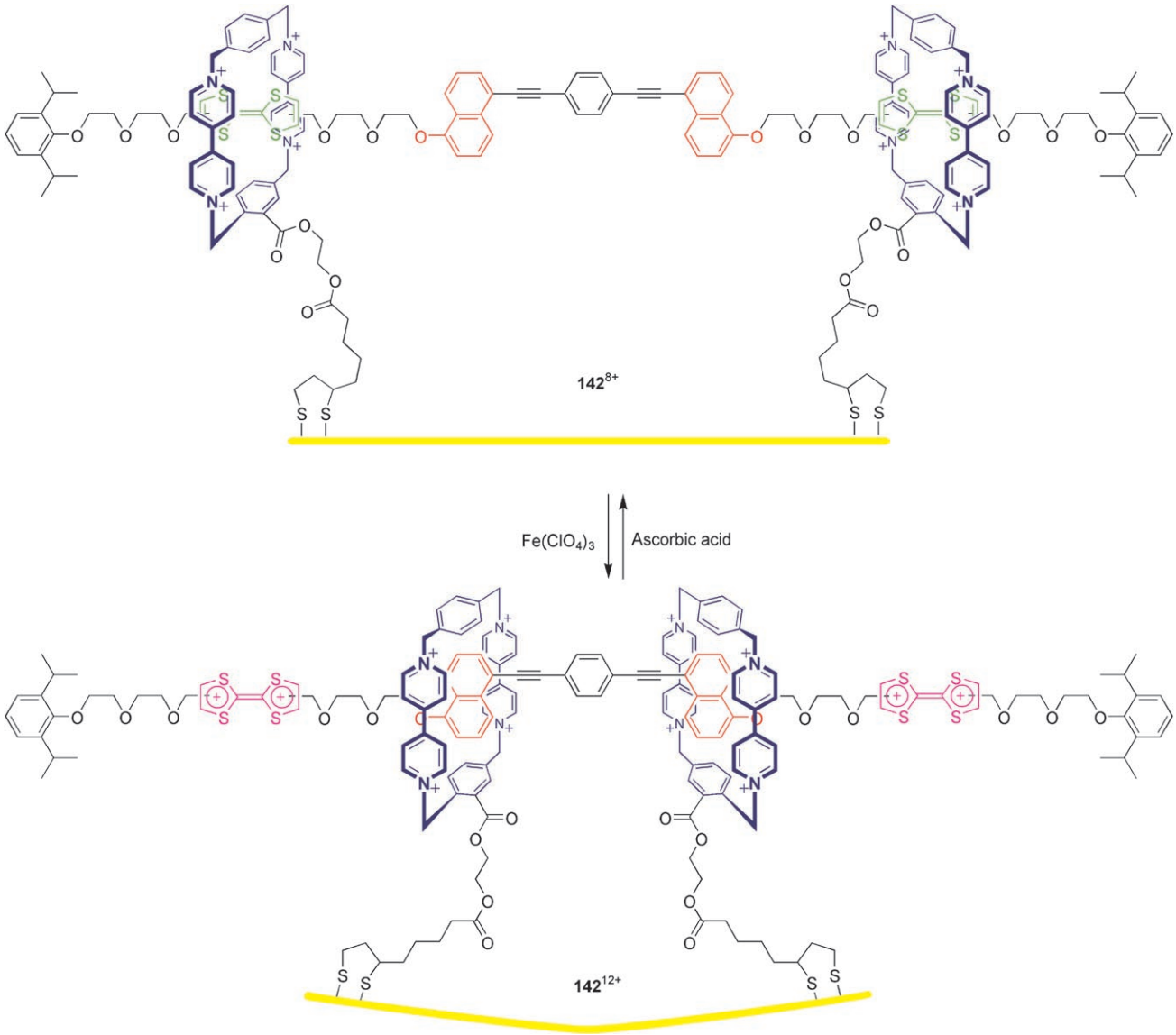

Scheme 85. Chemical structure of [3]rotaxane $\mathbf{142}^{8+}$ and schematic representation of its operation as a molecular actuator.[508]

environmentally responsive hydrogel polymers and polyelectrolytes, photoresponsive azobenzene-containing polymers, and dendritic polymers, as well as changes arising from microphase segregation mechanisms for block-copolymer and mixed polymer brushes. These approaches have been extensively reviewed elsewhere,[510,511] and can give rise to switchable surface patterning, wettability, adhesion, and control of other interfacial interactions. Integration of these functional organic structures with inorganic and biomaterials is an important current goal, particularly with a view to potential applications.[511d] For example, the intercalation of Au nanoparticles into an electrode-mounted solvent-responsive polymer gel allowed control of the interfacial conductivity through variation in the separation of the nanoparticles.[512] The encapsulation of a thermally responsive polymer in a porous inorganic matrix resulted in a switchable molecular filter,[513,514] while a covalently tethered monolayer of the same polymer has been used to reversibly adsorb proteins in an integrated microfluidics chip.[515]

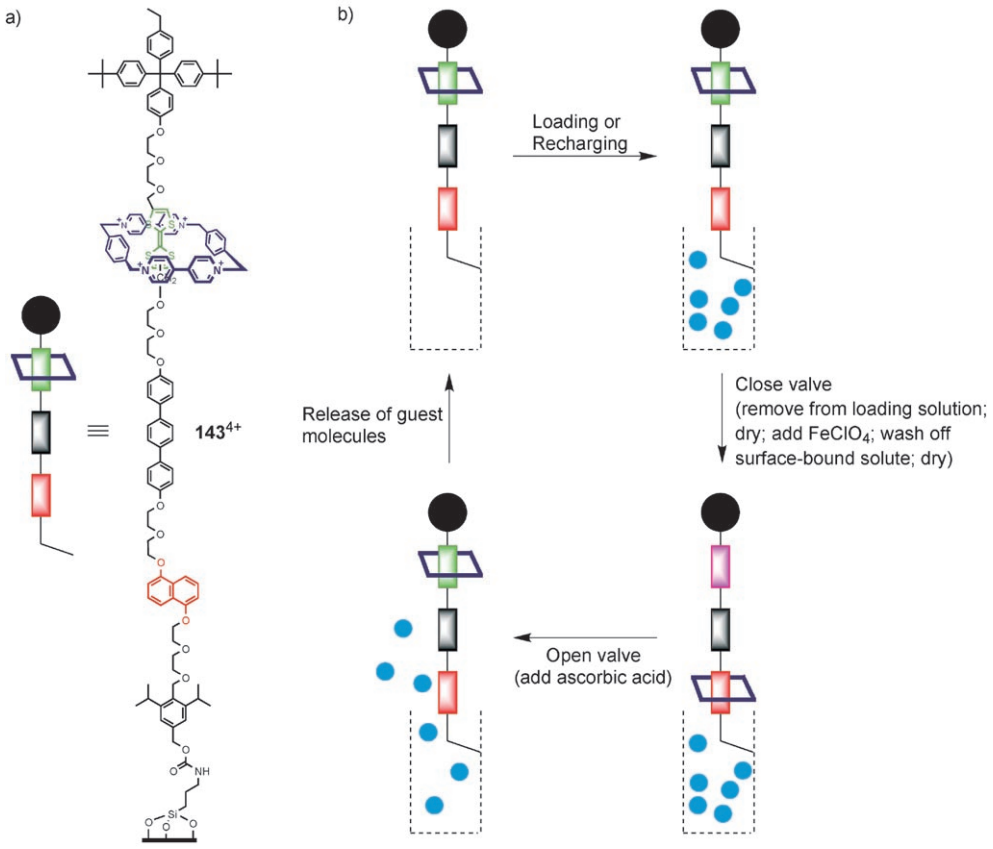

Figure 50. a) Chemical structure of a bistable [2]rotaxane ($\mathbf{143}^{4+}$) used to create a reversible molecular valve.[517] b) Schematic representation of the operating cycle for a reversible molecular valve. Colors not defined in (a) are: pink = TTF^{+}; light blue = guest molecules.

The direct deposition of bistable small molecules onto solid substrates as thin films can also result in interesting switching phenomena which amplify the molecular-level motion to give a large response. On polar surfaces such as mica, monolayer films of amphiphilic benzylic amide [2]catenane **91** (Scheme 53) prefer to adopt co-conformation alkyl-**91**, irrespective of the nature of the depositing solution.[516] Continued deposition from acetone results in stacked monomolecular terraces that are clearly observable by AFM. Further deposition from chloroform, however, results in the incoming molecules (adopting the amido-**91** form in the apolar environment) inducing a co-conformational change in the film so that amido-**91** is adopted by all the molecules, thus minimizing the packing energy. The result is a completely different morphology: decreased interaction with the substrate causes complete rupture of the film to give stacks several tens of nanometers in height.

A rotaxane-based molecular shuttle has been attached to mesoporous silica particles and used to control access to pores in the material (Figure 50)—a reversible analogue of an earlier pseudorotaxane-based design (Section 8.1).[517] When the $CBPQT^{4+}$ ring sits on the preferred TTF station, access to the interior of the nanoparticles is unrestricted and diffusion of solutes from the surrounding solution can occur. Chemically induced oxidation of the TTF unit results in a shuttling of the ring closer to the solid surface, thereby blocking access to the pores and trapping any solute molecules inside. Reduction of the TTF unit reverses the mechanical motion, thus releasing the guest molecules and returning the system to its initial state.

A potentially useful way of detecting and subsequently communicating the state of any type of molecular switch is to translate its state into an electrical signal.[97s,403e,518] This has been accomplished for a molecular shuttle attached through one end of the thread to the surface of a gold electrode.[519] Photochemically induced shuttling of a cyclodextrin ring closer to the electrode surface was detectable as an increase in the rate of electron transfer on oxidation of a redox-active ferrocene unit attached to the mobile ring. Shuttling has also been invoked to explain the operation of a remarkable device, in which a rotaxane connects the redox-active enzyme glucose oxidase to an electrode surface.[520] When the device is constructed without the rotaxane macrocycle (a $CBPQT^{4+}$ cyclophane) no electronic communication between the redox enzyme and the electrode is detected. With the rotaxane linker, however, bioelectrocatalyzed oxidation of glucose occurs. It is proposed that the cyclophane acts as a two-

electron relay, that is, acting as an intermediate for electron transfer between the enzyme and the electrode. It is likely that this role involves movement of the reduced ring towards the electrode as reduction destroys its charge-transfer interactions with the thread. Such a mechanism may also be at play in an earlier, fully synthetic, system where the ring acts as a relay between a photoelectroactive CdS nanoparticle and the electrode.[521] In a structurally simpler synthetic system (Scheme 86), electrochemically induced shuttling has been directly proven and shown to switch a number of properties of the functionalized electrode.[522] The cyclophane can be reversibly reduced and oxidized by applying appropriate potentials at the electrode. Chronoampometry demonstrates that the reductive electron transfer is significantly slower than the oxidation, thus indicating a shorter electrode–macrocycle separation in the reduced state. Positional integrity of the macrocycle in both states was quantitative to the limits of detection, however, fast two-potential-step chronoampometry experiments allowed a detailed study of the kinetics for shuttling (k_1 and k_2 in Scheme 86) in each direction at various temperatures and in solvent systems of differing viscosity.[522b] Impedance spectroscopy indicated a difference in the double-charge-layer capacitance in the two states, while the decrease of the cyclophane charge and shuttling to reveal the alkyl chain-based thread also increases the hydrophobicity of the electrode surface. This was demonstrated by a change in the contact angles for an electrolyte droplet placed on the electrode.[522a]

Inspired by a number of natural phenomena, the design of surfaces with special—and in particular switchable—wettability characteristics has attracted much interest in recent years.[523] Monolayers of various photochromic switches have been used to control the wettability of a surface.[510] In line with an earlier computational study,[524] variation of an electrostatic potential has been used to alter the conformation of a SAM of long-chain alkanethiols terminated with carboxylate groups and thus affect the surface hydrophobicity.[525] Applying a negative potential to the gold surface repels the carboxylate groups, which causes the chains to "stand up" and thus endows a strongly hydrophilic character to the surface; a positive Au potential attracts the carboxylate groups, which causes folding that exposes the hydrophobic alkyl chains at the surface. A low-density SAM must be utilized to allow significant conformational freedom. Similar switchable surface-wettability properties were also demonstrated by using positively charged bipyridinium end groups instead of the negatively charged carboxylate groups.[526] More recently, a carboxylate-terminated low-density SAM was manufactured by self-assembling cyclodextrin pseudorotaxanes on a gold surface before washing off the space-filling macrocycles with a polar solvent.[527] The resulting surface demonstrated conformational switching and could be used to reversibly adsorb both a cationic and a near-neutral protein at the interface.

A dramatic illustration of the power of controlled molecular-level motion is the use of conformationally switchable monolayers to control macroscopic liquid transport across surfaces. It has been shown both theoretically[528] and experimentally[529] that a liquid droplet on a surface with spatially inhomogeneous surface free energy will tend to move in the direction of the higher surface free energy.[530,531] Surface motions of droplets have been controlled by wettability gradients and steps in a number of different ways,[529,530,532,533] yet it remains a particular challenge to endow a surface with remotely controllable surface free energy so as to generate macroscopic motion of a droplet

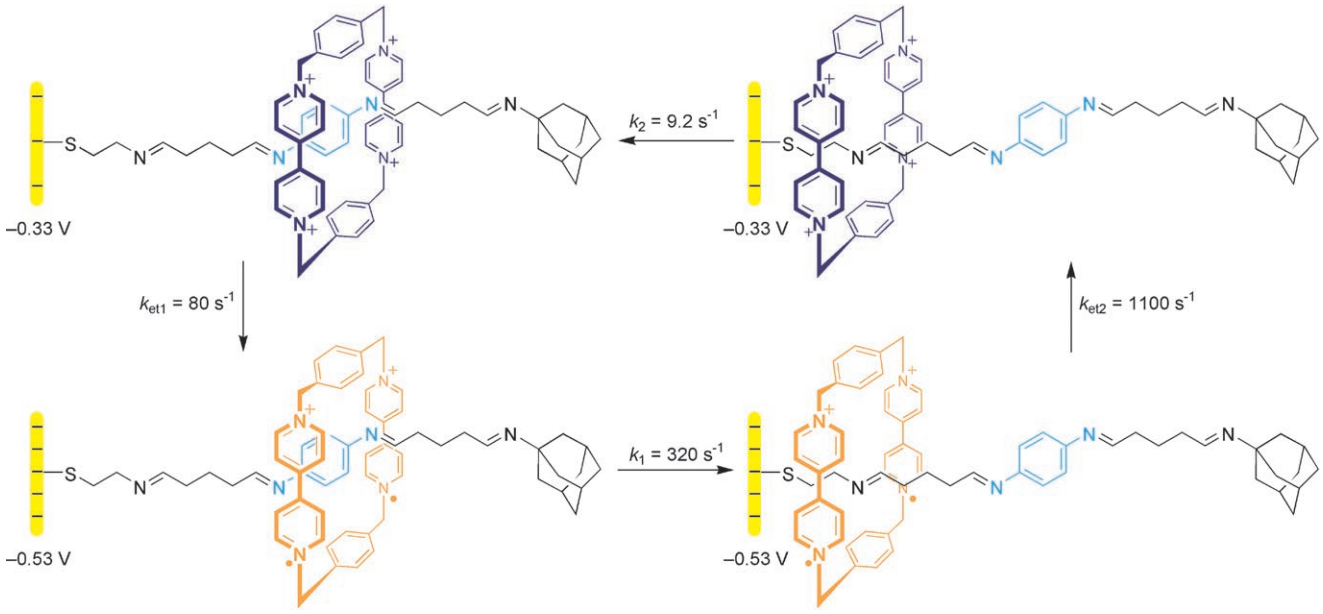

Scheme 86. Electrochemically induced shuttling on an electrode surface.[522] The submolecular co-conformational motion is transduced into an electronic signal in terms of a change in the electron-transfer kinetics and also results in a change in the capacitance and hydrophobicity of the monolayer. The rate constants shown for the shuttling steps (k_1 and k_2) are those measured at 25 °C in pure water. Only k_2 was found to vary with temperature, while both rates decreased with increasing solvent viscosity.

along any path.[534] As well as addressing a number of fundamental scientific issues, such a system would undoubtedly be of major value in the emerging fields of microfluidics and lab-on-a-chip technologies which currently rely on potentially damaging strong electric fields, air bubbles, or expensive microscopic pumps to transport small quantities of liquids.[535]

A monolayer of azobenzene-substituted calix[4]arene **144** (Scheme 87) provides a photoresponsive surface on which the

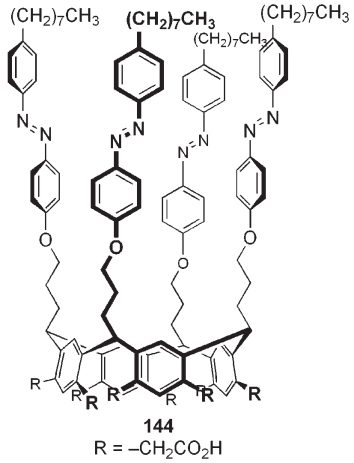

Scheme 87. Molecular structure of the azobenzene unit used to create a photoresponsive surface for the control of liquid motion.[536] The macrocyclic calix[4]arene scaffold ensures sufficient free volume to allow full configurational motion of the azobenzene moieties, even in a tightly packed monolayer.

motion of liquid droplets could be controlled simply by irradiation with light.[536] A droplet of olive oil on the all-*cis* surface was irradiated at 436 nm with an asymmetrical intensity so that more isomerization to the *trans* form occurred on one side of the droplet compared to the other. The resulting gradient in the surface free energy caused the droplet to move away from the *trans*-rich region. This motion could be continued by "chasing" the droplet with the light, or else by resetting the surface at the front of the drop to a *cis*-rich state with a spatially controlled irradiation at 365 nm, followed by a further cycle of 436 nm towards the rear and so on, with the motion carried out in a stepwise fashion. The potential utility of this approach was demonstrated in a number of ways: a liquid droplet could be used to move a millimeter-sized glass bead across the surface; the same approach could be used to functionalize a capillary tube and move liquids along it; and finally, an organic chemical reaction could be performed by bringing two droplets together, each containing one of the reactants.[536]

Recently, a similar effect was demonstrated using a photoresponsive surface based on molecular shuttles.[537] The millimeter-scale directional transport of diiodomethane drops across a surface (Figure 51) was achieved using the biased Brownian motion of the components of stimuli-responsive rotaxane **145** (Scheme 88) to expose or conceal fluoroalkane residues and thereby modify the surface tension.

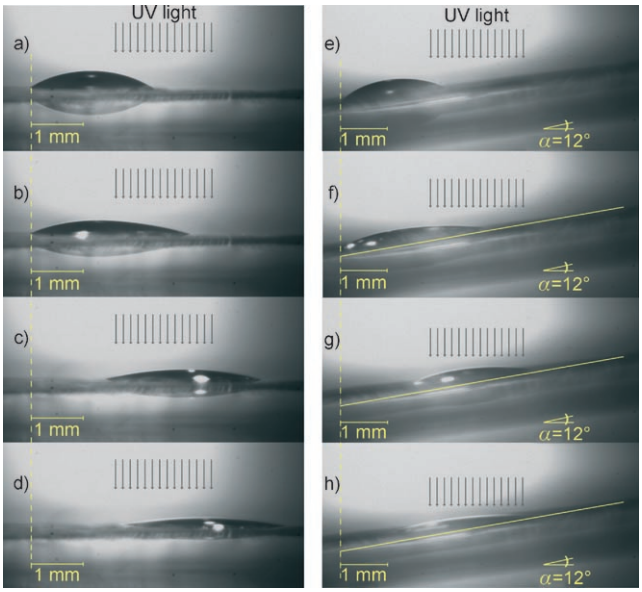

Figure 51. Lateral photographs of light-driven directional transport of a 1.25 μL drop of diiodomethane across the surface of an (*E*)-**145**·11-MUA·Au(111) substrate on mica arranged flat (a)–(d) and up a 12° incline (e)–(h).[537] a) Before irradiation (pristine (*E*)-**145**). b) After 215 s of irradiation (20 s prior to transport) with UV light in the position shown (the right edge of the droplet and the adjacent surface). c) After 370 s of irradiation (just after transport). d) After 580 s of irradiation (at the photostationary state). e) Before irradiation (pristine (*E*)-**145**). f) After 160 s of irradiation (just prior to transport) with UV light in the position shown (the right edge of the droplet and the adjacent surface). g) After 245 s of irradiation (just after transport). h) After 640 s irradiation (at the photostationary state). For clarity, a yellow line is used on photographs (f)–(h) to indicate the surface of the substrate.

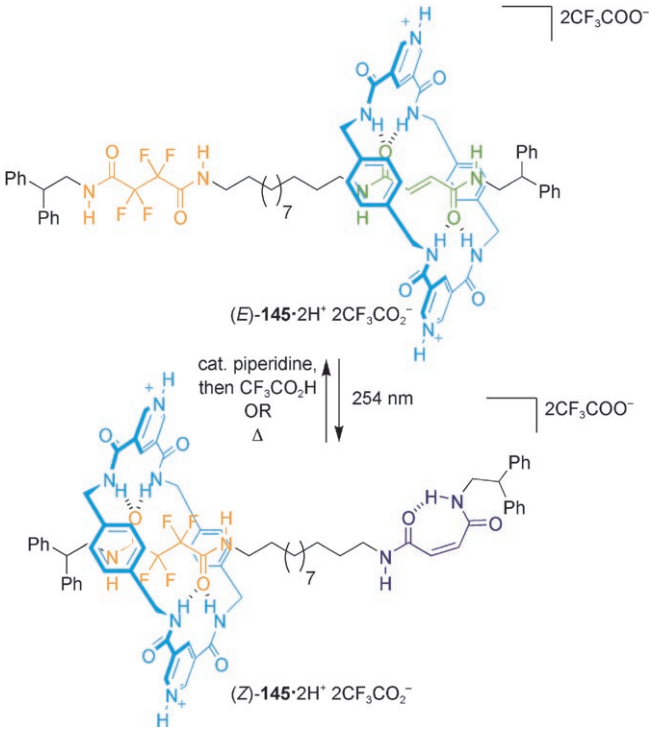

Scheme 88. Stimuli-induced positional change of the macrocycle in the fluorinated molecular shuttle **145**·2H$^+$.[537]

The collective operation of a monolayer of the molecular shuttles attached to a SAM of 11-mercaptoundecanoic acid (11-MUA) on Au(111) (Figure 52) was sufficient to power the movement of the microlitre droplet up a twelve degree incline

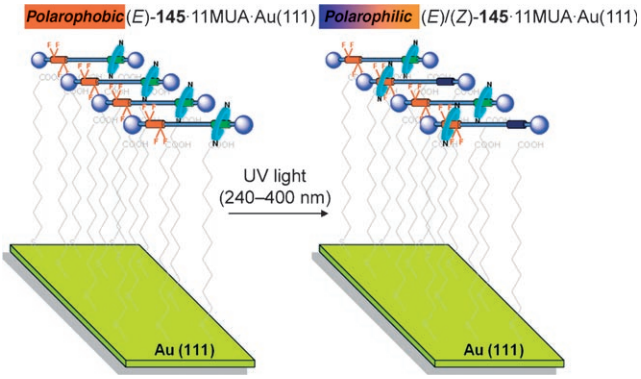

Figure 52. A photoresponsive surface based on switchable fluorinated molecular shuttles.[537] Light-switchable rotaxanes with the fluoroalkane region (orange) exposed ((*E*)-**145**) were physisorbed onto a self-assembled monolayer of 11-MUA on Au(111) deposited onto either glass or mica to create a polarophobic surface, (*E*)-**145**·11-MUA·Au-(111). Illumination with light of wavelength 240–400 nm isomerizes some of the *E* olefins to *Z* causing a nanometer displacement of the rotaxane threads in the *Z* shuttles which encapsulate the fluoroalkane units, thus leaving a more polarophilic surface, (*E*)/(*Z*)-**145**·11-MUA·Au(111). The contact angles of droplets of a wide range of liquids change in response to the isomerization process.

(Figure 51 e–h). In doing this, the molecular machines effectively employ the energy of the isomerizing photon to do work on the drop against gravity. In this experiment, approximately 50% of the light energy absorbed by the rotaxanes was used to overcome the effect of gravity, with the work done stored as potential energy (the raised position of the droplet up the incline).

The above examples demonstrate quite extraordinary application of collective submolecular motions to alter the macroscopic properties of a surface and in turn induce movement of a macroscopic object.[538] However, the changes in the surface free energy involved are relatively small. It is well known that surface roughness can amplify both hydrophobicity and hydrophilicity.[523] A micropatterned surface functionalized with a solvent-sensitive mixed polymer brush could switch between a hydrophilic and a superhydrophobic state.[539] Reversible switching between superhydrophobicity and superhydrophilicity has been achieved on a static micropatterned surface,[540] as well as on a dynamic nanostructured surface,[541] in both cases covered with a temperature-responsive polymer. A similar approach has been used to amplify the light-induced wettability switching for a spiropyran-functionalized surface.[542] As well as increasing the change in the contact angle relative to the smooth surface on irradiation, contact angle hysteresis was also reduced on the rough surface so that a water droplet could be moved across it on application of an asymmetric irradiation.

9. Artificial Biomolecular Machines

9.1. Hybrid Biomolecular Motors

Motor proteins provide both inspiration and important proofs-of-principle for the synthetic chemist trying to create artificial motor molecules. In turn, the increasing sophistication of the task carried out by synthetic structures may one day (perhaps sooner than one might think) start to aid our understanding of complex natural systems. However, the demonstration of such amazing mechanical functionality by motor proteins has also triggered a different approach to creating tiny mechanical devices: namely the direct application of complete biomolecular motor constructs in non-natural settings. Initially, interfacing operational motor proteins with artificial constructs was purely concerned with further dissecting the mechanochemical mechanisms of the natural systems. In a series of experiments which have achieved classic status, direct observation of directional rotation of the F_1-ATPase motor, driven by ATP hydrolysis, was realized for individual motors mounted on glass,[543] while the transmission of this motion to the F_0 motor in complete F_0F_1-ATPase constructs has also been observed.[544] The reverse process—ATP synthesis—has subsequently been achieved in a similar environment, by physically driving rotation of the F_1 motor in the opposite direction to that observed for the hydrolysis reaction; this is the first demonstration of artificial chemical synthesis driven by a vectorial force![545]

Mimicry and deconvolution of natural systems aside, methods by which biomolecular motors can be reliably incorporated into artificial systems are being pursued to create nanomechanical systems powered by ready-made molecular motors.[546] Such endeavors constitute a research area in their own right,[547] involving, for example, the integration of soft organic functional molecules with hard inorganic components and supports; the genetic engineering of motor proteins to adapt their function and interaction with synthetic components; and the engineering of switches whereby the natural motor can be turned on or off.

The use of myosin molecules immobilized on a solid substrate to transport actin strands across the surface was one of the earliest in vitro studies of motor protein mechanochemistry.[548] Analogous systems, many employing kinesin (or dynein) and microtubules as the motor and cargo components, respectively, are now being investigated with a view to practical applications.[549] The potential uses of such systems clearly include the transport of nanoscale cargoes and consequently the challenges of controlling and directing the motion, as well as capture and release of molecular materials, are actively being pursued.[11,547a,c] As mentioned in Section 8.3.3, temperature-responsive polymers can be used as control elements for motor proteins,[476] but recently it was shown that proteins themselves can be turned into novel polymer gel actuators. In particular, a chemically cross-linked actin gel has been shown to move over a cross-linked myosin gel in the presence of ATP, with speeds achieved similar to those of the native protein construct, thus opening up the

possibility of creating gel-based devices powered by protein motors rather than by osmotic effects.[550]

As for fully synthetic systems, any macroscopic mechanical application of biomolecular motors is likely to require the parallel operation of a great number of molecular devices—just as limb movement in an animal is the result of the coordinated effort of many millions of myosin motors. Recently, the self-assembly of muscle cells on silicon microdevices has been achieved. The advantage of using whole cells (cardiomyocytes in this case) to grow muscle bundles is that all the machinery for cooperative motion is automatically present and the result is the first microstructure which can move autonomously as a result of cooperative contraction of muscle bundles.[551]

A related active field is that of biomolecular electronics, in which native and genetically engineered proteins are deployed in molecular-based electronic and photonic devices. In many cases the electronic switching mechanism involves molecular-level motion, exemplified in particular by systems which rely on the photochromic and photoelectric properties of bacteriorhodopsin.[552]

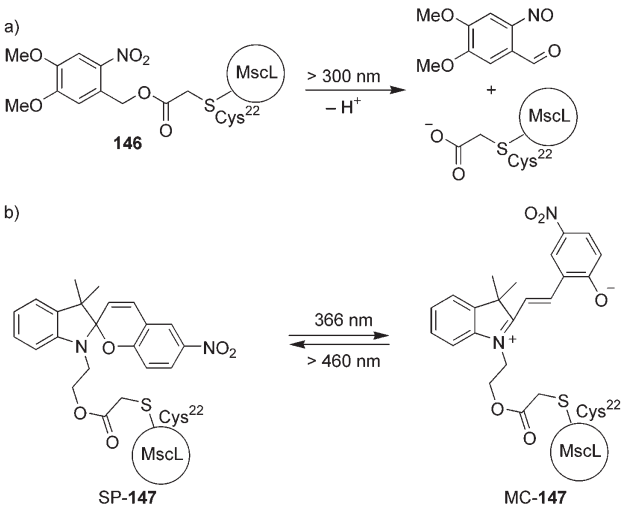

Scheme 89. Chemical structures of the photochromic switches used to create: a) irreversible and b) reversible light-triggered MscL.[556] As the MscL construct is a homopentamer, each channel features five sites for attachment of the photochromic units. SP = spiropyran form, MC = merocyanine form.

9.2. Hybrid Membrane-Bound Machines

The development of synthetic ionophores and ion channels has been a central goal of supramolecular chemistry for a number of decades and advanced functionality such as enantioselection and stimuli-controlled transport has been achieved.[553] Recently, however, biological channel proteins have been used in artificial settings and external control over their functions achieved. The mechanosensitive channel of large conductance (MscL) from *Escherichia coli* is a homopentameric protein channel which opens in response to internal pressure within the bacterium, thus allowing nonselective efflux of ions and small solutes.[554] It is known, however, that the introduction of polar or charged residues at a specific location in the protein can result in spontaneous opening of the pore.[555] Incorporation of a cysteine residue at this crucial amino acid position provided a handle to which Feringa and co-workers could attach artificial photoswitches, thereby creating light-switchable versions of this system.[556] In the first instance, an acetate unit protected by a photocleavable group was attached to the cysteine residue (Scheme 89a) and the resulting hybrid (**146**) incorporated in a synthetic lipid membrane. Photolysis of the protecting group revealed free acetate units, and concomitant opening of the channels was clearly observed on the single-molecule level by using patch-clamp techniques. A reversible analogue was created by appending a spiropyran switch to the cysteine residue (giving SP-**147**, Scheme 89b). Opening and closing of the channel was observed again in patch-clamp experiments, however, a significant decrease in the number of pores opening was observed on repeating the procedure for a second time. An efflux experiment was performed in which a self-quenching dye was released from liposomes on opening the channel. A clear increase in permeability on irradiation was demonstrated, although some leakage from the "closed" channels was also observed. A related approach has employed azobenzene chromophores to reversibly place a blocking group in Shaker K^+ ion channels in rat hippocampal neurons[557] and to bring an agonist into contact with the binding site in a ligand-gated ion channel, again in living cells.[558] The latter could, in principle, be a general method for creating optically switchable versions of many allosterically regulated proteins. Rather than postsynthetic functionalization of amino acid side chains, photoswitches can also be incorporated by chemical synthesis as non-natural amino acids in place of terminal residues. This approach has been used to create various photoswitchable analogues of the low-molecular-weight channel-forming peptide gramicidin.[559]

Artificial carrier mediated translocation of ions across a membrane can be coupled to redox reactions so that the carrier is oxidized and reduced at opposite sides of the membrane, thus adjusting its affinity for the transported species depending on its location.[560] A particularly impressive extension of this concept draws on the mechanism of photosynthetic energy conversion in nature—the photogeneration of charge-separated states.[561] Artificial photosynthetic reaction center **148** (Scheme 90) exploits components commonly used by nature—a porphyrin photosensitizer (P), a carotenoid polyene electron donor (D), and a naphthoquinone electron acceptor—to create charge-separated states of the form $D^{+\bullet}$-P-$A^{-\bullet}$. Directionally inserting **148** into liposome membranes results in a transmembrane electrochemical potential on irradiation with light. This allows the spatial control of the oxidation state for quinone-based carrier molecules which are dissolved and freely diffusing in the membrane. The change in oxidation state switches the pK_a value[562] or the calcium ion binding affinity[563] of the carrier molecules, depending on their proximity to the inner or outer surface of the membrane, so as to facilitate proton or calcium ion pumping across these "artificial photosynthetic membranes". Continual operation of the proton transport system and concomitant generation of a protonmotive force

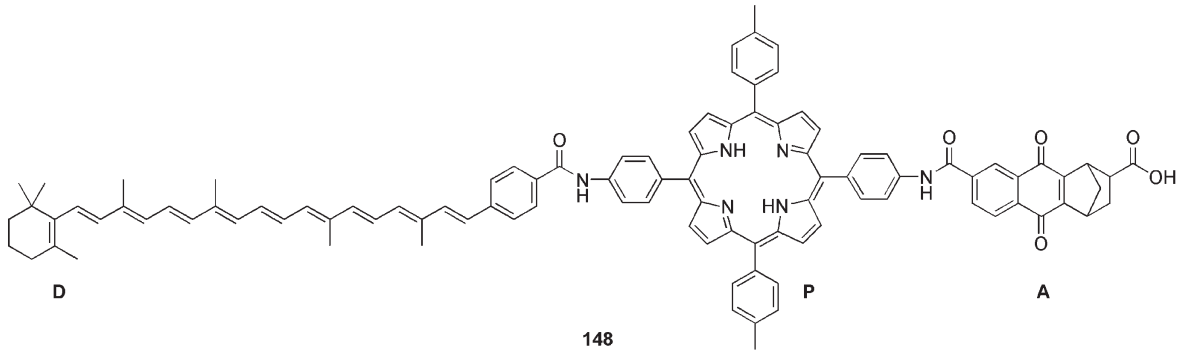

Scheme 90. Artificial photosynthetic reaction center **148** which was used to create a transmembrane electric potential so as to power proton[562,564] or calcium[563] transport.

was illustrated by incorporation of intact F_0F_1-ATPase into the artificial photosynthetic membrane, and in vitro ATP synthesis was successfully demonstrated.[564]

These systems harness directional electron transfer to set up the electrochemical gradient necessary for ion transport. They therefore correspond to the redox-loop (or Mitchell-loop) mechanisms for transport in nature (Section 1.3).[33] Synthetic examples of conformational pumps, on the other hand, have not yet been realized, although the design of potential components is being actively pursued.[565]

9.3. DNA-Based Switches and Motors: Molecules that Can Walk

It is also possible to borrow from nature, not the completed machine or some components thereof, but the materials used to build them. The use of nucleic acids as nanoscale construction materials have been exquisitely demonstrated over the past decade in a variety of ways.[566,567] Following an initial report on the control of double-stranded DNA branch migration,[568] the first artificial, well-defined, large amplitude DNA-based conformational switch was achieved by harnessing the ability of certain DNA sequences to change between right-handed B forms and left-handed Z forms, depending on the nature of the environment.[569] One such sequence was used to connect two rigid DNA double-crossover motifs to create a linear mechanical device. The B–Z transition results in a twisting of the device around the central unit (as well as a small change in length), thereby altering the separation of equivalent points on the two double-crossover units. This reversible process was monitored by fluorescence resonance energy transfer (FRET) between dyes attached to the double-crossover portions.[569]

The system depicted in Figure 53 is not only constructed from DNA but is also operated by the addition of specific oligonucleotide sequences. Three DNA strands (**A**, **B**, and **C**) self-assemble to give the "relaxed" structure. A fourth strand, the "fuel" **F**, has sequences complementary to the single-stranded regions of both **A** (red) and **B** (blue), and so hybridization occurs to give the "closed" form. However, **F** also contains an eight-base overhang (pink) at its 3′ end. This acts as a "toehold" for a "removal" strand **R**, which is complementary to the full length of **F**. Binding at the

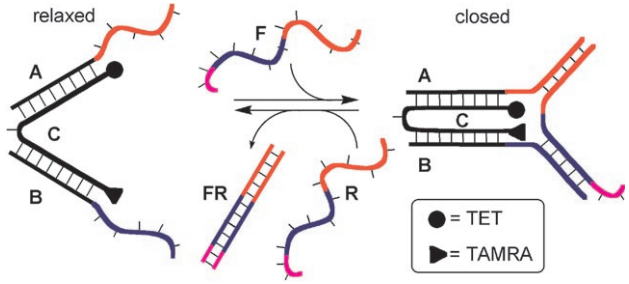

Figure 53. Operation of a pair of DNA tweezers.[570] Closing of the tweezers amounts to bringing the two rigid double-stranded regions (black) close together by hybridization of a fuel strand **F**. Removal of the fuel strand to restore the relaxed state is brought about by addition of a removal strand **R**, which binds initially at the toehold on **F**, then branch migration leads to complete removal of **F** from the device with concomitant formation of one molecule of duplex waste **FR**. The coloring scheme indicates the complementary regions on different threads; lines indicating base paring are purely schematic and do not represent a particular number of bases. TET = 5′-tetrachlorofluorescein phosphoramidite; TAMRA = carboxytetramethylrhodamine.

overhang is followed by continuing hybridization along the length of the two strands by a branch-migration process, until the inert "waste" duplex **FR** is formed and the machine returns to its original relaxed state. The process is reversible and reproducible over several cycles, as evidenced by FRET measurements which indicate a difference in the end–end distance between the two forms of approximately 6 nm.[570] A related device adopts the same strategy to switch between a relaxed state and an "open" state, where addition of the fuel strand results in an approximately linear conformation.[571] Finally, these two systems were combined to create a three-state device capable of switching repeatedly between conformationally well-defined open and closed forms through the more flexible relaxed state.[572] Switching between two well-defined conformations triggered by hybridization has also been achieved in an alternative system based on crossover motifs.[573] In this case, a 180° rotation of one end of a linear device relative to the other end results. One-dimensional oligomeric arrays of such devices were prepared, with a structurally rigid DNA substituent appended to each monomer. The switching motion could then be observed by AFM as a change in the relative orientation of the rigid subunits. A

related system has since been designed to exhibit lengthening and contraction of a linear DNA construct.[574] This device was incorporated into a 2D DNA lattice and its switching used to reversibly alter the dimensions of the lattice features, again evidenced by AFM.

Opening and closing or twisting of DNA devices could clearly be used to alter the relative orientations of a wide number of attached functionalities, in a manner similar to rotaxane-based co-conformational switches (Section 8.2.2), while it has also been postulated that these devices may be able to exert mechanical forces, again similar to the shuttle-based switches (Section 8.3.3). The use of specific oligonucleotides to trigger the molecular-level motion may have advantages for the development of more complex systems, where it should be possible to construct machines composed of a variety of subtly different molecular components. Each could then be selectively triggered by a specific oligonucleotide stimulus, allowing the fuel to act also as an information carrier between the operator and machine, or even between different machine components. On the downside, however, each operational cycle results in the production of a waste duplex strand and, from a practical point of view, dilution of the system. Both these factors have been shown to result in a decrease in the fluorescent response on increasing cycles. Furthermore, the hybridization processes are relatively slow: half-times for completion of these reactions are commonly of the order of tens of seconds. On the other hand, a DNA conformational switch which operates simply by adding and removing protons has now been created (Figure 54).[575]

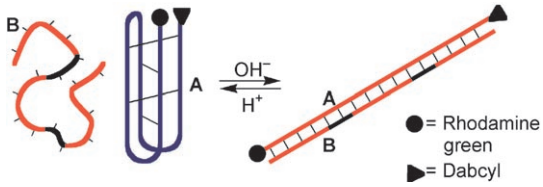

Figure 54. pH-switched quadruplex–duplex switching in a DNA molecular machine.[575] In acidic environments, the cytosine-rich strand **A** is partially protonated and forms the four-stranded self-complementary *i* motif. This holds the two dyes in proximity and FRET occurs. Increasing the pH value turns off the self-complementary interactions (blue→red) and the strand can now be captured by a partially complementary partner (**B**), thereby forming an extended duplex structure which holds the fluorophore and quencher units far apart and reducing the FRET response. The coloring scheme indicates the complementary regions on different threads; lines indicating base paring are purely schematic and do not represent a particular number of bases.

Certain cytosine-rich strands become partially protonated at low pH values and form a compact quadruplex structure known as the *i* motif. Raising the pH value disrupts this structure, thereby allowing the single-stranded DNA to be captured by a partially complementary strand waiting in solution, thus forming an extended duplex structure, as evidenced by a decrease in the FRET response between two attached dyes. If the binding between the two strands is not too strong, the generation of an acidic environment reforms the *i* motif. The system exhibits impressive fatigue resistance even after 30 cycles, while the switching processes both occur in about 5 s.[576] Two related triplex–duplex contraction–expansion systems, also triggered by controlling cytosine protonation, have also been reported.[577] Both are fully self-contained devices in which all the oligonucleotides (two stands in one case, three strands in the other) remain associated in both open and closed forms. Quadruplex–duplex contraction–expansion systems have also been achieved by using the competitive hybridization strategies discussed above,[578] and this has been combined with aptamer technology to create a device in which binding and release of a protein (the human blood clotting factor α-thrombin) can be reversibly achieved.[579] It is worth noting that these contraction–expansion systems bear some resemblance to the switchable helical oligomeric systems discussed in Section 2.1.4.

In most of the switches and motors we have discussed so far, at least two stimuli, applied consecutively, are required to send the machine through an operating cycle. A DNA-based open–closed conformational switch has been created, however, which can continuously cycle between two states without any external intervention as long as its fuel is present.[580] The two-stranded cyclic structure (Figure 55) consists of two duplex arms connected by a single base "hinge" at one end and a longer single-stranded region at the other. The 29-base single-stranded region (**E**) contains an RNA-cleaving 10–23 DNA enzyme (light blue) and in the absence of substrate (and in the presence of divalent cations)

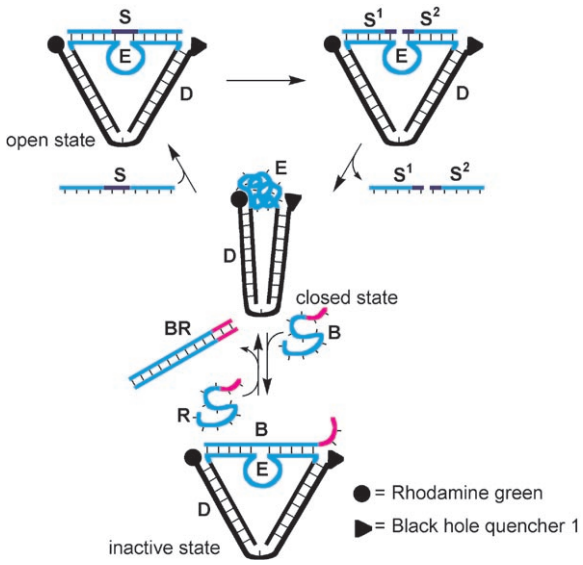

Figure 55. An autonomous DNA machine.[580,581] The machine consists of two single strands (**D** and **E**). The single-stranded 10–23 DNAzyme region (light blue) of **E** adopts a coiled-coil conformation so that the machine adopts a closed arrangement. Binding of a DNA–RNA chimera substrate (**S**) forces the machine to adopt an open state. Subsequent enzymatic action on the substrate creates two products ($\mathbf{S}^1$ and $\mathbf{S}^2$), each of which only has weak complementarity for the enzyme strand and so are released in favor of the closed conformation. Addition of an all-DNA strand **B** which is complementary to the active-site region, also forces formation of the open conformation, but halts enzyme action until **B** is removed by competitive hybridization using removal strand **R**. The coloring scheme indicates the complementary regions on different threads; lines indicating base paring are purely schematic and do not represent a particular number of bases.

it exists in a coiled-coil conformation which gives an overall closed state for the device. Substrates (**S**) for the DNAzyme are DNA–RNA chimeras complementary to regions either side of the catalytic site so that hybridization forces the structure to adopt an open arrangement. Cleavage of the substrate ensues and produces two fragments ($\mathbf{S^1}$ and $\mathbf{S^2}$), neither of which bind strongly to **E** and so are ejected in favor of forming the compact closed state once more. The device is now ready to undergo a second cycle of opening and closing and will continue to do so, without any external control, until no substrate "fuel" is left.

Also illustrated in Figure 55 is an external control mechanism whereby the autonomous machine can be switched on or off by addition or removal of a "brake" strand (**B**), which has greater affinity for **E** than the substrate but cannot itself be cleaved.[581] A different autonomous device has been realized based on the elegant use of topology to kinetically hinder a competitive hybridization reaction.[582] In this case, the "device" is simply a short oligonucleotide which oscillates between a random single-stranded state and a more-ordered duplex state.

As with the small-molecule organic systems, a key challenge for DNA-based machines is achieving directional processive motion, either in a linear or rotary form. In this regard, successful systems have recently been demonstrated by four independent research groups.[583] The first of these, from Sherman and Seeman, is shown in Figure 56.[584] A triple-crossover molecule acts as a rigid track from which protrudes a series of three single-stranded "footholds" (red, green, and light blue). A bipedal walking device is constructed from two helical domains ("legs"), each with a single-stranded "foot" (dark blue and orange) at one end and connected together by flexible linkers at the other. Attachment of the walker to the track occurs through "set" strands which have a specific foot-complementary sequence adjacent to a specific foothold-complementary sequence. Starting with both feet anchored to the track (Figure 56a), the "front" foot can be lifted by removing its set strand (Figure 56b). This is done by competitive hybridization initiated at a toehold region (pink) as discussed for the simpler machines above. Addition of a different set strand then anchors this foot to the next foothold (Figure 56c). Finally, the rear foot is freed (Figure 56d) and attached to the foothold just vacated by the front foot (Figure 56e). The walker can be returned to the starting position by a similar series of steps. Such a process, with the rear leg always trailing, has been described as an "inchworm" gait (see Section 4.4). The present system only contains three footholds and so there is no choice of direction for the walker to make at any stage; it is a positional switch rather than a motor. However, it may be possible to generate continued directional motion simply with a repeating sequence of three attachment points. It must be noted that the nature of the flexible linkers between the two legs is crucial here: they must be able to stretch across, say, the green foothold to link the red and light blue sites, but not so flexible as to allow motion in the wrong direction through passing of the front foot to the rear and attachment at a foothold on this side.

A similar strategy was used by Shin and Pierce to create a bipedal walker (Figure 57) that moves with a gait in which the rear leg advances to the front (a "passing-leg" gait, see

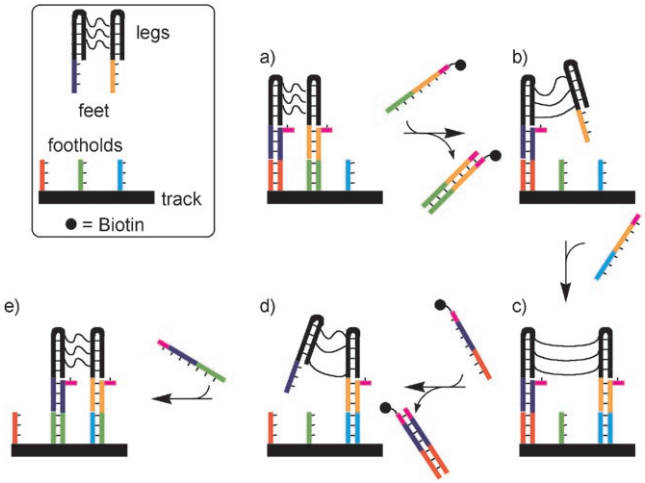

Figure 56. A non-autonomous DNA walker which moves using an inchworm-like gait.[584] Matching colors indicate complementary sequences between the strands; lines indicating base paring are purely schematic and do not represent a particular number of bases. a) The walker starts off attached to the track through both "feet", by means of "set" strands which each have regions complementary to the appropriate foot and "foothold" on the track. b) The front foot is released by removal of the appropriate set strand through competitive hybridization, initiated at a single-stranded toehold region (pink) on the set strand. The removal strand has biotin attached so that the resultant duplex waste can be easily removed. c) The front foot is attached to the next foothold on the track using a set strand of appropriate sequence. d) The rear foot is now released by competitive hybridization of its set strand. e) Finally, the rear foot is attached at its new position by the required set strand.

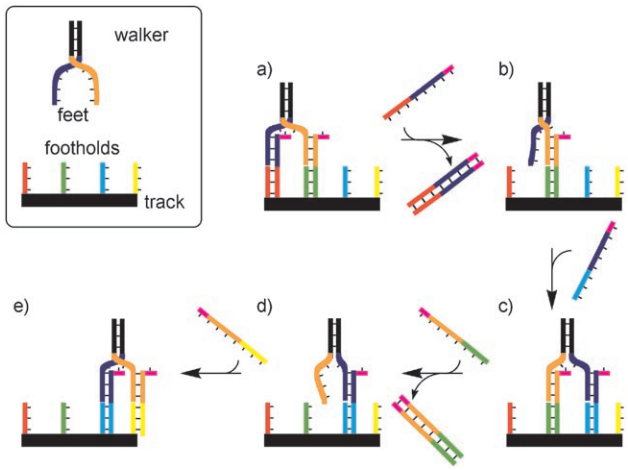

Figure 57. A non-autonomous DNA walker with a "passing-leg" gait.[585] Matching colors indicate complementary sequences between strands; lines indicating base paring are purely schematic and do not represent a particular number of bases. A sequence of removal strand and set strand additions removes the rear foot and reattaches it at the next foothold in front of the walker (see text for details). Each foothold is appended with a different fluorophore (not shown) and each foot a quencher, so that progression of the walker can be monitored by multiplexed fluorescence quenching measurements.

Section 4.4).[585] The track was constructed from six oligonucleotides which form a helical scaffold from which four 20-base single-stranded footholds (red, green, light-blue, and yellow) protrude at regular intervals. The walker consists of two partially complementary oligonucleotides which form a 20-base helix at one end, leaving two 23-base single-stranded legs (dark blue and orange). A sequence of set-strand-mediated attachment and removal by competitive hybridization results in unidirectional walking of the device, as illustrated in Figure 57.

A pair of DNA-based "gears" which can rotate unidirectionally against each other has been created by Ye and Mao by using the same principles (Figure 58).[586] This system comprises two DNA duplex circles composed of a central cyclic strand surrounded by three different linear strands, each of which has a single-stranded "tooth" at one end. The two gears can be connected through one tooth on each by a suitable set strand. The addition of a second set strand can attach the gears between two of the remaining teeth. Removal of the original set strand leaves a single linkage between the two gears again, but rotated by 120° with respect to the starting point. The process can be continued in either direction to generate a full 360° rotation.

A number of approaches for achieving an autonomously processive DNA-based device have been proposed,[587] and the first such system was recently reported by Turberfield and co-workers.[588] In this case, the walker is a 6-base fragment of DNA (colored red in Figure 59) which moves along three footholds on a track through a series of ligation and restriction steps catalyzed by a ligase and two different restriction endonucleases. In the initial state the walker is ligated to foothold **A**. However, it has a 3-base sticky end which is complementary to the single-stranded overhang of foothold **B**. The flexible single-stranded regions at the base of each foothold allows hybridization of the complementary components (Figure 59b), thus creating a substrate for T4 ligase and resulting in covalent attachment of the two DNA fragments (giving **A*****B**, Figure 59c). In turn, this creates a recognition site for a restriction enzyme (PflM 1). Crucially, the selectivity of the resulting cleavage is such that the walker is always transferred onto foothold **B** (Figure 59d) and the restriction site is destroyed. This means that although **B*** and **A** may associate again through hybridization (giving **A** + **B***, Figure 59e), and ligation may occur to give **A*****B** once more, this is simply an "idling" step as subsequent cleavage can only restore **B*** once more: the motion is essentially ratcheted by the selectivity of the restriction endonuclease. Foothold **C** has the same overhanging three bases as foothold **A**, however, and so hybridization in this "forward" direction may occur (giving **B*** + **C**, Figure 59f). The complex formed is again a substrate for T4 ligase, so **B*****C** is produced (Figure 59g). This creates a substrate for a second restriction endonuclease, BstAP 1, and cleavage occurs to give **C*** (Figure 59h). Again, an idling step involving religation with **B** may occur, but cleavage to give **B*** does not follow and so the motion cannot be reversed. This device then is an interesting example of an information ratchet (see Section 1.4.2). The free energy of the device at states **A***, **B***, or **C*** is virtually identical and invariant, and the directionality of motion is achieved irrespective of what foothold is occupied, with the kinetics for passage in one direction (left to right as drawn) being faster than passage in the opposite direction.

Two further autonomous walking systems have also been reported.[589,590] Both these machines involve tracks which display essentially identical footholds for the walker, together with a single enzyme which is able to cleave portions of the

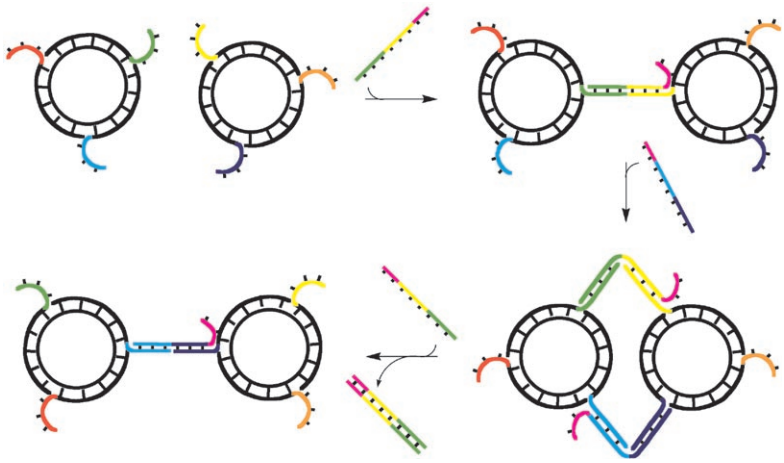

Figure 58. Unidirectional correlated rotation of a pair of DNA-based gears, driven by hybridization reactions.[586] Matching colors indicate complementary sequences between strands; lines indicating base paring are purely schematic and do not represent a particular number of bases.

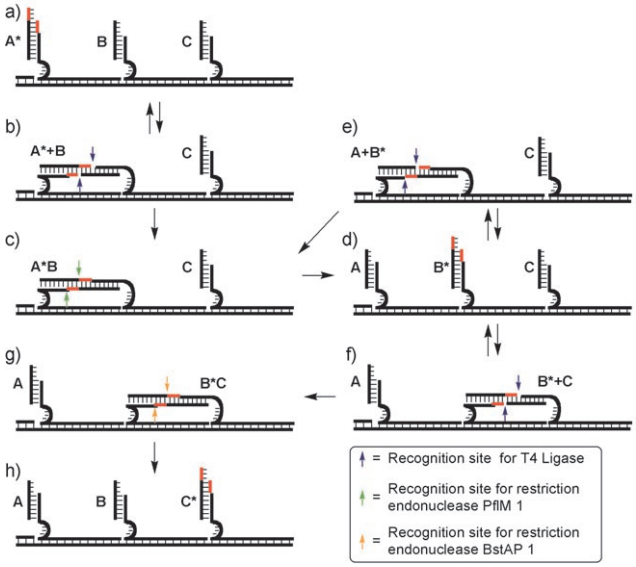

Figure 59. A unidirectional autonomous DNA walker.[588] The walker consists of the six-nucleotide base sequence colored red. Covalent attachment of the walker to a foothold is indicated by an asterisk; bridging between two footholds by hybridization is indicated by a plus sign; covalent attachment of the walker between two footholds is indicated thus: **X*****Y**. In practice, the sequences of footholds **A** and **C** are identical. Lines indicating base paring are purely schematic and do not represent a particular number of bases.

track only when the walker is bound. In one case,[589] a nicking enzyme is employed (Figure 60). This is a restriction endonuclease which binds double-stranded DNA at a specific sequence but then catalyzes the cleavage of only one strand.

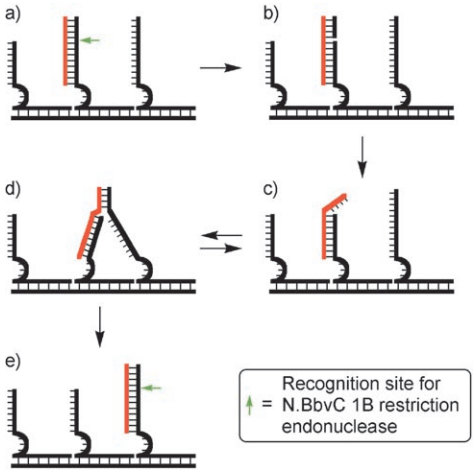

Figure 60. An autonomous DNA walker (red) starting midway through its journey from left to right.[589] Lines indicating base paring are purely schematic and do not represent a particular number of bases.

Hybridization of the walker oligonucleotide to a single-stranded foothold on the track provides the correct recognition sequence for the enzyme (Figure 60a), which subsequently cleaves the foothold strand eight bases from its end (Figure 60b). The resultant eight-base duplex has a melting temperature below the operating temperature of the device, so dissociation occurs (Figure 60c) to reveal an overhang on the walker through which it can seek (Figure 60d)—and then bind to—the next foothold along the track (Figure 60d→e). Motion continues in this way, with movement in the "backwards" direction prevented by the irreversible cleavage of each successive foothold. The walker can be stopped on any foothold by introducing a single mismatch in the enzyme recognition site. In the second example,[590] the walker itself is the enzyme—a 10–23 DNAzyme, similar to that used in the autonomous tweezers (Figure 55). The footholds are provided by DNA–RNA chimeras and duplex formation with the walker results directly in cleavage of the foothold between two RNA residues. In a manner similar to the previous example, this frees a portion of the walker to seek out the next foothold with which it can fully associate. Just like the autonomous walker in Figure 59, both these systems operate by imposing an almost infinite barrier to motion in the "backwards" direction. Unlike the first example, however, these systems completely destroy the track in their wake—the motion is entirely irreversible and the track not reusable—while waste oligonucleotides are produced in each cleavage step.[591]

The rapid progress in DNA-based molecular machines is testament to the power of this precisely programmable self-assembling construction and information-bearing material.[592] In living systems, oligonucleotides carry out a variety of roles within highly complex environments and the next advances in the artificial systems will surely see integration of these relatively simple machines, which exploit the structural properties of the material, with other emerging nucleotide-based technologies. Already a DNA tweezer device, closely related to that depicted in Figure 53, has been integrated with genetic DNA.[593] In this system, the genetic material is transcribed and produces a strand of mRNA which acts as the fuel strand, thereby closing the tweezers in an autonomous fashion. A similar process could be used to generate the removal strand, while mechanisms for regulating gene transcription have also been incorporated. The use of DNA as a templating scaffold for carrying out covalent chemistry is another emerging area where DNA switching technology has already been applied.[594] Here, a pH-controlled duplex–triplex switch is able to swap the reactivity of two chemically similar amines in an acylation reaction with a carboxylic acid. Furthermore, the machines described above exploit only a fraction of the structural characteristics and abilities of DNA, while DNA-templated assembly and nanofabrication of other materials is also of great interest.[566a,f–h,592,595] The recognition and mechanical properties of DNA have recently been exploited in a number of sensor systems. In particular, fluorophore-labeled DNA hairpins—so-called "molecular beacons"—are capable of very sensitive and specific detection of oligonucleotides.[596] The ability of certain DNA sequences to bind specific proteins, often resulting in a conformational change, has been exploited in a DNA-based device which can estimate binding free energies through a nanomechanical mechanism.[597] In another example, a DNA aptamer was combined with a fluorescently labeled, complementary oligonucleotide strand so that binding of the aptamer to its target (adenosine, in this case) is signaled by release of the tagged strand.[598] The released strand can then be designed to hybridize with another oligonucleotide in response to the analyte, while introduction of an enzyme that reacts with the guest molecule can reset the system. Indeed, the ability of oligonucleotides to selectively recognize specific sequences amongst a milieu of other molecular "noise", together with the highly refined enzymatic tools of molecular biology, form the basis of a rapidly increasing number of systems in which DNA molecules are used to perform logic and computational functions, both in vitro,[599] and in living cells.[600] Such networks may prove important in the control of more sophisticated DNA-based mechanical devices.

10. Conclusions and Outlook

In this Review we have outlined the current state-of-the-art with regards to how the relative positioning of the components of molecular-level structures can be switched, rotated, speeded up, slowed down, and directionally driven in response to stimuli. In doing so they can affect the nanoscopic and macroscopic properties of the system to which they belong. Whether one chooses to call such structures "motors" and "machines", or prefers to consider them more classically as specific triggered large amplitude conformational, configurational, and structural changes, is irrelevant. What is

important is that the use of controlled molecular-level motion to bring about property changes is fundamentally different—both in terms of how to do it and in what it can do—to methods that rely solely upon variations in the nature of functional groups or electrostatics.

Currently it is fair to say that there are two distinct design philosophies being used to try and prepare synthetic molecular-level machines: The first "hard matter" approach focuses on adapting mechanical principles and designs from the macroscopic world to molecules and is typified by the research efforts on field-driven rotors, molecular gyroscopes, molecular scissors, molecular wheelbarrows, nanocars, etc. In this approach, friction and binding interactions are avoided as much as possible and the molecules are designed to be rigid in all degrees of freedom except those involved in the desired motion. The input energy is designed to provide a directed force that pushes the molecular machine in the desired direction or exerts a torque to cause it to turn. This approach follows directly from that used in the design of macroscopic machines, which are designed to reduce friction and sticking and to eliminate jitter, vibration, and excess motion that dissipate energy and reduce the efficiency of the machine.

The second "soft matter" approach is more chemical in philosophy and seeks to adapt principles of chemistry (selective stabilization and destabilization of noncovalent bonding interactions, structural symmetry, and kinetic versus thermodynamic control of processes) to achieve efficient and controllable directional motion at the molecular level. This approach characterizes our own studies on catenanes and rotaxanes, for example, and also that of the DNA walkers, etc. Directed motion is achieved by a sequence of reactions in which different covalent and noncovalent-bonding arrangements are alternately stabilized and destabilized. The input energy is used to ensure that the sequence of reactions occurs in one order and not the reverse. The motion occurs by diffusion over an energy barrier, where the conformational changes are best described as thermally activated transitions from states that are in local equilibrium.

The advantage of the "hard matter" approach is that we understand macroscopic mechanics very well and so can easily see how to construct mechanical machines. The disadvantage is that, under most conditions, such machines must fight against the physics and chemistry intrinsic to their length scale. The advantage of the "soft matter" approach is that by using the principles outlined in Sections 1.4.2, 1.4.3, and 4.4 we can see how to exploit the natural features of the nanoscale environment. Its disadvantage is that there is no familiar macroscopic model to follow and nature's exquisite working examples are too complex in their detail to provide us with more than broad clues at present.

As outlined in this Review, both sets of design philosophies have already had many notable successes and they are not mutually exclusive. No doubt their combination will become increasingly important in the future.

Unfortunately, the hype surrounding science fictional "surgical nanobots" and the hysteria of "grey goo", has led to controversy and the questioning of expectations for synthetic molecular machines. In a commentary[601] on the exciting recent developments in catalytically driven microparticles (Section 6.1) the question was posed "What is the problem that requires having a nanomotor?". Perhaps the best way to appreciate the technological potential of controlled molecular-level motion it is to recognize that this question has been asked and answered repeatedly over four billion years of evolution with the result that nanomotors and molecular-level machines lie at the heart of virtually every significant biological process. Nature has not repeatedly chosen this solution without good reason. In stark contrast to biology, none of mankind's fantastic myriad of present day technologies (with the exception of liquid crystals) exploit controlled molecular-level motion in any way at all. When we learn how to build synthetic structures that can rectify random dynamic processes and interface their effects directly with other molecular-level substructures and the outside world, it has the potential to revolutionize every aspect of functional molecule and materials design. An improved understanding of physics and biology will surely also follow.

In this regard, we do not subscribe to the view that it will be impossible for synthetic chemists to develop molecular-level machine systems that use controlled motion to perform functions similar to those of biological machines simply because of the complexity of the latter (just as the tremendous successes in homogeneous and heterogeneous catalysis have been achieved without the need for the de novo design of enzymes). The first examples of molecular-level mechanical switching being used to perform functions on surfaces and in solution have already been demonstrated. However, a broad new range of synthetic strategies and methodologies are needed to take this further. It is only in the last decade that unnatural product synthesis has progressed to a level where the architectures necessary for biasing conformational and co-conformational motions can be constructed. However, this is not, in itself, enough to produce anything other than the most basic molecular-machine systems. Any machine more sophisticated than a switch must operate by manipulating non-equilibrium conformations and/or co-conformations of a substrate or itself. Although many methods for turning binding interactions "on" and "off" have been developed, relatively little is known about how to vary the kinetics of binding in response to external stimuli, and virtually nothing about how to do so in systems where the substrate is restricted from exchanging with the bulk.

Sections 2.1.2, 2.2, and 4.6 discussed the first examples of unidirectional motors based on rotation around single, double, and mechanical bonds, respectively. The development of molecular-level systems which carry out functions by responding to stimuli through Boolean logic operations[252] has clear relevance to the future development of interfaced and compartmentalized molecular machines which are more sophisticated than the current generation of mechanical switches and motors. While current efforts in molecular logic have concentrated on supramolecular systems rather than mechanical motion, their success suggests a way in which relatively simple molecular-machine components might be connected to produce useful devices at the next level of complexity (Section 4.4).

Developments in synthetic chemistry almost always go hand-in-hand with advances in measurement and instrumen-

tation. Spectacular advances in spectroscopy[602] and single-molecule manipulation techniques (see Section 7) have already had a major impact in the study of molecular-level machine systems and further breakthroughs appear more than likely over the next few years.

Despite the intrinsic simplicity of the current generation of synthetic molecular machines, attention is already turning to their application to perform useful tasks. Inspiration and assistance again comes from an increasing understanding of biological motor proteins and information processing, as well as the remarkable achievements of modern-day microelectronics and mechanical engineering. Yet we must bear in mind that mechanically based devices made by the synthetic chemist will have different characteristics, strengths, and weaknesses to their counterparts at other length scales. As with many fundamental developments in science—from electricity to manned-flight, the computer and the internet—it is not clear at the very beginning (and make no mistake that we are, indeed, at the very beginning in terms of experimental systems) in exactly what ways synthetic molecular-level machines are going to change technology. In the short term, changing surface properties, switching, and memory devices look particularly attractive. A greater challenge, however, is to transduce the energy input from an external source to a molecular machine into the directed transport of a cargo or the pumping of a substrate to reverse a chemical gradient. The organization and addressing of molecular machines on surfaces and at interfaces is an area where we can expect particularly important advances over the next few years.

The breadth of this Review is testament to the multidisciplinary nature of the subject matter. We hope it will be of interest to biologists to see what insights simpler molecular analogues might have for uncovering the workings of complex motor proteins. We hope it will be of interest to mathematicians and physicists to see what synthetic chemists can make (and cannot yet make) and the molecular design strategies that can be gleaned from their theories. We hope it will be of interest to materials and surface scientists to see what molecular-machine structures are available, which they can consider trying to organize, characterize, and utilize. We hope it will be of interest to engineers to see the kinds of property effects possible, and the stimuli that can be used, with molecules that need to be interfaced with the outside world. But most of all we hope it will of interest to chemists—synthetic, organic, inorganic, physical, and theoretical—and that it might inspire them to take up a challenge in which the rules of the game are only just being appreciated, and where there is much virgin territory to be trodden and major breakthroughs to be made.

Addendum (September 22, 2006)

In the time since this Review was accepted for publication, progress in the field has continued apace. The general importance and broad appeal of synthetic molecular machines has been reflected in the regular appearance of various short review articles focusing on the most recent advances in specific areas of the field, including: conformational switching in cavitands,[603] conformational control by stereochemical relays,[604] switching of chiral properties,[605] light-stimulated machines,[606] switchable molecular shuttles,[607] transition-metal-based molecular machines,[608] crystalline molecular machines,[609] self-locomotion,[610] electromechanical molecular electronic devices,[611] liquid-crystalline phase alignment,[612] liquid-crystalline elastomer actuators,[613] and biomotors used to power self-assembly processes.[614]

Recent experiment and theory has shown that interesting effects arise for ratchet systems in which there are several interacting particles moving over the same potential-energy surface.[615] This brings to mind the almost complete absence of polyrotaxane architectures from current synthetic molecular machine designs and suggests that these interlocked architectures may provide interesting systems in the future. Even today, the long-studied concept of correlated conformational motions continues to generate significant interest and advances,[616] including an investigation of a molecular-orbital-controlled gearing effect during a sigmatropic rearrangement.[616c] The more recent concept of molecular "gyroscope" structures has also seen new examples reported, with potentially interesting dynamic features.[617] Observed at the single-molecule level using STM, rotation of a porphyrin-based molecule on a silver surface has been shown to be reversibly switched on by addition of a small "hub" molecule.[618] Using an overcrowded alkene, a three-state luminescent switch has been demonstrated, whereby red-, blue-, and nonfluorescent states can be accessed by appropriate application of light, heat, and electrons.[619] Continuing the systematic investigation of unidirectional motors constructed from overcrowded alkenes, new members of the "second generation" series have been reported,[620] including the fastest-rotating example yet.

Understanding and characterization of isolated molecular mechanical switching units is now such that devices of greater complexity, incorporating a number of fundamental features, are within reach. Aida and co-workers have harnessed an azobenzene isomerization-induced change in conformation around a metallocene pivot to control the relative arrangement of two porphyrin substituents. These, in turn, can regulate the conformation of a kinetically bound guest.[621] In a related system, a photoresponsive guest has been used to switch the host molecule between two, kinetically stable, conformations.[622] An example of macroscopic-machine-inspired design can be found in a report on the construction and solution-phase characterization of an ambitious new member in the molecular "nanocar" series that combines the design features of the original STM-tip-driven molecules with an overcrowded alkene molecular motor as a proposed propulsion mechanism.[623]

In terms of rotaxane-based switches, recent advances include: the first quantitative force spectroscopy measurements on intercomponent interactions in a shuttle;[624] further characterization of amphiphilic shuttles arranged at the air–water interface[625] and the fabrication of solid-state electronic devices from monolayers; [626] theoretical and experimental work aimed at further clarifying the mechanism of operation for solid-state MSTJs;[627] and progress towards an electrically

powered actuator constructed from such rotaxanes.[628] In a truly novel addition to the dynamic interlocked molecules field, a rotaxane has been reported in which raising the temperature leads to *reduced* intercomponent motions, as a result of the reversible formation of imine bonds between the macrocycle and thread.[629]

Mechanical[630] and electrostatic[631] telescoping of MWNTs has recently been exploited to create a tunable nanoresonator and a nanoelectromechanical switch, respectively. Polymer-based actuator materials have continued their march towards useful devices, making progress on several fronts. The development of stimuli-responsive hydrogels that are biochemically degradable[632] and that respond to important biological analytes in relevant media[633] should prove to be important advances. In terms of engineering existing actuator materials, highlights include the use of stimuli-responsive hydrogels to control the focal length of liquid microlenses[634] and the direct conversion of chemical potential into work using charge- and heat-powered actuator materials by creating fuel-cell electrodes from carbon nanotube sheets and a shape memory alloy, respectively.[635]

In an interesting experiment, STM has been applied to investigate conformational changes in single chlorophyll-a molecules on injection of electrons, thus revealing a four-step switching scheme.[636] Further development of modified MscL channel proteins has led to a tunable pH-sensitive valve that may find application in drug-delivery systems,[637] while an entirely synthetic peptide has been used to form switchable channels which open in the presence of Fe(III) ions.[638] It has been shown that microtubules being transported down kinesin-coated channels can be directed at channel junctions by application of an electric field.[639] A pH-responsive conformational switch constructed from DNA has recently been attached to a solid substrate and coupled to an oscillating chemical reaction to power its operation.[640] Finally, a remarkable self-assembling system of aromatic chromophores has been shown to span a lipid bilayer and generate a photoinduced electric potential. This was used to power the reduction of quinones held inside vesicles formed by the membrane, thereby resulting in a transmembrane proton gradient. Addition of an aromatic intercalator irreversibly disrupted the complex, turning it into an ion channel through which the proton gradient could equilibrate.[641] If this is not quite a synthetic ion pump, it is well on the way there!

The first four decades of supramolecular chemistry were primarily concerned with the manipulation of molecular-level structures under thermodynamic control.[169] However, the most recent developments in molecular-level machines demonstrate yet again that to build sophisticated functional systems it will be necessary to develop a whole new field of supramolecular and molecular chemistry that operates, with control, far from equilibrium. The underlying principles that will allow chemists to do this are outlined in Sections 1.4.2, 1.4.3, and 4.4.

D.A.L. and F.Z. would like to thank all the members, past and present, of their research groups for their ideas, imagination, and enthusiasm over the past 15 years. We also thank the UK and Italian funding bodies, the EU, and the Carnegie Trust for their generous funding of our research programs in the area of molecular motors and machines.

Received: December 5, 2005
Published online: November 29, 2006

[1] a) R. P. Feynman, *Eng. Sci.* **1960**, *23*, 22–36; b) A. P. Davis, *Nature* **1999**, *401*, 120–121; c) V. Balzani, A. Credi, F. M. Raymo, J. F. Stoddart, *Angew. Chem.* **2000**, *112*, 3484–3530; *Angew. Chem. Int. Ed.* **2000**, *39*, 3349–3391; d) B. L. Feringa, *Nature* **2000**, *408*, 151–154; e) special issue on "Molecular Machines": *Acc. Chem. Res.* **2001**, *34*, 409–522; f) volume on "Molecular Machines and Motors": *Struct. Bonding (Berlin)* **2001**, *99*, 1–281; g) V. Balzani, A. Credi, M. Venturi, *Chem. Eur. J.* **2002**, *8*, 5524–5532; h) V. Balzani, M. Venturi, A. Credi, *Molecular Devices and Machines. A Journey into the Nanoworld*, Wiley-VCH, Weinheim, **2003**; i) C. J. Easton, S. F. Lincoln, L. Barr, H. Onagi, *Chem. Eur. J.* **2004**, *10*, 3120–3128; j) C. P. Mandl, B. König, *Angew. Chem.* **2004**, *116*, 1650–1652; *Angew. Chem. Int. Ed.* **2004**, *43*, 1622–1624; k) G. S. Kottas, L. I. Clarke, D. Horinek, J. Michl, *Chem. Rev.* **2005**, *105*, 1281–1376; l) K. Kinbara, T. Aida, *Chem. Rev.* **2005**, *105*, 1377–1400; m) E. R. Kay, D. A. Leigh in *Functional Artificial Receptors* (Eds.: T. Schrader, A. D. Hamilton), Wiley-VCH, Weinheim, **2005**, pp. 333–406; n) volume on "Molecular Machines": *Top. Curr. Chem.* **2005**, *262*, 1–236; for a recent view of the molecular-machines field from the perspective of the physics community, see: o) special issue on "Molecular Motors": *J. Phys.: Condens. Matter* **2005**, *17*, S3661–S4024.

[2] This is in no sense a criticism of the terminology used at the time to report these pioneering experiments, which filled a generation of chemists with excitement at the prospect of making molecular-sized machines. Language can only ever be used in the context of the knowledge of the day.

[3] E. R. Kay, D. A. Leigh, *Nature* **2006**, *440*, 286–287.

[4] a) R. E. Smalley, *Sci. Am.* **2001**, *285*(3), 68–69; b) G. M. Whitesides, *Sci. Am.* **2001**, *285*(3), 70–75; c) point/counterpoint debate between R. E. Smalley and K. E. Drexler, *Chem. Eng. News* **2003**, *81*(48), 37–42.

[5] In fact, physicists sometimes differentiate thermal ratchets from motors in that the former do not bear a load. However, as they are mechanistically identical, this distinction is unnecessary for the design of chemical systems.

[6] "Motor molecules" can also act as switches; the change in the distribution or position of the components can be used to affect a system as a function of state; see Sections 8.3.2 and 8.3.3.

[7] a) R. Brown, *Philos. Mag.* **1828**, *4*, 171–173; b) R. Brown, *Edinb. New Philos. J.* **1828**, *5*, 358–371; c) R. Brown, *Philos. Mag.* **1829**, *6*, 161–166; Brown's accounts of these investigations are also reprinted in d) R. Brown in *The Miscellaneous Botanical Works of Robert Brown*, *Vol. 1* (Ed.: J. J. Bennett), Ray Society, London, **1866**, pp. 463–486; for a modern reconstruction of the original experiments, see: e) B. J. Ford, *Microscope* **1992**, *40*, 235–241.

[8] A. Einstein, *Ann. Phys.* **1905**, *17*, 549–560; reprinted in *Einstein's Annalen Papers: The Complete Collection 1901–1922* (Ed.: J. Renn), Wiley-VCH, Weinheim, **2005**, pp. 182–193.

[9] J. Perrin, *Atoms* (English Translation: D. L. Hammick), 2nd English ed., Constable & Co., London, **1923**.

[10] For more detailed accounts of these discoveries and their impact on the scientific world, see: a) M. D. Haw, *J. Phys.: Condens. Matter* **2002**, *14*, 7769–7779; b) G. Parisi, *Nature* **2005**, *433*, 221–221; c) M. Haw, *Phys. World* **2005**, *18*(1), 19–22; d) P. Hänggi, F. Marchesoni, *Chaos* **2005**, *15*, 026101; e) J. Renn, *Ann. Phys.* **2005**, *14*, S23-S37; reprinted in *Einstein's Annalen*

Papers: The Complete Collection 1901–1922 (Ed.: J. Renn), Wiley-VCH, Weinheim, **2005**, pp. 23 – 37.

[11] *Molecular Motors* (Ed.: M. Schliwa), Wiley-VCH, Weinheim, **2003**.

[12] R. D. Astumian, P. Hänggi, *Phys. Today* **2002**, *55*(11), 33 – 39.

[13] R. A. L. Jones, *Soft Machines: Nanotechnology and Life*, Oxford University Press, Oxford, **2004**.

[14] For reprints of key papers and commentary on some of the main issues regarding Maxwell's demon, see: *Maxwell's Demon 2. Entropy, Classical and Quantum Information, Computing* (Eds.: H. S. Leff, A. F. Rex), Institute of Physics Publishing, Bristol, **2003**.

[15] The first a) private and b) public written discussions of the "temperature demon" were: a) J. C. Maxwell, *Letter to P. G. Tait*, *11 December 1867*; quoted in C. G. Knott, *Life and Scientific Work of Peter Guthrie Tait*, Cambridge University Press, London, **1911**, pp. 213 – 214; and reproduced in *The Scientific Letters and Papers of James Clerk Maxwell Vol. II 1862–1873* (Ed.: P. M. Harman), Cambridge University Press, Cambridge, **1995**, pp. 331 – 332; b) J. C. Maxwell, *Theory of Heat*, Longmans, Green and Co., London, **1871**, chap. 22; c) Maxwell introduced the idea of a "pressure demon" in a later letter to Tait (believed to date from early 1875); quoted in C. G. Knott, *Life and Scientific Work of Peter Guthrie Tait*, Cambridge University Press, London, **1911**, pp. 214 – 215; and reproduced in *The Scientific Letters and Papers of James Clerk Maxwell, Vol. III, 1874–1879* (Ed.: P. M. Harman), Cambridge University Press, Cambridge, **2002**, pp. 185 – 187; "Concerning Demons… Is the production of an inequality of temperature their only occupation? No, for less intelligent demons can produce a difference in pressure as well as temperature by merely allowing all particles going in one direction while stopping all those going the other way. This reduces the demon to a valve.". More formally, a pressure demon would operate in a system linked to a constant-temperature reservoir with the sole effect of using energy transferred as heat from that reservoir to do work (see Szilard's engine, Figure 3 and Ref. [17]). This is in conflict with the Kelvin–Planck form of the second law of thermodynamics, whereas the temperature demon challenges the Clausius definition.

[16] a) M. von Smoluchowski, *Physik. Z.* **1912**, *13*, 1069-1080; b) M. von Smoluchowski, *Vortrage über die Kinetische Theorie der Materie und der Elektrizitat* (Ed.: M. Planck), Teubner and Leipzig, Berlin, **1914**, pp. 89-121; Maxwell had earlier alluded to the basic premise behind Smoluchowski's trapdoor in private correspondence (c) J. C. Maxwell, *Letter to J. W. Strutt, 6 December 1870*. Reproduced in *The Scientific Letters and Papers of James Clerk Maxwell Vol. II 1862-1873* (Ed.: P. M. Harman), Cambridge University Press, Cambridge, **1995**, pp. 582-583), describing his "finite being" as a "doorkeeper, very intelligent and exceedingly quick" adding that "I do not see why even intelligence might not be dispensed with and the thing be made self-acting".

[17] L. Szilard, *Z. Phys.* **1929**, *53*, 840 – 856. An English translation by A. Rapoport and M. Knoller is reprinted in ref. [14], pp. 110–119.

[18] R. P. Feynman, R. B. Leighton, M. Sands, *The Feynman Lectures on Physics*, *Vol. 1*, Addison-Wesley, Reading, MA, **1963**, chapt. 46.

[19] *The Second Law of Thermodynamics. Memoirs by Carnot, Clausius and Thomson: Harper's Scientific Memoirs* (Ed.: W. F. Magie), Harper & Brothers, New York, **1899**.

[20] a) W. Ehrenberg, *Sci. Am.* **1967**, *217*(5), 103 – 110; b) C. H. Bennett, *Sci. Am.* **1987**, *257*(5), 88 – 96.

[21] W. Thomson, *Proc. R. Soc. Edinburgh* **1874**, *8*, 325 – 334.

[22] W. Thomson, *Nature* **1874**, *9*, 441 – 444.

[23] In fact, Thomson thought that Maxwell had coined the term "demon", but Maxwell corrects this in Ref. [15c].

[24] This insight is all the more remarkable coming as it did before the advent of the electronic computer. The deconstruction of the reasoning processes of a living being to simple computational steps is the basis for the modern field of cybernetics.

[25] For a modern critique of Feynman's analysis, see: a) J. M. R. Parrondo, P. Español, *Am. J. Phys.* **1996**, *64*, 1125 – 1130; b) K. Sekimoto, *J. Phys. Soc. Jpn.* **1997**, *66*, 1234 – 1237; and for other modern treatments of this model, see: c) H. Sakaguchi, *J. Phys. Soc. Jpn.* **1998**, *67*, 709 – 712; d) T. Hondou, F. Takagi, *J. Phys. Soc. Jpn.* **1998**, *67*, 2974 – 2976; e) M. O. Magnasco, G. Stolovitzky, *J. Stat. Phys.* **1998**, *93*, 615 – 632; f) C. Jarzynski, O. Mazonka, *Phys. Rev. E* **1999**, *59*, 6448 – 6459; g) D. Abbott, B. R. Davis, J. M. R. Parrondo, in *Proceedings of the Second International Conference on Unsolved Problems of Noise and Fluctuations* (Adelaide, 1999), *AIP Conf. Proc. 511* (Eds.: D. Abbott, L. B. Kiss), American Institute of Physics, New York, **2000**, pp. 213 – 218; h) S. Velasco, J. M. M. Roco, A. Medina, A. C. Hernandez, *J. Phys. D* **2001**, *34*, 1000 – 1006; i) R. Kawai, X. Sailer, L. Schimansky-Geier, C. Van den Broeck, *Phys. Rev. E* **2004**, *69*, 051109; j) C. Van den Broeck, R. Kawai, P. Meurs, *Phys. Rev. Lett.* **2004**, *93*, 090601; k) C. Van den Broeck, P. Meurs, R. Kawai, *New J. Phys.* **2005**, *7*, 10.

[26] In more recent times, Skordos and Zurek have carried out a simulation of the Smoluchowski trapdoor which showed Smoluchowski's intuitive conclusions (and Feynman's theoretical considerations) to be correct: a) P. A. Skordos, W. H. Zurek, *Am. J. Phys.* **1992**, *60*, 876 – 882; reprinted in Ref. [14], pp. 94–100; cooling the trapdoor every time it approaches the closed position results in the success of the ratcheting mechanism and creates a pressure gradient between the two compartments. Rex and Larsen have presented a similar analysis in which they quantified the statistical entropy loss on sorting the particles and showed this to be less than the thermodynamic entropy gained on cooling the trapdoor: b) A. F. Rex, R. Larsen in *Proceedings of the Workshop on Physics and Computation*, IEEE Computer Society Press, Los Alamitos (PhysComp, Dallas, 1992), **1992**, pp. 93–101; reprinted in Ref. [14], pp. 101–109.

[27] E. M. Purcell, *Am. J. Phys.* **1977**, *45*, 3 – 11.

[28] J. Siegel, *Science* **2005**, *310*, 63 – 64.

[29] R. B. Gennis, *Biomembranes—Molecular Structure and Function*, Springer, New York, **1989**.

[30] a) P. Läuger, *Electrogenic Ion Pumps*, Sinauer Associates, Sunderland, MA, **1991**; b) E. Gouaux, R. MacKinnon, *Science* **2005**, *310*, 1461 – 1465.

[31] a) C. Toyoshima, G. Inesi, *Annu. Rev. Biochem.* **2004**, *73*, 269 – 292; b) J. V. Møller, P. Nissen, T. L.-M. Sørensen, M. le Maire, *Curr. Opin. Struct. Biol.* **2005**, *15*, 387 – 393.

[32] M. N. Chatterjee, E. R. Kay, D. A. Leigh, *J. Am. Chem. Soc.* **2006**, *128*, 4058 – 4073.

[33] D. G. Nicholls, S. J. Ferguson, *Bioenergetics 3*, Academic Press, London, **2002**.

[34] The precise mechanisms in each case are, of course, complex and the details difficult to elucidate. In part this is because elements of a conformational and a gradient-driven pumping mechanism can be in operation at the same time.

[35] A close analogue, halorhodopsin, is a light-powered conformational chloride pump.

[36] a) J. K. Lanyi, H. Luecke, *Curr. Opin. Struct. Biol.* **2001**, *11*, 415 – 419; b) R. Neutze, E. Pebay-Peyroula, K. Edman, A. Royant, J. Navarro, E. M. Landau, *Biochim. Biophys. Acta* **2002**, *1565*, 144 – 167.

[37] L. Onsager, *Phys. Rev.* **1931**, *37*, 405 – 426.

[38] For an introduction to Brownian motors, see: Ref. [12] and R. D. Astumian, *Sci. Am.* **2001**, *285*(1), 56 – 64.

[39] For reviews on Brownian ratchet mechanisms, see: a) P. Hänggi, R. Bartussek in *Nonlinear Physics of Complex Systems—Current status and future trends: Lecture Notes in Physics*, *Vol. 476* (Eds.: J. Parisi, S. C. Müller, W. Zimmermann), Springer, Berlin, **1996**, pp. 294–308; b) R. D. Astumian, *Science* **1997**, *276*, 917–922; c) M. Bier, *Contemp. Phys.* **1997**, *38*, 371–379; d) F. Jülicher, A. Ajdari, J. Prost, *Rev. Mod. Phys.* **1997**, *69*, 1269–1281; e) special issue on "The constructive role of noise in fluctuation-driven transport and stochastic resonance": *Chaos* **1998**, *8*, 533–664; f) P. Reimann, *Phys. Rep.* **2002**, *361*, 57–265; g) P. Reimann, P. Hänggi, *Appl. Phys. A* **2002**, *75*, 169–178; h) J. M. R. Parrondo, B. J. De Cisneros, *Appl. Phys. A* **2002**, *75*, 179–191; i) J. M. R. Parrondo, L. Dinís, *Contemp. Phys.* **2004**, *45*, 147–157; j) B. J. Gabryś, K. Pesz, S. J. Bartkiewicz, *Physica A* **2004**, *336*, 112–122; k) H. Linke, M. T. Downton, M. J. Zuckermann, *Chaos* **2005**, *15*, 026111. The terms "thermal ratchet" and "Brownian ratchet" are often used interchangeably in the physics and biophysics literature ("Brownian rectifier" and "stochastic ratchet" are also occasionally used). This reflects the fact that *thermal* energy, in the form of *Brownian* motion, is the source of randomization in such schemes. Although the latter term is more common in the recent literature, it has to be said that some researchers (see, for example, Refs. [39f–h]) prefer the former on the basis that "Brownian ratchet" was first coined (l) S. M. Simon, C. S. Peskin, G. F. Oster, *Proc. Natl. Acad. Sci. USA* **1992**, *89*, 3770-3774) for the specific phenomenon of protein translocation through pores, during which Brownian motion is ratcheted by binding events on one side of the membrane. There can also be confusion between the terms "thermal ratchet" and "temperature ratchet"; the latter should properly be reserved only for ratchet systems that operate on the basis of temperature gradients, a subclass of thermal ratchets. We believe, therefore, that both force of numbers and the illustrative nature of the term "Brownian ratchet" commend it for use here, particularly as "Brownian motor" is commonly used to describe a machine which operates by such a mechanism (see Ref. [5]).

[40] Randomizing influences other than Brownian motion can be used in ratchet mechanisms; for example, in quantum ratchets, quantum effects such as tunneling or electron-wave interference play this role; see, for example: H. Linke, T. E. Humphrey, P. E. Lindelof, A. Lofgren, R. Newbury, P. Omling, A. O. Sushkov, R. P. Taylor, H. Xu, *Appl. Phys. A* **2002**, *75*, 237–246.

[41] The source of spatial inversion symmetry breaking is most commonly an inherently asymmetric (or "ratchet") potential. In certain cases, however, a symmetric potential is sufficient if the energy input (although unbiased) brings about spatial asymmetry. Also possible is spontaneous symmetry breaking in coupled symmetric systems driven away from equilibrium (not discussed here). Of course, spatial inversion symmetry may also be broken by a combination of the above.

[42] a) R. D. Astumian, M. Bier, *Biophys. J.* **1996**, *70*, 637–653; b) R. D. Astumian, I. Derényi, *Eur. Biophys. J.* **1998**, *27*, 474–489; c) L. Mahadevan, P. Matsudaira, *Science* **2000**, *288*, 95–99; d) R. Lipowsky in *Stochastic Processes in Physics, Chemistry and Biology: Lecture Notes in Physics*, *Vol. 557* (Eds.: J. A. Freund, T. Pöschel), Springer, Berlin, **2000**, pp. 21–31; e) C. Bustamante, D. Keller, G. Oster, *Acc. Chem. Res.* **2001**, *34*, 412–420; f) R. D. Astumian, *Appl. Phys. A* **2002**, *75*, 193–206; g) A. Mogilner, G. Oster, *Curr. Biol.* **2003**, *13*, R721–R733; h) G. Oster, H. Y. Wang, *Trends Cell Biol.* **2003**, *13*, 114–121; i) M. Kurzyński, P. Chełminiak, *Physica A* **2004**, *336*, 123–132.

[43] For a recent snapshot of the current status of experiment and application with respect to both biological systems and future technology, see: special issue on "Ratchets and Brownian motors: Basics, experiments and applications": *Appl. Phys. A* **2002**, *75*, 167–352.

[44] For a selection of experimental examples, see: a) J. Rousselet, L. Salome, A. Ajdari, J. Prost, *Nature* **1994**, *370*, 446–448; b) L. P. Faucheux, L. S. Bourdieu, P. D. Kaplan, A. J. Libchaber, *Phys. Rev. Lett.* **1995**, *74*, 1504–1507; c) L. P. Faucheux, G. Stolovitzky, A. Libchaber, *Phys. Rev. E* **1995**, *51*, 5239–5250; d) L. P. Faucheux, A. Libchaber, *J. Chem. Soc. Faraday Trans.* **1995**, 3163–3166; e) L. Gorre, E. Ioannidis, P. Silberzan, *Europhys. Lett.* **1996**, *33*, 267–272; f) L. Gorre-Talini, S. Jeanjean, P. Silberzan, *Phys. Rev. E* **1997**, *56*, 2025–2034; g) L. Gorre-Talini, P. Silberzan, *J. Phys. I* **1997**, *7*, 1475–1485; h) L. Gorre-Talini, J. P. Spatz, P. Silberzan, *Chaos* **1998**, *8*, 650–656; i) A. Lorke, S. Wimmer, B. Jager, J. P. Kotthaus, W. Wegscheider, M. Bichler, *Physica B* **1998**, *251*, 312–316; j) H. Linke, W. Sheng, A. Lofgren, H. Q. Xu, P. Omling, P. E. Lindelof, *Europhys. Lett.* **1998**, *44*, 341–347; k) C. Mennerat-Robilliard, D. Lucas, S. Guibal, J. Tabosa, C. Jurczak, J. Y. Courtois, G. Grynberg, *Phys. Rev. Lett.* **1999**, *82*, 851–854; l) A. van Oudenaarden, S. G. Boxer, *Science* **1999**, *285*, 1046–1048; m) J. S. Bader, R. W. Hammond, S. A. Henck, M. W. Deem, G. A. McDermott, J. M. Bustillo, J. W. Simpson, G. T. Mulhern, J. M. Rothberg, *Proc. Natl. Acad. Sci. USA* **1999**, *96*, 13165–13169; n) C. F. Chou, O. Bakajin, S. W. P. Turner, T. A. J. Duke, S. S. Chan, E. C. Cox, H. G. Craighead, R. H. Austin, *Proc. Natl. Acad. Sci. USA* **1999**, *96*, 13762–13765; o) M. Switkes, C. M. Marcus, K. Campman, A. C. Gossard, *Science* **1999**, *283*, 1905–1908; p) H. Linke, T. E. Humphrey, A. Lofgren, A. O. Sushkov, R. Newbury, R. P. Taylor, P. Omling, *Science* **1999**, *286*, 2314–2317; q) R. W. Hammond, J. S. Bader, S. A. Henck, M. W. Deem, G. A. McDermott, J. M. Bustillo, J. M. Rothberg, *Electrophoresis* **2000**, *21*, 74–80; r) H. Linke, W. D. Sheng, A. Svensson, A. Lofgren, L. Christensson, H. Q. Xu, P. Omling, P. E. Lindelof, *Phys. Rev. B* **2000**, *61*, 15914–15926; s) E. M. Hohberger, A. Lorke, W. Wegscheider, M. Bichler, *Appl. Phys. Lett.* **2001**, *78*, 2905–2907; t) C. Marquet, A. Buguin, L. Talini, P. Silberzan, *Phys. Rev. Lett.* **2002**, *88*, 168301; u) S. Matthias, F. Müller, *Nature* **2003**, *424*, 53–57; v) L. R. Huang, E. C. Cox, R. H. Austin, J. C. Sturm, *Anal. Chem.* **2003**, *75*, 6963–6967. The implications of Brownian ratchet theory, however, are far-reaching and elements of a wide range of noise-assisted physical phenomena may be modeled as ratchet processes, see Refs. [39f, 43].

[45] a) H. X. Zhou, Y.-D. Chen, *Phys. Rev. Lett.* **1996**, *77*, 194–197; b) I. Derényi, M. Bier, R. D. Astumian, *Phys. Rev. Lett.* **1999**, *83*, 903–906; c) A. Parmeggiani, F. Jülicher, A. Ajdari, J. Prost, *Phys. Rev. E* **1999**, *60*, 2127–2140.

[46] A power stroke is not intrinsically different in mechanistic terms to these ratchet mechanisms. The distinction is solely whether the particle is mostly under the influence of a force (that is, moving down an energy gradient) or not during its diffusion.

[47] A net flux of particles may also be achieved in a symmetric periodic potential if it is subject to a spatially periodic variation in temperature of the same periodicity as, but out of phase with, the potential. Such systems have their origin in the demonstration by Landauer that in a bistable potential well, a localized inhomogeneity in temperature can alter the relative stabilities of the two minima (a) R. Landauer, *Phys. Rev. A* **1975**, *12*, 636–638); Büttiker (b) M. Büttiker, *Z. Phys. B* **1987**, *68*, 161–167); and van Kampen (c) N. G. van Kampen, *IBM J. Res. Dev.* **1988**, *32*, 107–111) independently modeled this effect and showed that if extended to a periodic potential (that is, repeating the bistable well in a linear fashion or allowing motion in a closed loop), directional particle transport would occur; shortly after, Landauer further extended this model (d) R. Landauer, *J. Stat. Phys.* **1988**, *53*, 233–248) which is now often termed "Landauer's blowtorch" (see also: e) K. Sinha, F. Moss, *J. Stat. Phys.* **1989**, *54*, 1411–1423; f) M. Bekele, S.

Rajesh, G. Ananthakrishna, N. Kumar, *Phys. Rev. E* **1999**, *59*, 143 – 149). Although realization of such a scheme on a microscopic scale would be problematic (see Section 1.3), circulating currents in a closed loop were first observed in electronics by Thomas Johann Seebeck in 1821. An electric current flows in a circuit composed of two resistors which are held at different temperatures (the modern equivalent of such thermoelectric circuits is a thermogenerator, in which a semiconductor diode is held at a different temperature to the rest of a circuit). For this reason, particle transport over symmetric periodic potentials, driven by spatial variations in temperature, is also often known as a "Seebeck ratchet". Clearly, such schemes also bear a close resemblance to Feynman's ratchet-and-pawl (Section 1.2.1) when $T_1 \neq T_2$ and, indeed, mathematical equivalence of the two models can be shown, see ref. [25].

[48] R. Landauer, *IBM J. Res. Dev.* **1961**, *5*, 183 – 191.

[49] The switching between two different intrinsic periodic potentials (chemical reactions) according to the position of the particle is effectively a chemical manifestation of "Parrondo's paradox", a discovery in game theory that two losing repetitive gambling games, played stochastically or periodically one after another, can become winning; see Ref. [38] and a) P. V. E. McClintock, *Nature* **1999**, *401*, 23 – 24; b) G. P. Harmer, D. Abbott, *Nature* **1999**, *402*, 864; c) G. P. Harmer, D. Abbott, *Stat. Sci.* **1999**, *14*, 206 – 213.

[50] The directional threading that occurs in cyclodextrin and other unsymmetrical macrocycle-based rotaxanes, polyrotaxanes, and pseudorotaxanes could be used in this respect, but only if coupled to an appropriate energy input (for example, olefin or azobenzene isomerization), see: Section 4.3.1 and a) R. Isnin, A. E. Kaifer, *J. Am. Chem. Soc.* **1991**, *113*, 8188 – 8190; b) H. Yonemura, M. Kasahara, H. Saito, H. Nakamura, T. Matsuo, *J. Phys. Chem.* **1992**, *96*, 5765 – 5770; c) A. Abou-Hamdan, P. Bugnon, C. Saudan, P. G. Lye, A. E. Merbach, *J. Am. Chem. Soc.* **2000**, *122*, 592 – 602; d) J. E. H. Buston, J. R. Young, H. L. Anderson, *Chem. Commun.* **2000**, 905 – 906; e) M. R. Craig, M. G. Hutchings, T. D. W. Claridge, H. L. Anderson, *Angew. Chem.* **2001**, *113*, 1105 – 1108; *Angew. Chem. Int. Ed.* **2001**, *40*, 1071 – 1074; f) C. Saudan, F. A. Dunand, A. Abou-Hamdan, P. Bugnon, P. G. Lye, S. F. Lincoln, A. E. Merbach, *J. Am. Chem. Soc.* **2001**, *123*, 10290 – 10298; g) J. S. Lock, B. L. May, P. Clements, S. F. Lincoln, C. J. Easton, *Org. Biomol. Chem.* **2004**, *2*, 337 – 344; h) J. W. Park, H. J. Song, *Org. Lett.* **2004**, *6*, 4869 – 4872; i) J. W. Park, S. Y. Lee, H. J. Song, K. K. Park, *J. Org. Chem.* **2005**, *70*, 9505 – 9513; j) T. Oshikiri, Y. Takashima, H. Yamaguchi, A. Harada, *J. Am. Chem. Soc.* **2005**, *127*, 12186 – 12187; k) Q.-C. Wang, Q. Ma, D.-H. Qu, H. Tian, *Chem. Eur. J.* **2006**, *12*, 1088 – 1096; l) A. G. Cheetham, M. G. Hutchings, T. D. W. Claridge, H. L. Anderson, *Angew. Chem.* **2006**, *118*, 1626 – 1629; *Angew. Chem. Int. Ed.* **2006**, *45*, 1596 – 1599; m) G. Wenz, B.-H. Han, A. Müller, *Chem. Rev.* **2006**, *106*, 782 – 817.

[51] J. V. Hernández, E. R. Kay, D. A. Leigh, *Science* **2004**, *306*, 1532 – 1537.

[52] It seems to us that these ideas could prove useful in understanding protein folding and, perhaps, how some chaperones, foldases, and prions function.

[53] a) K. Mislow, *Acc. Chem. Res.* **1976**, *9*, 26 – 33; b) Z. Rappoport, S. E. Biali, *Acc. Chem. Res.* **1988**, *21*, 442 – 449; c) K. Mislow, *Chemtracts: Org. Chem.* **1989**, *2*, 151 – 174; d) Z. Rappoport, S. E. Biali, *Acc. Chem. Res.* **1997**, *30*, 307 – 314.

[54] M. Ōki, *Angew. Chem.* **1976**, *88*, 67 – 74; *Angew. Chem. Int. Ed. Engl.* **1976**, *15*, 87 – 93.

[55] For a joint summary of the work of the two research groups, see: H. Iwamura, K. Mislow, *Acc. Chem. Res.* **1988**, *21*, 175 – 182.

[56] For highlights of the work by Iwamura and co-workers, see: a) Y. Kawada, H. Iwamura, *J. Org. Chem.* **1980**, *45*, 2547 – 2548; b) Y. Kawada, H. Iwamura, *J. Am. Chem. Soc.* **1981**, *103*, 958 – 960; c) Y. Kawada, H. Iwamura, *Tetrahedron Lett.* **1981**, *22*, 1533 – 1536; d) Y. Kawada, H. Iwamura, *J. Am. Chem. Soc.* **1983**, *105*, 1449 – 1459; e) Y. Kawada, Y. Okamoto, H. Iwamura, *Tetrahedron Lett.* **1983**, *24*, 5359 – 5362; f) H. Iwamura, T. Ito, H. Ito, K. Toriumi, Y. Kawada, E. Osawa, T. Fujiyoshi, C. Jaime, *J. Am. Chem. Soc.* **1984**, *106*, 4712 – 4717; g) H. Iwamura, *J. Mol. Struct.* **1985**, *126*, 401 – 412; h) N. Koga, H. Iwamura, *J. Am. Chem. Soc.* **1985**, *107*, 1426 – 1427; i) N. Koga, H. Iwamura, *Chem. Lett.* **1986**, 247 – 250; j) Y. Kawada, H. Yamazaki, G. Koga, S. Murata, H. Iwamura, *J. Org. Chem.* **1986**, *51*, 1472 – 1477; k) Y. Kawada, J. Ishikawa, H. Yamazaki, G. Koga, S. Murata, H. Iwamura, *Tetrahedron Lett.* **1987**, *28*, 445 – 448.

[57] For highlights of the work by Mislow and co-workers, see: a) W. D. Hounshell, C. A. Johnson, A. Guenzi, F. Cozzi, K. Mislow, *Proc. Natl. Acad. Sci. USA* **1980**, *77*, 6961 – 6964; b) F. Cozzi, A. Guenzi, C. A. Johnson, K. Mislow, W. D. Hounshell, J. F. Blount, *J. Am. Chem. Soc.* **1981**, *103*, 957 – 958; c) C. A. Johnson, A. Guenzi, K. Mislow, *J. Am. Chem. Soc.* **1981**, *103*, 6240 – 6242; d) C. A. Johnson, A. Guenzi, R. B. Nachbar, J. F. Blount, O. Wennerstrom, K. Mislow, *J. Am. Chem. Soc.* **1982**, *104*, 5163 – 5168; e) H. B. Burgi, W. D. Hounshell, R. B. Nachbar, K. Mislow, *J. Am. Chem. Soc.* **1983**, *105*, 1427 – 1438; f) A. Guenzi, C. A. Johnson, F. Cozzi, K. Mislow, *J. Am. Chem. Soc.* **1983**, *105*, 1438 – 1448.

[58] The term "gearing" or "static gearing" is sometimes used to describe systems in which steric crowding results in the twisting and intermeshing of substituents on a planar framework, so as to all twist in the same direction. This is not, however, a sufficient condition for dynamic gearing (that is, correlated motion) of these substituents to occur.

[59] Like atropisomers, residual stereoisomers arise when two forms can interconvert through bond rotations but only at high energies. The term residual stereoisomer is used when each isolable species is not in fact a single conformational possibility, but rather a collection of rapidly interconverting permutations. Where these forms are interconverting by correlated rotations, the residual isomers may also be termed phase isomers.

[60] a) N. Koga, Y. Kawada, H. Iwamura, *J. Am. Chem. Soc.* **1983**, *105*, 5498 – 5499; b) N. Koga, Y. Kawada, H. Iwamura, *Tetrahedron* **1986**, *42*, 1679 – 1686.

[61] Y. Kawada, H. Sakai, M. Oguri, G. Koga, *Tetrahedron Lett.* **1994**, *35*, 139 – 142.

[62] a) G. Yamamoto, M. Ōki, *Chem. Lett.* **1979**, 1251 – 1254; b) G. Yamamoto, M. Ōki, *Chem. Lett.* **1979**, 1255 – 1258; c) G. Yamamoto, M. Ōki, *Bull. Chem. Soc. Jpn.* **1981**, *54*, 473 – 480; d) G. Yamamoto, M. Ōki, *Bull. Chem. Soc. Jpn.* **1981**, *54*, 481 – 487; e) G. Yamamoto, M. Ōki, *J. Org. Chem.* **1983**, *48*, 1233 – 1236; f) G. Yamamoto, *J. Mol. Struct.* **1985**, *126*, 413 – 420; g) G. Yamamoto, M. Ōki, *Bull. Chem. Soc. Jpn.* **1985**, *58*, 1953 – 1961; h) G. Yamamoto, M. Ōki, *Bull. Chem. Soc. Jpn.* **1986**, *59*, 3597 – 3603; i) G. Yamamoto, *Bull. Chem. Soc. Jpn.* **1989**, *62*, 4058 – 4060; j) G. Yamamoto, *Tetrahedron* **1990**, *46*, 2761 – 2772.

[63] A. M. Stevens, C. J. Richards, *Tetrahedron Lett.* **1997**, *38*, 7805 – 7808.

[64] For a review of investigations aimed at uncovering correlated motion in other crowded organometallic systems, see: S. Brydges, L. E. Harrington, M. J. McGlinchey, *Coord. Chem. Rev.* **2002**, *233*, 75 – 105.

[65] a) S. Hiraoka, K. Harano, T. Tanaka, M. Shiro, M. Shionoya, *Angew. Chem.* **2003**, *115*, 5340 – 5343; *Angew. Chem. Int. Ed.* **2003**, *42*, 5182 – 5185; b) S. Hiraoka, M. Shiro, M. Shionoya, *J. Am. Chem. Soc.* **2004**, *126*, 1214 – 1218; c) S. Hiraoka, K. Hirata, M. Shionoya, *Angew. Chem.* **2004**, *116*, 3902 – 3906; *Angew. Chem. Int. Ed.* **2004**, *43*, 3814 – 3818.

[66] a) M. Kuttenberger, M. Frieser, M. Hofweber, A. Mannschreck, *Tetrahedron: Asymmetry* **1998**, *9*, 3629 – 3645; b) J.

Clayden, J. H. Pink, *Angew. Chem.* **1998**, *110*, 2040 – 2043; *Angew. Chem. Int. Ed.* **1998**, *37*, 1937 – 1939; c) E. R. Johnston, R. Fortt, J. C. Barborak, *Magn. Reson. Chem.* **2000**, *38*, 932 – 936; d) R. A. Bragg, J. Clayden, *Org. Lett.* **2000**, *2*, 3351 – 3354; e) R. A. Bragg, J. Clayden, G. A. Morris, J. H. Pink, *Chem. Eur. J.* **2002**, *8*, 1279 – 1289.

[67] For accounts of the development of the Kelly systems, see: a) T. R. Kelly, *Acc. Chem. Res.* **2001**, *34*, 514 – 522; b) T. R. Kelly, J. P. Sestelo, *Struct. Bonding (Berlin)* **2001**, *99*, 19 – 53; c) J. P. Sestelo, T. R. Kelly, *Appl. Phys. A* **2002**, *75*, 337 – 343.

[68] T. R. Kelly, M. C. Bowyer, K. V. Bhaskar, D. Bebbington, A. Garcia, F. R. Lang, M. H. Kim, M. P. Jette, *J. Am. Chem. Soc.* **1994**, *116*, 3657 – 3658.

[69] Metal-ion binding to a 2,2′-bipyridyl unit has also been used to reversibly switch the orientation of two appended porphyrin units between a freely rotating and a rigid cofacial conformation, see: Y. Tomohiro, A. Satake, Y. Kobuke, *J. Org. Chem.* **2001**, *66*, 8442 – 8446.

[70] P. V. Jog, R. E. Brown, D. K. Bates, *J. Org. Chem.* **2003**, *68*, 8240 – 8243.

[71] Rotation around C_{aryl}–N bonds can be controlled by electrochemical switching between *p*-phenylenediamine (benzoid forms, rotation allowed) and *p*-quinonediimine (quinoid forms, no rotation) functionalities. This has been used to reversibly alter the geometry of a cyclophane, see: H. Kanazawa, M. Higuchi, K. Yamamoto, *J. Am. Chem. Soc.* **2005**, *127*, 16404 – 16405.

[72] a) T. R. Kelly, I. Tellitu, J. P. Sestelo, *Angew. Chem.* **1997**, *109*, 1969 – 1972; *Angew. Chem. Int. Ed. Engl.* **1997**, *36*, 1866 – 1868; b) T. R. Kelly, J. P. Sestelo, I. Tellitu, *J. Org. Chem.* **1998**, *63*, 3655 – 3665.

[73] a) A. P. Davis, *Angew. Chem.* **1998**, *110*, 953 – 954; *Angew. Chem. Int. Ed.* **1998**, *37*, 909 – 910; b) G. Musser, *Sci. Am.* **1999**, *280*(2), 24.

[74] P. W. Atkins, *Physical Chemistry*, 6th ed., Oxford University Press, Oxford, **1998**.

[75] The experimentally observed behavior of molecule **10** can be considered as a verification of both the second law of thermodynamics and the principle of detailed balance (see Section 1.4.1); for analysis, see: K. L. Sebastian, *Phys. Rev. E* **2000**, *61*, 937 – 939.

[76] a) T. R. Kelly, H. De Silva, R. A. Silva, *Nature* **1999**, *401*, 150 – 152; b) T. R. Kelly, R. A. Silva, H. De Silva, S. Jasmin, Y. J. Zhao, *J. Am. Chem. Soc.* **2000**, *122*, 6935 – 6949.

[77] W. L. Mock, K. J. Ochwat, *J. Phys. Org. Chem.* **2003**, *16*, 175 – 182.

[78] The presence of a kinetically unrestricted intermediate (bottom center in Scheme 4) reduces the ability of any molecular motor to progressively do work. Although an overall bias in the direction of the half-rotation should result from the molecular chirality, any attempt to achieve this against an opposing force (that is, to do work) would result in equilibration at this freely rotating intermediate. In the current case, preactivation of the "free" carboxylate prior to hydrolysis of the anhydride reduces the chance of reversal to give the starting enantiomer (an idling step) while also increasing the rate of the desired ring-closing reaction, in an attempt to minimize the effect of thermal randomization. However, it is likely that any opposing force would swamp this effect.

[79] B. J. Dahl, B. P. Branchaud, *Tetrahedron Lett.* **2004**, *45*, 9599 – 9602.

[80] Y. Lin, B. J. Dahl, B. P. Branchaud, *Tetrahedron Lett.* **2005**, *46*, 8359 – 8362.

[81] S. P. Fletcher, F. Dumur, M. M. Pollard, B. L. Feringa, *Science* **2005**, *310*, 80 – 82.

[82] a) K. Tashiro, K. Konishi, T. Aida, *Angew. Chem.* **1997**, *109*, 882 – 884; *Angew. Chem. Int. Ed. Engl.* **1997**, *36*, 856 – 858; b) K. Tashiro, T. Fujiwara, K. Konishi, T. Aida, *Chem. Commun.* **1998**, 1121 – 1122; c) K. Tashiro, K. Konishi, T. Aida, *J. Am. Chem. Soc.* **2000**, *122*, 7921 – 7926.

[83] Conversely, complexes formed around lanthanum(III) have been shown to rotate faster than the cerium(IV) parent compounds, see: M. Ikeda, M. Takeuchi, S. Shinkai, F. Tani, Y. Naruta, *Bull. Chem. Soc. Jpn.* **2001**, *74*, 739 – 746.

[84] a) S. Shinkai, M. Ikeda, A. Sugasaki, M. Takeuchi, *Acc. Chem. Res.* **2001**, *34*, 494 – 503; b) M. Takeuchi, M. Ikeda, A. Sugasaki, S. Shinkai, *Acc. Chem. Res.* **2001**, *34*, 865 – 873; c) S. Shinkai, M. Takeuchi, *Bull. Chem. Soc. Jpn.* **2005**, *78*, 40 – 51.

[85] a) M. Takeuchi, T. Imada, S. Shinkai, *Angew. Chem.* **1998**, *110*, 2242 – 2246; *Angew. Chem. Int. Ed.* **1998**, *37*, 2096 – 2099; b) A. Sugasaki, M. Ikeda, M. Takeuchi, A. Robertson, S. Shinkai, *J. Chem. Soc. Perkin Trans. 1* **1999**, 3259 – 3264.

[86] M. Yamamoto, A. Sugasaki, M. Ikeda, M. Takeuchi, K. Frimat, T. D. James, S. Shinkai, *Chem. Lett.* **2001**, 520 – 521.

[87] A. Robertson, M. Ikeda, M. Takeuchi, S. Shinkai, *Bull. Chem. Soc. Jpn.* **2001**, *74*, 883 – 888.

[88] a) M. Ikeda, T. Tanida, M. Takeuchi, S. Shinkai, *Org. Lett.* **2000**, *2*, 1803 – 1805; b) M. Ikeda, M. Takeuchi, S. Shinkai, F. Tani, Y. Naruta, S. Sakamoto, K. Yamaguchi, *Chem. Eur. J.* **2002**, *8*, 5542 – 5550.

[89] a) A. Sugasaki, M. Ikeda, M. Takeuchi, K. Koumoto, S. Shinkai, *Tetrahedron* **2000**, *56*, 4717 – 4723; b) A. Sugasaki, M. Ikeda, M. Takeuchi, S. Shinkai, *Angew. Chem.* **2000**, *112*, 3997 – 4000; *Angew. Chem. Int. Ed.* **2000**, *39*, 3839 – 3842; c) A. Sugasaki, K. Sugiyasu, M. Ikeda, M. Takeuchi, S. Shinkai, *J. Am. Chem. Soc.* **2001**, *123*, 10239 – 10244.

[90] G. Ercolani, *Org. Lett.* **2005**, *7*, 803 – 805.

[91] Allosteric receptors based on the braking of rotational motion have also been created from porphyrin-based systems, connected not by a common metal ion, but by single and triple C–C bonds, see: a) M. Ikeda, S. Shinkai, A. Osuka, *Chem. Commun.* **2000**, 1047 – 1048; b) Y. Kubo, M. Ikeda, A. Sugasaki, M. Takeuchi, S. Shinkai, *Tetrahedron Lett.* **2001**, *42*, 7435 – 7438; c) Y. Kubo, A. Sugasaki, M. Ikeda, K. Sugiyasu, K. Sonoda, A. Ikeda, M. Takeuchi, S. Shinkai, *Org. Lett.* **2002**, *4*, 925 – 928; d) M. Ayabe, A. Ikeda, Y. Kubo, M. Takeuchi, S. Shinkai, *Angew. Chem.* **2002**, *114*, 2914 – 2916; *Angew. Chem. Int. Ed.* **2002**, *41*, 2790 – 2792.

[92] R. K. Bohn, A. Haaland, *J. Organomet. Chem.* **1966**, *5*, 470 – 476.

[93] X.-B. Wang, B. Dai, H.-K. Woo, L.-S. Wang, *Angew. Chem.* **2005**, *117*, 6176 – 6178; *Angew. Chem. Int. Ed.* **2005**, *44*, 6022 – 6024.

[94] a) L. J. Todd, *Adv. Organomet. Chem.* **1970**, *8*, 87 – 115; b) M. F. Hawthorne, G. B. Dunks, *Science* **1972**, *178*, 462 – 471.

[95] a) L. F. Warren, M. F. Hawthorne, *J. Am. Chem. Soc.* **1970**, *92*, 1157 – 1173; b) D. St. Clair, A. Zalkin, D. H. Templeton, *J. Am. Chem. Soc.* **1970**, *92*, 1173 – 1179; c) M. R. Churchill, K. Gold, *J. Am. Chem. Soc.* **1970**, *92*, 1180 – 1187.

[96] M. F. Hawthorne, J. I. Zink, J. M. Skelton, M. J. Bayer, C. Liu, E. Livshits, R. Baer, D. Neuhauser, *Science* **2004**, *303*, 1849 – 1851.

[97] For reviews on triggering protein folding events to allow the study of this otherwise natural phenomenon, see: a) W. A. Eaton, P. A. Thompson, C. K. Chan, S. J. Hagen, J. Hofrichter, *Structure* **1996**, *4*, 1133 – 1139; b) special issue on "Protein Folding": *Acc. Chem. Res.* **1998**, *31*, 697 – 780; c) R. H. Callender, R. B. Dyer, R. Gilmanshin, W. H. Woodruff, *Annu. Rev. Phys. Chem.* **1998**, *49*, 173 – 202; d) C. M. Dobson, A. Šali, M. Karplus, *Angew. Chem.* **1998**, *110*, 908 – 935; *Angew. Chem. Int. Ed.* **1998**, *37*, 868 – 893; e) M. Gruebele, *Annu. Rev. Phys. Chem.* **1999**, *50*, 485 – 516; f) D. J. Brockwell, D. A. Smith, S. E. Radford, *Curr. Opin. Struct. Biol.* **2000**, *10*, 16 – 25; g) *Mechanisms of Protein Folding: Frontiers in Molecular Biology*,

Vol. 32, 2nd ed. (Ed.: R. H. Pain), Oxford University Press, Oxford, **2000**; h) M. Volk, *Eur. J. Org. Chem.* **2001**, 2605 – 2621; i) A. R. Fersht, V. Daggett, *Cell* **2002**, *108*, 573 – 582; for reviews on stimuli-induced control of synthetic polypeptide and polysaccharide secondary structures, see: j) M. Sisido, *Prog. Polym. Sci.* **1992**, *17*, 699 – 764; k) D. W. Urry, *Angew. Chem.* **1993**, *105*, 859 – 883; *Angew. Chem. Int. Ed. Engl.* **1993**, *32*, 819 – 841; l) D. M. Whitfield, S. Stojkovski, B. Sarkar, *Coord. Chem. Rev.* **1993**, *122*, 171 – 225; m) J. P. Schneider, J. W. Kelly, *Chem. Rev.* **1995**, *95*, 2169 – 2187; n) T. Kinoshita, *Prog. Polym. Sci.* **1995**, *20*, 527 – 583; o) I. Willner, S. Rubin, *Angew. Chem.* **1996**, *108*, 419 – 439; *Angew. Chem. Int. Ed. Engl.* **1996**, *35*, 367 – 385; p) I. Willner, *Acc. Chem. Res.* **1997**, *30*, 347 – 356; q) O. Pieroni, A. Fissi, G. Popova, *Prog. Polym. Sci.* **1998**, *23*, 81 – 123; r) O. Pieroni, A. Fissi, N. Angelini, F. Lenci, *Acc. Chem. Res.* **2001**, *34*, 9 – 17; s) I. Willner, B. Willner in *Molecular Switches* (Ed.: B. L. Feringa), Wiley-VCH, Weinheim, **2001**, pp. 165 – 218; t) F. Ciardelli, O. Pieroni in *Molecular Switches* (Ed.: B. L. Feringa), Wiley-VCH, Weinheim, **2001**, pp. 399 – 441; u) G. A. Woolley, *Acc. Chem. Res.* **2005**, *38*, 486 – 493.

[98] a) A. Fersht, *Enzyme Structure and Mechanism*, 2nd ed., W. H. Freeman and Company, New York, **1985**; b) M. F. Perutz, *Q. Rev. Biophys.* **1989**, *22*, 139 – 236; c) A. Mattevi, M. Rizzi, M. Bolognesi, *Curr. Opin. Struct. Biol.* **1996**, *6*, 824 – 829; d) J.-P. Changeux, S. J. Edelstein, *Neuron* **1998**, *21*, 959 – 980; e) W. A. Lim, *Curr. Opin. Struct. Biol.* **2002**, *12*, 61 – 68; f) J. A. Hardy, J. A. Wells, *Curr. Opin. Struct. Biol.* **2004**, *14*, 706 – 715; g) J.-P. Changeux, S. J. Edelstein, *Science* **2005**, *308*, 1424 – 1428.

[99] a) J. Rebek, Jr., *Acc. Chem. Res.* **1984**, *17*, 258 – 264; b) F. Vanveggel, W. Verboom, D. N. Reinhoudt, *Chem. Rev.* **1994**, *94*, 279 – 299; c) B. Linton, A. D. Hamilton, *Chem. Rev.* **1997**, *97*, 1669 – 1680; d) A. Robertson, S. Shinkai, *Coord. Chem. Rev.* **2000**, *205*, 157 – 199; e) S. Shinkai in *Molecular Switches* (Ed.: B. L. Feringa), Wiley-VCH, Weinheim, **2001**, pp. 281 – 307; f) L. Kovbasyuk, R. Krämer, *Chem. Rev.* **2004**, *104*, 3161 – 3187.

[100] a) J. Rebek, Jr., J. E. Trend, R. V. Wattley, S. Chakravorti, *J. Am. Chem. Soc.* **1979**, *101*, 4333 – 4337; b) J. Rebek, Jr., R. V. Wattley, *J. Am. Chem. Soc.* **1980**, *102*, 4853 – 4854.

[101] J. Rebek, Jr., T. Costello, L. Marshall, R. Wattley, R. C. Gadwood, K. Onan, *J. Am. Chem. Soc.* **1985**, *107*, 7481 – 7487.

[102] a) F.-G. Klärner, B. Kahlert, *Acc. Chem. Res.* **2003**, *36*, 919 – 932; b) M. Harmata, *Acc. Chem. Res.* **2004**, *37*, 862 – 873.

[103] a) R. P. Sijbesma, S. S. Wijmenga, R. J. M. Nolte, *J. Am. Chem. Soc.* **1992**, *114*, 9807 – 9813; b) J. N. H. Reek, H. Engelkamp, A. E. Rowan, J. Elemans, R. J. M. Nolte, *Chem. Eur. J.* **1998**, *4*, 716 – 722; c) A. E. Rowan, J. Elemans, R. J. M. Nolte, *Acc. Chem. Res.* **1999**, *32*, 995 – 1006.

[104] R. P. Sijbesma, R. J. M. Nolte, *J. Am. Chem. Soc.* **1991**, *113*, 6695 – 6696.

[105] a) Y. S. Chong, M. D. Smith, K. D. Shimizu, *J. Am. Chem. Soc.* **2001**, *123*, 7463 – 7464; b) C. F. Degenhardt, J. M. Lavin, M. D. Smith, K. D. Shimizu, *Org. Lett.* **2005**, *7*, 4079 – 4081.

[106] a) P. Leighton, J. K. M. Sanders, *J. Chem. Soc. Chem. Commun.* **1984**, 854 – 856; b) R. J. Abraham, P. Leighton, J. K. M. Sanders, *J. Am. Chem. Soc.* **1985**, *107*, 3472 – 3478.

[107] E. L. Eliel, S. H. Wilen, *Stereochemistry of Organic Compounds*, Wiley-Interscience, New York, **1994**.

[108] For reviews on conformational design, see: a) R. W. Hoffmann, *Angew. Chem.* **1992**, *104*, 1147 – 1157; *Angew. Chem. Int. Ed. Engl.* **1992**, *31*, 1124 – 1134; b) R. W. Hoffmann, *Angew. Chem.* **2000**, *112*, 2134 – 2150; *Angew. Chem. Int. Ed.* **2000**, *39*, 2054 – 2070.

[109] a) H. Yuasa, H. Hashimoto, *J. Am. Chem. Soc.* **1999**, *121*, 5089 – 5090; b) T. Izumi, H. Hashimoto, H. Yuasa, *Chem. Commun.* **2004**, 94 – 95.

[110] a) F. M. Menger, P. A. Chicklo, M. J. Sherrod, *Tetrahedron Lett.* **1989**, *30*, 6943 – 6946; b) S. M. Shirodkar, G. R. Weisman, *J. Chem. Soc. Chem. Commun.* **1989**, 236 – 238; c) M. Raban, D. L. Burch, E. R. Hortelano, D. Durocher, D. Kost, *J. Org. Chem.* **1994**, *59*, 1283 – 1287; d) M. Goodall, P. M. Kelly, D. Parker, K. Gloe, H. Stephan, *J. Chem. Soc. Perkin Trans. 2* **1997**, 59 – 69; e) V. A. Palyulin, S. V. Emets, V. A. Chertkov, C. Kasper, H.-J. Schneider, *Eur. J. Org. Chem.* **1999**, 3479 – 3482.

[111] a) D. S. Kemp, K. S. Petrakis, *J. Org. Chem.* **1981**, *46*, 5140 – 5143; b) V. V. Samoshin, V. A. Chertkov, L. P. Vatlina, E. K. Dobretsova, N. A. Simonov, L. P. Kastorsky, D. E. Gremyachinsky, H.-J. Schneider, *Tetrahedron Lett.* **1996**, *37*, 3981 – 3984; c) A. G. D. Santos, W. Klute, J. Torode, V. P. W. Bohm, E. Cabrita, J. Runsink, R. W. Hoffmann, *New J. Chem.* **1998**, *22*, 993 – 997.

[112] H. Yuasa, H. Hashimoto, *Trends Glycosci. Glycotechnol.* **2001**, *13*, 31 – 55.

[113] For a review of resorcinarenes, including their conformational dynamics, see: P. Timmerman, W. Verboom, D. N. Reinhoudt, *Tetrahedron* **1996**, *52*, 2663 – 2704.

[114] a) J. R. Moran, S. Karbach, D. J. Cram, *J. Am. Chem. Soc.* **1982**, *104*, 5826 – 5828; b) J. R. Moran, J. L. Ericson, E. Dalcanale, J. A. Bryant, C. B. Knobler, D. J. Cram, *J. Am. Chem. Soc.* **1991**, *113*, 5707 – 5714.

[115] a) P. J. Skinner, A. G. Cheetham, A. Beeby, V. Gramlich, F. Diederich, *Helv. Chim. Acta* **2001**, *84*, 2146 – 2153; b) V. A. Azov, F. Diederich, Y. Lill, B. Hecht, *Helv. Chim. Acta* **2003**, *86*, 2149 – 2155; c) V. A. Azov, B. Jaun, F. Diederich, *Helv. Chim. Acta* **2004**, *87*, 449 – 462.

[116] M. Frei, F. Marotti, F. Diederich, *Chem. Commun.* **2004**, 1362 – 1363.

[117] a) F. C. Tucci, D. M. Rudkevich, J. Rebek, Jr., *Chem. Eur. J.* **2000**, *6*, 1007 – 1016; b) T. Haino, D. M. Rudkevich, A. Shivanyuk, K. Rissanen, J. Rebek, Jr., *Chem. Eur. J.* **2000**, *6*, 3797 – 3805.

[118] a) D. M. Rudkevich, G. Hilmersson, J. Rebek, Jr., *J. Am. Chem. Soc.* **1997**, *119*, 9911 – 9912; b) D. M. Rudkevich, G. Hilmersson, J. Rebek, Jr., *J. Am. Chem. Soc.* **1998**, *120*, 12216 – 12225; c) S. H. Ma, D. M. Rudkevich, J. Rebek, Jr., *Angew. Chem.* **1999**, *111*, 2761 – 2764; *Angew. Chem. Int. Ed.* **1999**, *38*, 2600 – 2602.

[119] a) P. Amrhein, P. L. Wash, A. Shivanyuk, J. Rebek, Jr., *Org. Lett.* **2002**, *4*, 319 – 321; b) P. Amrhein, A. Shivanyuk, D. W. Johnson, J. Rebek, Jr., *J. Am. Chem. Soc.* **2002**, *124*, 10349 – 10358.

[120] a) C. D. Gutsche, *Calixarenes: Monographs in Supramolecular Chemistry, Vol. 1*, RSC, Cambridge, **1989**; b) *Calixarenes: A Versatile Class of Macrocyclic Compounds: Topics in Inclusion Science, Vol. 3* (Eds.: J. Vicens, V. Böhmer), Kluwer Academic, Dordrecht, **1991**.

[121] For reviews, see: a) A. Ikeda, S. Shinkai, *Chem. Rev.* **1997**, *97*, 1713 – 1734; b) S. Shinkai, A. Ikeda, *Pure Appl. Chem.* **1999**, *71*, 275 – 280.

[122] P. R. Ashton, R. Ballardini, V. Balzani, S. E. Boyd, A. Credi, M. T. Gandolfi, M. Gómez-López, S. Iqbal, D. Philp, J. A. Preece, L. Prodi, H. G. Ricketts, J. F. Stoddart, M. S. Tolley, M. Venturi, A. J. P. White, D. J. Williams, *Chem. Eur. J.* **1997**, *3*, 152 – 170.

[123] Similar conformational changes have been observed in a number of related analogues, see: a) P. R. Ashton, M. Gómez-López, S. Iqbal, J. A. Preece, J. F. Stoddart, *Tetrahedron Lett.* **1997**, *38*, 3635 – 3638; b) M. B. Nielsen, S. B. Nielsen, J. Becher, *Chem. Commun.* **1998**, 475 – 476; c) M. B. Nielsen, J. G. Hansen, J. Becher, *Eur. J. Org. Chem.* **1999**, 2807 – 2815; d) V. Balzani, P. Ceroni, A. Credi, M. Gómez-López, C. Hamers, J. F. Stoddart, R. Wolf, *New J. Chem.* **2001**, *25*, 25 – 31; e) Y. Liu, A. H. Flood, J. F. Stoddart, *J. Am. Chem. Soc.* **2004**, *126*, 9150 – 9151.

[124] See, for example: a) F. C. de Schryver, P. Collart, J. Vandendriessche, R. Goedeweeck, A. Swinnen, M. van der Auweraer, *Acc. Chem. Res.* **1987**, *20*, 159 – 166; b) H. Itagaki, W. Masuda, Y. Hirayanagi, *Chem. Phys. Lett.* **1999**, *309*, 402 – 406; c) H. Itagaki, W. Masuda, Y. Hirayanagi, S. Sugimoto, *J. Phys. Chem. B* **2002**, *106*, 3316 – 3322.

[125] See, for example: a) X. Y. Lauteslager, M. J. Bartels, J. J. Piet, J. M. Warman, J. W. Verhoeven, A. M. Brouwer, *Eur. J. Org. Chem.* **1998**, 2467 – 2481; b) X. Y. Lauteslager, I. H. M. van Stokkum, H. J. van Ramesdonk, A. M. Brouwer, J. W. Verhoeven, *J. Phys. Chem. A* **1999**, *103*, 653 – 659; c) T. D. M. Bell, K. A. Jolliffe, K. P. Ghiggino, A. M. Oliver, M. J. Shephard, S. J. Langford, M. N. Paddon-Row, *J. Am. Chem. Soc.* **2000**, *122*, 10661 – 10666; d) X. Y. Lauteslager, I. H. M. van Stokkum, H. J. van Ramesdonk, D. Bebelaar, J. Fraanje, K. Goubitz, H. Schenk, A. M. Brouwer, J. W. Verhoeven, *Eur. J. Org. Chem.* **2001**, 3105 – 3118.

[126] For reviews and highlights with general coverage, see: a) A. Williams, *Chem. Eur. J.* **1997**, *3*, 15 – 19; b) S. H. Gellman, *Acc. Chem. Res.* **1998**, *31*, 173 – 180; c) A. E. Rowan, R. J. M. Nolte, *Angew. Chem.* **1998**, *110*, 65 – 71; *Angew. Chem. Int. Ed.* **1998**, *37*, 63 – 68; d) M. S. Cubberley, B. L. Iverson, *Curr. Opin. Chem. Biol.* **2001**, *5*, 650 – 653; e) D. J. Hill, M. J. Mio, R. B. Prince, T. S. Hughes, J. S. Moore, *Chem. Rev.* **2001**, *101*, 3893 – 4011; f) C. Schmuck, *Angew. Chem.* **2003**, *115*, 2552 – 2556; *Angew. Chem. Int. Ed.* **2003**, *42*, 2448 – 2452; g) M. Albrecht, *Angew. Chem.* **2005**, *117*, 6606 – 6609; *Angew. Chem. Int. Ed.* **2005**, *44*, 6448 – 6451; on aromatic oligoamides: h) B. Gong, *Chem. Eur. J.* **2001**, *7*, 4336 – 4342; i) A. R. Sanford, K. Yamato, X. W. Yang, L. H. Yuan, Y. H. Han, B. Gong, *Eur. J. Biochem.* **2004**, *271*, 1416 – 1425; j) I. Huc, *Eur. J. Org. Chem.* **2004**, 17 – 29; on metal-templated helicates: k) E. C. Constable, *Tetrahedron* **1992**, *48*, 10013 – 10059; l) C. Piguet, G. Bernardinelli, G. Hopfgartner, *Chem. Rev.* **1997**, *97*, 2005 – 2062; m) M. Albrecht, *Chem. Rev.* **2001**, *101*, 3457 – 3497; on biomimetic foldamers, for example, β-peptides and peptide nucleic acid: n) D. Seebach, J. L. Matthews, *Chem. Commun.* **1997**, 2015 – 2022; o) P. E. Nielsen, G. Haaima, *Chem. Soc. Rev.* **1997**, *26*, 73 – 78; p) K. D. Stigers, M. J. Soth, J. S. Nowick, *Curr. Opin. Chem. Biol.* **1999**, *3*, 714 – 723; q) J. S. Nowick, *Acc. Chem. Res.* **1999**, *32*, 287 – 296; r) P. E. Nielsen, *Acc. Chem. Res.* **1999**, *32*, 624 – 630; s) K. Kirshenbaum, R. N. Zuckermann, K. A. Dill, *Curr. Opin. Struct. Biol.* **1999**, *9*, 530 – 535; t) P. Herdewijn, *Biochim. Biophys. Acta* **1999**, *1489*, 167 – 179; u) R. P. Cheng, S. H. Gellman, W. F. DeGrado, *Chem. Rev.* **2001**, *101*, 3219 – 3232; v) J. A. Patch, A. E. Barron, *Curr. Opin. Chem. Biol.* **2002**, *6*, 872 – 877; w) T. A. Martinek, F. Fülöp, *Eur. J. Biochem.* **2003**, *270*, 3657 – 3666; x) R. P. Cheng, *Curr. Opin. Struct. Biol.* **2004**, *14*, 512 – 520; y) G. Licini, L. J. Prins, P. Scrimin, *Eur. J. Org. Chem.* **2005**, 969 – 977.

[127] a) J. C. Nelson, J. G. Saven, J. S. Moore, P. G. Wolynes, *Science* **1997**, *277*, 1793 – 1796; b) R. B. Prince, J. G. Saven, P. G. Wolynes, J. S. Moore, *J. Am. Chem. Soc.* **1999**, *121*, 3114 – 3121; c) S. Lahiri, J. L. Thompson, J. S. Moore, *J. Am. Chem. Soc.* **2000**, *122*, 11315 – 11319; d) D. J. Hill, J. S. Moore, *Proc. Natl. Acad. Sci. USA* **2002**, *99*, 5053 – 5057; derivatization with suitable coordinating units allows metal ions to assist in the helix formation, see: e) R. B. Prince, T. Okada, J. S. Moore, *Angew. Chem.* **1999**, *111*, 245 – 249; *Angew. Chem. Int. Ed.* **1999**, *38*, 233 – 236.

[128] For solvent-induced switching of helical screw-sense in a chiral helical structure, see: A. L. Hofacker, J. R. Parquette, *Angew. Chem.* **2005**, *117*, 1077 – 1081; *Angew. Chem. Int. Ed.* **2005**, *44*, 1053 – 1057.

[129] a) V. Berl, I. Huc, R. G. Khoury, M. J. Krische, J.-M. Lehn, *Nature* **2000**, *407*, 720 – 723; b) V. Berl, I. Huc, R. G. Khoury, J.-M. Lehn, *Chem. Eur. J.* **2001**, *7*, 2798 – 2809; c) V. Berl, I. Huc, R. G. Khoury, J.-M. Lehn, *Chem. Eur. J.* **2001**, *7*, 2810 – 2820.

[130] C. Dolain, V. Maurizot, I. Huc, *Angew. Chem.* **2003**, *115*, 2844 – 2846; *Angew. Chem. Int. Ed.* **2003**, *42*, 2738 – 2740.

[131] E. Kolomiets, V. Berl, I. Odriozola, A. M. Stadler, N. Kyritsakas, J.-M. Lehn, *Chem. Commun.* **2003**, 2868 – 2869.

[132] D. Kanamori, T. A. Okamura, H. Yamamoto, N. Ueyama, *Angew. Chem.* **2005**, *117*, 991 – 994; *Angew. Chem. Int. Ed.* **2005**, *44*, 969 – 972.

[133] a) G. S. Hanan, J.-M. Lehn, N. Kyritsakas, J. Fischer, *J. Chem. Soc. Chem. Commun.* **1995**, 765 – 766; b) D. M. Bassani, J.-M. Lehn, G. Baum, D. Fenske, *Angew. Chem.* **1997**, *109*, 1931 – 1933; *Angew. Chem. Int. Ed. Engl.* **1997**, *36*, 1845 – 1847; c) M. Ohkita, J.-M. Lehn, G. Baum, D. Fenske, *Chem. Eur. J.* **1999**, *5*, 3471 – 3481.

[134] M. Barboiu, J.-M. Lehn, *Proc. Natl. Acad. Sci. USA* **2002**, *99*, 5201 – 5206.

[135] A. M. Stadler, N. Kyritsakas, J.-M. Lehn, *Chem. Commun.* **2004**, 2024 – 2025.

[136] M. Barboiu, G. Vaughan, N. Kyritsakas, J.-M. Lehn, *Chem. Eur. J.* **2003**, *9*, 763 – 769.

[137] A. Petitjean, R. G. Khoury, N. Kyritsakas, J.-M. Lehn, *J. Am. Chem. Soc.* **2004**, *126*, 6637 – 6647.

[138] F. Zhang, S. Bai, G. P. A. Yap, V. Tarwade, J. M. Fox, *J. Am. Chem. Soc.* **2005**, *127*, 10590 – 10599.

[139] a) R. B. Woodward, R. Hoffmann, *Angew. Chem.* **1969**, *81*, 797 – 869; *Angew. Chem. Int. Ed. Engl.* **1969**, *8*, 781 – 853; b) K. Fukui, *Acc. Chem. Res.* **1971**, *4*, 57 – 64; c) J. B. Hendrickson, *Angew. Chem.* **1974**, *86*, 71 – 100; *Angew. Chem. Int. Ed. Engl.* **1974**, *13*, 47 – 76; d) W. R. Dolbier, H. Koroniak, K. N. Houk, C. M. Sheu, *Acc. Chem. Res.* **1996**, *29*, 471 – 477.

[140] a) B. E. R. Schilling, R. Hoffmann, *J. Am. Chem. Soc.* **1978**, *100*, 6274 – 6274; b) B. E. R. Schilling, R. Hoffmann, *J. Am. Chem. Soc.* **1979**, *101*, 3456 – 3467; c) R. T. Edidin, J. R. Norton, K. Mislow, *Organometallics* **1982**, *1*, 561 – 562.

[141] H. Ushiyama, K. Takatsuka, *Angew. Chem.* **2005**, *117*, 1263 – 1266; *Angew. Chem. Int. Ed.* **2005**, *44*, 1237 – 1240.

[142] There are differences between the technical definition of the terms "configuration" and "conformation" and their common usage. While formally, configurational differences involve differences in bond angles and conformational differences suggest changes in torsion angles, here "configuration" is applied to *cis–trans* isomerism around double bonds as convention suggests. The same categorization can be extended to include isomerism around the C–N bond of amides, although this is often considered as a conformational change around a formal single bond. For further discussion, see Ref. [107]. The arrangement in space of the components of interlocked molecules and supramolecular complexes requires definition of another stereochemical term: "co-conformation". This refers to the relative positions of the noncovalently linked components with respect to each other, see: M. C. T. Fyfe, P. T. Glink, S. Menzer, J. F. Stoddart, A. J. P. White, D. J. Williams, *Angew. Chem.* **1997**, *109*, 2158 – 2160; *Angew. Chem. Int. Ed. Engl.* **1997**, *36*, 2068 – 2070.

[143] For a comprehensive review of isomerizations in both natural and synthetic systems, see: C. Dugave, L. Demange, *Chem. Rev.* **2003**, *103*, 2475 – 2532.

[144] a) D. H. Waldeck, *Chem. Rev.* **1991**, *91*, 415 – 436; b) H. Meier, *Angew. Chem.* **1992**, *104*, 1425 – 1446; *Angew. Chem. Int. Ed. Engl.* **1992**, *31*, 1399 – 1420; c) J. Saltiel, D. F. Sears, Jr., D.-H. Ko, K.-M. Park in *CRC Handbook of Organic Photochemistry and Photobiology* (Eds.: W. M. Horspool, P.-S. Song), CRC, Boca Raton, **1995**, pp. 3 – 15.

[145] A photochromic process is one in which a light-induced interconversion between two species results in a change in absorption spectrum.

[146] H. Suginome in *CRC Handbook of Organic Photochemistry and Photobiology* (Eds.: W. M. Horspool, P.-S. Song), CRC, Boca Raton, **1995**, pp. 824 – 840.

[147] a) M. Irie, *Pure Appl. Chem.* **1996**, *68*, 1367 – 1371; b) M. Irie, *Chem. Rev.* **2000**, *100*, 1685 – 1716.

[148] a) H. G. Heller in *CRC Handbook of Organic Photochemistry and Photobiology* (Eds.: W. M. Horspool, P.-S. Song), CRC, Boca Raton, **1995**, pp. 173 – 183; b) Y. Yokoyama, *Chem. Rev.* **2000**, *100*, 1717 – 1739; c) Y. Yokoyama in *Molecular Switches* (Ed.: B. L. Feringa), Wiley-VCH, Weinheim, **2001**, pp. 107 – 121.

[149] G. Berkovic, V. Krongauz, V. Weiss, *Chem. Rev.* **2000**, *100*, 1741 – 1753.

[150] a) B. L. Feringa, N. P. M. Huck, A. M. Schoevaars, *Adv. Mater.* **1996**, *8*, 681 – 684; b) B. L. Feringa, R. A. van Delden, N. Koumura, E. M. Geertsema, *Chem. Rev.* **2000**, *100*, 1789 – 1816; c) B. L. Feringa, R. A. van Delden, M. K. J. Ter Wiel in *Molecular Switches* (Ed.: B. L. Feringa), Wiley-VCH, Weinheim, **2001**, pp. 123 – 163.

[151] For reviews, see: a) B. L. Feringa, W. F. Jager, B. de Lange, *Tetrahedron* **1993**, *49*, 8267 – 8310; b) special issue on "Photochromism: Memories and Switches": *Chem. Rev.* **2000**, *100*, 1683 – 1890; c) *Molecular Switches* (Ed.: B. L. Feringa), Wiley-VCH, Weinheim, **2001**.

[152] a) G. Fischer, *Angew. Chem.* **1994**, *106*, 1479 – 1501; *Angew. Chem. Int. Ed. Engl.* **1994**, *33*, 1415 – 1436; b) G. Fischer, *Chem. Soc. Rev.* **2000**, *29*, 119 – 127; c) J. Balbach, F. X. Schmid in *Mechanisms of Protein Folding: Frontiers in Molecular Biology, Vol. 32* (Ed.: R. H. Pain), 2nd ed., Oxford University Press, Oxford, **2000**, pp. 212 – 249.

[153] C. Tie, J. C. Gallucci, J. R. Parquette, *J. Am. Chem. Soc.* **2006**, *128*, 1162 – 1171.

[154] For reviews, see: a) A. Momotake, T. Arai, *J. Photochem. Photobiol. C* **2004**, *5*, 1 – 25; b) A. Momotake, T. Arai, *Polymer* **2004**, *45*, 5369 – 5390.

[155] T. Muraoka, K. Kinbara, Y. Kobayashi, T. Aida, *J. Am. Chem. Soc.* **2003**, *125*, 5612 – 5613.

[156] Multiple azobenzene chromophores have previously been used to cause significant geometric changes in macrocyclic and macrobicyclic systems, see: a) S. Shinkai, Y. Honda, Y. Kusano, O. Manabe, *J. Chem. Soc. Chem. Commun.* **1982**, 848 – 850; b) M. Bauer, F. Vögtle, *Chem. Ber.* **1992**, *125*, 1675 – 1686.

[157] Y. Norikane, N. Tamaoki, *Org. Lett.* **2004**, *6*, 2595 – 2598.

[158] A. M. Schoevaars, W. Kruizinga, R. W. J. Zijlstra, N. Veldman, A. L. Spek, B. L. Feringa, *J. Org. Chem.* **1997**, *62*, 4943 – 4948.

[159] a) N. Harada, N. Koumura, B. L. Feringa, *J. Am. Chem. Soc.* **1997**, *119*, 7256 – 7264; b) N. Koumura, N. Harada, *Chem. Lett.* **1998**, 1151 – 1152.

[160] N. Koumura, R. W. J. Zijlstra, R. A. van Delden, N. Harada, B. L. Feringa, *Nature* **1999**, *401*, 152 – 155.

[161] For accounts on the development of the Feringa and Harada systems, see: a) B. L. Feringa, *Acc. Chem. Res.* **2001**, *34*, 504 – 513; b) B. L. Feringa, N. Koumura, R. A. van Delden, M. K. J. ter Wiel, *Appl. Phys. A* **2002**, *75*, 301 – 308; c) B. L. Feringa, R. A. van Delden, M. K. J. ter Wiel, *Pure Appl. Chem.* **2003**, *75*, 563 – 575.

[162] The more facile thermal helix inversion for *cis* isomers of this first generation series of overcrowded alkene molecular motors appears to be a general trend, see: a) N. Harada, A. Saito, N. Koumura, D. C. Roe, W. F. Jager, R. W. J. Zijlstra, B. de Lange, B. L. Feringa, *J. Am. Chem. Soc.* **1997**, *119*, 7249 – 7255; b) R. W. J. Zijlstra, W. F. Jager, B. de Lange, P. T. van Duijnen, B. L. Feringa, H. Goto, A. Saito, N. Koumura, N. Harada, *J. Org. Chem.* **1999**, *64*, 1667 – 1674.

[163] R. W. J. Zijlstra, P. T. van Duijnen, B. L. Feringa, T. Steffen, K. Duppen, D. A. Wiersma, *J. Phys. Chem. A* **1997**, *101*, 9828 – 9836.

[164] M. K. J. ter Wiel, R. A. van Delden, A. Meetsma, B. L. Feringa, *J. Am. Chem. Soc.* **2005**, *127*, 14208 – 14222.

[165] a) N. Koumura, E. M. Geertsema, A. Meetsma, B. L. Feringa, *J. Am. Chem. Soc.* **2000**, *122*, 12005 – 12006; b) N. Koumura, E. M. Geertsema, M. B. van Gelder, A. Meetsma, B. L. Feringa, *J. Am. Chem. Soc.* **2002**, *124*, 5037 – 5051; c) E. M. Geertsema, N. Koumura, M. K. J. ter Wiel, A. Meetsma, B. L. Feringa, *Chem. Commun.* **2002**, 2962 – 2963; d) R. A. van Delden, N. Koumura, A. Schoevaars, A. Meetsma, B. L. Feringa, *Org. Biomol. Chem.* **2003**, *1*, 33 – 35; e) D. Pijper, R. A. van Delden, A. Meetsma, B. L. Feringa, *J. Am. Chem. Soc.* **2005**, *127*, 17612 – 17613.

[166] a) M. K. J. ter Wiel, R. A. van Delden, A. Meetsma, B. L. Feringa, *J. Am. Chem. Soc.* **2003**, *125*, 15076 – 15086. Based on comparison of CD data with earlier analogues, the absolute stereochemistry of the single diastereomer of **50** produced in this report was originally assigned as (2*R*,2′*R*)-(*P*,*P*)-*trans*-**50**. A recent enantioselective synthesis and stereochemical study by X-ray crystallography, however, has shown that this assignment should be revised to (2*S*,2′*S*)-(*M*,*M*)-*trans*-**50**, see: b) T. Fujita, S. Kuwahara, N. Harada, *Eur. J. Org. Chem.* **2005**, 4533 – 4543; of course, this only affects the absolute sense of rotation of the two halves of the motor. Isolation and analysis of the unstable-*cis* isomer has been achieved, as has dectection of the unstable-*trans* form, thus indicating that rotation occurs through the same mechanism to the first and second generation systems, see: c) S. Kuwahara, T. Fujita, N. Harada, *Eur. J. Org. Chem.* **2005**, 4544 – 4556. In this third generation system, however, it appears that the unstable-*trans* form is more thermally labile than the unstable-*cis* form, in contrast to the first generation system (see Refs. [166a, 166c]).

[167] For **50**, it has recently been shown that the photostationary state ratios can be improved by more careful selection of irradiation wavelength, see Ref. [166c].

[168] M. K. J. ter Wiel, R. A. van Delden, A. Meetsma, B. L. Feringa, *Org. Biomol. Chem.* **2005**, *3*, 4071 – 4076.

[169] a) J.-M. Lehn, *Angew. Chem.* **1988**, *100*, 91 – 116; *Angew. Chem. Int. Ed. Engl.* **1988**, *27*, 89 – 112; b) D. J. Cram, *Angew. Chem.* **1988**, *100*, 1041 – 1052; *Angew. Chem. Int. Ed. Engl.* **1988**, *27*, 1009 – 1020; c) C. J. Pedersen, *Angew. Chem.* **1988**, *100*, 1053 – 1059; *Angew. Chem. Int. Ed. Engl.* **1988**, *27*, 1021 – 1027; d) J.-M. Lehn, *Supramolecular Chemistry: Concepts and Perspectives*, VCH, Weinheim, **1995**; e) *Comprehensive Supramolecular Chemistry* (Eds.: J.-M. Lehn, J. L. Atwood, J. E. D. Davies, D. D. MacNicol, F. Vögtle), Pergamon, Oxford, **1996**; f) special issue on "Molecular Recognition": *Chem. Rev.* **1997**, *97*, 1231 – 1734.

[170] Myosin requires an actin track to move along: a) S. M. Block, *Cell* **1996**, *87*, 151 – 157; while kinesin progresses along the pathway provided by microtubule filaments: b) S. M. Block, *Cell* **1998**, *93*, 5 – 8; even ion pumps operate through precisely defined structural channels: c) J. C. Skou, *Angew. Chem.* **1998**, *110*, 2452 – 2461; *Angew. Chem. Int. Ed.* **1998**, *37*, 2321 – 2328.

[171] S. Shinkai, T. Nakaji, T. Ogawa, K. Shigematsu, O. Manabe, *J. Am. Chem. Soc.* **1981**, *103*, 111 – 115.

[172] S. Shinkai, M. Ishihara, K. Ueda, O. Manabe, *J. Chem. Soc. Perkin Trans. 2* **1985**, 511 – 518.

[173] a) L. Fabbrizzi, M. Licchelli, P. Pallavicini, *Acc. Chem. Res.* **1999**, *32*, 846 – 853; b) V. Amendola, L. Fabbrizzi, C. Mangano, P. Pallavicini, *Acc. Chem. Res.* **2001**, *34*, 488 – 493; c) V. Amendola, L. Fabbrizzi, C. Mangano, P. Pallavicini, *Struct. Bonding (Berlin)* **2001**, *99*, 79 – 115.

[174] L. Fabbrizzi, F. Gatti, P. Pallavicini, E. Zambarbieri, *Chem. Eur. J.* **1999**, *5*, 682 – 690.

[175] A similar anion translocation process has also been achieved in a related trinuclear, multicomponent system, see: G. DeSantis,

L. Fabbrizzi, D. Iacopino, P. Pallavicini, A. Perotti, A. Poggi, *Inorg. Chem.* **1997**, *36*, 827 – 832.

[176] A. Ikeda, T. Tsudera, S. Shinkai, *J. Org. Chem.* **1997**, *62*, 3568 – 3574.

[177] L. Zelikovich, J. Libman, A. Shanzer, *Nature* **1995**, *374*, 790 – 792.

[178] Metal-ion translocation between two binding sites has been achieved in a number of other systems based either on switching the oxidation state of the metal or on the protonation state of the receptor, see: Refs. [173b, 173c] and a) E. Kimura, Y. Kurogi, T. Tojo, M. Shionoya, M. Shiro, *J. Am. Chem. Soc.* **1991**, *113*, 4857 – 4864; b) C. Belle, J. L. Pierre, E. Saint-Aman, *New J. Chem.* **1998**, *22*, 1399 – 1402; c) T. R. Ward, A. Lutz, S. P. Parel, J. Ensling, P. Gütlich, P. Buglyo, C. Orvig, *Inorg. Chem.* **1999**, *38*, 5007 – 5017; d) V. Amendola, L. Fabbrizzi, C. Mangano, P. Pallavicini, A. Perotti, A. Taglietti, *J. Chem. Soc. Dalton Trans.* **2000**, 185 – 189; e) D. Kalny, M. Elhabiri, T. Moav, A. Vaskevich, I. Rubinstein, A. Shanzer, A.-M. Albrecht-Gary, *Chem. Commun.* **2002**, 1426 – 1427; f) V. Amendola, L. Fabbrizzi, C. Mangano, H. Miller, P. Pallavicini, A. Perotti, A. Taglietti, *Angew. Chem.* **2002**, *114*, 2665 – 2668; *Angew. Chem. Int. Ed.* **2002**, *41*, 2553 – 2556; g) L. Fabbrizzi, F. Foti, S. Patroni, P. Pallavicini, A. Taglietti, *Angew. Chem.* **2004**, *116*, 5183 – 5187; *Angew. Chem. Int. Ed.* **2004**, *43*, 5073 – 5077.

[179] For representative examples of pseudorotaxane architectures based on polyether macrocycles bound to nitrogen-based cationic linear components, see: a) P. R. Ashton, P. J. Campbell, E. J. T. Chrystal, P. T. Glink, S. Menzer, D. Philp, N. Spencer, J. F. Stoddart, P. A. Tasker, D. J. Williams, *Angew. Chem.* **1995**, *107*, 1997 – 2001; *Angew. Chem. Int. Ed. Engl.* **1995**, *34*, 1865 – 1869; b) P. R. Ashton, E. J. T. Chrystal, P. T. Glink, S. Menzer, C. Schiavo, J. F. Stoddart, P. A. Tasker, D. J. Williams, *Angew. Chem.* **1995**, *107*, 2001 – 2004; *Angew. Chem. Int. Ed. Engl.* **1995**, *34*, 1869 – 1871; c) P. R. Ashton, E. J. T. Chrystal, P. T. Glink, S. Menzer, C. Schiavo, N. Spencer, J. F. Stoddart, P. A. Tasker, A. J. P. White, D. J. Williams, *Chem. Eur. J.* **1996**, *2*, 709 – 728; d) P. R. Ashton, M. C. T. Fyfe, P. T. Glink, S. Menzer, J. F. Stoddart, A. J. P. White, D. J. Williams, *J. Am. Chem. Soc.* **1997**, *119*, 12514 – 12524; e) S. J. Loeb, J. A. Wisner, *Angew. Chem.* **1998**, *110*, 3010 – 3013; *Angew. Chem. Int. Ed.* **1998**, *37*, 2838 – 2840; f) P. R. Ashton, I. Baxter, M. C. T. Fyfe, F. M. Raymo, N. Spencer, J. F. Stoddart, A. J. P. White, D. J. Williams, *J. Am. Chem. Soc.* **1998**, *120*, 2297 – 2307; g) P. R. Ashton, M. C. T. Fyfe, M.-V. Martínez-Díaz, S. Menzer, C. Schiavo, J. F. Stoddart, A. J. P. White, D. J. Williams, *Chem. Eur. J.* **1998**, *4*, 1523 – 1534; h) T. Clifford, A. Abushamleh, D. H. Busch, *Proc. Natl. Acad. Sci. USA* **2002**, *99*, 4830 – 4836; i) H. W. Gibson, N. Yamaguchi, J. W. Jones, *J. Am. Chem. Soc.* **2003**, *125*, 3522 – 3533; j) S. J. Loeb, J. Tiburcio, S. J. Vella, *Org. Lett.* **2005**, *7*, 4923 – 4926.

[180] For examples of pseudorotaxane architectures based on π-donor guest and π-acceptor cyclophane interactions, see: a) P. L. Anelli, P. R. Ashton, N. Spencer, A. M. Z. Slawin, J. F. Stoddart, D. J. Williams, *Angew. Chem.* **1991**, *103*, 1052 – 1054; *Angew. Chem. Int. Ed. Engl.* **1991**, *30*, 1036 – 1039; b) L. Grubert, D. Jacobi, K. Buck, W. Abraham, C. Mugge, E. Krause, *Eur. J. Org. Chem.* **2001**, 3921 – 3932; c) J. O. Jeppesen, J. Becher, J. F. Stoddart, *Org. Lett.* **2002**, *4*, 557 – 560; d) W. Abraham, L. Grubert, S. Schmidt-Schäffer, K. Buck, *Eur. J. Org. Chem.* **2005**, 374 – 386.

[181] For examples of other types of pseudorotaxane architectures, see: Refs. [50b,c,f,i] and a) A. Mirzoian, A. E. Kaifer, *Chem. Eur. J.* **1997**, *3*, 1052 – 1058; b) H. Yonemura, S. Kusano, T. Matsuo, S. Yamada, *Tetrahedron Lett.* **1998**, *39*, 6915 – 6918; c) K. Eliadou, K. Yannakopoulou, A. Rontoyianni, I. M. Mavridis, *J. Org. Chem.* **1999**, *64*, 6217 – 6226; d) K. M. Huh, T. Ooya, S. Sasaki, N. Yui, *Macromolecules* **2001**, *34*, 2402 – 2404; e) J. A. Wisner, P. D. Beer, M. G. B. Drew, *Angew. Chem.* **2001**, *113*, 3718 – 3721; *Angew. Chem. Int. Ed.* **2001**, *40*, 3606 – 3609; f) J. A. Wisner, P. D. Beer, N. G. Berry, B. Tomapatanaget, *Proc. Natl. Acad. Sci. USA* **2002**, *99*, 4983 – 4986; g) A. Arduini, F. Calzavacca, A. Pochini, A. Secchi, *Chem. Eur. J.* **2003**, *9*, 793 – 799; h) F. H. Huang, F. R. Fronczek, H. W. Gibson, *J. Am. Chem. Soc.* **2003**, *125*, 9272 – 9273; i) F. H. Huang, H. W. Gibson, W. S. Bryant, D. S. Nagvekar, F. R. Fronczek, *J. Am. Chem. Soc.* **2003**, *125*, 9367 – 9371; j) Y. Inoue, T. Kanbara, T. Yamamoto, *Tetrahedron Lett.* **2004**, *45*, 4603 – 4606; k) M. R. Sambrook, P. D. Beer, J. A. Wisner, R. L. Paul, A. R. Cowley, F. Szemes, M. G. B. Drew, *J. Am. Chem. Soc.* **2005**, *127*, 2292 – 2302; l) B. A. Blight, K. A. Van Noortwyk, J. A. Wisner, M. C. Jennings, *Angew. Chem.* **2005**, *117*, 1523 – 1528; *Angew. Chem. Int. Ed.* **2005**, *44*, 1499 – 1504; m) T. Kraus, M. Buděšínský, J. C. Cvaèka, J.-P. Sauvage, *Angew. Chem.* **2006**, *118*, 264 – 267; *Angew. Chem. Int. Ed.* **2006**, *45*, 258 – 261; n) M. V. Rekharsky, H. Yamamura, M. Kawai, I. Osaka, R. Arakawa, A. Sato, Y. H. Ko, N. Selvapalam, K. Kim, Y. Inoue, *Org. Lett.* **2006**, *8*, 815 – 818.

[182] The *IUPAC Compendium of Chemical Terminology* (A. D. McNaught, A. Wilkinson, 2nd ed., Blackwell Science, **1997**) defines rotaxanes as "molecules in which a ring encloses another, rod-like molecule having end groups too large to pass through the ring opening, and thus holds the rod-like molecule in position without covalent bonding.". This definition formally excludes threaded host–guest complexes (pseudorotaxanes).

[183] For a brief account of a number of such systems, see: V. Balzani, A. Credi, M. Venturi, *Proc. Natl. Acad. Sci. USA* **2002**, *99*, 4814 – 4817.

[184] a) R. Ballardini, V. Balzani, M. T. Gandolfi, L. Prodi, M. Venturi, D. Philp, H. G. Ricketts, J. F. Stoddart, *Angew. Chem.* **1993**, *105*, 1362 – 1364; *Angew. Chem. Int. Ed. Engl.* **1993**, *32*, 1301 – 1303; b) M. Montalti, R. Ballardini, L. Prodi, V. Balzani, *Chem. Commun.* **1996**, 2011 – 2012; c) R. Ballardini, V. Balzani, A. Credi, M. T. Gandolfi, S. J. Langford, S. Menzer, L. Prodi, J. F. Stoddart, M. Venturi, D. J. Williams, *Angew. Chem.* **1996**, *108*, 1056 – 1059; *Angew. Chem. Int. Ed. Engl.* **1996**, *35*, 978 – 981; d) M. Asakawa, P. R. Ashton, V. Balzani, A. Credi, G. Mattersteig, O. A. Matthews, M. Montalti, N. Spencer, J. F. Stoddart, M. Venturi, *Chem. Eur. J.* **1997**, *3*, 1992 – 1996; e) A. Credi, V. Balzani, S. J. Langford, J. F. Stoddart, *J. Am. Chem. Soc.* **1997**, *119*, 2679 – 2681; f) P. R. Ashton, R. Ballardini, V. Balzani, M. Gómez-López, S. E. Lawrence, M.-V. Martínez-Díaz, M. Montalti, A. Piersanti, L. Prodi, J. F. Stoddart, D. J. Williams, *J. Am. Chem. Soc.* **1997**, *119*, 10641 – 10651; g) W. Devonport, M. A. Blower, M. R. Bryce, L. M. Goldenberg, *J. Org. Chem.* **1997**, *62*, 885 – 887; h) M. Montalti, L. Prodi, *Chem. Commun.* **1998**, 1461 – 1462; i) O. A. Matthews, F. M. Raymo, J. F. Stoddart, A. J. P. White, D. J. Williams, *New J. Chem.* **1998**, *22*, 1131 – 1134; j) M. Asakawa, P. R. Ashton, V. Balzani, S. E. Boyd, A. Credi, G. Mattersteig, S. Menzer, M. Montalti, F. M. Raymo, C. Ruffilli, J. F. Stoddart, M. Venturi, D. J. Williams, *Eur. J. Org. Chem.* **1999**, 985 – 994; k) M. Asakawa, P. R. Ashton, V. Balzani, C. L. Brown, A. Credi, O. A. Matthews, S. P. Newton, F. M. Raymo, A. N. Shipway, N. Spencer, A. Quick, J. F. Stoddart, A. J. P. White, D. J. Williams, *Chem. Eur. J.* **1999**, *5*, 860 – 875; l) V. Balzani, A. Credi, G. Mattersteig, O. A. Matthews, F. M. Raymo, J. F. Stoddart, M. Venturi, A. J. P. White, D. J. Williams, *J. Org. Chem.* **2000**, *65*, 1924 – 1936; m) V. Balzani, J. Becher, A. Credi, M. B. Nielsen, F. M. Raymo, J. F. Stoddart, A. M. Talarico, M. Venturi, *J. Org. Chem.* **2000**, *65*, 1947 – 1956; n) V. Balzani, A. Credi, F. Marchioni, J. F. Stoddart, *Chem. Commun.* **2001**, 1860 – 1861; o) T. Fujimoto, A. Nakamura, Y. Inoue, Y. Sakata, T. Kaneda, *Tetrahedron Lett.* **2001**, *42*, 7987 – 7989; p) M. Horie, Y. Suzaki, K. Osakada, *J. Am. Chem. Soc.* **2004**, *126*, 3684 – 3685; q) A.

Credi, S. Dumas, S. Silvi, M. Venturi, A. Arduini, A. Pochini, A. Secchi, *J. Org. Chem.* **2004**, *69*, 5881 – 5887; r) K. J. Chang, Y. J. An, H. Uh, K. S. Jeong, *J. Org. Chem.* **2004**, *69*, 6556 – 6563; s) G. Kaiser, T. Jarrosson, S. Otto, Y. F. Ng, A. D. Bond, J. K. M. Sanders, *Angew. Chem.* **2004**, *116*, 1993 – 1996; *Angew. Chem. Int. Ed.* **2004**, *43*, 1959 – 1962; t) M. Venturi, S. Dumas, V. Balzani, J. G. Cao, J. F. Stoddart, *New J. Chem.* **2004**, *28*, 1032 – 1037; u) S. Nygaard, B. W. Laursen, A. H. Flood, C. N. Hansen, J. O. Jeppesen, J. F. Stoddart, *Chem. Commun.* **2006**, 144 – 146.

[185] a) M. Asakawa, S. Iqbal, J. F. Stoddart, N. D. Tinker, *Angew. Chem.* **1996**, *108*, 1053 – 1056; *Angew. Chem. Int. Ed. Engl.* **1996**, *35*, 976 – 978; b) A. Credi, M. Montalti, V. Balzani, S. J. Langford, F. M. Raymo, J. F. Stoddart, *New J. Chem.* **1998**, *22*, 1061 – 1065; c) P. R. Ashton, V. Balzani, J. Becher, A. Credi, M. C. T. Fyfe, G. Mattersteig, S. Menzer, M. B. Nielsen, F. M. Raymo, J. F. Stoddart, M. Venturi, D. J. Williams, *J. Am. Chem. Soc.* **1999**, *121*, 3951 – 3957.

[186] a) W. L. Mock, J. Pierpont, *J. Chem. Soc. Chem. Commun.* **1990**, 1509 – 1511; b) S. I. Jun, J. W. Lee, S. Sakamoto, K. Yamaguchi, K. Kim, *Tetrahedron Lett.* **2000**, *41*, 471 – 475; c) J. O. Jeppesen, S. A. Vignon, J. F. Stoddart, *Chem. Eur. J.* **2003**, *9*, 4611 – 4625.

[187] a) P. R. Ashton, V. Balzani, O. Kocian, L. Prodi, N. Spencer, J. F. Stoddart, *J. Am. Chem. Soc.* **1998**, *120*, 11 190 – 11 191; b) E. Ishow, A. Credi, V. Balzani, F. Spadola, L. Mandolini, *Chem. Eur. J.* **1999**, *5*, 984 – 989; c) R. Ballardini, V. Balzani, M. Clemente-Leon, A. Credi, M. T. Gandolfi, E. Ishow, J. Perkins, J. F. Stoddart, H.-R. Tseng, S. Wenger, *J. Am. Chem. Soc.* **2002**, *124*, 12 786 – 12 795.

[188] For examples of mechanical devices based on kinetically stable pseudorotaxane systems, see: a) J.-P. Collin, P. Gaviña, J.-P. Sauvage, *Chem. Commun.* **1996**, 2005 – 2006; b) J. W. Lee, K. P. Kim, K. Kim, *Chem. Commun.* **2001**, 1042 – 1043; c) W. S. Jeon, A. Y. Ziganshina, J. W. Lee, Y. H. Ko, J. K. Kang, C. Lee, K. Kim, *Angew. Chem.* **2003**, *115*, 4231 – 4234; *Angew. Chem. Int. Ed.* **2003**, *42*, 4097 – 4100; d) W. S. Jeon, E. Kim, Y. H. Ko, I. H. Hwang, J. W. Lee, S. Y. Kim, H. J. Kim, K. Kim, *Angew. Chem.* **2005**, *117*, 89 – 93; *Angew. Chem. Int. Ed.* **2005**, *44*, 87 – 91.

[189] a) G. Schill, *Catenanes, Rotaxanes and Knots*, Academic Press, New York, **1971**; b) D. M. Walba, *Tetrahedron* **1985**, *41*, 3161 – 3212; c) D. B. Amabilino, J. F. Stoddart, *Chem. Rev.* **1995**, *95*, 2725 – 2828; d) S. A. Nepogodiev, J. F. Stoddart, *Chem. Rev.* **1998**, *98*, 1959 – 1976; e) D. A. Leigh, A. Murphy, *Chem. Ind.* **1999**, 178 – 183; f) G. A. Breault, C. A. Hunter, P. C. Mayers, *Tetrahedron* **1999**, *55*, 5265 – 5293; g) *Molecular Catenanes Rotaxanes and Knots* (Eds.: J.-P. Sauvage, C. O. Dietrich-Buchecker), Wiley-VCH, Weinheim, **1999**.

[190] There are some examples of catenanes and rotaxanes constructed under thermodynamic control by using dynamic processes such as olefin metathesis or formation of an imine bond (see for example: R. L. E. Furlan, S. Otto, J. K. M. Sanders, *Proc. Natl. Acad. Sci. USA* **2002**, *99*, 4801 – 4804, and references therein). Such systems cannot act as molecular machines if they exchange components with the bulk quicker than the timescale of their stimuli-induced motion.

[191] For reviews on the development of interlocked molecules as molecular machines, see: Refs. [1c,h,m] and a) A. C. Benniston, *Chem. Soc. Rev.* **1996**, *25*, 427 – 435; b) M. Gómez-López, J. A. Preece, J. F. Stoddart, *Nanotechnology* **1996**, *7*, 183 – 192; c) V. Balzani, M. Gómez-López, J. F. Stoddart, *Acc. Chem. Res.* **1998**, *31*, 405 – 414; d) J.-P. Sauvage, *Acc. Chem. Res.* **1998**, *31*, 611 – 619; e) J.-C. Chambron, J.-P. Sauvage, *Chem. Eur. J.* **1998**, *4*, 1362 – 1366; f) J.-P. Collin, P. Gaviña, V. Heitz, J.-P. Sauvage, *Eur. J. Inorg. Chem.* **1998**, 1 – 14; g) M.-J. Blanco, M. C. Jiménez, J.-C. Chambron, V. Heitz, M. Linke, J.-P. Sauvage, *Chem. Soc. Rev.* **1999**, *28*, 293 – 305; h) A. R. Pease, J. O. Jeppesen, J. F. Stoddart, Y. Luo, C. P. Collier, J. R. Heath, *Acc. Chem. Res.* **2001**, *34*, 433 – 444; i) A. Harada, *Acc. Chem. Res.* **2001**, *34*, 456 – 464; j) C. A. Schalley, K. Beizai, F. Vögtle, *Acc. Chem. Res.* **2001**, *34*, 465 – 476; k) J.-P. Collin, C. Dietrich-Buchecker, P. Gaviña, M. C. Jimenez-Molero, J.-P. Sauvage, *Acc. Chem. Res.* **2001**, *34*, 477 – 487; l) L. Raehm, J.-P. Sauvage, *Struct. Bonding (Berlin)* **2001**, *99*, 55 – 78; m) R. Ballardini, V. Balzani, A. Credi, M. T. Gandolfi, M. Venturi, *Struct. Bonding (Berlin)* **2001**, *99*, 163 – 188; n) A. R. Pease, J. F. Stoddart, *Struct. Bonding (Berlin)* **2001**, *99*, 189 – 236; o) V. Balzani, A. Credi, *Chem. Rec.* **2001**, *1*, 422 – 435; p) F. M. Raymo, J. F. Stoddart in *Molecular Switches* (Ed.: B. L. Feringa), Wiley-VCH, Weinheim, **2001**, pp. 219 – 248; q) J.-P. Collin, J.-M. Kern, L. Raehm, J.-P. Sauvage in *Molecular Switches* (Ed.: B. L. Feringa), Wiley-VCH, Weinheim, **2001**, pp. 249 – 280; r) B. X. Colasson, C. Dietrich-Buchecker, M. C. Jimenez-Molero, J.-P. Sauvage, *J. Phys. Org. Chem.* **2002**, *15*, 476 – 483; s) V. Balzani, A. Credi, M. Venturi, *Pure Appl. Chem.* **2003**, *75*, 541 – 547; t) A. M. Brouwer, S. M. Fazio, C. Frochot, F. G. Gatti, D. A. Leigh, J. K. Y. Wong, G. W. H. Wurpel, *Pure Appl. Chem.* **2003**, *75*, 1055 – 1060; u) C. Dietrich-Buchecker, M. C. Jimenez-Molero, V. Sartor, J.-P. Sauvage, *Pure Appl. Chem.* **2003**, *75*, 1383 – 1393; v) M. C. Jimenez-Molero, C. Dietrich-Buchecker, J.-P. Sauvage, *Chem. Commun.* **2003**, 1613 – 1616; w) M. J. Gunter, *Eur. J. Org. Chem.* **2004**, 1655 – 1673; x) A. H. Flood, R. J. A. Ramirez, W.-Q. Deng, R. P. Muller, W. A. Goddard, J. F. Stoddart, *Aust. J. Chem.* **2004**, *57*, 301 – 322; y) P. M. Mendes, A. H. Flood, J. F. Stoddart, *Appl. Phys. A* **2005**, *80*, 1197 – 1209; z) J.-P. Sauvage, *Chem. Commun.* **2005**, 1507 – 1510; aa) J.-P. Collin, J.-P. Sauvage, *Chem. Lett.* **2005**, *34*, 742 – 747; ab) V. Balzani, A. Credi, B. Ferrer, S. Silvi, M. Venturi, *Top. Curr. Chem.* **2005**, *262*, 1 – 27; ac) J.-P. Collin, V. Heitz, J.-P. Sauvage, *Top. Curr. Chem.* **2005**, *262*, 29 – 62; ad) N. N. P. Moonen, A. H. Flood, J. M. Fernández, J. F. Stoddart, *Top. Curr. Chem.* **2005**, *262*, 99 – 132; ae) E. R. Kay, D. A. Leigh, *Top. Curr. Chem.* **2005**, *262*, 133 – 177; af) A. B. Braunschweig, B. H. Northrop, J. F. Stoddart, *J. Mater. Chem.* **2006**, *16*, 32 – 44.

[192] Numbers in square brackets preceding the names of interlocked compounds indicate the number of mechanically interlocked species, for example, a [2]rotaxane consists of a single macrocycle locked onto one thread; two macrocycles on one thread would constitute a [3]rotaxane.

[193] According to Prelog, the concept of a molecular catenane was discussed by Willstätters prior to 1912 (see Refs. [189a,b]). The first synthesis of a catenane (using statistical threading with no assisting template effects) was achieved by Wasserman in 1960: a) E. Wasserman, *J. Am. Chem. Soc.* **1960**, *82*, 4433 – 4434; proving the viability of such interlocked and otherwise topologically interesting molecules: b) H. L. Frisch, E. Wasserman, *J. Am. Chem. Soc.* **1961**, *83*, 3789 – 3795; the first directed synthesis of a catenane was reported by Schill and Lüttringhaus in 1964: c) G. Schill, A. Lüttringhaus, *Angew. Chem.* **1964**, *76*, 567 – 568; *Angew. Chem. Int. Ed. Engl.* **1964**, *3*, 546 – 547; the first rotaxane was synthesized (using statistical methods) by Harrison and Harrison in 1967: d) I. T. Harrison, S. Harrison, *J. Am. Chem. Soc.* **1967**, *89*, 5723 – 5724; e) I. T. Harrison, *J. Chem. Soc. Perkin Trans. 1* **1974**, 301 – 304.

[194] Another synthetic strategy, "slippage", theoretically provides a route to rotaxanes under thermodynamic control. However, the chemical assemblies prepared thus far by this route clearly do not satisfy the structural requirements of a rotaxane since the components can be separated from each other without breaking covalent bonds. Rather they are pseudorotaxanes—threaded host–guest complexes—which are (reasonably) kinetically stable at room temperature. The misclassification (see Ref. [182]) is not normally an issue because the physical behavior of kinetically stable pseudorotaxanes generally mir-

rors that of rotaxanes. However, it increasingly appears to be confusing nonspecialists into thinking that rotaxanes are supramolecular species or that pseudorotaxanes that are not kinetically stable can act as molecular machines. Slippage could be used as a strategy to form rotaxanes if the stabilization gained from the ring binding on the thread was sufficient to mean that covalent bond breaking is less energetically demanding than dethreading of the rings over the stoppers. However, to date no structures of this type have been reported.

[195] For general reviews on template synthesis, with particular regard to the development of methods for the assembly of mechanically interlocked species, see: Ref. [189] and a) C. O. Dietrich-Buchecker, J.-P. Sauvage, *Chem. Rev.* **1987**, *87*, 795–810; b) S. Anderson, H. L. Anderson, J. K. M. Sanders, *Acc. Chem. Res.* **1993**, *26*, 469–475; c) R. Hoss, F. Vögtle, *Angew. Chem.* **1994**, *106*, 389–398; *Angew. Chem. Int. Ed. Engl.* **1994**, *33*, 375–384; d) *Templated Organic Synthesis* (Eds.: F. Diederich, P. J. Stang), Wiley-VCH, Weinheim, **1999**; e) T. J. Hubin, D. H. Busch, *Coord. Chem. Rev.* **2000**, *200*, 5–52; for particular accounts on the synthesis of interlocked architectures with metals as templates and/or as part the framework, see: f) J.-P. Sauvage, *Acc. Chem. Res.* **1990**, *23*, 319–327; g) D. H. Busch, N. A. Stephenson, *Coord. Chem. Rev.* **1990**, *100*, 119–154; h) M. Fujita, K. Ogura, *Coord. Chem. Rev.* **1996**, *148*, 249–264; i) M. Fujita, *Acc. Chem. Res.* **1999**, *32*, 53–61; j) C. Dietrich-Buchecker, G. Rapenne, J.-P. Sauvage, *Coord. Chem. Rev.* **1999**, *185–186*, 167–176; k) J.-C. Chambron, J.-P. Collin, V. Heitz, D. Jouvenot, J.-M. Kern, P. Mobian, D. Pomeranc, J.-P. Sauvage, *Eur. J. Org. Chem.* **2004**, 1627–1638; l) S. J. Cantrill, K. S. Chichak, A. J. Peters, J. F. Stoddart, *Acc. Chem. Res.* **2005**, *38*, 1–9; see also: m) A.-M. Fuller, D. A. Leigh, P. J. Lusby, I. D. H. Oswald, S. Parsons, D. B. Walker, *Angew. Chem.* **2004**, *116*, 4004–4008; *Angew. Chem. Int. Ed.* **2004**, *43*, 3914–3918; for accounts focusing on the synthesis of interlocked molecules templated by a combination of hydrogen bonds and π–π interactions, see: n) D. Philp, J. F. Stoddart, *Synlett* **1991**, 445–458; o) J. F. Stoddart, *Chem. Br.* **1991**, *27*, 714–718; p) F. M. Raymo, J. F. Stoddart, *Pure Appl. Chem.* **1996**, *68*, 313–322; q) R. E. Gillard, F. M. Raymo, J. F. Stoddart, *Chem. Eur. J.* **1997**, *3*, 1933–1940; r) C. G. Claessens, J. F. Stoddart, *J. Phys. Org. Chem.* **1997**, *10*, 254–272; s) F. M. Raymo, J. F. Stoddart, *Chemtracts: Org. Chem.* **1998**, *11*, 491–511; t) P. T. Glink, J. F. Stoddart, *Pure Appl. Chem.* **1998**, *70*, 419–424 (the latter also contains a brief account of templated synthesis based on ammonium ion/crown ether hydrogen bonds); for accounts of amide-based hydrogen bond directed synthesis of interlocked architectures, see: u) R. Jäger, F. Vögtle, *Angew. Chem.* **1997**, *109*, 966–980; *Angew. Chem. Int. Ed. Engl.* **1997**, *36*, 930–944; v) A. G. Johnston, D. A. Leigh, R. J. Pritchard, M. D. Deegan, *Angew. Chem.* **1995**, *107*, 1324–1327; *Angew. Chem. Int. Ed. Engl.* **1995**, *34*, 1209–1212; w) A. G. Johnston, D. A. Leigh, L. Nezhat, J. P. Smart, M. D. Deegan, *Angew. Chem.* **1995**, *107*, 1327–1331; *Angew. Chem. Int. Ed. Engl.* **1995**, *34*, 1212–1216; x) A. G. Johnston, D. A. Leigh, A. Murphy, J. P. Smart, M. D. Deegan, *J. Am. Chem. Soc.* **1996**, *118*, 10662–10663; y) F. Biscarini, M. Cavallini, D. A. Leigh, S. León, S. J. Teat, J. K. Y. Wong, F. Zerbetto, *J. Am. Chem. Soc.* **2002**, *124*, 225–233; z) V. Aucagne, D. A. Leigh, J. S. Lock, A. R. Thomson, *J. Am. Chem. Soc.* **2006**, *128*, 1784–1785; for phenolate templates, see: aa) C. Seel, F. Vögtle, *Chem. Eur. J.* **2000**, *6*, 21–24; for a discussion of the template-directed construction of interlocked architectures under thermodynamic control, see Ref. [190] and ab) T. J. Kidd, D. A. Leigh, A. J. Wilson, *J. Am. Chem. Soc.* **1999**, *121*, 1599–1600; ac) D. A. Leigh, P. J. Lusby, S. J. Teat, A. J. Wilson, J. K. Y. Wong, *Angew. Chem.* **2001**, *113*, 1586–1591; *Angew. Chem. Int. Ed.* **2001**, *40*, 1538–1543; ad) J. S. Hannam, T. J. Kidd, D. A. Leigh, A. J. Wilson, *Org. Lett.* **2003**, *5*, 1907–1910; ae) L. Hogg, D. A. Leigh, P. J. Lusby, A. Morelli, S. Parsons, J. K. Y. Wong, *Angew. Chem.* **2004**, *116*, 1238–1241; *Angew. Chem. Int. Ed.* **2004**, *43*, 1218–1221; for a route to rotaxanes that only requires a catalytic amount of template, see: af) V. Aucagne, K. D. Hänni, D. A. Leigh, P. J. Lusby, D. B. Walker, *J. Am. Chem. Soc.* **2006**, *128*, 2186–2187.

[196] With the notable exception of the earliest statistically constructed [2]rotaxanes (see Refs. [193d,e]) and those assembled by covalent bond-directed synthesis (a) G. Schill, H. Zollenkopf, *Justus Liebigs Ann. Chem.* **1969**, *721*, 53–74; b) K. Hiratani, J. Suga, Y. Nagawa, H. Houjou, H. Tokuhisa, M. Numata, K. Watanabe, *Tetrahedron Lett.* **2002**, *43*, 5747–5750; c) N. Kameta, A. Hiratani, Y. Nagawa, *Chem. Commun.* **2004**, 466–467; d) Y. Nagawa, J. Suga, K. Hiratani, E. Koyama, M. Kanesato, *Chem. Commun.* **2005**, 749–751), there are few examples of rotaxanes without significant noncovalent recognition elements between macrocycle and thread; however, see: Ref. [195aa,af] and e) G. M. Hübner, J. Glaser, C. Seel, F. Vögtle, *Angew. Chem.* **1999**, *111*, 395–398; *Angew. Chem. Int. Ed.* **1999**, *38*, 383–386; f) C. Reuter, W. Wienand, G. M. Hübner, C. Seel, F. Vögtle, *Chem. Eur. J.* **1999**, *5*, 2692–2697; g) C. A. Schalley, G. Silva, C. F. Nising, P. Linnartz, *Helv. Chim. Acta* **2002**, *85*, 1578–1596; h) J. M. Mahoney, R. Shukla, R. A. Marshall, A. M. Beatty, J. Zajicek, B. D. Smith, *J. Org. Chem.* **2002**, *67*, 1436–1440; i) X. Y. Li, J. Illigen, M. Nieger, S. Michel, C. A. Schalley, *Chem. Eur. J.* **2003**, *9*, 1332–1347; j) J. S. Hannam, S. M. Lacy, D. A. Leigh, C. G. Saiz, A. M. Z. Slawin, S. G. Stitchell, *Angew. Chem.* **2004**, *116*, 3322–3326; *Angew. Chem. Int. Ed.* **2004**, *43*, 3260–3264.

[197] P. L. Anelli, N. Spencer, J. F. Stoddart, *J. Am. Chem. Soc.* **1991**, *113*, 5131–5133.

[198] a) P. R. Ashton, D. Philp, N. Spencer, J. F. Stoddart, *J. Chem. Soc. Chem. Commun.* **1992**, 1124–1128; b) P. R. Ashton, M. R. Johnston, J. F. Stoddart, M. S. Tolley, J. W. Wheeler, *J. Chem. Soc. Chem. Commun.* **1992**, 1128–1131.

[199] A. S. Lane, D. A. Leigh, A. Murphy, *J. Am. Chem. Soc.* **1997**, *119*, 11092–11093.

[200] D. A. Leigh, A. Murphy, J. P. Smart, A. M. Z. Slawin, *Angew. Chem.* **1997**, *109*, 752–756; *Angew. Chem. Int. Ed. Engl.* **1997**, *36*, 728–732.

[201] The rate of submolecular motion in the analogous benzylic amide catenanes exhibits similar solvent effects, see: a) D. A. Leigh, A. Murphy, J. P. Smart, M. S. Deleuze, F. Zerbetto, *J. Am. Chem. Soc.* **1998**, *120*, 6458–6467; b) M. S. Deleuze, D. A. Leigh, F. Zerbetto, *J. Am. Chem. Soc.* **1999**, *121*, 2364–2379; c) D. A. Leigh, A. Troisi, F. Zerbetto, *Chem. Eur. J.* **2001**, *7*, 1450–1454.

[202] P. Ghosh, G. Federwisch, M. Kogej, C. A. Schalley, D. Haase, W. Saak, A. Lützen, R. M. Gschwind, *Org. Biomol. Chem.* **2005**, *3*, 2691–2700.

[203] Cleavage of covalent bonds, in the form of acid-mediated *N*-butyloxycarbamate cleavage to reveal an ammonium binding site has been used to initiate degenerate shuttling, see: J. G. Cao, M. C. T. Fyfe, J. F. Stoddart, G. R. L. Cousins, P. T. Glink, *J. Org. Chem.* **2000**, *65*, 1937–1946.

[204] a) L. S. Jiang, J. Okano, A. Orita, J. Otera, *Angew. Chem.* **2004**, *116*, 2173–2176; *Angew. Chem. Int. Ed.* **2004**, *43*, 2121–2124; b) for another system in which either metal coordination or organic substrate binding blocks the shuttling of the macrocycle in a [2]rotaxane, see D. A. Leigh, P. J. Lusby, A. M. Z. Slawin, D. B. Walker, *Angew. Chem.* **2005**, *117*, 4633–4640; *Angew. Chem. Int. Ed.* **2005**, *44*, 4557–4564.

[205] D. A. Leigh, A. Troisi, F. Zerbetto, *Angew. Chem.* **2000**, *112*, 358–361; *Angew. Chem. Int. Ed.* **2000**, *39*, 350–353.

[206] Even in 1991, when reporting the first degenerate molecular shuttle,[197] Stoddart noted that: "The opportunity now exists to desymmetrize the molecular shuttle by inserting nonidentical

'stations' along the polyether 'thread' in such a manner that these different 'stations' can be addressed selectively by chemical, electrochemical, or photochemical means and so provide a mechanism to drive the 'bead' to and fro between 'stations' along the 'thread'.".

[207] a) A. C. Benniston, A. Harriman, *Angew. Chem.* **1993**, *105*, 1553 – 1555; *Angew. Chem. Int. Ed. Engl.* **1993**, *32*, 1459 – 1461; b) A. C. Benniston, A. Harriman, V. M. Lynch, *Tetrahedron Lett.* **1994**, *35*, 1473 – 1476; c) A. C. Benniston, A. Harriman, V. M. Lynch, *J. Am. Chem. Soc.* **1995**, *117*, 5275 – 5291.

[208] W. Clegg, C. Gimenez-Saiz, D. A. Leigh, A. Murphy, A. M. Z. Slawin, S. J. Teat, *J. Am. Chem. Soc.* **1999**, *121*, 4124 – 4129.

[209] M. Asakawa, G. Brancato, M. Fanti, D. A. Leigh, T. Shimizu, A. M. Z. Slawin, J. K. Y. Wong, F. Zerbetto, S. W. Zhang, *J. Am. Chem. Soc.* **2002**, *124*, 2939 – 2950.

[210] a) H. Murakami, A. Kawabuchi, K. Kotoo, M. Kunitake, N. Nakashima, *J. Am. Chem. Soc.* **1997**, *119*, 7605 – 7606; b) H. Murakami, A. Kawabuchi, R. Matsumoto, T. Ido, N. Nakashima, *J. Am. Chem. Soc.* **2005**, *127*, 15891 – 15899.

[211] C. A. Stanier, S. J. Alderman, T. D. W. Claridge, H. L. Anderson, *Angew. Chem.* **2002**, *114*, 1847 – 1850; *Angew. Chem. Int. Ed.* **2002**, *41*, 1769 – 1772.

[212] Intriguingly, insertion of an alkyl spacer beyond the viologen units restores the ability to undergo $E \rightarrow Z$ photoisomerization, concomitant with shuttling of the ring to this remote site (see Ref [210b]). Shuttling back to the central unit does not occur immediately on re-isomerization back to the *E* isomer, on account of the large kinetic barrier for passage over the viologen unit. It may be appropriate to regard this analogue, and therefore indeed **66**, as two-station shuttles. However, any favorable interactions with the alkyl "stations" in either case are rather weak and poorly defined.

[213] A molecular mechanics study of **66** yielded results consistent with the experimental observations for this shuttle. Although no comment is made of it, the optimized *Z*-**66** co-conformation has the wider 3-rim of the α-CD closest to the azobenzene unit, in contrast to the experimental findings for **67**, see: K. Sohlberg, B. G. Sumpter, D. W. Noid, *J. Mol. Struct.* **1999**, *491*, 281 – 286.

[214] For examples with cyclodextrin macrocycles, see Ref. [50]. Similar effects have been observed when forming either pseudorotaxanes or rotaxanes by threading though the cavity in calixarenes, see: Ref. [181g] and A. Arduini, F. Ciesa, M. Fragassi, A. Pochini, A. Secchi, *Angew. Chem.* **2005**, *117*, 282 – 285; *Angew. Chem. Int. Ed.* **2005**, *44*, 278 – 281.

[215] Providing the chemical reaction is fast with respect to the movement of the macrocycle.

[216] R. A. Bissell, E. Córdova, A. E. Kaifer, J. F. Stoddart, *Nature* **1994**, *369*, 133 – 137.

[217] The subsequent proliferation of molecular machines based on $CBPQT^{4+}$ recognition has inspired a number of computational studies on complexation by this species, see: a) R. Castro, M. J. Berardi, E. Córdova, M. O. de Olza, A. E. Kaifer, J. D. Evanseck, *J. Am. Chem. Soc.* **1996**, *118*, 10257 – 10268; b) R. Castro, K. R. Nixon, J. D. Evanseck, A. E. Kaifer, *J. Org. Chem.* **1996**, *61*, 7298 – 7303; c) R. Castro, P. D. Davidov, K. A. Kumar, A. P. Marchand, J. D. Evanseck, A. E. Kaifer, *J. Phys. Org. Chem.* **1997**, *10*, 369 – 382; d) G. A. Kaminski, W. L. Jorgensen, *J. Chem. Soc. Perkin Trans. 2* **1999**, 2365 – 2375; e) A. T. Macias, K. A. Kumar, A. P. Marchand, J. D. Evanseck, *J. Org. Chem.* **2000**, *65*, 2083 – 2089; f) G. Ercolani, P. Mencarelli, *J. Org. Chem.* **2003**, *68*, 6470 – 6473; g) K. C. Zhang, L. Liu, T. W. Mu, Q. X. Guo, *Chem. Phys. Lett.* **2001**, *333*, 195 – 198; h) X. Grabuleda, P. Ivanov, C. Jaime, *J. Org. Chem.* **2003**, *68*, 1539 – 1547; these, in turn, have provoked the development of computational methods by which the related bistable shuttles themselves can be studied. Particular issues highlighted from this work are the importance of solvent interactions and thread folding in determining the preferred co-conformation; see: i) X. Grabuleda, C. Jaime, *J. Org. Chem.* **1998**, *63*, 9635 – 9643; j) X. Grabuleda, P. Ivanov, C. Jaime, *J. Phys. Chem. B* **2003**, *107*, 7582 – 7588.

[218] See: Ref. [179] and a) A. G. Kolchinski, D. H. Busch, N. W. Alcock, *J. Chem. Soc. Chem. Commun.* **1995**, 1289 – 1291; b) P. T. Glink, C. Schiavo, J. F. Stoddart, D. J. Williams, *Chem. Commun.* **1996**, 1483 – 1490; c) P. R. Ashton, P. T. Glink, J. F. Stoddart, P. A. Tasker, A. J. P. White, D. J. Williams, *Chem. Eur. J.* **1996**, *2*, 729 – 736; d) S. J. Cantrill, A. R. Pease, J. F. Stoddart, *J. Chem. Soc. Dalton Trans.* **2000**, 3715 – 3734.

[219] a) M.-V. Martínez-Díaz, N. Spencer, J. F. Stoddart, *Angew. Chem.* **1997**, *109*, 1991 – 1994; *Angew. Chem. Int. Ed. Engl.* **1997**, *36*, 1904 – 1907; b) P. R. Ashton, R. Ballardini, V. Balzani, I. Baxter, A. Credi, M. C. T. Fyfe, M. T. Gandolfi, M. Gómez-López, M.-V. Martínez-Díaz, A. Piersanti, N. Spencer, J. F. Stoddart, M. Venturi, A. J. P. White, D. J. Williams, *J. Am. Chem. Soc.* **1998**, *120*, 11932 – 11942; c) S. Garaudée, S. Silvi, M. Venturi, A. Credi, A. H. Flood, J. F. Stoddart, *ChemPhysChem* **2005**, *6*, 2145 – 2152.

[220] Terms such as "all-or-nothing" or "quantitative" are inappropriate descriptors for an equilibrium.

[221] Molecular mechanics calculations on both forms of this system are in agreement with these experimental results, see: L. Frankfort, K. Sohlberg, *J. Mol. Struct.* **2003**, *621*, 253 – 260.

[222] For an example of another pH-switched shuttle from the Stoddart group, see: A. M. Elizarov, S.-H. Chiu, J. F. Stoddart, *J. Org. Chem.* **2002**, *67*, 9175 – 9181.

[223] a) J. D. Badjić, V. Balzani, A. Credi, S. Silvi, J. F. Stoddart, *Science* **2004**, *303*, 1845 – 1849; b) J. D. Badjić, C. M. Ronconi, J. F. Stoddart, V. Balzani, S. Silvi, A. Credi, *J. Am. Chem. Soc.* **2006**, *128*, 1489 – 1499.

[224] C. M. Keaveney, D. A. Leigh, *Angew. Chem.* **2004**, *116*, 1242 – 1244; *Angew. Chem. Int. Ed.* **2004**, *43*, 1222 – 1224.

[225] a) P. R. Ashton, R. A. Bissell, N. Spencer, J. F. Stoddart, M. S. Tolley, *Synlett* **1992**, 914 – 918; b) P. R. Ashton, R. A. Bissell, R. Gorski, D. Philp, N. Spencer, J. F. Stoddart, M. S. Tolley, *Synlett* **1992**, 919 – 922; c) P. R. Ashton, R. A. Bissell, N. Spencer, J. F. Stoddart, M. S. Tolley, *Synlett* **1992**, 923 – 926; d) P. L. Anelli, M. Asakawa, P. R. Ashton, R. A. Bissell, G. Clavier, R. Gorski, A. E. Kaifer, S. J. Langford, G. Mattersteig, S. Menzer, D. Philp, A. M. Z. Slawin, N. Spencer, J. F. Stoddart, M. S. Tolley, D. J. Williams, *Chem. Eur. J.* **1997**, *3*, 1113 – 1135; e) D. B. Amabilino, P. R. Ashton, S. E. Boyd, M. Gómez-López, W. Hayes, J. F. Stoddart, *J. Org. Chem.* **1997**, *62*, 3062 – 3075.

[226] Shuttle **69** also shows a certain degree of electrochemical switching in the deprotonated state when electrochemical reduction of the bipyridinium unit causes movement of the macrocycle back towards the amine moiety. In this state however, the electron-rich macrocycle has no significant favorable interactions with the thread and its position is not well-defined, see Ref. [219a].

[227] H.-R. Tseng, S. A. Vignon, J. F. Stoddart, *Angew. Chem.* **2003**, *115*, 1529 – 1533; *Angew. Chem. Int. Ed.* **2003**, *42*, 1491 – 1495.

[228] a) M. Asakawa, P. R. Ashton, V. Balzani, A. Credi, C. Hamers, G. Mattersteig, M. Montalti, A. N. Shipway, N. Spencer, J. F. Stoddart, M. S. Tolley, M. Venturi, A. J. P. White, D. J. Williams, *Angew. Chem.* **1998**, *110*, 357 – 361; *Angew. Chem. Int. Ed.* **1998**, *37*, 333 – 337; b) J. O. Jeppesen, J. Perkins, J. Becher, J. F. Stoddart, *Angew. Chem.* **2001**, *113*, 1256 – 1261; *Angew. Chem. Int. Ed.* **2001**, *40*, 1216 – 1221; c) J. O. Jeppesen, K. A. Nielsen, J. Perkins, S. A. Vignon, A. Di Fabio, R. Ballardini, M. T. Gandolfi, M. Venturi, V. Balzani, J. Becher, J. F. Stoddart, *Chem. Eur. J.* **2003**, *9*, 2982 – 3007; d) H.-R. Tseng, S. A. Vignon, P. C. Celestre, J. Perkins, J. O. Jeppesen, A. Di Fabio, R. Ballardini, M. T. Gandolfi, M. Venturi, V. Balzani, J. F. Stoddart, *Chem. Eur. J.* **2004**, *10*, 155 – 172; e) S. S. Kang, S. A.

Vignon, H.-R. Tseng, J. F. Stoddart, *Chem. Eur. J.* **2004**, *10*, 2555 – 2564; f) A. H. Flood, A. J. Peters, S. A. Vignon, D. W. Steuerman, H.-R. Tseng, S. Kang, J. R. Heath, J. F. Stoddart, *Chem. Eur. J.* **2004**, *10*, 6558 – 6564; g) B. W. Laursen, S. Nygaard, J. O. Jeppesen, J. F. Stoddart, *Org. Lett.* **2004**, *6*, 4167 – 4170; h) J. O. Jeppesen, S. Nygaard, S. A. Vignon, J. F. Stoddart, *Eur. J. Org. Chem.* **2005**, 196 – 220; i) J. W. Choi, A. H. Flood, D. W. Steuerman, S. Nygaard, A. B. Braunschweig, N. N. P. Moonen, B. W. Laursen, Y. Luo, E. DeIonno, A. J. Peters, J. O. Jeppesen, K. Xu, J. F. Stoddart, J. R. Heath, *Chem. Eur. J.* **2006**, *12*, 261 – 279. For a review of the development of these systems, see Ref. [191ad].

[229] a) A. M. Brouwer, C. Frochot, F. G. Gatti, D. A. Leigh, L. Mottier, F. Paolucci, S. Roffia, G. W. H. Wurpel, *Science* **2001**, *291*, 2124 – 2128; b) A. Altieri, F. G. Gatti, E. R. Kay, D. A. Leigh, D. Martel, F. Paolucci, A. M. Z. Slawin, J. K. Y. Wong, *J. Am. Chem. Soc.* **2003**, *125*, 8644 – 8654.

[230] For an independent computational study of this system which shows excellent agreement with the experimental results, see: X. G. Zheng, K. Sohlberg, *J. Phys. Chem. A* **2003**, *107*, 1207 – 1215.

[231] N. Armaroli, V. Balzani, J.-P. Collin, P. Gaviña, J.-P. Sauvage, B. Ventura, *J. Am. Chem. Soc.* **1999**, *121*, 4397 – 4408.

[232] For other examples of electrochemically switched shuttles, see: a) R. Ballardini, V. Balzani, W. Dehaen, A. E. Dell'Erba, F. M. Raymo, J. F. Stoddart, M. Venturi, *Eur. J. Org. Chem.* **2000**, 591 – 602; b) P. R. Ashton, R. Ballardini, V. Balzani, A. Credi, K. R. Dress, E. Ishow, C. J. Kleverlaan, O. Kocian, J. A. Preece, N. Spencer, J. F. Stoddart, M. Venturi, S. Wenger, *Chem. Eur. J.* **2000**, *6*, 3558 – 3574 (for an example of light- and electrochemically triggered shuttling, see also Section 4.3.8); c) N. Kihara, M. Hashimoto, T. Takata, *Org. Lett.* **2004**, *6*, 1693 – 1696.

[233] a) S. A. Vignon, T. Jarrosson, T. Iijima, H.-R. Tseng, J. K. M. Sanders, J. F. Stoddart, *J. Am. Chem. Soc.* **2004**, *126*, 9884 – 9885; b) T. Iijima, S. A. Vignon, H.-R. Tseng, T. Jarrosson, J. K. M. Sanders, F. Marchioni, M. Venturi, E. Apostoli, V. Balzani, J. F. Stoddart, *Chem. Eur. J.* **2004**, *10*, 6375 – 6392.

[234] D. S. Marlin, D. González Cabrera, D. A. Leigh, A. M. Z. Slawin, *Angew. Chem.* **2006**, *118*, 83 – 89; *Angew. Chem. Int. Ed.* **2006**, *45*, 77 – 83.

[235] D. S. Marlin, D. González Cabrera, D. A. Leigh, A. M. Z. Slawin, *Angew. Chem.* **2006**, *118*, 1413 – 1418; *Angew. Chem. Int. Ed.* **2006**, *45*, 1385 – 1390.

[236] The binding of Cd^{II} ions to the BPA-glycine carbonyl oxygen atom lowers the pK_a value of the adjacent NH proton, thus allowing selective deprotonation at this site. Model studies also show that deprotonation cannot occur while the macrocycle resides on the glycylglycine station and so the reaction must only occur in the minor translational isomer; once again, it is important to remember that the co-conformations in a simple [2]rotaxane are always in equilibrium.

[237] D. A. Leigh, E. M. Pérez, *Chem. Commun.* **2004**, 2262 – 2263.

[238] W. Abraham, L. Grubert, U. W. Grummt, K. Buck, *Chem. Eur. J.* **2004**, *10*, 3562 – 3568.

[239] S. Schmidt-Schäffer, L. Grubert, U. W. Grummt, K. Buck, W. Abraham, *Eur. J. Org. Chem.* **2006**, 378 – 398.

[240] A. Altieri, G. Bottari, F. Dehez, D. A. Leigh, J. K. Y. Wong, F. Zerbetto, *Angew. Chem.* **2003**, *115*, 2398 – 2402; *Angew. Chem. Int. Ed.* **2003**, *42*, 2296 – 2300.

[241] F. G. Gatti, D. A. Leigh, S. A. Nepogodiev, A. M. Z. Slawin, S. J. Teat, J. K. Y. Wong, *J. Am. Chem. Soc.* **2001**, *123*, 5983 – 5989.

[242] V. Balzani, M. Clemente-León, A. Credi, B. Ferrer, M. Venturi, A. H. Flood, J. F. Stoddart, *Proc. Natl. Acad. Sci. USA* **2006**, *103*, 1178 – 1183. Similar to **73**, shuttling in [2]rotaxane **81** can also be triggered by using an external source of electrons in an electrochemical cell.

[243] G. W. H. Wurpel, A. M. Brouwer, I. H. M. van Stokkum, A. Farran, D. A. Leigh, *J. Am. Chem. Soc.* **2001**, *123*, 11327 – 11328.

[244] Heat has been used to bring about *cis*→*trans* isomerization in **80** that results in a concomitant net change of the position of the ring (see Ref. [240]), while a temperature increase has also been used to overcome a significant kinetic barrier to shuttling following a chemical change in a kinetically stable pseudorotaxane (see Ref. [188b]). In neither of these cases is the process reversible on cooling the material without some other stimulus being applied. In a number of the π-donor-/π-acceptor-based molecular shuttles the population distribution can exhibit a certain degree of temperature sensitivity. This can occur when a large difference exists in the enthalpy of binding at each station and/or because of the formation of "alongside" interactions between the unoccupied electron-rich station and the outer surface of the positively charged macrocycle, which incurs entropic losses and enthalpic gains. See, for example, Refs. [191ad, 228b,c,h,i].

[245] G. Bottari, F. Dehez, D. A. Leigh, P. J. Nash, E. M. Pérez, J. K. Y. Wong, F. Zerbetto, *Angew. Chem.* **2003**, *115*, 6066 – 6069; *Angew. Chem. Int. Ed.* **2003**, *42*, 5886 – 5889.

[246] A C_{12} chain has more than 500000 (3^{12}) possible C–C rotamers and a significant number of these degrees of freedom must be lost upon forming the **83** structure.

[247] A series of theoretical designs for entropy-driven mechanical motion in mechanically interlocked molecules have been suggested, see: A. Hanke, R. Metzler, *Chem. Phys. Lett.* **2002**, *359*, 22 – 26.

[248] There are some clear limitations in using temperature as an entropy-driven switching mechanism: for example, it would be very difficult to address a small region of a larger array of shuttles in this way.

[249] T. Da Ros, D. M. Guldi, A. F. Morales, D. A. Leigh, M. Prato, R. Turco, *Org. Lett.* **2003**, *5*, 689 – 691.

[250] a) C. G. Gong, H. W. Gibson, *Angew. Chem.* **1997**, *109*, 2426 – 2428; *Angew. Chem. Int. Ed. Engl.* **1997**, *36*, 2331 – 2333; b) C. G. Gong, T. E. Glass, H. W. Gibson, *Macromolecules* **1998**, *31*, 308 – 313.

[251] If it did, this would correspond to a type of information ratchet mechanism (see Section 1.4.2).

[252] Molecular-scale logic systems which, in the main, do not rely on mechanical motions, and which operate through combinational logic processes, have been created. For reviews, see: a) P. Ball, *Nature* **2000**, *406*, 118 – 120; b) A. P. de Silva, N. D. McClenaghan, C. P. McCoy in *Molecular Switches* (Ed.: B. L. Feringa), Wiley-VCH, Weinheim, **2001**, pp. 339 – 361; c) F. M. Raymo, *Adv. Mater.* **2002**, *14*, 401 – 414; d) G. J. Brown, A. P. de Silva, S. Pagliari, *Chem. Commun.* **2002**, 2461 – 2463; e) V. Balzani, A. Credi, M. Venturi, *ChemPhysChem* **2003**, *4*, 49 – 59; f) A. P. de Silva, N. D. McClenaghan, *Chem. Eur. J.* **2004**, *10*, 574 – 586.

[253] a) A. P. Malvino, J. A. Brown, *Digital Computer Electronics*, 3rd ed., Glencoe, Lake Forest, **1993**; b) R. J. Mitchell, *Microprocessor Systems: An introduction*, Macmillan, London, **1995**.

[254] A series of stimuli-responsive molecular shuttles have been shown to exhibit relatively long-lived non-equilibrium ("metastable") states when operating in self-assembled monolayers, a polymer electrolyte, or at low temperatures (see Refs. [191ad, 228f,i] and Sections 8.1 and 8.3). This may account for the junction hysteresis observed in solid-state electronic devices that utilize such rotaxanes (see Section 8.3.1). Kinetically stable non-equilibrium co-conformations have also been observed in a cyclodextrin-based shuttle, see Ref. [210b].

[255] The term "Brownian motor", in the form of the German "Brownsche Motoren", was introduced by Bartussek and Hänggi (R. Bartussek, P. Hänggi, *Phys. Bl.* **1995**, *51*, 506 – 507) to describe load-bearing thermal ratchets and is also

widely used in molecular biology. We have tried to place the term in a chemical context which is consistent with its meaning in biology and physics.

[256] In principle, directional rotation of the macrocycle in a rotaxane could be induced by using rapid thermal fluctuations (or similar) and a chiral rotaxane (such as those in G. Brancato, F. Coutrot, D. A. Leigh, A. Murphy, J. K. Y. Wong, F. Zerbetto, *Proc. Natl. Acad. Sci. USA* **2002**, *99*, 4967 – 4971)—see the "temperature ratchet" mechanism, Section 1.4.2. However, it cannot occur for a macrocycle undergoing Brownian motion in a chiral rotaxane at equilibrium, although this has been incorrectly suggested several times (O. Lukin, T. Kubota, Y. Okamoto, F. Schelhase, A. Yoneva, W. M. Müller, U. Müller, F. Vögtle, *Angew. Chem.* **2003**, *115*, 4681 – 4684; *Angew. Chem. Int. Ed.* **2003**, *42*, 4542 – 4545 and Ref. [191j]).

[257] V. Bermudez, N. Capron, T. Gase, F. G. Gatti, F. Kajzar, D. A. Leigh, F. Zerbetto, S. W. Zhang, *Nature* **2000**, *406*, 608 – 611.

[258] a) A. Kapitulnik, S. Casalnuovo, K. C. Lim, A. J. Heeger, *Phys. Rev. Lett.* **1984**, *53*, 469 – 472; b) K. C. Lim, A. Kapitulnik, R. Zacher, A. J. Heeger, *J. Chem. Phys.* **1985**, *82*, 516 – 521.

[259] F. G. Gatti, S. León, J. K. Y. Wong, G. Bottari, A. Altieri, M. A. F. Morales, S. J. Teat, C. Frochot, D. A. Leigh, A. M. Brouwer, F. Zerbetto, *Proc. Natl. Acad. Sci. USA* **2003**, *100*, 10 – 14.

[260] a) R. Shukla, M. J. Deetz, B. D. Smith, *Chem. Commun.* **2000**, 2397 – 2398; b) M. J. Deetz, R. Shukla, B. D. Smith, *Tetrahedron* **2002**, *58*, 799 – 805; c) X. Fradera, M. Marquez, B. D. Smith, M. Orozco, F. J. Luque, *J. Org. Chem.* **2003**, *68*, 4663 – 4673.

[261] M. Linke, J.-C. Chambron, V. Heitz, J.-P. Sauvage, V. Semetey, *Chem. Commun.* **1998**, 2469 – 2470.

[262] a) L. Raehm, J.-M. Kern, J.-P. Sauvage, *Chem. Eur. J.* **1999**, *5*, 3310 – 3317; b) J.-M. Kern, L. Raehm, J.-P. Sauvage, B. Divisia-Blohorn, P. L. Vidal, *Inorg. Chem.* **2000**, *39*, 1555 – 1560; c) N. Weber, C. Hamann, J.-M. Kern, J.-P. Sauvage, *Inorg. Chem.* **2003**, *42*, 6780 – 6792; d) I. Poleschak, J.-M. Kern, J.-P. Sauvage, *Chem. Commun.* **2004**, 474 – 476; e) U. Létinois-Halbes, D. Hanss, J. M. Beierle, J.-P. Collin, J.-P. Sauvage, *Org. Lett.* **2005**, *7*, 5753 – 5756.

[263] a) F. Vögtle, W. M. Müller, U. Müller, M. Bauer, K. Rissanen, *Angew. Chem.* **1993**, *105*, 1356 – 1358; *Angew. Chem. Int. Ed. Engl.* **1993**, *32*, 1295 – 1297; b) M. Bauer, W. M. Müller, U. Müller, K. Rissanen, F. Vögtle, *Liebigs Ann.* **1995**, 649 – 656.

[264] P. Ceroni, D. A. Leigh, L. Mottier, F. Paolucci, S. Roffia, D. Tetard, F. Zerbetto, *J. Phys. Chem. B* **1999**, *103*, 10171 – 10179.

[265] M. J. Gunter, M. R. Johnston, *J. Chem. Soc. Chem. Commun.* **1994**, 829 – 830.

[266] L. Flamigni, A. M. Talarico, S. Serroni, F. Puntoriero, M. J. Gunter, M. R. Johnston, T. P. Jeynes, *Chem. Eur. J.* **2003**, *9*, 2649 – 2659.

[267] D. A. Leigh, K. Moody, J. P. Smart, K. J. Watson, A. M. Z. Slawin, *Angew. Chem.* **1996**, *108*, 326 – 331; *Angew. Chem. Int. Ed. Engl.* **1996**, *35*, 306 – 310.

[268] Both experimental and computational studies have shown solvation effects to be important in determining the co-conformational preference of certain cyclobis(paraquat-*p*-phenylene)/diarene macrocyclic polyether [2]catenanes, see: a) P. R. Ashton, M. Blower, D. Philp, N. Spencer, J. F. Stoddart, M. S. Tolley, R. Ballardini, M. Ciano, V. Balzani, M. T. Gandolfi, L. Prodi, C. H. McLean, *New J. Chem.* **1993**, *17*, 689 – 695; b) F. M. Raymo, K. N. Houk, J. F. Stoddart, *J. Org. Chem.* **1998**, *63*, 6523 – 6528; c) R. Ballardini, V. Balzani, M. T. Gandolfi, R. E. Gillard, J. F. Stoddart, E. Tabellini, *Chem. Eur. J.* **1998**, *4*, 449 – 459.

[269] As well as demonstrating co-conformational preferences for both oxidation states which are in line with the experimental findings, a computational study of [2]catenane **92** also showed evidence for charge localization in the TTF unit of the singly oxidized species, thus resulting in a barrierless, coulombic repulsion-driven $TTF^{+}\rightarrow$DNP shuttling step, see: X. G. Zheng, K. Sohlberg, *Phys. Chem. Chem. Phys.* **2004**, *6*, 809 – 815; a further computational study employed a novel molecular dynamics approach to model the entire period of the shuttling motion (a timescale normally outside traditional molecular dynamics approaches). So-far only the $TTF^{+}\rightarrow$DNP step has been modeled, and important features to emerge include a virtually barrier-free potential-energy profile and a key role for counterions in the shuttling mechanism, see: M. Ceccarelli, F. Mercuri, D. Passerone, M. Parrinello, *J. Phys. Chem. B* **2005**, *109*, 17094 – 17099.

[270] For other examples of switchable motion in [2]catenanes from the Stoddart group, see: a) P. R. Ashton, R. Ballardini, V. Balzani, M. T. Gandolfi, D. J.-F. Marquis, L. Pérez-García, L. Prodi, J. F. Stoddart, M. Venturi, *J. Chem. Soc. Chem. Commun.* **1994**, 177 – 180; b) P. R. Ashton, R. Ballardini, V. Balzani, A. Credi, M. T. Gandolfi, S. Menzer, L. Pérez-García, L. Prodi, J. F. Stoddart, M. Venturi, A. J. P. White, D. J. Williams, *J. Am. Chem. Soc.* **1995**, *117*, 11171 – 11197 (redox switching); c) V. Balzani, A. Credi, S. J. Langford, F. M. Raymo, J. F. Stoddart, M. Venturi, *J. Am. Chem. Soc.* **2000**, *122*, 3542 – 3543 (chemical switching); d) P. R. Ashton, V. Baldoni, V. Balzani, A. Credi, H. D. A. Hoffmann, M.-V. Martínez-Díaz, F. M. Raymo, J. F. Stoddart, M. Venturi, *Chem. Eur. J.* **2001**, *7*, 3482 – 3493 (redox and pH switching).

[271] Electrochemistry has been used to trigger co-conformational changes in a neutral π-donor/π-acceptor catenane; see: D. G. Hamilton, M. Montalti, L. Prodi, M. Fontani, P. Zanello, J. K. M. Sanders, *Chem. Eur. J.* **2000**, *6*, 608 – 617.

[272] B. Korybut-Daszkiewicz, A. Więckowska, R. Bilewicz, S. Domagała, K. Woźniak, *Angew. Chem.* **2004**, *116*, 1700 – 1704; *Angew. Chem. Int. Ed.* **2004**, *43*, 1668 – 1672.

[273] C. O. Dietrich-Buchecker, J.-P. Sauvage, J. P. Kintzinger, *Tetrahedron Lett.* **1983**, *24*, 5095 – 5098.

[274] a) C. O. Dietrich-Buchecker, J.-P. Sauvage, J.-M. Kern, *J. Am. Chem. Soc.* **1984**, *106*, 3043 – 3045; b) M. Cesario, C. O. Dietrich-Buchecker, J. Guilhem, C. Pascard, J.-P. Sauvage, *J. Chem. Soc. Chem. Commun.* **1985**, 244 – 247; c) A.-M. Albrecht-Gary, Z. Saad, C. O. Dietrich-Buchecker, J.-P. Sauvage, *J. Am. Chem. Soc.* **1985**, *107*, 3205 – 3209; d) C. Dietrich-Buchecker, J.-P. Sauvage, *Tetrahedron* **1990**, *46*, 503 – 512.

[275] a) M. Cesario, C. O. Dietrich, A. Edel, J. Guilhem, J. P. Kintzinger, C. Pascard, J.-P. Sauvage, *J. Am. Chem. Soc.* **1986**, *108*, 6250 – 6254; b) A.-M. Albrecht-Gary, C. Dietrich-Buchecker, Z. Saad, J.-P. Sauvage, *J. Am. Chem. Soc.* **1988**, *110*, 1467 – 1472; c) C. Dietrich-Buchecker, J.-P. Sauvage, J.-M. Kern, *J. Am. Chem. Soc.* **1989**, *111*, 7791 – 7800; d) A.-M. Albrecht-Gary, C. Dietrich-Buchecker, Z. Saad, J.-P. Sauvage, *J. Chem. Soc. Chem. Commun.* **1992**, 280 – 282; e) N. Armaroli, L. Decola, V. Balzani, J.-P. Sauvage, C. O. Dietrich-Buchecker, J.-M. Kern, A. Bailal, *J. Chem. Soc. Dalton Trans.* **1993**, 3241 – 3247.

[276] Similar effects have been observed in a number of other metal-templated interlocked systems, see: a) J.-P. Sauvage, J. Weiss, *J. Am. Chem. Soc.* **1985**, *107*, 6108 – 6110; b) C. O. Dietrich-Buchecker, A. Khemiss, J.-P. Sauvage, *J. Chem. Soc. Chem. Commun.* **1986**, 1376 – 1378; c) B. Mohr, J.-P. Sauvage, R. H. Grubbs, M. Weck, *Angew. Chem.* **1997**, *109*, 1365 – 1367; *Angew. Chem. Int. Ed. Engl.* **1997**, *36*, 1308 – 1310; d) M. Koizumi, C. Dietrich-Buchecker, J.-P. Sauvage, *Eur. J. Org. Chem.* **2004**, 770 – 775.

[277] D. B. Amabilino, C. O. Dietrich-Buchecker, A. Livoreil, L. Pérez-García, J.-P. Sauvage, J. F. Stoddart, *J. Am. Chem. Soc.* **1996**, *118*, 3905 – 3913.

[278] A. Andrievsky, F. Ahuis, J. L. Sessler, F. Vögtle, D. Gudat, M. Moini, *J. Am. Chem. Soc.* **1998**, *120*, 9712 – 9713.

[279] A. M. L. Fuller, D. A. Leigh, P. J. Lusby, A. M. Z. Slawin, D. B. Walker, *J. Am. Chem. Soc.* **2005**, *127*, 12612 – 12619.
[280] D. A. Leigh, P. J. Lusby, A. M. Z. Slawin, D. B. Walker, *Chem. Commun.* **2005**, 4919 – 4921.
[281] a) A. C. Laemmel, J.-P. Collin, J.-P. Sauvage, *Eur. J. Inorg. Chem.* **1999**, 383 – 386; b) E. Baranoff, J.-P. Collin, Y. Furusho, A. C. Laemmel, J.-P. Sauvage, *Chem. Commun.* **2000**, 1935 – 1936; c) J.-P. Collin, A. C. Laemmel, J.-P. Sauvage, *New J. Chem.* **2001**, *25*, 22 – 24; d) A. C. Laemmel, J.-P. Collin, J.-P. Sauvage, G. Accorsi, N. Armaroli, *Eur. J. Inorg. Chem.* **2003**, 467 – 474; e) S. Bonnet, J.-P. Collin, J.-P. Sauvage, *Chem. Commun.* **2005**, 3195 – 3197; f) J.-P. Collin, D. Jouvenot, M. Koizumi, J.-P. Sauvage, *Inorg. Chem.* **2005**, *44*, 4693 – 4698.
[282] P. Mobian, J.-M. Kern, J.-P. Sauvage, *Angew. Chem.* **2004**, *116*, 2446 – 2449; *Angew. Chem. Int. Ed.* **2004**, *43*, 2392 – 2395.
[283] This reversible process has been shown to tolerate other catenane and also rotaxane structures, see: a) F. Arico, P. Mobian, J.-M. Kern, J.-P. Sauvage, *Org. Lett.* **2003**, *5*, 1887 – 1890; b) D. Pomeranc, D. Jouvenot, J.-C. Chambron, J.-P. Collin, V. Heitz, J.-P. Sauvage, *Chem. Eur. J.* **2003**, *9*, 4247 – 4254.
[284] a) A. Livoreil, C. O. Dietrich-Buchecker, J.-P. Sauvage, *J. Am. Chem. Soc.* **1994**, *116*, 9399 – 9400; b) F. Baumann, A. Livoreil, W. Kaim, J.-P. Sauvage, *Chem. Commun.* **1997**, 35 – 36; c) A. Livoreil, J.-P. Sauvage, N. Armaroli, V. Balzani, L. Flamigni, B. Ventura, *J. Am. Chem. Soc.* **1997**, *119*, 12114 – 12124.
[285] D. J. Cardenas, A. Livoreil, J.-P. Sauvage, *J. Am. Chem. Soc.* **1996**, *118*, 11980 – 11981.
[286] D. A. Leigh, J. K. Y. Wong, F. Dehez, F. Zerbetto, *Nature* **2003**, *424*, 174 – 179.
[287] A similar mechanism for achieving unidirectional rotation in a [2]catenane has been explored theoretically, see: R. D. Astumian, *Proc. Natl. Acad. Sci. USA* **2005**, *102*, 1843 – 1847.
[288] a) A. Troisi, M. A. Ratner, *J. Am. Chem. Soc.* **2002**, *124*, 14528 – 14529; b) P. E. Kornilovitch, A. M. Bratkovsky, R. S. Williams, *Phys. Rev. B* **2002**, *66*, 245413; c) A. W. Ghosh, T. Rakshit, S. Datta, *Nano Lett.* **2004**, *4*, 565 – 568.
[289] A. Troisi, M. A. Ratner, *Nano Lett.* **2004**, *4*, 591 – 595.
[290] T. Seideman, *J. Phys.: Condens. Matter* **2003**, *15*, R521-R549.
[291] a) K. Hoki, M. Yamaki, S. Koseki, Y. Fujimura, *J. Chem. Phys.* **2003**, *118*, 497 – 504; b) K. Hoki, M. Yamaki, Y. Fujimura, *Angew. Chem.* **2003**, *115*, 3084 – 3086; *Angew. Chem. Int. Ed.* **2003**, *42*, 2976 – 2978.
[292] In actual fact, **104** would be a poor choice practically as racemization is likely to occur through keto–enol tautomerism. However, this does not affect the validity of the principles involved.
[293] K. Hoki, M. Yamaki, S. Koseki, Y. Fujimura, *J. Chem. Phys.* **2003**, *119*, 12393 – 12398.
[294] For theory, see: a) P. Reimann, M. Grifoni, P. Hänggi, *Phys. Rev. Lett.* **1997**, *79*, 10 – 13; b) S. Yukawa, M. Kikuchi, G. Tatara, H. Matsukawa, *J. Phys. Soc. Jpn.* **1997**, *66*, 2953 – 2956; c) I. Goychuk, P. Hänggi, *Europhys. Lett.* **1998**, *43*, 503 – 509; for experiment, see Ref. [44p].
[295] a) M. Yamaki, K. Hoki, Y. Ohtsuki, H. Kono, Y. Fujimura, *J. Am. Chem. Soc.* **2005**, *127*, 7300 – 7301; b) M. Yamaki, K. Hoki, Y. Ohtsuki, H. Kono, Y. Fujimura, *Phys. Chem. Chem. Phys.* **2005**, *7*, 1900 – 1904.
[296] For a review of the work in this area during the 1990s, see: A. Globus, C. W. Bauschlicher, J. Han, R. L. Jaffe, C. Levit, D. Srivastava, *Nanotechnology* **1998**, *9*, 192 – 199.
[297] a) K. E. Drexler, *Engines of Creation: The Coming Era of Nanotechnology*, Fourth Estate, London, **1990**; b) K. E. Drexler, *Nanosystems: Molecular Machinery, Manufacturing and Computation*, Wiley, Chichester, **1992**.
[298] a) J. C. Charlier, J. P. Michenaud, *Phys. Rev. Lett.* **1993**, *70*, 1858 – 1861; b) R. C. Merkle, *Nanotechnology* **1993**, *4*, 86 – 90; c) Y. K. Kwon, D. Tomanek, *Phys. Rev. B* **1998**, *58*, R16001 – R16004; d) A. H. R. Palser, *Phys. Chem. Chem. Phys.* **1999**, *1*, 4459 – 4464; e) A. N. Kolmogorov, V. H. Crespi, *Phys. Rev. Lett.* **2000**, *85*, 4727 – 4730; f) R. Saito, R. Matsuo, T. Kimura, G. Dresselhaus, M. S. Dresselhaus, *Chem. Phys. Lett.* **2001**, *348*, 187 – 193; g) M. Damnjanovic, T. Vukovic, I. Milosevic, *Eur. Phys. J. B* **2002**, *25*, 131 – 134; h) T. Vukovic, M. Damnjanovic, I. Milosevic, *Physica E* **2003**, *16*, 259 – 268; i) M. Damnjanovic, E. Dobardzic, I. Milosevic, T. Vukovic, B. Nikolic, *New J. Phys.* **2003**, *6*, 148; j) J. Servantie, P. Gaspard, *Phys. Rev. Lett.* **2003**, *91*, 185503; k) A. V. Belikov, Y. E. Lozovik, A. G. Nikolaev, A. M. Popov, *Chem. Phys. Lett.* **2004**, *385*, 72 – 78; l) E. Bichoutskaia, A. M. Popov, A. El-Barbary, M. I. Heggie, Y. E. Lozovik, *Phys. Rev. B* **2005**, *71*, 113403.
[299] a) R. E. Tuzun, D. W. Noid, B. G. Sumpter, *Nanotechnology* **1995**, *6*, 64 – 74; b) K. Sohlberg, R. E. Tuzun, B. G. Sumpter, D. W. Noid, *Nanotechnology* **1997**, *8*, 103 – 111; c) R. E. Tuzun, K. Sohlberg, D. W. Noid, B. G. Sumpter, *Nanotechnology* **1998**, *9*, 37 – 48.
[300] a) Y. E. Lozovik, A. Minogin, A. M. Popov, *Phys. Lett. A* **2003**, *313*, 112 – 121; b) Y. E. Lozovik, A. V. Minogin, A. M. Popov, *JETP Lett.* **2003**, *77*, 631 – 635.
[301] J. Han, A. Globus, R. Jaffe, G. Deardorff, *Nanotechnology* **1997**, *8*, 95 – 102.
[302] R. E. Tuzun, D. W. Noid, B. G. Sumpter, *Nanotechnology* **1995**, *6*, 52 – 63.
[303] D. Srivastava, *Nanotechnology* **1997**, *8*, 186 – 192.
[304] For an example of a proposed molecular bearing in which chiral nanotubes could exhibit unidirectional relative rotation driven by temperature variations (that is, a temperature ratchet), see: a) Z. C. Tu, Z. C. Ou-Yang, *J. Phys.: Condens. Matter* **2004**, *16*, 1287 – 1292; for a similar case, driven by a fluctuating electric field (that is, a fluctuating potential ratchet), see: b) Z. C. Tu, X. Hu, *Phys. Rev. B* **2005**, *72*, 033404.
[305] a) L. Forró, *Science* **2000**, *289*, 560 – 561; b) Q. S. Zheng, Q. Jiang, *Phys. Rev. Lett.* **2002**, *88*, 045503; c) Q. S. Zheng, J. Z. Liu, Q. Jiang, *Phys. Rev. B* **2002**, *65*, 245409; d) S. B. Legoas, V. R. Coluci, S. F. Braga, P. Z. Coura, S. O. Dantas, D. S. Galvão, *Phys. Rev. Lett.* **2003**, *90*, 055504; e) W. Guo, Y. Guo, H. Gao, Q. Zheng, W. Zhong, *Phys. Rev. Lett.* **2003**, *91*, 125501; f) Y. Zhao, C. C. Ma, G. H. Chen, Q. Jiang, *Phys. Rev. Lett.* **2003**, *91*, 175504; g) S. B. Legoas, V. R. Coluci, S. F. Braga, P. Z. Coura, S. Dantas, D. S. Galvão, *Nanotechnology* **2004**, *15*, S184 – S189; h) P. Tangney, S. G. Louie, M. L. Cohen, *Phys. Rev. Lett.* **2004**, *93*, 065503.
[306] J. W. Kang, H. J. Hwang, *J. Appl. Phys.* **2004**, *96*, 3900 – 3905.
[307] J. W. Kang, K. O. Song, O. K. Kwon, H. J. Hwang, *Nanotechnology* **2005**, *16*, 2670 – 2676.
[308] D. Tasis, N. Tagmatarchis, A. Bianco, M. Prato, *Chem. Rev.* **2006**, *106*, 1105 – 1136.
[309] a) J. Cumings, A. Zettl, *Science* **2000**, *289*, 602 – 604; b) M. F. Yu, B. I. Yakobson, R. S. Ruoff, *J. Phys. Chem. B* **2000**, *104*, 8764 – 8767.
[310] The first examples of nanoelectromechanical systems incorporating moving nanotube components have been reported and exemplify the state of the art in terms of both construction and electric-field-driven manipulation for devices of this type, see: a) A. M. Fennimore, T. D. Yuzvinsky, W. Q. Han, M. S. Fuhrer, J. Cumings, A. Zettl, *Nature* **2003**, *424*, 408 – 410; b) P. A. Williams, S. J. Papadakis, A. M. Patel, M. R. Falvo, S. Washburn, R. Superfine, *Appl. Phys. Lett.* **2003**, *82*, 805 – 807; c) B. Bourlon, D. C. Glattli, C. Miko, L. Forró, A. Bachtold, *Nano Lett.* **2004**, *4*, 709 – 712; d) S. J. Papadakis, A. R. Hall, P. A. Williams, L. Vicci, M. R. Falvo, R. Superfine, S. Washburn, *Phys. Rev. Lett.* **2004**, *93*, 146101; e) B. C. Regan, S. Aloni, R. O. Ritchie, U. Dahmen, A. Zettl, *Nature* **2004**, *428*, 924 – 927; f) B. C. Regan, S. Aloni, K. Jensen, R. O. Ritchie, A. Zettl,

Nano Lett. **2005**, *5*, 1730 – 1733; g) J. C. Meyer, M. Paillet, S. Roth, *Science* **2005**, *309*, 1539 – 1541; h) T. Ikuno, S.-I. Honda, T. Yasuda, K. Oura, M. Katayama, J. G. Lee, H. Mori, *Appl. Phys. Lett.* **2005**, *87*, 213104; i) T. D. Yuzvinsky, A. M. Fennimore, A. Kis, A. Zettl, *Nanotechnology* **2006**, *17*, 434 – 438.

[311] In the computational studies of rotation in **104**, Fujimura and co-workers also considered motion driven by circularly polarised laser pulses. It was confirmed that the necessary asymmetry derives from the photon helicity, and rotational direction is independent of molecular chirality. The direction of rotation for a randomly oriented population of rotors is therefore defined in the laboratory fixed frame (the frame of the applied field) and now the magnitude of rotation does depend on which enantiomer is used, see Ref. [291a].

[312] J. Vacek, J. Michl, *Proc. Natl. Acad. Sci. USA* **2001**, *98*, 5481 – 5486.

[313] For a review of such supramolecular grid structures, see: J. Michl, T. F. Magnera, *Proc. Natl. Acad. Sci. USA* **2002**, *99*, 4788 – 4792.

[314] For theoretical studies and preliminary experimental results on two structurally simpler azimuthal rotor (that is, axle perpendicular to the surface) systems, see: a) L. I. Clarke, D. Horinek, G. S. Kottas, N. Varaksa, T. F. Magnera, T. P. Hinderer, R. D. Horansky, J. Michl, J. C. Price, *Nanotechnology* **2002**, *13*, 533 – 540; b) D. Horinek, J. Michl, *J. Am. Chem. Soc.* **2003**, *125*, 11900 – 11910.

[315] a) X. L. Zheng, M. E. Mulcahy, D. Horinek, F. Galeotti, T. F. Magnera, J. Michl, *J. Am. Chem. Soc.* **2004**, *126*, 4540 – 4542; b) T. F. Magnera, J. Michl, *Top. Curr. Chem.* **2005**, *262*, 63 – 97.

[316] At room temperature, it was observed that the molecules adopting a nonrotating conformation were interconverting with rotating forms on a timescale of minutes.

[317] D. Horinek, J. Michl, *Proc. Natl. Acad. Sci. USA* **2005**, *102*, 14175 – 14180.

[318] At low temperatures (thermal energy less than maximum barrier heights), this motion is predicted to be near-synchronous given a strong enough electric field that is not too high in frequency. The mechanism is similar to a flashing ratchet except the electric field both varies the potential-energy surface and powers motion over the surface. At temperatures which permit thermal crossing of the barrier, lower strength electric fields perform best, with the mechanism taking on the features of a true flashing Brownian ratchet. Interconversion between the residual diastereomers in the current structures is expected to scramble the unidirectional nature of the motion at ambient temperature. Analogues more resistant to isomerization should, however, be relatively easy to design.

[319] a) D. C. Caskey, R. K. Shoemaker, J. Michl, *Org. Lett.* **2004**, *6*, 2093 – 2096; b) D. C. Caskey, J. Michl, *J. Org. Chem.* **2005**, *70*, 5442 – 5448.

[320] H. Jian, J. M. Tour, *J. Org. Chem.* **2003**, *68*, 5091 – 5103.

[321] J. Karczmarek, J. Wright, P. Corkum, M. Ivanov, *Phys. Rev. Lett.* **1999**, *82*, 3420 – 3423.

[322] D. M. Villeneuve, S. A. Aseyev, P. Dietrich, M. Spanner, M. Y. Ivanov, P. B. Corkum, *Phys. Rev. Lett.* **2000**, *85*, 542 – 545.

[323] An experimental example of direct momentum transfer from a linear flow to rotational motion of a chiral propeller-like molecule has been observed in a liquid-crystal monolayer (Y. Tabe, H. Yokoyama, *Nat. Mater.* **2003**, *2*, 806 – 809). When a chiral liquid-crystal monolayer was deposited as a Langmuir film on a glycerol surface, a "target pattern" of expanding concentric circles was observed under reflected-light polarizing microscopy. The linear molecules align end-on but with a common tilt angle and undergo cooperative precession driven by the diffusion of water across the liquid/vapor interface. Molecules furthest from defects in the monolayer rotate most easily and transfer their changing orientation outwards, thereby giving rise to the observed expanding pattern. The self-ordering properties of liquid crystals are essential for amplifying a small molecular-level effect which would otherwise be swamped by thermal motion.

[324] J. Vacek, J. Michl, *New J. Chem.* **1997**, *21*, 1259 – 1268.

[325] Driving a nanoscale rotor constructed from carbon nanotube components with a flow of gas has recently been considered: J. W. Kang, H. J. Hwang, *Nanotechnology* **2004**, *15*, 1633 – 1638.

[326] K. Hoki, M. Sato, M. Yamaki, R. Sahnoun, L. González, S. Koseki, Y. Fujimura, *J. Phys. Chem. B* **2004**, *108*, 4916 – 4921.

[327] Y. Fujimura, L. González, D. Kröner, J. Manz, I. Mehdaoui, B. Schmidt, *Chem. Phys. Lett.* **2004**, *386*, 248 – 253.

[328] a) J. D. Dunitz, E. F. Maverick, K. N. Trueblood, *Angew. Chem.* **1988**, *100*, 910 – 926; *Angew. Chem. Int. Ed. Engl.* **1988**, *27*, 880 – 895; b) F. Horii, H. Kaji, H. Ishida, K. Kuwabara, K. Masuda, T. Tai, *J. Mol. Struct.* **1998**, *441*, 303 – 311.

[329] a) Z. Dominguez, H. Dang, M. J. Strouse, M. A. Garcia-Garibay, *J. Am. Chem. Soc.* **2002**, *124*, 2398 – 2399; b) C. E. Godinez, G. Zepeda, M. A. Garcia-Garibay, *J. Am. Chem. Soc.* **2002**, *124*, 4701 – 4707; c) Z. Dominguez, H. Dang, M. J. Strouse, M. A. Garcia-Garibay, *J. Am. Chem. Soc.* **2002**, *124*, 7719 – 7727; d) Z. Dominguez, T. A. V. Khuong, H. Dang, C. N. Sanrame, J. E. Nunez, M. A. Garcia-Garibay, *J. Am. Chem. Soc.* **2003**, *125*, 8827 – 8837; e) T. A. V. Khuong, G. Zepeda, R. Ruiz, S. I. Khan, M. A. Garcia-Garibay, *Cryst. Growth Des.* **2004**, *4*, 15 – 18; f) C. E. Godinez, G. Zepeda, C. J. Mortko, H. Dang, M. A. Garcia-Garibay, *J. Org. Chem.* **2004**, *69*, 1652 – 1662; g) S. D. Karlen, M. A. Garcia-Garibay, *Chem. Commun.* **2005**, 189 – 191; h) S. D. Karlen, S. I. Khan, M. A. Garcia-Garibay, *Cryst. Growth Des.* **2005**, *5*, 53 – 55; i) S. D. Karlen, R. Ortiz, O. L. Chapman, M. A. Garcia-Garibay, *J. Am. Chem. Soc.* **2005**, *127*, 6554 – 6555; j) R. D. Horansky, L. I. Clarke, J. C. Price, T. A. V. Khuong, P. D. Jarowski, M. A. Garcia-Garibay, *Phys. Rev. B* **2005**, *72*, 014302.

[330] For recent accounts of this work, see: a) M. A. Garcia-Garibay, *Proc. Natl. Acad. Sci. USA* **2005**, *102*, 10771 – 10776; b) S. D. Karlen, M. A. Garcia-Garibay, *Top. Curr. Chem.* **2005**, *262*, 179 – 227.

[331] An earlier, but related, structure is the "molecular turnstile" designed and created by Beddard and Moore: T. C. Bedard, J. S. Moore, *J. Am. Chem. Soc.* **1995**, *117*, 10662 – 10671.

[332] The diborate congener of **110**, in which the trityl carbon atoms are replaced by boron, has also been reported: J. R. Gardinier, P. J. Pellechia, M. D. Smith, *J. Am. Chem. Soc.* **2005**, *127*, 12448 – 12449. Compared to **110**, a more open packing arrangement is found in the crystalline state owing to coulombic repulsion which results in a lower barrier to rotary motion.

[333] T. Shima, F. Hampel, J. A. Gladysz, *Angew. Chem.* **2004**, *116*, 5653 – 5656; *Angew. Chem. Int. Ed.* **2004**, *43*, 5537 – 5540.

[334] T. Akutagawa, K. Shitagami, S. Nishihara, S. Takeda, T. Hasegawa, T. Nakamura, Y. Hosokoshi, K. Inoue, S. Ikeuchi, Y. Miyazaki, K. Saito, *J. Am. Chem. Soc.* **2005**, *127*, 4397 – 4402.

[335] For an overview of recent experimental results in nanoscale locomotion, see: G. A. Ozin, I. Manners, S. Fournier-Bidoz, A. Arsenault, *Adv. Mater.* **2005**, *17*, 3011 – 3018.

[336] a) N. O. Young, J. S. Goldstein, M. J. Block, *J. Fluid Mech.* **1959**, *6*, 350 – 356; b) A. W. Adamson, *Physical Chemistry of Surfaces*, 5th ed., Wiley, New York, **1990**.

[337] For an historical perspective, see: L. E. Scriven, C. V. Sternling, *Nature* **1960**, *187*, 186 – 188.

[338] a) K. D. Barton, R. S. Subramanian, *J. Colloid Interface Sci.* **1989**, *133*, 211 – 222; b) A. M. Cazabat, F. Heslot, S. M. Troian, P. Carles, *Nature* **1990**, *346*, 824 – 826.

[339] a) M. A. Burns, C. H. Mastrangelo, T. S. Sammarco, F. P. Man, J. R. Webster, B. N. Johnson, B. Foerster, D. Jones, Y. Fields, A. R. Kaiser, D. T. Burke, *Proc. Natl. Acad. Sci. USA* **1996**, *93*,

5556 – 5561; b) D. E. Kataoka, S. M. Troian, *Nature* **1999**, *402*, 794 – 797.

[340] a) C. D. Bain, G. D. Burnetthall, R. R. Montgomerie, *Nature* **1994**, *372*, 414 – 415; b) D. F. Dossantos, T. Ondarçuhu, *Phys. Rev. Lett.* **1995**, *75*, 2972 – 2975; c) M. E. R. Shanahan, P. G. de Gennes, *C. R. Acad. Sci. Ser. IIb* **1997**, *324*, 261 – 268; d) P. G. de Gennes, *Europhys. Lett.* **1997**, *39*, 407 – 412; e) P. G. de Gennes, *Physica A* **1998**, *249*, 196 – 205; f) S. W. Lee, P. E. Laibinis, *J. Am. Chem. Soc.* **2000**, *122*, 5395 – 5396; g) Y. Sumino, N. Magome, T. Hamada, K. Yoshikawa, *Phys. Rev. Lett.* **2005**, *94*, 068301.

[341] A similar effect can be induced in mercury droplets by a redox reaction. This may be controlled by application of an electric field in suitable electrolytes and has been used to move mercury droplets by a Brownian ratchet mechanism, see Refs. [44e,g]. Another related phenomenon is observed because of the solvent-swelling of amphiphilic polymer gels: T. Mitsumata, K. Ikeda, J. P. Gong, Y. Osada, *Appl. Phys. Lett.* **1998**, *73*, 2366 – 2368.

[342] R. F. Ismagilov, A. Schwartz, N. Bowden, G. M. Whitesides, *Angew. Chem.* **2002**, *114*, 674 – 676; *Angew. Chem. Int. Ed.* **2002**, *41*, 652 – 654.

[343] W. F. Paxton, K. C. Kistler, C. C. Olmeda, A. Sen, S. K. St Angelo, Y. Y. Cao, T. E. Mallouk, P. E. Lammert, V. H. Crespi, *J. Am. Chem. Soc.* **2004**, *126*, 13424 – 13431.

[344] a) R. Golestanian, T. B. Liverpool, A. Ajdari, *Phys. Rev. Lett.* **2005**, *94*, 220801; b) W. E. Paxton, A. Sen, T. E. Mallouk, *Chem. Eur. J.* **2005**, *11*, 6462 – 6470; an alternative mechanism considered herein is "self-electrophoresis", whereby two ends of a conducting object catalyze two different electrochemical half-cell reactions, essentially generating its own electic field. This would result in a flow of electrons within the particle, accompanied by a concomitant balancing flow of protons (or other electrolyte ions) across its surface, thus resulting in propulsion of the object with respect to the fluid. Experimentally, this mechanism has very recently been investigated as a method for mixing a solution over a metallic surface, see: c) T. R. Kline, W. F. Paxton, Y. Wang, D. Velegol, T. E. Mallouk, A. Sen, *J. Am. Chem. Soc.* **2005**, *127*, 17150 – 17151; and in an example where enzymes are empolyed as the redox-active species to propel a macroscopic conducting carbon fiber, see: d) N. Mano, A. Heller, *J. Am. Chem. Soc.* **2005**, *127*, 11574 – 11575.

[345] P. Dhar, T. M. Fischer, Y. Wang, T. E. Mallouk, W. F. Paxton, A. Sen, *Nano Lett.* **2006**, *6*, 66 – 72.

[346] J. M. Catchmark, S. Subramanian, A. Sen, *Small* **2005**, *1*, 202 – 206.

[347] T. R. Kline, W. F. Paxton, T. E. Mallouk, A. Sen, *Angew. Chem.* **2005**, *117*, 754 – 756; *Angew. Chem. Int. Ed.* **2005**, *44*, 744 – 746.

[348] S. Fournier-Bidoz, A. C. Arsenault, I. Manners, G. A. Ozin, *Chem. Commun.* **2005**, 441 – 443.

[349] J. Vicario, R. Eelkema, W. R. Browne, A. Meetsma, R. M. La Crois, B. L. Feringa, *Chem. Commun.* **2005**, 3936 – 3938.

[350] G. Taylor, *Proc. R. Soc. London Ser. A* **1951**, *209*, 447 – 461.

[351] a) L. E. Becker, S. A. Koehler, H. A. Stone, *J. Fluid Mech.* **2003**, *490*, 15 – 35; b) R. Dreyfus, J. Baudry, H. A. Stone, *Eur. Phys. J. B* **2005**, *47*, 161 – 164.

[352] a) A. Najafi, R. Golestanian, *Phys. Rev. E* **2004**, *69*, 062901; b) A. Najafi, R. Golestanian, *J. Phys.: Condens. Matter* **2005**, *17*, S1203 – S1208.

[353] a) A. Shapere, F. Wilczek, *Phys. Rev. Lett.* **1987**, *58*, 2051 – 2054; b) A. Shapere, F. Wilczek, *J. Fluid Mech.* **1989**, *198*, 557 – 585; c) A. Shapere, F. Wilczek, *J. Fluid Mech.* **1989**, *198*, 587 – 599; d) H. A. Stone, A. D. T. Samuel, *Phys. Rev. Lett.* **1996**, *77*, 4102 – 4104; e) E. M. Purcell, *Proc. Natl. Acad. Sci. USA* **1997**, *94*, 11307 – 11311; f) C. H. Wiggins, R. E. Goldstein, *Phys. Rev. Lett.* **1998**, *80*, 3879 – 3882; g) A. Ajdari, H. A. Stone, *Phys. Fluids* **1999**, *11*, 1275 – 1277; h) S. Camalet, F. Jülicher, J. Prost, *Phys. Rev. Lett.* **1999**, *82*, 1590 – 1593; i) J. E. Avron, O. Gat, O. Kenneth, *Phys. Rev. Lett.* **2004**, *93*, 186001; j) J. E. Avron, O. Kenneth, D. H. Oaknin, *New J. Phys.* **2005**, *7*, 234; two related mechanisms for mechanical non-Brownian propulsion across a periodic but symmetrical surface have also recently been considered. These can be regarded as "self-propelled" walkers (see Section 4.4) in which all steps in the mechanism involve changes to the moving object, while the track remains passive throughout, see: k) M. Porto, M. Urbakh, J. Klafter, *Phys. Rev. Lett.* **2000**, *84*, 6058 – 6061; l) Z. Wang, *Phys. Rev. E* **2004**, *70*, 031903.

[354] R. Dreyfus, J. Baudry, M. L. Roper, M. Fermigier, H. A. Stone, J. Bibette, *Nature* **2005**, *437*, 862 – 865.

[355] D.-H. Qu, Q.-C. Wang, H. Tian, *Angew. Chem.* **2005**, *117*, 5430 – 5433; *Angew. Chem. Int. Ed.* **2005**, *44*, 5296 – 5299.

[356] The suggestion of photo/thermal imine isomerization was made to us by Jean-Marie Lehn in 2004 during discussions on possible means to break time-reversal symmetry in chemical reactions. These ideas were recently published in the context of rotary motors: J.-M. Lehn, *Chem. Eur. J.* **2006**, *12*, 5910 – 5915.

[357] a) N. B. Baranova, B. Y. Zel'dovich, *Chem. Phys. Lett.* **1978**, *57*, 435 – 437; b) B. Space, H. Rabitz, A. Lörincz, P. Moore, *J. Chem. Phys.* **1996**, *105*, 9515 – 9524.

[358] a) G. Binnig, H. Rohrer, C. Gerber, E. Weibel, *Phys. Rev. Lett.* **1982**, *49*, 57 – 61; b) G. Binnig, H. Rohrer, *Rev. Mod. Phys.* **1987**, *59*, 615 – 625.

[359] G. Binnig, C. F. Quate, C. Gerber, *Phys. Rev. Lett.* **1986**, *56*, 930 – 933.

[360] For general reviews on the use of probe microscopies to manipulate single atoms and molecules, see: a) special issue on "Force and Tunneling Microscopy": *Chem. Rev.* **1997**, *97*, 1015 – 1230; b) J. K. Gimzewski, C. Joachim, *Science* **1999**, *283*, 1683 – 1688; for reviews on the early development of single atom and molecule STM manipulation, see: c) J. A. Stroscio, D. M. Eigler, *Science* **1991**, *254*, 1319 – 1326; d) P. Avouris, *Acc. Chem. Res.* **1995**, *28*, 95 – 102; for reviews on the development of STM manipulation of large molecules, see: e) J. K. Gimzewski, T. A. Jung, M. T. Cuberes, R. R. Schlittler, *Surf. Sci.* **1997**, *386*, 101 – 114; f) F. Rosei, M. Schunack, Y. Naitoh, P. Jiang, A. Gourdon, E. Laegsgaard, I. Stensgaard, C. Joachim, F. Besenbacher, *Prog. Surf. Sci.* **2003**, *71*, 95 – 146; for reviews on the development of and advances in AFM, see: g) H. Takano, J. R. Kenseth, S. S. Wong, J. C. O'Brien, M. D. Porter, *Chem. Rev.* **1999**, *99*, 2845 – 2890; h) M. Guthold, M. Falvo, W. G. Matthews, S. Paulson, J. Mullin, S. Lord, D. Erie, S. Washburn, R. Superfine, F. P. Brooks, R. M. Taylor, *J. Mol. Graphics Modell.* **1999**, *17*, 187 – 197; i) F. J. Giessibl, *Rev. Mod. Phys.* **2003**, *75*, 949 – 983; for reviews on the use of AFM to probe the intramolecular interactions in single biomolecules and intermolecular interactions of biological complexes, see: j) C. Bustamante, D. Keller, *Phys. Today* **1995**, *48*(12), 32 – 38; k) A. Engel, H. E. Gaub, D. J. Müller, *Curr. Biol.* **1999**, *9*, R133 – R136; l) H. Clausen-Schaumann, M. Seitz, R. Krautbauer, H. E. Gaub, *Curr. Opin. Chem. Biol.* **2000**, *4*, 524 – 530; m) B. Samori, *Chem. Eur. J.* **2000**, *6*, 4249 – 4255; n) A. Janshoff, M. Neitzert, Y. Oberdörfer, H. Fuchs, *Angew. Chem.* **2000**, *112*, 3346 – 3374; *Angew. Chem. Int. Ed.* **2000**, *39*, 3212 – 3237; o) M. Rief, H. Grubmüller, *ChemPhysChem* **2002**, *3*, 255 – 261; p) R. B. Best, J. Clarke, *Chem. Commun.* **2002**, 183 – 192; for reviews on the use of STM to induce single-molecule chemical reactions, see: q) S. W. Hla, G. Meyer, K.-H. Rieder, *ChemPhysChem* **2001**, *2*, 361 – 366; for reviews on the role of probe microscopies in the development of molecular electronics, see: Ref. [290] and r) C. Joachim, J. K. Gimzewski, *Proc. IEEE* **1998**, *86*, 184 – 190; s) C. Joachim, J. K. Gimzewski, A. Aviram,

Nature **2000**, *408*, 541 – 548; t) F. Moresco, *Phys. Rep.* **2004**, *399*, 175 – 225.

[361] For a futuristic vision of molecular manufacturing based on the atom-by-atom manipulation of matter by nanoscale machines, see Ref. [297].

[362] D. M. Eigler, C. P. Lutz, W. E. Rudge, *Nature* **1991**, *352*, 600 – 603.

[363] T. A. Jung, R. R. Schlittler, J. K. Gimzewski, H. Tang, C. Joachim, *Science* **1996**, *271*, 181 – 184.

[364] Free rotation around the porphyrin–phenyl bond means that different leg–porphyrin angles are observed on different surfaces (from virtually perpendicular to coplanar). In all cases, however, the planar porphyrin core is insulated from the surface by the bulky *tert*-butyl groups: a) T. A. Jung, R. R. Schlittler, J. K. Gimzewski, *Nature* **1997**, *386*, 696 – 698; b) F. Moresco, G. Meyer, K.-H. Rieder, H. Ping, H. Tang, C. Joachim, *Surf. Sci.* **2002**, *499*, 94 – 102.

[365] Note this method of "pushing" the molecule away from a moving STM tip is in fact different from the strategy used to move single atoms and simple molecules at low temperature, where the mobile species is trapped directly under the tip by electrostatic or van der Waals interactions before "sliding" to the new position.

[366] A modified technique was required to effect motion of the same molecule at low temperature; however this then allowed a detailed description of the precise conformational changes and their effect on the tunneling current between the tip and substrate, see: a) F. Moresco, G. Meyer, K.-H. Rieder, H. Tang, A. Gourdon, C. Joachim, *Appl. Phys. Lett.* **2001**, *78*, 306 – 308; b) F. Moresco, G. Meyer, K.-H. Rieder, H. Tang, A. Gourdon, C. Joachim, *Phys. Rev. Lett.* **2001**, *87*, 088302.

[367] F. Biscarini, W. Gebauer, D. Di Domenico, R. Zamboni, J. I. Pascual, D. A. Leigh, A. Murphy, D. Tetard, *Synth. Met.* **1999**, *102*, 1466 – 1467.

[368] P. Samori, F. Jackel, O. Unsal, A. Godt, J. P. Rabe, *ChemPhysChem* **2001**, *2*, 461 – 464.

[369] H. Shigekawa, K. Miyake, J. Sumaoka, A. Harada, M. Komiyama, *J. Am. Chem. Soc.* **2000**, *122*, 5411 – 5412.

[370] M. T. Cuberes, R. R. Schlittler, J. K. Gimzewski, *Appl. Phys. Lett.* **1996**, *69*, 3016 – 3018.

[371] M. Feng, X. Guo, X. Lin, X. He, W. Ji, S. Du, D. Zhang, D. Zhu, H. Gao, *J. Am. Chem. Soc.* **2005**, *127*, 15338 – 15339.

[372] K. Kitagawa, T. Morita, S. Kimura, *Angew. Chem.* **2005**, *117*, 6488 – 6491; *Angew. Chem. Int. Ed.* **2005**, *44*, 6330 – 6333.

[373] A related phenomenon has been reported for gold-supported self-assembled monolayers of a rotaxane. A change in surface height was observed after applying a positive voltage with a conducting AFM tip, see: D. Wu, X. Yin, X. Zhang, H.-R. Tseng, J. F. Stoddart, *IEEE Trans: Nanotechnol.* **2003**, *2*, 606 – 608.

[374] J. K. Gimzewski, C. Joachim, R. R. Schlittler, V. Langlais, H. Tang, I. Johannsen, *Science* **1998**, *281*, 531 – 533.

[375] For an example of an STM-imaged rotation of a guest molecule in a cavity within a 2D lattice, where the guest and lattice molecules are different, see: S. J. H. Griessl, M. Lackinger, F. Jamitzky, T. Markert, M. Hietschold, W. M. Heckl, *Langmuir* **2004**, *20*, 9403 – 9407.

[376] For an interesting discussion which places the aforementioned results in the context of ultimately creating, and observing, a single-molecule unidirectional rotor, see: C. Joachim, J. K. Gimzewski, *Struct. Bonding (Berlin)* **2001**, *99*, 1 – 18.

[377] The incorporation of a "small-molecule" fragment into a polymer of known force–extension behavior can be used to circumvent such problems in certain cases.

[378] a) M. Cavallini, F. Biscarini, S. León, F. Zerbetto, G. Bottari, D. A. Leigh, *Science* **2003**, *299*, 531 – 531; b) J. F. Moulin, J. C. Kengne, R. Kshirsagar, M. Cavallini, F. Biscarini, S. León, F. Zerbetto, G. Bottari, D. A. Leigh, *J. Am. Chem. Soc.* **2006**, *128*, 526 – 532.

[379] a) F. Moresco, G. Meyer, K.-H. Rieder, H. Tang, A. Gourdon, C. Joachim, *Phys. Rev. Lett.* **2001**, *86*, 672 – 675; b) C. Loppacher, M. Guggisberg, O. Pfeiffer, E. Meyer, M. Bammerlin, R. Luthi, R. Schlittler, J. K. Gimzewski, H. Tang, C. Joachim, *Phys. Rev. Lett.* **2003**, *90*, 066107.

[380] C. Viala, A. Seechi, A. Gourdon, *Eur. J. Org. Chem.* **2002**, 4185 – 4189.

[381] a) A. Gourdon, *Eur. J. Org. Chem.* **1998**, 2797 – 2801; b) V. J. Langlais, R. R. Schlittler, H. Tang, A. Gourdon, C. Joachim, J. K. Gimzewski, *Phys. Rev. Lett.* **1999**, *83*, 2809 – 2812; c) F. Moresco, L. Gross, L. Grill, M. Alemani, A. Gourdon, C. Joachim, K.-H. Rieder, *Appl. Phys. A* **2005**, *80*, 913 – 920, and references therein; this work has recently been summarized, see: d) F. Moresco, A. Gourdon, *Proc. Natl. Acad. Sci. USA* **2005**, *102*, 8809 – 8814.

[382] L. Soukiassian, A. J. Mayne, G. Comtet, L. Hellner, G. Dujardin, A. Gourdon, *J. Chem. Phys.* **2005**, *122*, 134704.

[383] M. Lastapis, M. Martin, D. Riedel, L. Hellner, G. Comtet, G. Dujardin, *Science* **2005**, *308*, 1000 – 1003.

[384] a) C. Joachim, H. Tang, F. Moresco, G. Rapenne, G. Meyer, *Nanotechnology* **2002**, *13*, 330 – 335; b) G. Jimenez-Bueno, G. Rapenne, *Tetrahedron Lett.* **2003**, *44*, 6261 – 6263.

[385] G. Rapenne, *Org. Biomol. Chem.* **2005**, *3*, 1165 – 1169.

[386] L. Grill, K.-H. Rieder, F. Moresco, G. Jimenez-Bueno, C. Wang, G. Rapenne, C. Joachim, *Surf. Sci.* **2005**, *584*, L153 L158.

[387] Nanoscale friction is still a matter of intense investigation and debate, see: a) B. Bhushan, J. N. Israelachvili, U. Landman, *Nature* **1995**, *374*, 607 – 616; b) B. Luan, M. O. Robbins, *Nature* **2005**, *435*, 929 – 932.

[388] a) A. Buldum, J. P. Lu, *Phys. Rev. Lett.* **1999**, *83*, 5050 – 5053; b) B. Ni, S. B. Sinnott, *Surf. Sci.* **2001**, *487*, 87 – 96; c) J. W. Kang, H. J. Hwang, *Nanotechnology* **2004**, *15*, 614 – 621; d) N. Sasaki, K. Miura, *Jpn. J. Appl. Phys.* **2004**, *43*, 4486 – 4491.

[389] a) M. R. Falvo, R. M. Taylor, A. Helser, V. Chi, F. P. Brooks, S. Washburn, R. Superfine, *Nature* **1999**, *397*, 236 – 238; b) M. R. Falvo, J. Steele, R. M. Taylor, R. Superfine, *Phys. Rev. B* **2000**, *62*, R10665 – R10667; c) K. Miura, T. Takagi, S. Kamiya, T. Sahashi, M. Yamauchi, *Nano Lett.* **2001**, *1*, 161 – 163.

[390] a) P. Moriarty, Y. R. Ma, M. D. Upward, P. H. Beton, *Surf. Sci.* **1998**, *407*, 27 – 35; b) K. Miura, S. Kamiya, N. Sasaki, *Phys. Rev. Lett.* **2003**, *90*, 055509; c) D. L. Keeling, M. J. Humphry, R. H. J. Fawcett, P. H. Beton, C. Hobbs, L. Kantorovich, *Phys. Rev. Lett.* **2005**, *94*, 146104.

[391] Y. Shirai, A. J. Osgood, Y. Zhao, K. F. Kelly, J. M. Tour, *Nano Lett.* **2005**, *5*, 2330 – 2334.

[392] a) B. Das, K. L. Sebastian, *Chem. Phys. Lett.* **2000**, *330*, 433 – 439; b) B. Das, K. L. Sebastian, *Chem. Phys. Lett.* **2002**, *357*, 25 – 31.

[393] Y. Fujikawa, J. T. Sadowski, K. F. Kelly, K. S. Nakayama, E. T. Mickelson, R. H. Hauge, J. L. Margrave, T. Sakurai, *Jpn. J. Appl. Phys.* **2002**, *41*, 245 – 249.

[394] a) S. J. Stranick, M. M. Kamna, P. S. Weiss, *Science* **1994**, *266*, 99 – 102; b) R. Otero, F. Hummelink, F. Sato, S. B. Legoas, P. Thostrup, E. Laegsgaard, I. Stensgaard, D. S. Galvão, F. Besenbacher, *Nat. Mater.* **2004**, *3*, 779 – 782.

[395] K. Y. Kwon, K. L. Wong, G. Pawin, L. Bartels, S. Stolbov, T. S. Rahman, *Phys. Rev. Lett.* **2005**, *95*, 166101.

[396] A. Carella, G. Rapenne, J. P. Launay, *New J. Chem.* **2005**, *29*, 288 – 290.

[397] A. Carella, J. Jaud, G. Rapenne, J. P. Launay, *Chem. Commun.* **2003**, 2434 – 2435.

[398] For reviews, see: a) S. M. Block, *Nature* **1992**, *360*, 493 – 495; b) S. C. Kuo, M. P. Sheetz, *Trends Cell Biol.* **1992**, *2*, 116 – 118; c) T. Yanagida, Y. Harada, A. Ishijima, *Trends Biochem. Sci.* **1993**, *18*, 319 – 324; d) K. Svoboda, S. M. Block, *Annu. Rev.*

Biophys. Biomol. Struct. **1994**, *23*, 247 – 285; e) A. D. Mehta, M. Rief, J. A. Spudich, D. A. Smith, R. M. Simmons, *Science* **1999**, *283*, 1689 – 1695; f) C. Bustamante, J. C. Macosko, G. J. L. Wuite, *Nat. Rev. Mol. Cell Biol.* **2000**, *1*, 130 – 136; g) J. F. Allemand, D. Bensimon, V. Croquette, *Curr. Opin. Struct. Biol.* **2003**, *13*, 266 – 274; h) X. Zhuang, *Science* **2004**, *305*, 188 – 190; i) K. C. Neuman, S. M. Block, *Rev. Sci. Instrum.* **2004**, *75*, 2787 – 2809.

[399] Y. Arai, R. Yasuda, K. Akashi, Y. Harada, H. Miyata, K. Kinosita, H. Itoh, *Nature* **1999**, *399*, 446 – 448.

[400] a) P. Y. Chiou, A. T. Ohta, M. C. Wu, *Nature* **2005**, *436*, 370 – 372; b) K. Dholakia, *Nat. Mater.* **2005**, *4*, 579 – 580.

[401] For reviews, see: a) W. E. Moerner, T. Basché, *Angew. Chem.* **1993**, *105*, 537 – 557; *Angew. Chem. Int. Ed. Engl.* **1993**, *32*, 457 – 476; b) W. E. Moerner, *Science* **1994**, *265*, 46 – 53; c) W. E. Moerner, *Acc. Chem. Res.* **1996**, *29*, 563 – 571; d) X. S. Xie, *Acc. Chem. Res.* **1996**, *29*, 598 – 606; e) P. M. Goodwin, W. P. Ambrose, R. A. Keller, *Acc. Chem. Res.* **1996**, *29*, 607 – 613; f) S. M. Nie, R. N. Zare, *Annu. Rev. Biophys. Biomol. Struct.* **1997**, *26*, 567 – 596; g) T. Plakhotnik, E. A. Donley, U. P. Wild, *Annu. Rev. Phys. Chem.* **1997**, *48*, 181 – 212; h) X. S. Xie, J. K. Trautman, *Annu. Rev. Phys. Chem.* **1998**, *49*, 441 – 480; i) W. E. Moerner, M. Orrit, *Science* **1999**, *283*, 1670 – 1676; j) S. Weiss, *Science* **1999**, *283*, 1676 – 1683; k) W. P. Ambrose, P. M. Goodwin, J. H. Jett, A. Van Orden, J. H. Werner, R. A. Keller, *Chem. Rev.* **1999**, *99*, 2929 – 2956; l) A. A. Deniz, T. A. Laurence, M. Dahan, D. S. Chemla, P. G. Schultz, S. Weiss, *Annu. Rev. Phys. Chem.* **2001**, *52*, 233 – 253; m) W. E. Moerner, *J. Phys. Chem. B* **2002**, *106*, 910 – 927; n) R. A. Keller, W. P. Ambrose, A. A. Arias, H. Gai, S. R. Emory, P. M. Goodwin, J. H. Jett, *Anal. Chem.* **2002**, *74*, 316a – 324a; o) special issue on "Single-Molecule Physics and Chemistry": *J. Chem. Phys.* **2002**, *117*, 10923–11033; p) M. Bohmer, J. Enderlein, *ChemPhysChem* **2003**, *4*, 793 – 808; q) W. E. Moerner, D. P. Fromm, *Rev. Sci. Instrum.* **2003**, *74*, 3597 – 3619; r) P. Tinnefeld, M. Sauer, *Angew. Chem.* **2005**, *117*, 2698 – 2728; *Angew. Chem. Int. Ed.* **2005**, *44*, 2642 – 2671; s) special issue on "Single-Molecule Spectroscopy": *Acc. Chem. Res.* **2005**, *38*, 503 – 610.

[402] N. Fang, H. Lee, C. Sun, X. Zhang, *Science* **2005**, *308*, 534 – 537.

[403] For reviews see: a) R. M. Crooks, A. J. Ricco, *Acc. Chem. Res.* **1998**, *31*, 219 – 227; b) L. M. Goldenberg, M. R. Bryce, M. C. Petty, *J. Mater. Chem.* **1999**, *9*, 1957 – 1974; c) S. Flink, F. C. J. M. van Veggel, D. N. Reinhoudt, *Adv. Mater.* **2000**, *12*, 1315 – 1328; d) A. N. Shipway, E. Katz, I. Willner, *ChemPhysChem* **2000**, *1*, 18 – 52; e) E. Katz, I. Willner, *Electroanalysis* **2003**, *15*, 913 – 947; f) G. Cooke, *Angew. Chem.* **2003**, *115*, 5008 – 5018; *Angew. Chem. Int. Ed.* **2003**, *42*, 4860 – 4870; g) D. Astruc, M.-C. Daniel, J. Ruiz, *Chem. Commun.* **2004**, 2637 – 2649; h) U. Drechsler, B. Erdogan, V. M. Rotello, *Chem. Eur. J.* **2004**, *10*, 5570 – 5579.

[404] A reversible recognition event has also been observed in a nanoporous silicate matrix, see: a) S. Y. Chia, J. Cao, J. F. Stoddart, J. I. Zink, *Angew. Chem.* **2001**, *113*, 2513 – 2517; *Angew. Chem. Int. Ed.* **2001**, *40*, 2447 – 2451; for other molecular-recognition processes occurring within solids, see: b) T. E. Mallouk, J. A. Gavin, *Acc. Chem. Res.* **1998**, *31*, 209 – 217.

[405] R. Hernandez, H.-R. Tseng, J. W. Wong, J. F. Stoddart, J. I. Zink, *J. Am. Chem. Soc.* **2004**, *126*, 3370 – 3371.

[406] T. Gase, D. Grando, P. A. Chollet, F. Kajzar, A. Murphy, D. A. Leigh, *Adv. Mater.* **1999**, *11*, 1303 – 1305.

[407] For a computational study of the conformations and co-conformational dynamics of the same molecule on a graphite surface, see: M. S. Deleuze, *J. Am. Chem. Soc.* **2000**, *122*, 1130 – 1143.

[408] G. Bidan, M. Billon, B. Divisia-Blohorn, J.-M. Kern, L. Raehm, J.-P. Sauvage, *New J. Chem.* **1998**, *22*, 1139 – 1141.

[409] L. Raehm, J.-M. Kern, J.-P. Sauvage, C. Hamann, S. Palacin, J. P. Bourgoin, *Chem. Eur. J.* **2002**, *8*, 2153 – 2162.

[410] H.-R. Tseng, D. M. Wu, N. X. L. Fang, X. Zhang, J. F. Stoddart, *ChemPhysChem* **2004**, *5*, 111 – 116.

[411] T. J. Huang, H.-R. Tseng, L. Sha, W. X. Lu, B. Brough, A. H. Flood, B.-D. Yu, P. C. Celestre, J. P. Chang, J. F. Stoddart, C.-M. Ho, *Nano Lett.* **2004**, *4*, 2065 – 2071.

[412] B. Long, K. Nikitin, D. Fitzmaurice, *J. Am. Chem. Soc.* **2003**, *125*, 15490 – 15498.

[413] K. Nikitin, D. Fitzmaurice, *J. Am. Chem. Soc.* **2005**, *127*, 8067 – 8076.

[414] R. A. van Delden, M. K. J. ter Wiel, M. M. Pollard, J. Vicario, N. Koumura, B. L. Feringa, *Nature* **2005**, *437*, 1337 – 1340.

[415] Attachment of triptycene-based rotors (such as those discussed in Sections 2.1.1 and 2.1.2) to surfaces has been simulated computationally, see: S. M. Hou, T. Sagara, D. C. Xu, T. R. Kelly, E. Ganz, *Nanotechnology* **2003**, *14*, 566 – 570.

[416] a) T. E. Glass, *J. Am. Chem. Soc.* **2000**, *122*, 4522 – 4523; b) J. Raker, T. E. Glass, *Tetrahedron* **2001**, *57*, 10233 – 10240; c) J. Raker, T. E. Glass, *J. Org. Chem.* **2001**, *66*, 6505 – 6512; d) J. Raker, T. E. Glass, *J. Org. Chem.* **2002**, *67*, 6113 – 6116.

[417] For an example of binding-induced conformational control leading to changes in the electronic properties of oligothiophenes, see: a) B. Jousselme, P. Blanchard, E. Levillain, J. Delaunay, M. Allain, P. Richomme, D. Rondeau, N. Gallego-Planas, J. Roncali, *J. Am. Chem. Soc.* **2003**, *125*, 1363 – 1370; in polyether-substituted poly(thiophene)s—and in other conjugated polymers—changes in electronic properties can often be attributed to electrostatic interactions on ion doping. For examples where binding-induced conformational changes of the polymer backbone are thought to play a role, see: b) J. Roncali, R. Garreau, D. Delabouglise, F. Garnier, M. Lemaire, *J. Chem. Soc. Chem. Commun.* **1989**, 679 – 681; c) J. Roncali, L. H. Shi, F. Garnier, *J. Phys. Chem.* **1991**, *95*, 8983 – 8989; d) M. J. Marsella, T. M. Swager, *J. Am. Chem. Soc.* **1993**, *115*, 12214 – 12215; e) M. J. Marsella, R. J. Newland, P. J. Carroll, T. M. Swager, *J. Am. Chem. Soc.* **1995**, *117*, 9842 – 9848; for an example of similar effects in bipyridyl-substitued poly(phenylvinylene), see: f) B. Wang, M. R. Wasielewski, *J. Am. Chem. Soc.* **1997**, *119*, 12 – 21.

[418] For reviews on functionalised poly(thiophene)s, see: a) J. Roncali, *J. Mater. Chem.* **1999**, *9*, 1875 – 1893; b) D. T. McQuade, A. E. Pullen, T. M. Swager, *Chem. Rev.* **2000**, *100*, 2537 – 2574; c) G. Barbarella, M. Melucci, G. Sotgiu, *Adv. Mater.* **2005**, *17*, 1581 – 1593.

[419] Similar changes to electronic properties can be observed on application of a photonic stimulus to oligothiophenes appended with an azobenzene moiety, see: a) B. Jousselme, P. Blanchard, N. Gallego-Planas, J. Delaunay, M. Allain, P. Richomme, E. Levillain, J. Roncali, *J. Am. Chem. Soc.* **2003**, *125*, 2888 – 2889; b) B. Jousselme, P. Blanchard, N. Gallego-Planas, E. Levillain, J. Delaunay, M. Allain, P. Richomme, J. Roncali, *Chem. Eur. J.* **2003**, *9*, 5297 – 5306.

[420] D. H. R. Barton, *Science* **1970**, *169*, 539 – 544.

[421] J. Clayden, A. Lund, L. S. Vallverdu, M. Helliwell, *Nature* **2004**, *431*, 966 – 971.

[422] a) H. Yuasa, N. Miyagawa, T. Izumi, M. Nakatani, M. Izumi, H. Hashimoto, *Org. Lett.* **2004**, *6*, 1489 – 1492; for other examples of chair-flip-based conformational switches, see: b) C. Monahan, J. T. Bien, B. D. Smith, *Chem. Commun.* **1998**, 431 – 432.

[423] M. Barboiu, L. Prodi, M. Montalti, N. Zaccheroni, N. Kyritsakas, J.-M. Lehn, *Chem. Eur. J.* **2004**, *10*, 2953 – 2959.

[424] M. Linke-Schaetzel, C. E. Anson, A. K. Powell, G. Buth, E. Palomares, J. D. Durrant, T. S. Balaban, J.-M. Lehn, *Chem. Eur. J.* **2006**, *12*, 1931 – 1940; for an example of using the cation-triggered conformational change of terpyridines to vary the through-space electronic properties of two quinone substitu-

ents, see: M. Buschel, M. Helldobler, J. Daub, *Chem. Commun.* **2002**, 1338 – 1339.

[425] a) J. Berninger, R. Krauss, H. G. Weinig, U. Koert, B. Ziemer, K. Harms, *Eur. J. Org. Chem.* **1999**, 875 – 884; b) R. Krauss, H. G. Weinig, M. Seydack, J. Bendig, U. Koert, *Angew. Chem.* **2000**, *112*, 1905 – 1908; *Angew. Chem. Int. Ed.* **2000**, *39*, 1835 – 1837; c) H. G. Weinig, R. Krauss, M. Seydack, J. Bendig, U. Koert, *Chem. Eur. J.* **2001**, *7*, 2075 – 2088.

[426] U. Koert, R. Krauss, H. G. Weinig, C. Heumann, B. Ziemer, C. Mugge, M. Seydack, J. Bendig, *Eur. J. Org. Chem.* **2001**, 575 – 586.

[427] M. Karle, D. Bockelmann, D. Schumann, C. Griesinger, U. Koert, *Angew. Chem.* **2003**, *115*, 4684 – 4687; *Angew. Chem. Int. Ed.* **2003**, *42*, 4546 – 4549.

[428] V. A. Azov, A. Schlegel, F. Diederich, *Angew. Chem.* **2005**, *117*, 4711 – 4715; *Angew. Chem. Int. Ed.* **2005**, *44*, 4635 – 4638.

[429] a) M. C. Jiménez, C. Dietrich-Buchecker, J.-P. Sauvage, *Angew. Chem.* **2000**, *112*, 3422 – 3425; *Angew. Chem. Int. Ed.* **2000**, *39*, 3284 – 3287; b) M. C. Jiménez-Molero, C. Dietrich-Buchecker, J.-P. Sauvage, *Chem. Eur. J.* **2002**, *8*, 1456 – 1466.

[430] E. M. Pérez, D. T. F. Dryden, D. A. Leigh, G. Teobaldi, F. Zerbetto, *J. Am. Chem. Soc.* **2004**, *126*, 12210 – 12211.

[431] G. Bottari, D. A. Leigh, E. M. Pérez, *J. Am. Chem. Soc.* **2003**, *125*, 13360 – 13361.

[432] In a related photoswitched system, the position of a pyridinium-containing macrocycle is used to influence the interaction between two fluorophores attached to the thread, thus illiciting an optical response on shuttling, see a) Y. J. Li, H. Li, Y. L. Li, H. B. Liu, S. Wang, X. R. He, N. Wang, D. B. Zhu, *Org. Lett.* **2005**, *7*, 4835 – 4838; modification of a FRET response between fluorophores appended to the macrocycle and thread has also been demonstrated in a solvent-switchable hydrogen-bonded system, see b) H. Onagi, J. Rebek, Jr., *Chem. Commun.* **2005**, 4604 – 4606.

[433] Q.-C. Wang, D.-H. Qu, J. Ren, K. Chen, H. Tian, *Angew. Chem.* **2004**, *116*, 2715 – 2719; *Angew. Chem. Int. Ed.* **2004**, *43*, 2661 – 2665.

[434] During synthesis, the directional isomer of (*E*)-**133**·2H shown in Scheme 79 was formed exclusively but seems to arise by a kinetic trapping mechanism rather than from the thermodynamic stability of this product, see: Section 4.3.1 and Ref. [50k].

[435] a) D.-H. Qu, Q.-C. Wang, J. Ren, H. Tian, *Org. Lett.* **2004**, *6*, 2085 – 2088; b) D.-H. Qu, Q.-C. Wang, H. Tian, *Mol. Cryst. Liq. Cryst.* **2005**, *430*, 59 – 65.

[436] As well as a photochemical switching mechanism, it was found in one example that the position of the ring—and therefore the fluorescence intensities—could also be controlled by temperature, see Ref. [435b].

[437] D.-H. Qu, Q.-C. Wang, X. Ma, H. Tian, *Chem. Eur. J.* **2005**, *11*, 5929 – 5937.

[438] J. Elemans, E. J. A. Bijsterveld, A. E. Rowan, R. J. M. Nolte, *Chem. Commun.* **2000**, 2443 – 2444.

[439] a) P. Thordarson, E. J. A. Bijsterveld, A. E. Rowan, R. J. M. Nolte, *Nature* **2003**, *424*, 915 – 918; b) P. Thordarson, R. J. M. Nolte, A. E. Rowan, *Aust. J. Chem.* **2004**, *57*, 323 – 327; c) P. R. Carlier, *Angew. Chem.* **2004**, *116*, 2654 – 2657; *Angew. Chem. Int. Ed.* **2004**, *43*, 2602 – 2605.

[440] For detailed accounts of the development of these devices, see Refs. [191h,x,y].

[441] a) C. P. Collier, E. W. Wong, M. Belohradský, F. M. Raymo, J. F. Stoddart, P. J. Kuekes, R. S. Williams, J. R. Heath, *Science* **1999**, *285*, 391 – 394; b) E. W. Wong, C. P. Collier, M. Bìhloradský, F. M. Raymo, J. F. Stoddart, J. R. Heath, *J. Am. Chem. Soc.* **2000**, *122*, 5831 – 5840.

[442] a) R. C. Ahuja, P.-L. Caruso, D. Möbius, G. Wildburg, H. Ringsdorf, D. Philp, J. A. Preece, J. F. Stoddart, *Langmuir* **1993**, *9*, 1534 – 1544; b) R. C. Ahuja, P.-L. Caruso, D. Möbius, D. Philp, J. A. Preece, H. Ringsdorf, J. F. Stoddart, G. Wildburg, *Thin Solid Films* **1996**, *285*, 671 – 677; c) C. L. Brown, U. Jonas, J. A. Preece, H. Ringsdorf, M. Seitz, J. F. Stoddart, *Langmuir* **2000**, *16*, 1924 – 1930; d) M. Asakawa, M. Higuchi, G. Mattersteig, T. Nakamura, A. R. Pease, F. M. Raymo, T. Shimizu, J. F. Stoddart, *Adv. Mater.* **2000**, *12*, 1099 – 1102.

[443] C. P. Collier, G. Mattersteig, E. W. Wong, Y. Luo, K. Beverly, J. Sampaio, F. M. Raymo, J. F. Stoddart, J. R. Heath, *Science* **2000**, *289*, 1172 – 1175.

[444] C. P. Collier, J. O. Jeppesen, Y. Luo, J. Perkins, E. W. Wong, J. R. Heath, J. F. Stoddart, *J. Am. Chem. Soc.* **2001**, *123*, 12632 – 12641.

[445] Y. Luo, C. P. Collier, J. O. Jeppesen, K. A. Nielsen, E. Delonno, G. Ho, J. Perkins, H.-R. Tseng, T. Yamamoto, J. F. Stoddart, J. R. Heath, *ChemPhysChem* **2002**, *3*, 519 – 525.

[446] D. W. Steuerman, H.-R. Tseng, A. J. Peters, A. H. Flood, J. O. Jeppesen, K. A. Nielsen, J. F. Stoddart, J. R. Heath, *Angew. Chem.* **2004**, *116*, 6648 – 6653; *Angew. Chem. Int. Ed.* **2004**, *43*, 6486 – 6491.

[447] W.-Q. Deng, R. P. Muller, W. A. Goddard, *J. Am. Chem. Soc.* **2004**, *126*, 13562 – 13563.

[448] a) I. C. Lee, C. W. Frank, T. Yamamoto, H.-R. Tseng, A. H. Flood, J. F. Stoddart, *Langmuir* **2004**, *20*, 5809 – 5828; b) K. Nørgaard, J. O. Jeppesen, B. A. Laursen, J. B. Simonsen, M. J. Weygand, K. Kjaer, J. F. Stoddart, T. Bjørnholm, *J. Phys. Chem. B* **2005**, *109*, 1063 – 1066.

[449] S. S. Jang, Y. H. Jang, Y. H. Kim, W. A. Goddard, J. W. Choi, J. R. Heath, B. W. Laursen, A. H. Flood, J. F. Stoddart, K. Nørgaard, T. Bjørnholm, *J. Am. Chem. Soc.* **2005**, *127*, 14804 – 14816.

[450] Y. H. Jang, S. G. Hwang, Y. H. Kim, S. S. Jang, W. A. Goddard, *J. Am. Chem. Soc.* **2004**, *126*, 12636 – 12645.

[451] a) S. S. Jang, Y. H. Jang, Y. H. Kim, W. A. Goddard, A. H. Flood, B. W. Laursen, H.-R. Tseng, J. F. Stoddart, J. O. Jeppesen, J. W. Choi, D. W. Steuerman, E. Delonno, J. R. Heath, *J. Am. Chem. Soc.* **2005**, *127*, 1563 – 1575; b) Y. H. Jang, S. S. Jang, W. A. Goddard, *J. Am. Chem. Soc.* **2005**, *127*, 4959 – 4964.

[452] Y. H. Kim, S. S. Jang, Y. H. Jang, W. A. Goddard, *Phys. Rev. Lett.* **2005**, *94*, 156801.

[453] J. H. Huang, A. H. Flood, C.-W. Chu, S. Kang, T.-F. Guo, T. Yamamoto, H.-R. Tseng, B.-D. Yu, Y. Yang, J. F. Stoddart, C.-M. Ho, *IEEE Trans: Nanotechnol.* **2003**, *2*, 698 – 701.

[454] K. Nørgaard, B. W. Laursen, S. Nygaard, K. Kjaer, H.-R. Tseng, A. H. Flood, J. F. Stoddart, T. Bjørnholm, *Angew. Chem.* **2005**, *117*, 7197 – 7201; *Angew. Chem. Int. Ed.* **2005**, *44*, 7035 – 7039.

[455] a) H. B. Yu, Y. Luo, K. Beverly, J. F. Stoddart, H.-R. Tseng, J. R. Heath, *Angew. Chem.* **2003**, *115*, 5884 – 5889; *Angew. Chem. Int. Ed.* **2003**, *42*, 5706 – 5711; b) Y. Chen, D. A. A. Ohlberg, X. M. Li, D. R. Stewart, R. S. Williams, J. O. Jeppesen, K. A. Nielsen, J. F. Stoddart, D. L. Olynick, E. Anderson, *Appl. Phys. Lett.* **2003**, *82*, 1610 – 1612; c) Y. Chen, G. Y. Jung, D. A. A. Ohlberg, X. M. Li, D. R. Stewart, J. O. Jeppesen, K. A. Nielsen, J. F. Stoddart, R. S. Williams, *Nanotechnology* **2003**, *14*, 462 – 468; d) D. R. Stewart, D. A. A. Ohlberg, P. A. Beck, Y. Chen, R. S. Williams, J. O. Jeppesen, K. A. Nielsen, J. F. Stoddart, *Nano Lett.* **2004**, *4*, 133 – 136.

[456] J. R. Heath, M. A. Ratner, *Phys. Today* **2003**, *56*(5), 43 – 49. In fact, Williams and co-workers have investigated the possibility of using filament formation between two metal electrodes, separated by an insulating organic single-molecule layer, to create a switching device, see: C. N. Lau, D. R. Stewart, R. S. Williams, M. Bockrath, *Nano Lett.* **2004**, *4*, 569 – 572.

[457] M. R. Diehl, D. W. Steuerman, H.-R. Tseng, S. A. Vignon, A. Star, P. C. Celestre, J. F. Stoddart, J. R. Heath, *ChemPhysChem* **2003**, *4*, 1335 – 1339.

[458] a) K. Ichimura, *Chem. Rev.* **2000**, *100*, 1847 – 1873; b) N. Tamaoki, *Adv. Mater.* **2001**, *13*, 1135 – 1147; c) T. Ikeda, A.

Kanazawa in *Molecular Switches* (Ed.: B. L. Feringa), Wiley-VCH, Weinheim, **2001**, pp. 363 – 397.

[459] a) T. Kosa, E. Weinan, P. Palffy-Muhoray, *Int. J. Eng. Sci.* **2000**, *38*, 1077 – 1084; b) P. Palffy-Muhoray, T. Kosa, E. Weinan, *Mol. Cryst. Liq. Cryst.* **2002**, *375*, 577 – 591; c) P. Palffy-Muhoray, T. Kosa, E. Weinan, *Appl. Phys. A* **2002**, *75*, 293 – 300; d) P. Palffy-Muhoray, T. Kosa, W. E, *Braz. J. Phys.* **2002**, *32*, 552 – 563.

[460] R. A. van Delden, T. Mecca, C. Rosini, B. L. Feringa, *Chem. Eur. J.* **2004**, *10*, 61 – 70.

[461] a) For the switching of the cholesteric screw sense by photoconversion between two pseudoenantiomeric overcrowded alkene diastereomers, see: B. L. Feringa, N. P. M. Huck, H. A. Vandoren, *J. Am. Chem. Soc.* **1995**, *117*, 9929 – 9930; b) for inversion of handedness in the liquid-crystal phase by generating an enantiomeric excess (of extremely low magnitude) in an overcrowded alkene dopant by irradiation with circularly polarized light, see: N. P. M. Huck, W. F. Jager, B. de Lange, B. L. Feringa, *Science* **1996**, *273*, 1686 – 1688; c) for reversal of handedness in the cholesteric phase using two competing chiral dopants—one of switchable twisting ability, the other one photoinert—see: T. Sagisaka, Y. Yokoyama, *Bull. Chem. Soc. Jpn.* **2000**, *73*, 191 – 196; d) for color control through variation of pitch in a cholesteric liquid-crystalline film by photoinduced alteration of the pseudoenantiomeric ratio for an overcrowded alkene dopant, followed by fixing of the state by photopolymerization, see: R. A. van Delden, M. B. van Gelder, N. P. M. Huck, B. L. Feringa, *Adv. Funct. Mater.* **2003**, *13*, 319 – 324.

[462] R. A. van Delden, N. Koumura, N. Harada, B. L. Feringa, *Proc. Natl. Acad. Sci. USA* **2002**, *99*, 4945 – 4949.

[463] D. A. Leigh, M. A. F. Morales, E. M. Pérez, J. K. Y. Wong, C. G. Saiz, A. M. Z. Slawin, A. J. Carmichael, D. M. Haddleton, A. M. Brouwer, W. J. Buma, G. W. H. Wurpel, S. León, F. Zerbetto, *Angew. Chem.* **2005**, *117*, 3122 – 3127; *Angew. Chem. Int. Ed.* **2005**, *44*, 3062 – 3067.

[464] W.-Q. Deng, A. H. Flood, J. F. Stoddart, W. A. Goddard, *J. Am. Chem. Soc.* **2005**, *127*, 15 994 – 15 995.

[465] For reviews which compare the characteristics of various different actuator materials, see: a) J. D. W. Madden, N. A. Vandesteeg, P. A. Anquetil, P. G. A. Madden, A. Takshi, R. Z. Pytel, S. R. Lafontaine, P. A. Wieringa, I. W. Hunter, *IEEE J. Oceanic Eng.* **2004**, *29*, 706 – 728; b) R. H. Baughman, *Science* **2005**, *308*, 63 – 65; for reviews concentrating on specific molecular strategies, see below.

[466] For reviews on the development of this field, and progress towards applications, see: a) T. Tanaka, *Sci. Am.* **1981**, *244*(1), 110 – 123; b) H. G. Schild, *Prog. Polym. Sci.* **1992**, *17*, 163 – 249; c) K. Kajiwara, S. B. Ross-Murphy, *Nature* **1992**, *355*, 208 – 209; d) Y. Osada, J. P. Gong, *Prog. Polym. Sci.* **1993**, *18*, 187 – 226; e) Y. Osada, S. B. Ross-Murphy, *Sci. Am.* **1993**, *268*(5), 82 – 87; f) Y. Osada, J. P. Gong, *Adv. Mater.* **1998**, *10*, 827 – 837; g) M. Shahinpoor, Y. Bar-Cohen, J. O. Simpson, J. Smith, *Smart Mater. Struct.* **1998**, *7*, R15-R30.

[467] a) I. Z. Steinberg, A. Oplatka, A. Katchalsky, *Nature* **1966**, *210*, 568 – 571; b) M. V. Sussman, A. Katchalsky, *Science* **1970**, *167*, 45 – 47.

[468] Rather than using entirely synthetic gels, in practice Katchalsky's devices employed cross-linked collagen fibres. The ability of various natural polypeptides and protein bodies to undergo reversible, stimuli-induced conformational changes resulting in free-energy transduction has since been extensively studied, both from the perspective of understanding such processes in nature and also for artificial applications. For reviews, see: Ref. [97k] and a) D. W. Urry, *J. Phys. Chem. B* **1997**, *101*, 11 007 – 11 028; b) D. W. Urry, *Biopolymers* **1998**, *47*, 167 – 178; c) C. Mavroidis, A. Dubey, *Nat. Mater.* **2003**, *2*, 573 – 574.

[469] S. Juodkazis, N. Mukai, R. Wakaki, A. Yamaguchi, S. Matsuo, H. Misawa, *Nature* **2000**, *408*, 178 – 181.

[470] a) R. Yoshida, T. Takahashi, T. Yamaguchi, H. Ichijo, *J. Am. Chem. Soc.* **1996**, *118*, 5134 – 5135; b) R. Yoshida, E. Kokufuta, T. Yamaguchi, *Chaos* **1999**, *9*, 260 – 266; c) R. Yoshida, G. Otoshi, T. Yamaguchi, E. Kokufuta, *J. Phys. Chem. A* **2001**, *105*, 3667 – 3672; d) C. J. Crook, A. Smith, R. A. L. Jones, A. J. Ryan, *Phys. Chem. Chem. Phys.* **2002**, *4*, 1367 – 1369; e) R. Yoshida, K. Takei, T. Yamaguchi, *Macromolecules* **2003**, *36*, 1759 – 1761; f) J. R. Howse, P. Topham, C. J. Crook, A. J. Gleeson, W. Bras, R. A. L. Jones, A. J. Ryan, *Nano Lett.* **2006**, *6*, 73 – 77.

[471] a) C. D. Jones, L. A. Lyon, *Macromolecules* **2000**, *33*, 8301 – 8306; b) I. Berndt, W. Richtering, *Macromolecules* **2003**, *36*, 8780 – 8785; c) I. Berndt, J. S. Pedersen, W. Richtering, *J. Am. Chem. Soc.* **2005**, *127*, 9372 – 9373; d) I. Berndt, C. Popescu, F. J. Wortmann, W. Richtering, *Angew. Chem.* **2006**, *118*, 1099 – 1102; *Angew. Chem. Int. Ed.* **2006**, *45*, 1081 – 1085; e) I. Berndt, J. S. Pedersen, W. Richtering, *Angew. Chem.* **2006**, *118*, 1769 – 1773; *Angew. Chem. Int. Ed.* **2006**, *45*, 1737 – 1741.

[472] a) S. Kiyonaka, K. Sugiyasu, S. Shinkai, I. Hamachi, *J. Am. Chem. Soc.* **2002**, *124*, 10 954 – 10 955; b) S. L. Zhou, S. Matsumoto, H. D. Tian, H. Yamane, A. Ojida, S. Kiyonaka, I. Hamachi, *Chem. Eur. J.* **2005**, *11*, 1130 – 1136.

[473] a) T. Tanaka, C. N. Wang, V. Pande, A. Y. Grosberg, A. English, S. Masamune, H. Gold, R. Levy, K. King, *Faraday Discuss.* **1995**, *101*, 201 – 206; b) T. Oya, T. Enoki, A. Y. Grosberg, S. Masamune, T. Sakiyama, Y. Takeoka, K. Tanaka, G. Q. Wang, Y. Yilmaz, M. S. Feld, R. Dasari, T. Tanaka, *Science* **1999**, *286*, 1543 – 1545.

[474] a) D. J. Beebe, J. S. Moore, J. M. Bauer, Q. Yu, R. H. Liu, C. Devadoss, B. H. Jo, *Nature* **2000**, *404*, 588 – 590; b) Q. Yu, J. M. Bauer, J. S. Moore, D. J. Beebe, *Appl. Phys. Lett.* **2001**, *78*, 2589 – 2591; c) R. H. Liu, Q. Yu, D. J. Beebe, *J. Microelectromech. Syst.* **2002**, *11*, 45 – 53.

[475] Y. Osada, H. Okuzaki, H. Hori, *Nature* **1992**, *355*, 242 – 244.

[476] a) S. S. Pennadam, M. D. Lavigne, C. F. Dutta, K. Firman, D. Mernagh, D. C. Górecki, C. Alexander, *J. Am. Chem. Soc.* **2004**, *126*, 13 208 – 13 209; b) S. S. Pennadam, K. Firman, C. Alexander, D. C. Górecki, *J. Nanobiotechnology* **2004**, *2*, 8.

[477] For reviews, see: a) I. Y. Galaev, B. Mattiasson, *Trends Biotechnol.* **1999**, *17*, 335 – 340; b) N. A. Peppas, Y. Huang, M. Torres-Lugo, J. H. Ward, J. Zhang, *Annu. Rev. Biomed. Eng.* **2000**, *2*, 9 – 29; c) Y. Qiu, K. Park, *Adv. Drug Delivery Rev.* **2001**, *53*, 321 – 339; d) B. Jeong, A. Gutowska, *Trends Biotechnol.* **2002**, *20*, 305 – 311; e) J. Kopecek, *Nature* **2002**, *417*, 388 – 391; f) R. Langer, D. A. Tirrell, *Nature* **2004**, *428*, 487 – 492.

[478] a) E. Kokufata, Y.-Q. Zhang, T. Tanaka, *Nature* **1991**, *351*, 302 – 304; b) M. Irie, Y. Misumi, T. Tanaka, *Polymer* **1993**, *34*, 4531 – 4535; c) J. H. Holtz, S. A. Asher, *Nature* **1997**, *389*, 829 – 832; d) J. H. Holtz, J. S. W. Holtz, C. H. Munro, S. A. Asher, *Anal. Chem.* **1998**, *70*, 780 – 791; e) T. Miyata, N. Asami, T. Uragami, *Nature* **1999**, *399*, 766 – 769; f) K. Lee, S. A. Asher, *J. Am. Chem. Soc.* **2000**, *122*, 9534 – 9537; g) C. E. Reese, M. E. Baltusavich, J. P. Keim, S. A. Asher, *Anal. Chem.* **2001**, *73*, 5038 – 5042; h) S. A. Asher, V. L. Alexeev, A. V. Goponenko, A. C. Sharma, I. K. Lednev, C. S. Wilcox, D. N. Finegold, *J. Am. Chem. Soc.* **2003**, *125*, 3322 – 3329; i) S. A. Asher, A. C. Sharma, A. V. Goponenko, M. M. Ward, *Anal. Chem.* **2003**, *75*, 1676 – 1683; j) V. L. Alexeev, A. C. Sharma, A. V. Goponenko, S. Das, I. K. Lednev, C. S. Wilcox, D. N. Finegold, S. A. Asher, *Anal. Chem.* **2003**, *75*, 2316 – 2323; k) C. E. Reese, S. A. Asher, *Anal. Chem.* **2003**, *75*, 3915 – 3918; l) H.-J. Schneider, T. J. Liu, N. Lomadze, *Angew. Chem.* **2003**, *115*, 3668 – 3671; *Angew. Chem. Int. Ed.* **2003**, *42*, 3544 – 3546; m) V. L. Alexeev, S. Das, D. N. Finegold, S. A. Asher, *Clin. Chem.* **2004**, *50*, 2353 – 2360; n) A. C. Sharma, T. Jana, R. Kesavamoorthy, L. J. Shi, M. A.

Virji, D. N. Finegold, S. A. Asher, *J. Am. Chem. Soc.* **2004**, *126*, 2971 – 2977; o) H.-J. Schneider, T. J. Liu, *Chem. Commun.* **2004**, 100 – 101; p) H.-J. Schneider, L. Tianjun, N. Lomadze, *Chem. Commun.* **2004**, 2436 – 2437; q) H.-J. Schneider, T. J. Liu, N. Lomadze, B. Palm, *Adv. Mater.* **2004**, *16*, 613 – 615; r) A. V. Goponenko, S. A. Asher, *J. Am. Chem. Soc.* **2005**, *127*, 10753 – 10759.

[479] For reviews covering shape memory in a number of polymeric systems, see: a) Z. G. Wei, R. Sandstrom, S. Miyazaki, *J. Mater. Sci.* **1998**, *33*, 3743 – 3762; b) A. Lendlein, S. Kelch, *Angew. Chem.* **2002**, *114*, 2138 – 2162; *Angew. Chem. Int. Ed.* **2002**, *41*, 2034 – 2057.

[480] T. F. Scott, A. D. Schneider, W. D. Cook, C. N. Bowman, *Science* **2005**, *308*, 1615 – 1617.

[481] A. Lendlein, H. Y. Jiang, O. Junger, R. Langer, *Nature* **2005**, *434*, 879 – 882.

[482] For reviews see: a) R. H. Baughman, *Synth. Met.* **1996**, *78*, 339 – 353; b) T. F. Otero, J. M. Sansiñena, *Adv. Mater.* **1998**, *10*, 491 – 494; c) E. W. H. Jager, E. Smela, O. Inganas, *Science* **2000**, *290*, 1540 – 1545; d) E. Smela, *Adv. Mater.* **2003**, *15*, 481 – 494.

[483] J. M. Sansiñena, V. Olazábal, T. F. Otero, C. N. P. da Fonseca, M.-A. De Paoli, *Chem. Commun.* **1997**, 2217 – 2218.

[484] J. D. Madden, R. A. Cush, T. S. Kanigan, C. J. Brenan, I. W. Hunter, *Synth. Met.* **1999**, *105*, 61 – 64.

[485] W. Lu, A. G. Fadeev, B. H. Qi, E. Smela, B. R. Mattes, J. Ding, G. M. Spinks, J. Mazurkiewicz, D. Z. Zhou, G. G. Wallace, D. R. MacFarlane, S. A. Forsyth, M. Forsyth, *Science* **2002**, *297*, 983 – 987.

[486] L. M. Low, S. Seetharaman, K. Q. He, M. J. Madou, *Sens. Actuators B* **2000**, *67*, 149 – 160.

[487] K. J. Lin, S. J. Fu, C. Y. Cheng, W. H. Chen, H. M. Kao, *Angew. Chem.* **2004**, *116*, 4282 – 4285; *Angew. Chem. Int. Ed.* **2004**, *43*, 4186 – 4189.

[488] R. H. Baughman, C. X. Cui, A. A. Zakhidov, Z. Iqbal, J. N. Barisci, G. M. Spinks, G. G. Wallace, A. Mazzoldi, D. De Rossi, A. G. Rinzler, O. Jaschinski, S. Roth, M. Kertesz, *Science* **1999**, *284*, 1340 – 1344.

[489] B. Raguse, K.-H. Müller, L. Wieczorek, *Adv. Mater.* **2003**, *15*, 922 – 926.

[490] C. D. Eisenbach, *Polymer* **1980**, *21*, 1175 – 1179.

[491] For extensive reviews of azo-containing polymers and their various switchable properties, see: a) G. S. Kumar, D. C. Neckers, *Chem. Rev.* **1989**, *89*, 1915 – 1925; b) S. Xie, A. Natansohn, P. Rochon, *Chem. Mater.* **1993**, *5*, 403 – 411; c) A. Natansohn, P. Rochon, *Chem. Rev.* **2002**, *102*, 4139 – 4175.

[492] a) T. Hugel, N. B. Holland, A. Cattani, L. Moroder, M. Seitz, H. E. Gaub, *Science* **2002**, *296*, 1103 – 1106; b) N. B. Holland, T. Hugel, G. Neuert, A. Cattani-Scholz, C. Renner, D. Oesterhelt, L. Moroder, M. Seitz, H. E. Gaub, *Macromolecules* **2003**, *36*, 2015 – 2023.

[493] a) Y. Okamoto, T. Nakano, *Chem. Rev.* **1994**, *94*, 349 – 372; b) T. Nakano, Y. Okamoto, *Chem. Rev.* **2001**, *101*, 4013 – 4038.

[494] G. Maxein, R. Zentel, *Macromolecules* **1995**, *28*, 8438 – 8440.

[495] J. Li, G. B. Schuster, K. S. Cheon, M. M. Green, J. V. Selinger, *J. Am. Chem. Soc.* **2000**, *122*, 2603 – 2612.

[496] This process is exactly analogous to the generation of photo-induced anisotropy in azo-containing liquid crystals (see Section 8.3.2) and is also applicable to polymer systems containing other photoisomerizable molecules. It is also related to the "all optical poling" method for ordering non-centrosymmetric chromophores in polymers. For a discussion of these mechanims, see: M. Dumont, A. El Osman, *Chem. Phys.* **1999**, *245*, 437 – 462.

[497] J. A. Delaire, K. Nakatani, *Chem. Rev.* **2000**, *100*, 1817 – 1845.

[498] a) P. Rochon, E. Batalla, A. Natansohn, *Appl. Phys. Lett.* **1995**, *66*, 136 – 138; b) D. Y. Kim, S. K. Tripathy, L. Li, J. Kumar, *Appl. Phys. Lett.* **1995**, *66*, 1166 – 1168; for accounts of the observation of this remarkable effect, see: c) N. K. Viswanathan, D. Y. Kim, S. P. Bian, J. Williams, W. Liu, L. Li, L. Samuelson, J. Kumar, S. K. Tripathy, *J. Mater. Chem.* **1999**, *9*, 1941 – 1955; d) K. G. Yager, C. J. Barrett, *Curr. Opin. Solid State Mater. Sci.* **2001**, *6*, 487 – 494.

[499] The precise mechanism whereby mass transport occurs during photoorientation is still a topic of intense investigation, see, for example: Refs. [491c, 497, 498c,d] and a) F. L. Labarthet, J. L. Bruneel, T. Buffeteau, C. Sourisseau, M. R. Huber, S. J. Zilker, T. Bieringer, *Phys. Chem. Chem. Phys.* **2000**, *2*, 5154 – 5167; b) B. M. Schulz, M. R. Huber, T. Bieringer, G. Krausch, S. J. Zilker, *Synth. Met.* **2001**, *124*, 155 – 157.

[500] For a review, see: a) P. Xie, R. Zhang, *J. Mater. Chem.* **2005**, *15*, 2529 – 2550; for the first example of a microscopic device in which this technology is used, see: b) A. Buguin, M. H. Li, P. Silberzan, B. Ladoux, P. Keller, *J. Am. Chem. Soc.* **2006**, *128*, 1088 – 1089.

[501] a) H. Finkelmann, E. Nishikawa, G. G. Pereira, M. Warner, *Phys. Rev. Lett.* **2001**, *87*, 015501; b) P. M. Hogan, A. R. Tajbakhsh, E. M. Terentjev, *Phys. Rev. E* **2002**, *65*, 041720; c) J. Cviklinski, A. R. Tajbakhsh, E. M. Terentjev, *Eur. Phys. J. E* **2002**, *9*, 427 – 434; d) T. Ikeda, M. Nakano, Y. L. Yu, O. Tsutsumi, A. Kanazawa, *Adv. Mater.* **2003**, *15*, 201 – 205; e) M. H. Li, P. Keller, B. Li, X. G. Wang, M. Brunet, *Adv. Mater.* **2003**, *15*, 569 – 572; f) Y. L. Yu, M. Nakano, T. Ikeda, *Nature* **2003**, *425*, 145 – 145; g) M. Camacho-Lopez, H. Finkelmann, P. Palffy-Muhoray, M. Shelley, *Nat. Mater.* **2004**, *3*, 307 – 310.

[502] It has been proposed that the photoinduced macroscopic mechanical changes in both azo-containing liquid-crystal elastomers and spin-cast films arise from the same "photomechanical" effect at the molecular level and attention is now turning to the proper characterization of these phenomena, see: O. M. Tanchak, C. J. Barrett, *Macromolecules* **2005**, *38*, 10566 – 10570.

[503] R. Eelkema, M. M. Pollard, J. Vicario, N. Katsonis, B. S. Ramon, C. W. M. Bastiaansen, D. J. Broer, B. L. Feringa, *Nature* **2006**, *440*, 163.

[504] M. Kaneko, K. Kaneto, *Synth. Met.* **1999**, *102*, 1350 – 1353.

[505] a) M. J. Marsella, R. J. Reid, *Macromolecules* **1999**, *32*, 5982 – 5984; b) M. J. Marsella, R. J. Reid, S. Estassi, L. S. Wang, *J. Am. Chem. Soc.* **2002**, *124*, 12507 – 12510; c) M. J. Marsella, G. Z. Piao, F. S. Tham, *Synthesis* **2002**, 1133 – 1135; d) M. J. Marsella, *Acc. Chem. Res.* **2002**, *35*, 944 – 951.

[506] H. H. Yu, B. Xu, T. M. Swager, *J. Am. Chem. Soc.* **2003**, *125*, 1142 – 1143.

[507] a) H. H. Yu, T. M. Swager, *IEEE J. Oceanic Eng.* **2004**, *29*, 692 – 695; b) D. A. Scherlis, N. Marzari, *J. Am. Chem. Soc.* **2005**, *127*, 3207 – 3212; c) J. Casanovas, D. Zanuy, C. Aleman, *Angew. Chem.* **2006**, *118*, 1121 – 1123; *Angew. Chem. Int. Ed.* **2006**, *45*, 1103 – 1105.

[508] a) T. J. Huang, B. Brough, C.-M. Ho, Y. Liu, A. H. Flood, P. A. Bonvallet, H.-R. Tseng, J. F. Stoddart, M. Baller, S. Magonov, *Appl. Phys. Lett.* **2004**, *85*, 5391 – 5393; b) Y. Liu, A. H. Flood, P. A. Bonvallet, S. A. Vignon, B. H. Northrop, H.-R. Tseng, J. O. Jeppesen, T. J. Huang, B. Brough, M. Baller, S. Magonov, S. D. Solares, W. A. Goddard, C.-M. Ho, J. F. Stoddart, *J. Am. Chem. Soc.* **2005**, *127*, 9745 – 9759.

[509] Surface-stress-induced bending of microcantilevers has also been shown to be an extremely sensitive probe of molecular-recognition processes occurring at surface-mounted species (particularly for biomolecules), see for example: a) J. Fritz, M. K. Baller, H. P. Lang, H. Rothuizen, P. Vettiger, E. Meyer, H. J. Guntherodt, C. Gerber, J. K. Gimzewski, *Science* **2000**, *288*, 316 – 318; b) G. H. Wu, H. F. Ji, K. Hansen, T. Thundat, R. Datar, R. Cote, M. F. Hagan, A. K. Chakraborty, A. Majumdar, *Proc. Natl. Acad. Sci. USA* **2001**, *98*, 1560 – 1564; c) G. H. Wu,

R. H. Datar, K. M. Hansen, T. Thundat, R. J. Cote, A. Majumdar, *Nat. Biotechnol.* **2001**, *19*, 856 – 860; d) R. McKendry, J. Y. Zhang, Y. Arntz, T. Strunz, M. Hegner, H. P. Lang, M. K. Baller, U. Certa, E. Meyer, H. J. Guntherodt, C. Gerber, *Proc. Natl. Acad. Sci. USA* **2002**, *99*, 9783 – 9788; e) B. Dhayal, W. A. Henne, D. D. Doorneweerd, R. G. Reifenberger, P. S. Low, *J. Am. Chem. Soc.* **2006**, *128*, 3716 – 3721; mechanical changes have also been achieved in response to photoisomerization of an azobenzene monolayer (f) H. F. Ji, Y. Feng, X. H. Xu, V. Purushotham, T. Thundat, G. M. Brown, *Chem. Commun.* **2004**, 2532 – 2533); and pH-switched conformational changes in an oligonucleotide monolayer (g) W. M. Shu, D. S. Liu, M. Watari, C. K. Riener, T. Strunz, M. E. Welland, S. Balasubramanian, R. A. McKendry, *J. Am. Chem. Soc.* **2005**, *127*, 17054 – 17060); finally, a photoinduced, surface-catalyzed chemical reaction has been used to reversibly bend a microcantilever (h) M. Su, V. P. Dravid, *Nano Lett.* **2005**, *5*, 2023 – 2028).

[510] For a recent review, see: Y. Liu, L. Mu, B. H. Liu, J. L. Kong, *Chem. Eur. J.* **2005**, *11*, 2622 – 2631.

[511] a) S. T. Milner, *Science* **1991**, *251*, 905 – 914; b) V. V. Tsukruk, *Prog. Polym. Sci.* **1997**, *22*, 247 – 311; c) T. P. Russell, *Science* **2002**, *297*, 964 – 967; d) N. Nath, A. Chilkoti, *Adv. Mater.* **2002**, *14*, 1243 – 1247; e) I. Luzinov, S. Minko, V. V. Tsukruk, *Prog. Polym. Sci.* **2004**, *29*, 635 – 698.

[512] V. Pardo-Yissar, R. Gabai, A. N. Shipway, T. Bourenko, I. Willner, *Adv. Mater.* **2001**, *13*, 1320 – 1323.

[513] a) G. V. R. Rao, G. P. López, *Adv. Mater.* **2000**, *12*, 1692 – 1695; b) G. V. R. Rao, S. Balamurugan, D. E. Meyer, A. Chilkoti, G. P. López, *Langmuir* **2002**, *18*, 1819 – 1824; c) G. V. R. Rao, M. E. Krug, S. Balamurugan, H. F. Xu, Q. Xu, G. P. López, *Chem. Mater.* **2002**, *14*, 5075 – 5080.

[514] Control over mass transport through porous materials has similarly been controlled using photoresponsive (a) N. G. Liu, D. R. Dunphy, P. Atanassov, S. D. Bunge, Z. Chen, G. P. López, T. J. Boyle, C. J. Brinker, *Nano Lett.* **2004**, *4*, 551 – 554) and pH-responsive (b) R. Casasús, M. D. Marcos, R. Martínez-Máñez, J. V. Ros-Lis, J. Soto, L. A. Villaescusa, P. Amorós, D. Beltrán, C. Guillem, J. Latorre, *J. Am. Chem. Soc.* **2004**, *126*, 8612 – 8613) oligomers incorporated into the inorganic matrix.

[515] D. L. Huber, R. P. Manginell, M. A. Samara, B. I. Kim, B. C. Bunker, *Science* **2003**, *301*, 352 – 354.

[516] M. Cavallini, R. Lazzaroni, R. Zamboni, F. Biscarini, D. Timpel, F. Zerbetto, G. J. Clarkson, D. A. Leigh, *J. Phys. Chem. B* **2001**, *105*, 10826 – 10830.

[517] T. D. Nguyen, H.-R. Tseng, P. C. Celestre, A. H. Flood, Y. Liu, J. F. Stoddart, J. I. Zink, *Proc. Natl. Acad. Sci. USA* **2005**, *102*, 10029 – 10034.

[518] a) I. Willner, B. Willner, *J. Mater. Chem.* **1998**, *8*, 2543 – 2556; b) V. Pardo-Yissar, E. Katz, I. Willner, A. B. Kotlyar, C. Sanders, H. Lill, *Faraday Discuss.* **2000**, 119 – 134; c) A. N. Shipway, I. Willner, *Acc. Chem. Res.* **2001**, *34*, 421 – 432.

[519] I. Willner, V. Pardo-Yissar, E. Katz, K. T. Ranjit, *J. Electroanal. Chem.* **2001**, *497*, 172 – 177.

[520] E. Katz, L. Sheeney-Haj-Ichia, I. Willner, *Angew. Chem.* **2004**, *116*, 3354 – 3362; *Angew. Chem. Int. Ed.* **2004**, *43*, 3292 – 3300.

[521] L. Sheeney-Haj-Ichia, I. Willner, *J. Phys. Chem. B* **2002**, *106*, 13094 – 13097.

[522] a) E. Katz, O. Lioubashevsky, I. Willner, *J. Am. Chem. Soc.* **2004**, *126*, 15520 – 15532; b) E. Katz, R. Baron, I. Willner, N. Richke, R. D. Levine, *ChemPhysChem* **2005**, *6*, 2179 – 2189.

[523] a) R. Blossey, *Nat. Mater.* **2003**, *2*, 301 – 306; b) T. L. Sun, L. Feng, X. F. Gao, L. Jiang, *Acc. Chem. Res.* **2005**, *38*, 644 – 652.

[524] A. J. Pertsin, M. Grunze, H. J. Kreuzer, R. L. C. Wang, *Phys. Chem. Chem. Phys.* **2000**, *2*, 1729 – 1733.

[525] J. Lahann, S. Mitragotri, T. N. Tran, H. Kaido, J. Sundaram, I. S. Choi, S. Hoffer, G. A. Somorjai, R. Langer, *Science* **2003**, *299*, 371 – 374.

[526] X. M. Wang, A. B. Kharitonov, E. Katz, I. Willner, *Chem. Commun.* **2003**, 1542 – 1543.

[527] Y. Liu, L. Mu, B. H. Liu, S. Zhang, P. Y. Yang, J. L. Kong, *Chem. Commun.* **2004**, 1194 – 1195.

[528] a) H. P. Greenspan, *J. Fluid Mech.* **1978**, *84*, 125 – 143; b) F. Brochard, *Langmuir* **1989**, *5*, 432 – 438.

[529] a) T. Ondarçuhu, M. Veyssié, *J. Phys. II* **1991**, *1*, 75 – 85; b) M. K. Chaudhury, G. M. Whitesides, *Science* **1992**, *256*, 1539 – 1541.

[530] The difference in surface free energy leads to different equilibrium values for the contact angle on opposite sides of the droplet. The implied asymmetric droplet shape however is in fact never achieved as it sets up a Laplace pressure gradient inside the droplet, which rapidly equilibrates to give a symmetric shape with dynamic contact angles at either side of roughly equal values, intermediate between the two equilibrium values. It is this imbalance in contact angles which leads to a directional force on the droplet so that motion occurs. A difference in contact angles is the thermodynamic driving force for the motion, but it is not the sole requirement. A kinetic requirement is a low contact angle hysteresis (that is, small differences between receding and advancing contact angles for the surface–liquid system in use). The problem of significant hysteresis can be surmounted by coupling the system to a source of random energy, while using the surface energy gradient to bias the droplet motion, in a ratchetlike mechanism. This has been investigated for rapidly condensing droplets from steam: a) S. Daniel, M. K. Chaudhury, J. C. Chen, *Science* **2001**, *291*, 633 – 636; and for droplets subjected to mechanical vibrations: b) S. Daniel, S. Sircar, J. Gliem, M. K. Chaudhury, *Langmuir* **2004**, *20*, 4085 – 4092.

[531] Earlier, the directional motion of cells over artificial surfaces with a chemical composition gradient had been observed: a) S. B. Carter, *Nature* **1965**, *208*, 1183 – 1187; b) S. B. Carter, *Nature* **1967**, *213*, 256 – 260; and a brief theoretical explanation used similar arguments to those developed in more detail later: c) J. L. Moilliet, *Nature* **1967**, *213*, 260 – 261.

[532] a) H. Gau, S. Herminghaus, P. Lenz, R. Lipowsky, *Science* **1999**, *283*, 46 – 49; b) B. S. Gallardo, V. K. Gupta, F. D. Eagerton, L. I. Jong, V. S. Craig, R. R. Shah, N. L. Abbott, *Science* **1999**, *283*, 57 – 60; c) S. Daniel, M. K. Chaudhury, *Langmuir* **2002**, *18*, 3404 – 3407; d) H. Suda, S. Yamada, *Langmuir* **2003**, *19*, 529 – 531; e) S. H. Choi, B. M. Z. Newby, *Langmuir* **2003**, *19*, 7427 – 7435.

[533] See also self-propelled droplets on homogeneous surfaces operating by the chemical Marangoni effect (Section 6).

[534] M. Grunze, *Science* **1999**, *283*, 41 – 42.

[535] a) G. M. Whitesides, A. D. Stroock, *Phys. Today* **2001**, *54*(6), 42 – 48; b) D. R. Reyes, D. Iossifidis, P. A. Auroux, A. Manz, *Anal. Chem.* **2002**, *74*, 2623 – 2636.

[536] a) K. Ichimura, S. K. Oh, M. Nakagawa, *Science* **2000**, *288*, 1624 – 1626; b) S. K. Oh, M. Nakagawa, K. Ichimura, *J. Mater. Chem.* **2002**, *12*, 2262 – 2269.

[537] J. Berná, D. A. Leigh, M. Lubomska, S. M. Mendoza, E. M. Pérez, P. Rudolf, G. Teobaldi, F. Zerbetto, *Nat. Mater.* **2005**, *4*, 704 – 710.

[538] Motion of an organic droplet along a thin-film metal electrode immersed in an aqueous electrolyte has very recently been observed in a system which does not employ significant submolecular motion to alter the surface free energy, see: R. Yamada, H. Tada, *Langmuir* **2005**, *21*, 4254 – 4256.

[539] S. Minko, M. Müller, M. Motornov, M. Nitschke, K. Grundke, M. Stamm, *J. Am. Chem. Soc.* **2003**, *125*, 3896 – 3900.

[540] T. L. Sun, G. J. Wang, L. Feng, B. Q. Liu, Y. M. Ma, L. Jiang, D. B. Zhu, *Angew. Chem.* **2004**, *116*, 361 – 364; *Angew. Chem. Int. Ed.* **2004**, *43*, 357 – 360.

[541] Q. Fu, G. V. R. Rao, S. B. Basame, D. J. Keller, K. Artyushkova, J. E. Fulghum, G. P. López, *J. Am. Chem. Soc.* **2004**, *126*, 8904 – 8905.

[542] R. Rosario, D. Gust, A. A. Garcia, M. Hayes, J. L. Taraci, T. Clement, J. W. Dailey, S. T. Picraux, *J. Phys. Chem. B* **2004**, *108*, 12640 – 12642.

[543] a) H. Noji, R. Yasuda, M. Yoshida, K. Kinosita, *Nature* **1997**, *386*, 299 – 302; b) R. Yasuda, H. Noji, K. Kinosita, M. Yoshida, *Cell* **1998**, *93*, 1117 – 1124; c) K. Adachi, R. Yasuda, H. Noji, H. Itoh, Y. Harada, M. Yoshida, K. Kinosita, *Proc. Natl. Acad. Sci. USA* **2000**, *97*, 7243 – 7247; d) R. Yasuda, H. Noji, M. Yoshida, K. Kinosita, H. Itoh, *Nature* **2001**, *410*, 898 – 904.

[544] Y. Sambongi, Y. Iko, M. Tanabe, H. Omote, A. Iwamoto-Kihara, I. Ueda, T. Yanagida, Y. Wada, M. Futai, *Science* **1999**, *286*, 1722 – 1724.

[545] H. Itoh, A. Takahashi, K. Adachi, H. Noji, R. Yasuda, M. Yoshida, K. Kinosita, *Nature* **2004**, *427*, 465 – 468.

[546] a) C. Montemagno, G. Bachand, *Nanotechnology* **1999**, *10*, 225 – 231; b) R. K. Soong, G. D. Bachand, H. P. Neves, A. G. Olkhovets, H. G. Craighead, C. D. Montemagno, *Science* **2000**, *290*, 1555 – 1558.

[547] A number of reviews cover the various aspects of this field in greater detail than we are able to achieve here, see: a) H. Hess, V. Vogel, *Rev. Mol. Biotechnol.* **2001**, *82*, 67 – 85; b) J. J. Schmidt, C. D. Montemagno in *Molecular Motors* (Ed.: M. Schliwa), Wiley-VCH, Weinheim, **2003**, pp. 541 – 558; c) H. Hess, G. D. Bachand, V. Vogel, *Chem. Eur. J.* **2004**, *10*, 2110 – 2116; d) C. Mavroidis, A. Dubey, M. L. Yarmush, *Annu. Rev. Biomed. Eng.* **2004**, *6*, 363 – 395; e) M. Knoblauch, W. S. Peters, *Cell. Mol. Life Sci.* **2004**, *61*, 2497 – 2509; for a recent review which places artificial molecular machines side-by-side with motor proteins, see Ref. [1l].

[548] a) S. J. Kron, J. A. Spudich, *Proc. Natl. Acad. Sci. USA* **1986**, *83*, 6272 – 6276; b) Y. Y. Toyoshima, S. J. Kron, E. M. McNally, K. R. Niebling, C. Toyoshima, J. A. Spudich, *Nature* **1987**, *328*, 536 – 539; c) Y. Harada, K. Sakurada, T. Aoki, D. D. Thomas, T. Yanagida, *J. Mol. Biol.* **1990**, *216*, 49 – 68.

[549] Unfortunately, such systems are sometimes called "molecular shuttles", thus risking confusion with their unrelated rotaxane-based namesakes (see Sections 4.2–4.3).

[550] a) A. Kakugo, S. Sugimoto, J. P. Gong, Y. Osada, *Adv. Mater.* **2002**, *14*, 1124 – 1126; b) A. Kakugo, K. Shikinaka, K. Matsumoto, J. P. Gong, Y. Osada, *Bioconjugate Chem.* **2003**, *14*, 1185 – 1190; c) A. Kakugo, K. Shikinaka, N. Takekawa, S. Sugimoto, Y. Osada, J. P. Gong, *Biomacromolecules* **2005**, *6*, 845 – 849; d) A. Kakugo, K. Shikinaka, J. P. Gong, Y. Osada, *Polymer* **2005**, *46*, 7759 – 7770.

[551] J. Z. Xi, J. J. Schmidt, C. D. Montemagno, *Nat. Mater.* **2005**, *4*, 180 – 184.

[552] For reviews, see: a) G. A. Schick, A. F. Lawrence, R. R. Birge, *Trends Biotechnol.* **1988**, *6*, 159 – 163; b) R. R. Birge, *Annu. Rev. Phys. Chem.* **1990**, *41*, 683 – 733; c) D. Oesterhelt, C. Brauchle, N. Hampp, *Q. Rev. Biophys.* **1991**, *24*, 425 – 478; d) Z. P. Chen, R. R. Birge, *Trends Biotechnol.* **1993**, *11*, 292 – 300; e) N. Hampp, A. Silber, *Pure Appl. Chem.* **1996**, *68*, 1361 – 1366; f) R. R. Birge, N. B. Gillespie, E. W. Izaguirre, A. Kusnetzow, A. F. Lawrence, D. Singh, Q. W. Song, E. Schmidt, J. A. Stuart, S. Seetharaman, K. J. Wise, *J. Phys. Chem. B* **1999**, *103*, 10746 – 10766; g) N. Hampp, *Chem. Rev.* **2000**, *100*, 1755 – 1776.

[553] For reviews, see: Ref. [169d], chapt. 6 and a) J.-M. Lehn in *Physical Chemistry of Transmembrane Ion Motions* (Ed.: G. Spach), Elsevier, Amsterdam, **1983**, pp. 181 – 207; b) G. W. Gokel, O. Murillo, *Acc. Chem. Res.* **1996**, *29*, 425 – 432; c) T. M. Fyles, *Curr. Opin. Chem. Biol.* **1997**, *1*, 497 – 505; d) T. W. Bell, *Curr. Opin. Chem. Biol.* **1998**, *2*, 711 – 716; e) G. W. Gokel, A. Mukhopadhyay, *Chem. Soc. Rev.* **2001**, *30*, 274 – 286; f) J. M. Boon, B. D. Smith, *Curr. Opin. Chem. Biol.* **2002**, *6*, 749 – 756; g) B. D. Smith, T. N. Lambert, *Chem. Commun.* **2003**, 2261 – 2268; h) special issue on "Synthetic Ion Channels": *Bioorg. Med. Chem.* **2004**, *12*, 1277 – 1350; i) S. Matile, A. Som, N. Sorde, *Tetrahedron* **2004**, *60*, 6405 – 6435.

[554] S. Sukharev, A. Anishkin, *Trends Neurosci.* **2004**, *27*, 345 – 351.

[555] a) K. Yoshimura, A. Batiza, M. Schroeder, P. Blount, C. Kung, *Biophys. J.* **1999**, *77*, 1960 – 1972; b) K. Yoshimura, A. Batiza, C. Kung, *Biophys. J.* **2001**, *80*, 2198 – 2206.

[556] A. Kocer, M. Walko, W. Meijberg, B. L. Feringa, *Science* **2005**, *309*, 755 – 758.

[557] M. Banghart, K. Borges, E. Isacoff, D. Trauner, R. H. Kramer, *Nat. Neurosci.* **2004**, *7*, 1381 – 1386.

[558] M. Volgraf, P. Gorostiza, R. Numano, R. H. Kramer, E. Y. Isacoff, D. Trauner, *Nat. Chem. Biol.* **2006**, *2*, 47 – 52.

[559] a) V. Borisenko, D. C. Burns, Z. H. Zhang, G. A. Woolley, *J. Am. Chem. Soc.* **2000**, *122*, 6364 – 6370; b) T. Lougheed, V. Borisenko, T. Hennig, K. Ruck-Braun, G. A. Woolley, *Org. Biomol. Chem.* **2004**, *2*, 2798 – 2801.

[560] a) S. S. Anderson, I. G. Lyle, R. Paterson, *Nature* **1976**, *259*, 147 – 148; b) J. J. Grimaldi, S. Boileau, J.-M. Lehn, *Nature* **1977**, *265*, 229 – 230; c) T. Shinbo, K. Kurihara, Y. Kobatake, N. Kamo, *Nature* **1977**, *270*, 277 – 278; d) J. J. Grimaldi, J.-M. Lehn, *J. Am. Chem. Soc.* **1979**, *101*, 1333 – 1334.

[561] A number of synthetic systems now exist in which relatively long-lived, long-distance photoinduced intramolecular charge-separated states can be generated and currently ways of utilizing this electrical potential are being investigated, for reviews, see: a) T. J. Meyer, *Acc. Chem. Res.* **1989**, *22*, 163 – 170; b) M. R. Wasielewski, *Chem. Rev.* **1992**, *92*, 435 – 461; c) D. Gust, T. A. Moore, A. L. Moore, *Acc. Chem. Res.* **1993**, *26*, 198 – 205; d) K. Maruyama, A. Osuka, N. Mataga, *Pure Appl. Chem.* **1994**, *66*, 867 – 872; e) M. N. Paddon-Row, *Acc. Chem. Res.* **1994**, *27*, 18 – 25; f) H. Kurreck, M. Huber, *Angew. Chem.* **1995**, *107*, 929 – 947; *Angew. Chem. Int. Ed. Engl.* **1995**, *34*, 849 – 866; g) V. Balzani, A. Credi, M. Venturi, *Curr. Opin. Chem. Biol.* **1997**, *1*, 506 – 513; h) D. Gust, T. A. Moore, A. L. Moore, *Acc. Chem. Res.* **2001**, *34*, 40 – 48; i) H. Dürr, S. Bossmann, *Acc. Chem. Res.* **2001**, *34*, 905 – 917; j) L. C. Sun, L. Hammarstrom, B. Åkermark, S. Styring, *Chem. Soc. Rev.* **2001**, *30*, 36 – 49; k) D. Holten, D. F. Bocian, J. S. Lindsey, *Acc. Chem. Res.* **2002**, *35*, 57 – 69; l) D. M. Guldi, *Chem. Soc. Rev.* **2002**, *31*, 22 – 36; m) H. Imahori, Y. Mori, Y. Matano, *J. Photochem. Photobiol. C* **2003**, *4*, 51 – 83; n) H. Imahori, *Org. Biomol. Chem.* **2004**, *2*, 1425 – 1433; o) J. H. Alstrum-Acevedo, M. K. Brennaman, T. J. Meyer, *Inorg. Chem.* **2005**, *44*, 6802 – 6827.

[562] G. Steinberg-Yfrach, P. A. Liddell, S. C. Hung, A. L. Moore, D. Gust, T. A. Moore, *Nature* **1997**, *385*, 239 – 241.

[563] I. M. Bennett, H. M. V. Farfano, F. Bogani, A. Primak, P. A. Liddell, L. Otero, L. Sereno, J. J. Silber, A. L. Moore, T. A. Moore, D. Gust, *Nature* **2002**, *420*, 398 – 401.

[564] G. Steinberg-Yfrach, J. L. Rigaud, E. N. Durantini, A. L. Moore, D. Gust, T. A. Moore, *Nature* **1998**, *392*, 479 – 482.

[565] Z. C. He, S. B. Colbran, D. C. Craig, *Chem. Eur. J.* **2003**, *9*, 116 – 129.

[566] For reviews, see: a) C. M. Niemeyer, *Angew. Chem.* **1997**, *109*, 603 – 606; *Angew. Chem. Int. Ed. Engl.* **1997**, *36*, 585 – 587; b) N. C. Seeman, *Angew. Chem.* **1998**, *110*, 3408 – 3428; *Angew. Chem. Int. Ed.* **1998**, *37*, 3220 – 3238; c) N. C. Seeman, *Annu. Rev. Biophys. Biomol. Struct.* **1998**, *27*, 225 – 248; d) N. C. Seeman, H. Wang, X. P. Yang, F. R. Liu, C. D. Mao, W. Q. Sun, L. Wenzler, Z. Y. Shen, R. J. Sha, H. Yan, M. H. Wong, P. Sa-Ardyen, B. Liu, H. X. Qiu, X. J. Li, J. Qi, S. M. Du, Y. W. Zhang, J. E. Mueller, T. J. Fu, Y. L. Wang, J. H. Chen, *Nano-*

technology **1998**, *9*, 257 – 273; e) N. C. Seeman, *Trends Biotechnol.* **1999**, *17*, 437 – 443; f) C. M. Niemeyer, *Appl. Phys. A* **1999**, *68*, 119 – 124; g) C. M. Niemeyer, *Curr. Opin. Chem. Biol.* **2000**, *4*, 609 – 618; h) N. C. Seeman, A. M. Belcher, *Proc. Natl. Acad. Sci. USA* **2002**, *99*, 6451 – 6455; i) N. C. Seeman, *Nature* **2003**, *421*, 427 – 431; j) N. C. Seeman, *Biochemistry* **2003**, *42*, 7259 – 7269; k) N. C. Seeman, *Chem. Biol.* **2003**, *10*, 1151 – 1159; l) N. C. Seeman, *Sci. Am.* **2004**, *290*(6), 34 – 43; m) H. Yan, *Science* **2004**, *306*, 2048 – 2049.

[567] For reviews of DNA-based machines, see: a) C. M. Niemeyer, M. Adler, *Angew. Chem.* **2002**, *114*, 3933 – 3937; *Angew. Chem. Int. Ed.* **2002**, *41*, 3779 – 3783; b) N. C. Seeman, *Trends Biochem. Sci.* **2005**, *30*, 119 – 125; c) F. C. Simmel, W. U. Dittmer, *Small* **2005**, *1*, 284 – 299.

[568] X. P. Yang, A. V. Vologodskii, B. Liu, B. Kemper, N. C. Seeman, *Biopolymers* **1998**, *45*, 69 – 83.

[569] C. D. Mao, W. Q. Sun, Z. Y. Shen, N. C. Seeman, *Nature* **1999**, *397*, 144 – 146.

[570] B. Yurke, A. J. Turberfield, A. P. Mills, F. C. Simmel, J. L. Neumann, *Nature* **2000**, *406*, 605 – 608.

[571] F. C. Simmel, B. Yurke, *Phys. Rev. E* **2001**, *6304*, 041913.

[572] F. C. Simmel, B. Yurke, *Appl. Phys. Lett.* **2002**, *80*, 883 – 885.

[573] H. Yan, X. P. Zhang, Z. Y. Shen, N. C. Seeman, *Nature* **2002**, *415*, 62 – 65.

[574] L. P. Feng, S. H. Park, J. H. Reif, H. Yan, *Angew. Chem.* **2003**, *115*, 4478 – 4482; *Angew. Chem. Int. Ed.* **2003**, *42*, 4342 – 4346.

[575] D. S. Liu, S. Balasubramanian, *Angew. Chem.* **2003**, *115*, 5912 – 5914; *Angew. Chem. Int. Ed.* **2003**, *42*, 5734 – 5736.

[576] This process has been monitored for surface-mounted arrays of DNA strands by fluorescence switching when a dye is attached (D. S. Liu, A. Bruckbauer, C. Abell, S. Balasubramanian, D. J. Kang, D. Klenerman, D. J. Zhou, *J. Am. Chem. Soc.* **2006**, *128*, 2067 – 2071) and by mechanical changes when the strands are mounted on microcantilever beams (Ref. [509g]).

[577] a) Y. Chen, S. H. Lee, C. Mao, *Angew. Chem.* **2004**, *116*, 5449 – 5452; *Angew. Chem. Int. Ed.* **2004**, *43*, 5335 – 5338; b) M. Brucale, G. Zuccheri, B. Samori, *Org. Biomol. Chem.* **2005**, *3*, 575 – 577.

[578] a) J. W. J. Li, W. H. Tan, *Nano Lett.* **2002**, *2*, 315 – 318; b) P. Alberti, J. L. Mergny, *Proc. Natl. Acad. Sci. USA* **2003**, *100*, 1569 – 1573.

[579] W. U. Dittmer, A. Reuter, F. C. Simmel, *Angew. Chem.* **2004**, *116*, 3634 – 3637; *Angew. Chem. Int. Ed.* **2004**, *43*, 3550 – 3553.

[580] Y. Chen, M. Wang, C. Mao, *Angew. Chem.* **2004**, *116*, 3638 – 3641; *Angew. Chem. Int. Ed.* **2004**, *43*, 3554 – 3557.

[581] Y. Chen, C. Mao, *J. Am. Chem. Soc.* **2004**, *126*, 8626 – 8627.

[582] A. J. Turberfield, J. C. Mitchell, B. Yurke, A. P. Mills, M. I. Blakey, F. C. Simmel, *Phys. Rev. Lett.* **2003**, *90*, 118102.

[583] For an overview of this series of publications, see: T. R. Kelly, *Angew. Chem.* **2005**, *117*, 4194 – 4198; *Angew. Chem. Int. Ed.* **2005**, *44*, 4124 – 4127.

[584] W. B. Sherman, N. C. Seeman, *Nano Lett.* **2004**, *4*, 1203 – 1207.

[585] J. S. Shin, N. A. Pierce, *J. Am. Chem. Soc.* **2004**, *126*, 10834 – 10835.

[586] T. Ye, C. Mao, *J. Am. Chem. Soc.* **2004**, *126*, 11410 – 11411.

[587] a) J. H. Reif in *DNA Computing: 8th International Workshop on DNA-based Computers: Lecture Notes in Computer Science, Vol. 2568* (Eds.: M. Hagiya, A. Ohuchi), Springer, Berlin, **2003**, pp. 22 – 37; b) P. Yin, A. J. Turberfield, J. H. Reif in *DNA Computing: 10th International Workshop on DNA Computing: Lecture Notes in Computer Science, Vol. 3384* (Eds.: C. Ferretti, G. Mauri, C. Zandron), Springer, Berlin, **2005**, pp. 410 – 425.

[588] P. Yin, H. Yan, X. G. Daniell, A. J. Turberfield, J. H. Reif, *Angew. Chem.* **2004**, *116*, 5014 – 5019; *Angew. Chem. Int. Ed.* **2004**, *43*, 4906 – 4911.

[589] J. Bath, S. J. Green, A. J. Turberfield, *Angew. Chem.* **2005**, *117*, 4432 – 4435; *Angew. Chem. Int. Ed.* **2005**, *44*, 4358 – 4361.

[590] Y. Tian, Y. He, Y. Chen, P. Yin, C. Mao, *Angew. Chem.* **2005**, *117*, 4429 – 4432; *Angew. Chem. Int. Ed.* **2005**, *44*, 4355 – 4358.

[591] Although related to an information ratchet, mechanisms for Brownian particle motion based on particle-induced irreversible changes to a symmetrical, periodic potential-energy surface have been studied in their own right and have been termed "burnt-bridges" mechanisms; see Section 4.4 and: a) J. Mai, I. M. Sokolov, A. Blumen, *Phys. Rev. E* **2001**, *64*, 011102; b) T. Antal, P. L. Krapivsky, *Phys. Rev. E* **2005**, *72*, 046104.

[592] B. Samori, G. Zuccheri, *Angew. Chem.* **2005**, *117*, 1190 – 1206; *Angew. Chem. Int. Ed.* **2005**, *44*, 1166 – 1181.

[593] a) W. U. Dittmer, F. C. Simmel, *Nano Lett.* **2004**, *4*, 689 – 691; b) W. U. Dittmer, S. Kempter, J. O. Rädler, F. C. Simmel, *Small* **2005**, *1*, 708 – 712

[594] Y. Chen, C. Mao, *J. Am. Chem. Soc.* **2004**, *126*, 13240 – 13241.

[595] a) J. J. Storhoff, C. A. Mirkin, *Chem. Rev.* **1999**, *99*, 1849 – 1862; b) E. Braun, K. Keren, *Adv. Phys.* **2004**, *53*, 441 – 496; c) J. Wengel, *Org. Biomol. Chem.* **2004**, *2*, 277 – 280; d) U. Feldkamp, C. M. Niemeyer, *Angew. Chem.* **2006**, *118*, 1888 – 1910; *Angew. Chem. Int. Ed.* **2006**, *45*, 1856 – 1876.

[596] a) N. E. Broude, *Trends Biotechnol.* **2002**, *20*, 249 – 256; b) W. H. Tan, K. M. Wang, T. J. Drake, *Curr. Opin. Chem. Biol.* **2004**, *8*, 547 – 553.

[597] W. Q. Shen, M. F. Bruist, S. D. Goodman, N. C. Seeman, *Angew. Chem.* **2004**, *116*, 4854 – 4856; *Angew. Chem. Int. Ed.* **2004**, *43*, 4750 – 4752.

[598] R. Nutiu, Y. F. Li, *Angew. Chem.* **2005**, *117*, 5600 – 5603; *Angew. Chem. Int. Ed.* **2005**, *44*, 5464 – 5467.

[599] For highlights and reviews, see: a) A. Gibbons, M. Amos, D. Hodgson, *Curr. Opin. Biotechnol.* **1997**, *8*, 103 – 106; b) J. C. Cox, D. S. Cohen, A. D. Ellington, *Trends Biotechnol.* **1999**, *17*, 151 – 154; c) A. J. Ruben, L. F. Landweber, *Nat. Rev. Mol. Cell Biol.* **2000**, *1*, 69 – 72; d) S. D. Gillmor, P. P. Rugheimer, M. G. Lagally, *Surf. Sci.* **2002**, *500*, 699 – 721; e) J. H. Reif, *Science* **2002**, *296*, 478 – 479; f) M. S. Livstone, D. van Noort, L. F. Landweber, *Trends Biotechnol.* **2003**, *21*, 98 – 101; g) A. Condon, *Nature* **2004**, *429*, 351 – 352.

[600] For reviews, see: a) J. Hasty, D. McMillen, J. J. Collins, *Nature* **2002**, *420*, 224 – 230; b) R. Weiss, S. Basu, S. Hooshangi, A. Kalmbach, D. Karig, R. Mehreja, I. Netravali, *Nat. Comput.* **2003**, *2*, 47 – 84.

[601] M. Freemantle, *Chem. Eng. News* **2005**, *83*, 33 – 35.

[602] a) P. Hamm, M. Lim, W. F. DeGrado, R. M. Hochstrasser, *Proc. Natl. Acad. Sci. USA* **1999**, *96*, 2036 – 2041; b) J. Bredenbeck, J. Helbing, A. Sieg, T. Schrader, W. Zinth, C. Renner, R. Behrendt, L. Moroder, J. Wachtveitl, P. Hamm, *Proc. Natl. Acad. Sci. USA* **2003**, *100*, 6452 – 6457; c) J. Bredenbeck, J. Helbing, P. Hamm, *J. Am. Chem. Soc.* **2004**, *126*, 990 – 991; d) M. L. Cowan, B. D. Bruner, N. Huse, J. R. Dwyer, B. Chugh, E. T. J. Nibbering, T. Elsaesser, R. J. D. Miller, *Nature* **2005**, *434*, 199 – 202; e) J. Zheng, K. Kwak, J. Ashbury, X. Chen, I. R. Piletic, M. D. Fayer, *Science* **2005**, *309*, 1338 – 1343; f) H. S. Chung, M. Khalil, A. W. Smith, Z. Ganim, A. Tokmakoff, *Proc. Natl. Acad. Sci. USA* **2005**, *102*, 612 – 617; g) O. F. A. Larsen, P. Bodis, W. J. Buma, J. S. Hannam, D. A. Leigh, S. Woutersen, *Proc. Natl. Acad. Sci. USA* **2005**, *102*, 13378 – 13382.

[603] V. A. Azov, A. Beeby, M. Cacciarini, A. G. Cheetham, F. Diederich, M. Frei, J. K. Gimzewski, V. Gramlich, B. Hecht, B. Jaun, T. Latychevskaia, A. Lieb, Y. Lill, F. Marotti, A. Schlegel, R. R. Schlittler, P. J. Skinner, P. Seiler, Y. Yamakoshi, *Adv. Funct. Mater.* **2006**, *16*, 147 – 156.

[604] J. Clayden, N. Vassiliou, *Org. Biomol. Chem.* **2006**, *4*, 2667 – 2678.

[605] D. A. Leigh, E. M. Pérez, *Top. Curr. Chem.* **2006**, *265*, 185 – 208.

[606] A. Credi, *Aust. J. Chem.* **2006**, *59*, 157 – 169.

[607] H. Tian, Q.-C. Wang, *Chem. Soc. Rev.* **2006**, *35*, 361 – 374.

[608] S. Bonnet, J.-P. Collin, M. Koizumi, P. Mobian, J.-P. Sauvage, *Adv. Mater.* **2006**, *18*, 1239 – 1250.
[609] T.-A. V. Khuong, J. E. Nuñez, C. E. Godinez, M. A. Garcia-Garibay, *Acc. Chem. Res.* **2006**, *39*, 413 – 422.
[610] W. F. Paxton, S. Sundararajan, T. E. Mallouk, A. Sen, *Angew. Chem.* **2006**, *118*, 5546 – 5556; *Angew. Chem. Int. Ed.* **2006**, *45*, 5420 – 5429.
[611] R. Beckman, K. Beverly. A. Boukai, Y. Bunimovich, J. W. Choi, E. DeIonno, J. Green, E. Johnston-Halperin, Y. Luo, B. Sheriff, J. F. Stoddart, J. R. Heath, *Faraday Discuss.* **2006**, *131*, 9 – 22.
[612] J. Hoogboom, T. Rasing, A. E. Rowan, R. J. M. Nolte, *J. Mater. Chem.* **2006**, *16*, 1305 – 1314.
[613] Y. Yu, T. Ikeda, *Angew. Chem.* **2006**, *118*, 5542 – 5544; *Angew. Chem. Int. Ed.* **2006**, *45*, 5416 – 5418.
[614] H. Hess, *Soft Matter* **2006**, *2*, 669 – 677.
[615] C. C. de Souza Silva, J. Van de Vondel, M. Morelle, V. V. Moshchalkov, *Nature* **2006**, *440*, 651 – 654.
[616] a) R. Romeo, S. Carnabuci, L. Fenech, M. Rosaria Plutino, A. Albinati, *Angew. Chem.* **2006**, *118*, 4606 – 4610; *Angew. Chem. Int. Ed.* **2006**, *45*, 4494 – 4498; b) T. Benincori, G. Celentano, T. Pilati, A. Ponti, S. Rizzo, F. Sannicolò, *Angew. Chem.* **2006**, *118*, 6339 – 6342; *Angew. Chem. Int. Ed.* **2006**, *45*, 6193 – 6196; c) R. E. Bulo, F. Allaart, A. W. Ehlers, F. J. J. de Kanter, M. Schakel, M. Lutz, A. L. Spek, K. Lammertsma, *J. Am. Chem. Soc.* **2006**, *128*, 12169 – 12173.
[617] a) A. J. Nawara, T. Shima, F. Hampel, J. A. Gladysz, *J. Am. Chem. Soc.* **2006**, *128*, 4962 – 4963; b) L. Wang, F. Hampel, J. A. Gladysz, *Angew. Chem.* **2006**, *118*, 4479 – 4482; *Angew. Chem. Int. Ed.* **2006**, *45*, 4372 – 4375; c) S. D. Karlen, C. E. Godinez, M. A. Garcia-Garibay, *Org. Lett.* **2006**, *8*, 3417 – 3420.
[618] O. P. H. Vaughan, F. J. Williams, N. Bampos, R. M. Lambert, *Angew. Chem.* **2006**, *118*, 3863 – 3865; *Angew. Chem. Int. Ed.* **2006**, *45*, 3779 – 3781.
[619] W. R. Browne, M. M. Pollard, B. de Lange, A. Meetsma, B. L. Feringa, *J. Am. Chem. Soc.* **2006**, *128*, 12412 – 12413.
[620] J. Vicario, M. Walko, A. Meetsma, B. L. Feringa, *J. Am. Chem. Soc.* **2006**, *128*, 5127 – 5135.
[621] a) T. Muraoka, K. Kinbara, T. Aida, *Nature* **2006**, *440*, 512 – 515; for a highlight of this work, see: b) F. M. Raymo, *Angew. Chem.* **2006**, *118*, 5375 – 5377; *Angew. Chem. Int. Ed.* **2006**, *45*, 5249 – 5251.
[622] T. Muraoka, K. Kinbara, T. Aida, *J. Am. Chem. Soc.* **2006**, *128*, 11600 – 11605.
[623] J.-F. Morin, Y. Shirai, J. M. Tour, *Org. Lett.* **2006**, *8*, 1713 – 1716.
[624] B. Brough, B. H. Northrop, J. J. Schmidt, H.-R. Tseng, K. N. Houk, J. F. Stoddart, C.-M. Ho, *Proc. Natl. Acad. Sci. USA* **2006**, *103*, 8583 – 8588.
[625] P. M. Mendes, W. Lu, H.-R. Tseng, S. Shinder, T. Iijima, M. Miyaji, C. M. Knobler, J. F. Stoddart, *J. Phys. Chem. B* **2006**, *110*, 3845 – 3848.
[626] E. DeIonno, H.-R. Tseng, D. D. Harvey, J. F. Stoddart, J. R. Heath, *J. Phys. Chem. B* **2006**, *110*, 7609 – 7612.
[627] a) A. H. Flood, E. W. Wong, J. F. Stoddart, *Chem. Phys.* **2006**, *324*, 280-290; b) A. H. Flood, S. Nygaard, B. W. Laursen, J. O. Jeppesen, J. F. Stoddart, *Org. Lett.* **2006**, *8*, 2205 – 2208.
[628] T. J. Huang, A. H. Flood, B. Brough, Y. Liu, P. A. Bonvallet, S. Kang, C.-W. Chu, T.-F. Guo, W. Lu, Y. Yang, J. F. Stoddart, C.-M. Ho, *IEEE Trans. Autom. Sci. Eng.* **2006**, *3*, 254 – 259.
[629] H. Kawai, T. Umehara, K. Fujiwara, T. Tsuji, T. Suzuki, *Angew. Chem.* **2006**, *118*, 4387 – 4392; *Angew. Chem. Int. Ed.* **2006**, *45*, 4281 – 4286.
[630] K. Jensen, Ç. Girit, W. Mickelson, A. Zettl, *Phys. Rev. Lett.* **2006**, *96*, 215503.
[631] V. V. Deshpande, H.-Y. Chiu, H. W. Ch. Postma, C. Milkó, L. Forró, M. Bockrath, *Nano Lett.* **2006**, *6*, 1092 – 1095.
[632] C. Li, J. Madsen, S. P. Armes, A. L. Lewis, *Angew. Chem.* **2006**, *118*, 3590 – 3593; *Angew. Chem. Int. Ed.* **2006**, *45*, 3510 – 3513.
[633] G. K. Samoei, W. Wang, J. O. Escobedo, X. Xu, H.-J. Schneider, R. L. Cook, R. M. Strongin, *Angew. Chem.* **2006**, *118*, 5445 – 5448; *Angew. Chem. Int. Ed.* **2006**, *45*, 5319 – 5322.
[634] L. Dong, A. K. Agarwal, D. J. Beebe, H. Jiang, *Nature* **2006**, *442*, 551 – 554.
[635] a) V. H. Ebron, Z. Yang, D. J. Seyer, M. E. Kozlov, J. Oh, H. Xie, J. Razal, L. J. Hall, J. P. Ferraris, A. J. MacDiarmid, R. H. Baughman, *Science* **2006**, *311*, 1580 – 1583; for a highlight of this work, see: b) J. D. Madden, *Science* **2006**, *311*, 1559 – 1560.
[636] V. Iancu, S.-W. Hla, *Proc. Natl. Acad. Sci. USA* **2006**, *103*, 13718 – 13721.
[637] A. Koçer, M. Walko, E. Bulten, E. Halza, B. L. Feringa, W. Meijberg, *Angew. Chem.* **2006**, *118*, 3198 – 3202; *Angew. Chem. Int. Ed.* **2006**, *45*, 3126 – 3130.
[638] T. Kiwada, K. Sonomura, Y. Sugiura, K. Asami, S. Futaki, *J. Am. Chem. Soc.* **2006**, *128*, 6010 – 6011.
[639] a) M. G. L. van den Heuvel, M. P. de Graaff, C. Dekker, *Science* **2006**, *312*, 910 – 914; for a highlight of this work, see: b) H. Hess, *Science* **2006**, *312*, 860 – 861.
[640] T. Liedl, M. Olapinski, F. C. Simmel, *Angew. Chem.* **2006**, *118*, 5129 – 5132; *Angew. Chem. Int. Ed.* **2006**, *45*, 5007 – 5010.
[641] a) S. Bhosale, A. L. Sisson, P. Talukdar, A. Fürstenberg, N. Banerji, E. Vauthey, G. Bollot, J. Mareda, C. Röger, F. Würthner, N. Sakai, S. Matile, *Science* **2006**, *313*, 84 – 86; for a highlight of this work, see: b) K. Kinbara, T. Aida, *Science* **2006**, *313*, 51 – 52.